

**Local and systemic delivery of a novel group of inhibitors of
transglutaminase enzyme: A potential approach for treating of
catheter-related complications and liver fibrosis**

Nooshin Daneshpour

Doctor of Philosophy

Aston University

August 2010

This copy of the thesis has been supplied on condition that anyone who consults it is understood to recognise that its copyright rests with its author and that no quotation from the thesis and no information derived from it may be published without proper acknowledgement.

Contents

Chapter 1:

| | |
|--|----|
| Introduction..... | 1 |
| 1.1 Introduction..... | 2 |
| 1.2 Central venous catheters | 2 |
| 1.2.1 General introduction and background..... | 2 |
| 1.2.2 Central venous catheter complications | 3 |
| 1.2.2.1 Catheter sheath formation | 3 |
| 1.2.2.2 Catheter-related blood vessel thrombosis (DVT) | 3 |
| 1.2.2.3 Catheter-related infection..... | 4 |
| 1.2.3 Epidemiology for CRBSI..... | 7 |
| 1.2.3 Current treatment options for CRCs | 9 |
| 1.2.4 Transglutaminases (TGs): Nature's biological glues | 10 |
| 1.2.5 Plasma factor XIII..... | 12 |
| 1.2.6 FXIIIa inhibitors: a new approach to the treatment of catheter-related infection and thrombosis..... | 13 |
| 1.3 Liver fibrosis/ Cirrhosis | 14 |
| 1.3.1 General introduction and background..... | 14 |
| 1.3.2 Etiology of liver cirrhosis | 16 |
| 1.3.3 Epidemiology of liver cirrhosis in European countries | 16 |
| 1.3.4 Epidemiology of liver cirrhosis in United States..... | 17 |
| 1.3.5 Current options for treatment of liver fibrosis/ cirrhosis | 18 |
| 1.3.6 Problems of current interventions in treatment of liver fibrosis/ cirrhosis | 18 |
| 1.3.7 Tissue transglutaminase (TG2) inhibitors: a new approach to the treatment of liver cirrhosis. | 19 |
| 1.4 Aims and objectives..... | 21 |

Chapter 2:

| | |
|---|----|
| Characterisation of fluorescent derivatives as potential probes for novel TG inhibitors | 23 |
| 2.1 Introduction | 24 |
| 2.1.1 Irreversible non-fluorescent TG inhibitor (R281)..... | 24 |
| 2.1.2 Irreversible fluorescent TG inhibitor..... | 25 |
| 2.2 Aim and objectives | 26 |
| 2.3 Material..... | 28 |

| | |
|---|----|
| 2.4 Methods | 28 |
| 2.4.1 Determination of excitation/emission spectra | 28 |
| 2.4.2 Analytical method for quantification of the TG inhibitors | 29 |
| 2.4.2.1 Fluorescence spectrophotometry | 29 |
| 2.4.2.2 High performance liquid chromatography (HPLC) | 29 |
| 2.4.3 Inhibition of TG activity: ELSA (enzyme linked sorbent assay) | 30 |
| 2.4.4 Half maximal inhibitory concentration (IC ₅₀) | 31 |
| 2.4.5 Cell culture studies | 32 |
| 2.4.5.1 Thawing cells from storage | 32 |
| 2.4.5.2 Passage of cells | 32 |
| 2.4.5.3 Incubation of cells with the TG inhibitors | 33 |
| 2.4.5.4 <i>In vitro</i> toxicological studies cytotoxicity studies | 33 |
| 2.4.5.4.1 Cell proliferation assay with XTT reagent | 34 |
| 2.4.5.4.2 Trypan blue cell viability test | 34 |
| 2.5 Statistical analysis | 35 |
| 2.6 Results and discussions | 35 |
| 2.6.1 Determination of excitation/ emission spectra | 35 |
| 2.6.2 Construction of the calibration curve using spectrofluorometry | 35 |
| 2.6.3 Construction of the calibration curve using HPLC | 38 |
| 2.6.4 Inhibition of TG activity | 39 |
| 2.6.5 Determination of the half maximal inhibitory concentration (IC ₅₀) of the TG inhibitors | 42 |
| 2.6.6 XTT cell proliferation assay | 44 |
| 2.6.7 Trypan Blue test | 46 |
| 2.7 Conclusion | 47 |
| Chapter 3: | |
| Controlled release of FXIIIa inhibitor from polyurethane catheters | 48 |
| 3.1 Introduction | 49 |
| 3.1.1 Catheter requirements | 49 |
| 3.1.2 Types of polymeric coatings | 50 |
| 3.1.3 Hydrogels: General introduction and background | 51 |
| 3.1.4 Hydrogel coating | 52 |
| 3.2 Aim and objectives | 53 |
| 3.3 Materials | 54 |
| 3.4 Methods | 54 |
| 3.4.1 Polyurethane sheet | 54 |

| | |
|--|----|
| 3.4.2 Cleaning | 55 |
| 3.4.3 Key requirements for an effective polymer coating | 55 |
| 3.4.4 Choice of polymer..... | 56 |
| 3.4.5 Choice of solvent..... | 56 |
| 3.4.6 Dip-coating method..... | 57 |
| 3.4.7 in vitro release study of FXIIIa inhibitor..... | 58 |
| 3.5 Results and Discussion..... | 59 |
| 3.5.1 Drying time..... | 59 |
| 3.5.2 Flexibility, Smoothness and consistency of finish..... | 61 |
| 3.5.3 Thickness..... | 62 |
| 3.5.4 Rate-controlled release in drug delivery and targeting..... | 63 |
| 3.5.4.1 Initial burst drug release from the PU strips..... | 65 |
| 3.5.4.2 Delayed drug release from the PU strips..... | 68 |
| 3.5.4.3 Sustained drug release from the PU strips..... | 70 |
| 3.6 Conclusion..... | 74 |
| Chapter 4: | |
| Controlled release of FXIIIa inhibitor from self-lubricating silicone elastomers..... | 76 |
| 4.1 Introduction..... | 77 |
| 4.2 Aim and objectives | 79 |
| 4.3 Materials and methods | 80 |
| 4.3.1 Materials | 80 |
| 4.3.2 Preparation of silicone elastomer strips integrating the FXIIIa inhibitor: sustained drug release | 80 |
| 4.3.3 Production of a smart polymeric coating on the silicone strips: initial immediate drug release | 82 |
| 4.3.4 FXIIIa inhibitor release from the silicone elastomer strips <i>in vitro</i> | 83 |
| 4.3.5 Biological activity of the released FXIIIa inhibitor..... | 83 |
| 4.3.6 Morphological analysis..... | 84 |
| 4.3.6.1 Scanning electron microscopy (SEM) | 84 |
| 4.3.6.2 Digital images | 84 |
| 4.3.6.3 Optical microscopy | 84 |
| 4.3.7 Swelling studies | 84 |
| 4.3.8 Mechanical properties..... | 85 |

| | |
|---|-----|
| 4.3.8.1 Tensile strength..... | 85 |
| 4.3.8.2 Force-extension curve..... | 86 |
| 4.3.8.3 Young's modulus (modulus of elasticity) (elastic modulus) (Tensile modulus). | 86 |
| 4.3.9 Statistical analysis..... | 87 |
| 4.4 Results and discussions..... | 87 |
| 4.4.1 Drug release mechanism..... | 87 |
| 4.4.2 Influence of additives on release behaviour..... | 90 |
| 4.4.2.1 Sustained drug release from the silicone elastomer strips | 90 |
| 4.4.2.2 Initial immediate drug release..... | 94 |
| 4.4.3 Biological activity of the released inhibitors | 95 |
| 4.4.4 Scanning electron microscopy | 96 |
| 4.4.5 Macroscopic morphology | 101 |
| 4.4.6 Optical microscopy | 102 |
| 4.4.7 Swelling studies | 107 |
| 4.4.8 Mechanical properties of silicone strips | 108 |
| 4.4.8.1 Tensile strength..... | 108 |
| 4.4.8.2 Force-extension curve..... | 110 |
| 4.4.8.3 Young's modulus (modulus of elasticity) (elastic modulus) (Tensile modulus) | 116 |
| 4.4.9 Summary | 117 |
| 4.4.10 Conclusion | 119 |
| Chapter 5: | |
| Biodistribution and pharmacokinetic studies of the TG2 inhibitor | 120 |
| 5.1 Introduction | 121 |
| 5.2 Aim..... | 121 |
| 5.3 Animals..... | 121 |
| 5.4 Study design, drug administration and sample collection | 122 |
| 5.5 Results and discussions | 122 |
| 5.5.1 Biodistribution and pharmacokinetic of the TG2 inhibitor..... | 122 |
| 5.6 Conclusion | 128 |
| Chapter 6: | |
| Transglutaminase inhibitor loaded liposomes: a new approach to the treatment of liver fibrosis..... | 129 |

| | |
|---|-----|
| 6.1 Targeted delivery of the TG2 inhibitors into the liver | 130 |
| 6.2 Liposomes | 131 |
| 6.2.1 General background and application | 131 |
| 6.2.2 Liposomes | 132 |
| 6.2.3 Why liposomes are formed? | 132 |
| 6.2.4 Advantages of liposomes for drug delivery | 133 |
| 6.2.5 Manufacturing problems and limitations..... | 133 |
| 6.2.6 Classification of liposomes..... | 135 |
| 6.2.6.1 Multilamellar vesicles (MLV)..... | 135 |
| 6.2.6.2 Unilamellar vesicles of small size (SUV)..... | 135 |
| 6.2.6.3 Large unilamellar vesicles (LUV) | 136 |
| 6.2.6.4 Reverse phase evaporation vesicles (REV) | 136 |
| 6.2.6.5 Vesicles produced using the extrusion technique (VET)..... | 136 |
| 6.2.6.6 Dehydration-rehydration vesicles | 136 |
| 6.2.7 Parameters which influence <i>in vivo</i> behavior of liposomes..... | 137 |
| 6.2.7.1 Bi-layer fluidity..... | 137 |
| 6.2.7.2 Surface charge..... | 137 |
| 6.2.7.3 Liposome size | 138 |
| 6.2.8 Optimization of liposome composition..... | 139 |
| 6.3 Aim and objectives | 140 |
| 6.4 Materials | 140 |
| 6.5 Methods..... | 141 |
| 6.5.1 Liposome production | 141 |
| 6.5.1.1 Production of multilamellar vesicle incorporating the TG2 inhibitor | 141 |
| 6.5.1.2 Production of small unilamellar vesicles incorporating the TG2 inhibitor..... | 142 |
| 6.5.2 Separation of non-incorporated drug from liposome suspension | 142 |
| 6.5.2.1 Size-exclusion chromatography | 143 |
| 6.5.2.2 Centrifugation | 144 |
| 6.5.3 Characterisation of liposomes..... | 144 |
| 6.5.3.1 Determination of the liposome size and polydispersity | 144 |
| 6.5.3.2 Measuring zeta potential | 145 |
| 6.5.3.3 Drug encapsulation studies | 145 |
| 6.5.4 The effect of salt on the physico-chemical properties of liposomes..... | 147 |

| | |
|--|-----|
| 6.5.5 Stability studies in buffer and serum | 147 |
| 6.5.5.1 Drug retention | 147 |
| 6.5.5.2 Liposome stability: Particle size and zeta potential | 147 |
| 6.5.6 Bio-distribution of liposomes loaded with the enzyme inhibitor in mice | 148 |
| 6.6 Results and discussion | 149 |
| 6.6.1 Liposomal characteristics..... | 149 |
| 6.6.1.1 Characteristics of the TG2 inhibitor incorporated multi-lamellar vesicles..... | 149 |
| 6.6.1.2 Characteristics of the TG2 inhibitor incorporated small unilamellar vesicles..... | 152 |
| 6.6.1.2.1 Particle size and zeta potential of SUV..... | 152 |
| 6.6.1.2.2 Encapsulation efficiency | 155 |
| 6.6.2 The formulation of choice for further <i>in vivo</i> studies | 156 |
| 6.6.3 The effect of salt on the physico-chemical properties of liposome | 157 |
| 6.6.4 The influence of sonication time on physico-chemical characteristics of neutral and anionic liposomes..... | 158 |
| 6.6.5 Stability studies in serum | 161 |
| 6.6.5.1 Liposome stability: drug retention | 162 |
| 6.6.5.2 Liposome stability: vesicle size and zeta potential studies..... | 163 |
| 6.6.6 Bio-distribution studies of the liposome-TG2 inhibitor system in mice... | 165 |
| 6.6.7 Conclusion..... | 169 |
| Chapter 7: | |
| General discussion | 170 |
| 7.1 Summary and Implications of Research Findings..... | 171 |
| 7.2 Future directions..... | 173 |
| Thesis Publications..... | 174 |
| References..... | 177 |
| Appendix..... | 198 |

List of Figures

| | |
|--|----|
| Figure 1.1 Multi-lumen Central Venous Catheter Systems (web image 1)..... | 3 |
| Figure 1.2 Central venous catheter inserted into subclavian vein (web image 2) | 3 |
| Figure 1.3 Taking out of the catheter with the surrounding fresh thrombus material with the help of a clamp (web image 3)..... | 4 |
| Figure 1.4 Parts of Cava-fix catheter and cover thrombus surrounding it (inside) (web image 4). | 4 |
| Figure 1.5 A tube-site infection. Most catheter-related infections involve local cellulitis, as shown here, with erythema and tenderness. These infections frequently respond to local wound care and oral antibiotics (web image 5)..... | 5 |
| Figure 1.6 Appearance of a central venous catheter associated with bacteremia(web image 6) | 5 |
| Figure 1.7 Potential routes of catheter infection (web image 7). | 6 |
| Figure 1.8 Extra costs of catheter-related bloodstream infection (CRBSI) per implanted central venous catheter per country (France, Germany, Italy and the UK).. | 9 |
| Figure 1.9 Cross-linking reaction of transglutaminases (web image 8). | 11 |
| Figure 1.10 Crystal structure of human Factor XIII (web image 9). | 12 |
| Figure 1.11 Effect of the FXIIIa inhibitors (R281 & R283, excising inhibitors) on release of Staphylococcus aureus from human thrombi. | 14 |
| Figure 1.12 A healthy liver in adults (left). A liver damaged by alcoholism shows a buildup of fatty tissue (middle), and a liver with cirrhosis is enlarged and swollen (right) (web image 10). | 14 |
| Figure 1.13 Alterations in the hepatic structure in a fibrotic liver caused by accumulation of ECM proteins..... | 15 |
| Figure 1.14 Chronic liver disease and cirrhosis mortality rates per 100,000 populations, 1950-2006..... | 17 |
| Figure 1.15 Overall structure of a human tissue transglutaminase (TG) (web image 11)..... | 19 |
| Figure 2.1 The schematic structure of irreversible non-fluorescent transglutaminase inhibitor (R281) | 25 |
| Figure 2.2 Graphic representation of the calibration record of AM1/99. | 35 |
| Figure 2.3 Scanning the emission wavelengths of different concentrations of AM1/99 (0-200 μ M) in a fixed excitation wavelength (340 nm) using spectrofluorometry | 36 |

| | |
|---|----|
| Figure 2.4 Scanning the excitation wavelengths of different concentrations (0-200 μ M) of AM1/99 in a fixed emission wavelength (456 nm) using spectrofluorometry. | 36 |
| Figure 2.5 Graphic representation of the calibration record of AM1/107. | 37 |
| Figure 2.6 Graphic representation of the calibration record of AM2/97. | 37 |
| Figure 2.7 Graphic representation of the calibration record of AM2/169. | 38 |
| Figure 2.8 Graphic representation of the calibration record of AM2/169. | 39 |
| Figure 2.9 The inhibition of FXIIIa and TG2 by R281. | 40 |
| Figure 2.10 The inhibition of FXIIIa and TG2 by AM1/99..... | 41 |
| Figure 2.11 The inhibition of FXIIIa and TG2 by AM1/107..... | 41 |
| Figure 2.12 The inhibition of FXIIIa and TG2 by AM2/97..... | 42 |
| Figure 2.13 The inhibition of FXIIIa and TG2 by AM2/169..... | 42 |
| Figure 2.14 Effect of different concentrations of the TG inhibitors on fibroblast cell viability | 44 |
| Figure 2.15 Cytotoxicity of various TG inhibitors to fibroblast cells..... | 44 |
| Figure 2.16 Effect of the TG inhibitors on fibroblast cell death..... | 46 |
| Figure 3.1 Poly (urethane) sheet | 54 |
| Figure 3.2 The polymer-coated strips were hanged from a stand in a vertical position and dried at room temperature subsequent to coating. | 55 |
| Figure 3.3 The schematic of dip-coating of the polyurethane strips in the polymer solution containing the fluorescent inhibitor | 57 |
| Figure 3.4 The inhibitor-and polymer-coated polyurethane strips placed in PBS..... | 58 |
| Figure 3.5 Drying time (minute) of the PU strips at different concentrations of the polymeric-coating solution. | 59 |
| Figure 3.6 Partial delamination of the polymeric coating of the PU strips..... | 61 |
| Figure 3.7 The polymeric coating of the PU strips with partial delamination and cracks | 61 |
| Figure 3.8 Complete delamination of the polymeric coating of the PU strips..... | 62 |
| Figure 3.9 The thickness of the polymer-coated polyurethane strips, using SEM. | 62 |
| Figure 3.10 A-C epifluorescent microscope images of the 2, 3 and 4 times inhibitor- and polymer-coated polyurethane strips, using 4 x objectives | 63 |
| Figure 3.11 Cumulative releases (μ mole/ml) of the fluorescent FXIIIa inhibitor (AM2/97) into 10 ml PBS from the individually coated polyurethane strips over 60 minutes under sink condition. | 66 |

| | |
|---|----|
| Figure 3.12 Cumulative percentage release of the fluorescent FXIIIa inhibitor (AM2/97) into 10 ml PBS from the individually coated polyurethane strips over 60 minutes under sink condition. | 66 |
| Figure 3.13 Cumulative releases ($\mu\text{mole/ ml}$) of the fluorescent FXIIIa inhibitor (AM2/97) into 10 ml PBS from the individually coated polyurethane strips over 60 minutes under sink condition. | 67 |
| Figure 3.14 Cumulative percentage release of the fluorescent FXIIIa inhibitor (AM2/97) into 10 ml PBS from the individually coated polyurethane strips over 60 minutes under sink condition. | 68 |
| Figure 3.15 Cumulative releases ($\mu\text{mole/ ml}$) of the fluorescent FXIIIa inhibitor (AM2/97) into 10 ml PBS from the individually coated polyurethane strips over 7 days under sink condition. | 69 |
| Figure 3.16 Cumulative percentage release of the fluorescent FXIIIa inhibitor (AM2/97) into 10 ml PBS from the individually coated polyurethane strips over 7 days under sink condition. | 69 |
| Figure 3.17 Cumulative releases ($\mu\text{mole/ ml}$) of the fluorescent FXIIIa inhibitor (AM2/97) into 10 ml PBS, from the individually coated polyurethane strips over 7 days under sink condition. | 71 |
| Figure 3.18 Cumulative percentage release of the fluorescent FXIIIa inhibitor (AM2/97) into 10 ml PBS from the individually coated polyurethane strips over 7 days under sink condition. | 71 |
| Figure 3.19 Cumulative releases ($\mu\text{mole/ ml}$) of the fluorescent FXIIIa inhibitor (AM2/97) into PBS: FBS 50:50 (v/v) from the individually coated polyurethane strips over 14 days under sink condition. | 72 |
| Figure 3.20 Cumulative percentage release of the fluorescent FXIIIa inhibitor (AM2/97) into 10 ml PBS: FBS 50:50 (v/v) from the individually coated polyurethane strips over 14 days under sink condition..... | 73 |
| Figure 3.21 Cumulative releases ($\mu\text{mole/ ml}$) of the fluorescent FXIIIa inhibitor (AM2/97) into PBS: FBS 50:50 (v/v) from the individually coated polyurethane strips over 14 days under sink condition. | 73 |
| Figure 3.22 Cumulative percentage release of the fluorescent FXIIIa inhibitor (AM2/97) into PBS: FBS 50:50 (v/v) from the individually coated polyurethane strips over 14 days under sink condition. | 74 |

| | |
|---|----|
| Figure 4.1 The 3-D polymer structure of silicone elastomer. Silicone elastomers are cross linked linear silicone fluids or gums with a three-dimensional structure. | 77 |
| Figure 4.2 Cross-linking chemistry between hydroxy-terminated poly(dimethylsiloxane) and tetrapropoxysilane(TPOS)in the production of condensation cured silicone elastomer..... | 81 |
| Figure 4.3 Hounsfield H10KS Universal Testing Machine..... | 85 |
| Figure 4.4 Measuring the tensile strength and Young’s modulus of the silicone strips by a Hounsfield Universal Tester. | 87 |
| Figure 4.5 Fick’s law of diffusion in diffusion controlled devices. | 88 |
| Figure 4.6 Release mechanisms of drugs with different physiochemical properties from a silicone carrier. | 89 |
| Figure 4.7 Cumulative releases ($\mu\text{mole/ ml}$) of the fluorescent FXIIIa inhibitor (AM2/97) into 10 ml PBS from the silicone elastomer strips over 30 days under sink condition.. | 91 |
| Figure 4.8 Cumulative percentage release of the fluorescent FXIIIa inhibitor (AM2/97) into 10 ml PBS from the silicone elastomer strips over 30 days under sink condition. | 91 |
| Figure 4.9 Diagrams demonstrating the process of drug release from a silicone carrier. | 92 |
| Figure 4.10 Cumulative releases ($\mu\text{mole/ ml}$) of the fluorescent FXIIIa inhibitor (AM2/97) into 10 ml PBS from the silicone elastomer strips over 40 days under sink condition.. | 93 |
| Figure 4.11 Cumulative percentage release of the fluorescent FXIIIa inhibitor (AM2/97) into 10 ml PBS from the silicone elastomer strips over 40 days under sink condition. | 93 |
| Figure 4.12 Cumulative release ($\mu\text{mole/ ml}$) of the fluorescent FXIIIa inhibitor (AM2/97) into 10 ml PBS from the silicone elastomer strips with 2, 3 and 4x PVP coatings over 60 minute under sink condition. | 94 |
| Figure 4.13 Cumulative percentage release of the fluorescent FXIIIa inhibitor (AM2/97) into 10 ml PBS from the silicone strips with 2, 3 and 4x PVP coatings over 60 minutes under sink condition. | 95 |
| Figure 4.14 Cross sectional SEM images from the silicone elastomer strips containing 0% to 30% (w/w) CA: SB (a to d), prior to incubation in PBS at 29 x, 49 x and 10 3x magnification respectively. | 97 |

| | |
|--|-----|
| Figure 4.15 Cross sectional SEM images from the silicone elastomer strips containing 0 % to 30 % (w/w) CA: SB (a to d), subsequent to 1 day incubation in PBS at 29 x, 49 x and 103 x magnification respectively. | 98 |
| Figure 4.16 Cross sectional SEM images from the silicone elastomer strips containing 0 % to 30 % (w/w) CA: SB (a to d), subsequent to 1 week incubation in PBS at 29 x, 49 x and 103 x magnification respectively. | 99 |
| Figure 4.17 Cross sectional SEM images from the silicone elastomer strips containing 0 % to 30 % (w/w) CA: SB (a to d), subsequent to 1 month incubation in PBS at 29 x, 49 x and 103 x magnification respectively. | 100 |
| Figure 4.18 Macroscopic photographs of the silicone elastomer strips before and after one-month incubation in PBS. | 101 |
| Figure 4.19 a-d Optical images from the surface of the silicone elastomer strips containing 0 % (1), 5 % (2), 15 % (3) and 30 % (4) (w/w) CA: SB, prior to incubation in PBS at 25x (A) and 50x (B) magnifications respectively, using a Reichert-Jung Polyvar microscope..... | 103 |
| Figure 4.20 a-d Optical images from the surface of the silicone elastomer strips containing 0 % (1), 5 % (2), 15 % (3) and 30 % (4) (w/w) CA: SB, after 1 day incubation in PBS (37 °C) at 25x (A) and 50x (B) magnifications respectively, using a Reichert-Jung Polyvar microscope | 104 |
| Figure 4.21 a-d Optical images from the surface of the silicone elastomer strips containing 0 % (1), 5 % (2), 15 % (3) and 30 % (4) (w/w) CA: SB, after 1 week incubation in PBS (37 °C) at 25x (A) and 50x (B) magnifications respectively, using a Reichert-Jung Polyvar microscope | 105 |
| Figure 4.22 a-d Optical images from the surface of the silicone elastomer strips containing 0 % (1), 5 % (2), 15 % (3) and 30 % (4) (w/w) CA: SB, after 1 month incubation in PBS (37 °C) at 25x (A) and 50x (B) magnifications respectively, using a Reicher-Jung Polyvar microscope | 106 |
| Figure 4.23 Percent change in volume (%) of the silicone elastomer strips integrating 0 %, 5 %, 15 % and 30 % CA: SB after incubation (1 day, 1 week and 1 month) in PBS (pH 7.4, 37 °C)..... | 107 |
| Figure 4.24 The true tensile strength of the silicone elastomer strips incorporating 0 %, 5 %, 15 % and 30 % CA: SB previous to and after incubation (1 day, 1 week and 1 month) in PBS (pH 7.4, 37 °C). | 110 |

| | |
|---|-----|
| Figure 4.25 a-d Force-extension curve of the silicone elastomer strip containing 0 % (w/w) CA: SB, prior to incubation in PBS (1) and after 1 day (2) 1 week (3) and 1 month (4) incubation in PBS (pH 7.4, 37 °C)..... | 112 |
| Figure 4.26 a-d Force-extension curve of the silicone elastomer strip containing 5 % (w/w) CA: SB, prior to incubation in PBS (1) and after 1 day (2) 1 week (3) and 1 month (4) incubation in PBS (pH 7.4, 37 °C)..... | 113 |
| Figure 4.27 a-d Force-extension curve of the silicone elastomer strip containing 15 % (w/w) CA: SB, prior to incubation in PBS (1) and after 1 day (2) 1 week (3) and 1 month (4) incubation in PBS (pH 7.4, 37 °C)..... | 114 |
| Figure 4.28 a-d Force-extension curve of the silicone elastomer strip containing 30 % (w/w) CA: SB, prior to incubation in PBS (1) and after 1 day (2) 1 week (3) and 1 month (4) incubation in PBS (pH 7.4, 37 °C)..... | 115 |
| Figure 4.29 Young's modulus of the silicone elastomer strips incorporating 0 %, 5 %, 15 % and 30 % CA: SB previous to and after incubation (1 day, 1 week and 1 month) in PBS (pH 7.4, 37°C)..... | 116 |
| Figure 5.1a A linear plot of the decline in the mean plasma concentration of AM2/169 following an IP dose of 50 mg/kg to a group of male Wistar rats. | 123 |
| Figure 5.1b A semi logarithmic plot of the decline in the mean plasma concentration of AM2/169 following an IP dose of 50 mg/kg to a group of male Wistar rats. The time scale is the same as Figure 5.1a (0.083 to 2 hours time points time points), however the ordinate (concentration) scale is logarithmic. | 123 |
| Figure 5.1c A semi logarithmic plot of the decline in the mean plasma concentration of AM2/169 following an IP dose of 50 mg/kg to a group of male Wistar rats. The time scale is from a 0.33 hour time point (the time the drug has reached the maximum blood concentration) to a 2 hour time point (the time the drug has completely cleared from the blood stream)..... | 124 |
| Figure 5.2 Bio-distribution of AM2/169 in Wistar rats..... | 127 |
| Figure 6.1 Diagrammatic representation of a liposome and its bi-layer forming lipid molecule in an aqueous medium..... | 131 |
| Figure 6.2 Diagrammatic illustration of a phospholipid molecule with a polar (water soluble) and a non polar group (oil like), a phospholipid bi-layer and a self-assembled liposome. | 133 |
| Figure 6.3 Multilamellar vesicle (MLV)..... | 135 |
| Figure 6.4 Small unilamellar vesicles (SUV) | 136 |

| | |
|--|-----|
| Figure 6.5 Large unilamellar vesicles (LUV) | 136 |
| Figure 6.6 Schematic representation of the preparation of MLV by ‘hand-shaking’ method..... | 142 |
| Figure 6.7 Preparation of small unilamellar vesicles by sonication of MLV suspension..... | 142 |
| Figure 6.8 Schematic representation of size-exclusion chromatography..... | 143 |
| Figure 6.9 Volume mean diameter (VMD) and particle size distributions (PSD) of various TG2 incorporated multi-lamellar vesicle formulations..... | 150 |
| Figure 6.10 Zeta potential (mV) of various TG2 incorporated multi-lamellar vesicle formulations..... | 151 |
| Figure 6.11 Particle size (nm) and polydispersity of various small unilamellar vesicle formulations..... | 152 |
| Figure 6.12 Zeta potential (mV) of various small unilamellar vesicles formulations. | 153 |
| Figure 6.13 Percentage of drug entrapment for various liposomal formulations using size-exclusion chromatography.. .. | 156 |
| Figure 6.14 The influence of sonication time on z-average diameter and polydispersity of the neutral liposomes. | 159 |
| Figure 6.15 The influence of sonication time on zeta potential of the neutral liposomes. | 159 |
| Figure 6.16 The influence of sonication time on z-average diameter and polydispersity of anionic liposomes..... | 160 |
| Figure 6.17 The influence of sonication time on zeta potential of anionic liposomes. | 161 |
| Figure 6.18 Vesicle stability (size and zeta potential) of the neutral liposomes in serum..... | 164 |
| Figure 6.19 Vesicle stability (size and zeta potential) of the anionic liposomes in serum..... | 165 |
| Figure 6.20 Organ distribution of the liposomes-TG2 inhibitor system in mice at various time points following I.V. injection. | 168 |

List of Tables

| | | |
|------------------|---|-----|
| Table 1.1 | Key results of a Medline literature review of published epidemiological studies, economic evaluations and cost studies in the field CRBSIs..... | 8 |
| Table 1.2 | Identified active types of TGs in mammals..... | 12 |
| Table 2.1 | The name, chemical structure, molecular weight and components of the fluorescent and non- fluorescent TG inhibitors investigated..... | 27 |
| Table 2.2 | Parameters for the elution of the TG inhibitor from the RP-304 C4 column..... | 30 |
| Table 2.3 | IC50 values of the TG inhibitors on the two types of the enzyme TG (TG2 and FXIIIa)..... | 43 |
| Table 3.1 | Comparison of properties of common coating substances..... | 51 |
| Table 4.1 | Composition of silicone elastomer formulations..... | 82 |
| Table 4.2 | Experimental setup of Hounsfield Universal Tester for measuring the tensile strength of the silicone strips..... | 86 |
| Table 4.3 | Measurement of biological activity of the released inhibitors, using an enzyme linked sorbent assay..... | 95 |
| Table 4.4 | The data obtained from measuring tensile strength of the silicone elastomer strips by a Hounsfield Universal Tester. The experimental conditions involved; 0 %, 5 %, 15 % and 30 % CA/ SB incorporated formulations, and prior to incubation in PBS..... | 118 |
| Table 4.5 | The data obtained from measuring tensile strength of the silicone elastomer strips by a Hounsfield Universal Tester. The experimental conditions involved; 0 %, 5 %, 15 % and 30 % CA/ SB incorporated formulations, and after one day incubation in PBS..... | 118 |
| Table 4.6 | The data obtained from measuring tensile strength of the silicone elastomer strips by a Hounsfield Universal Tester. The experimental conditions involved; 0 %, 5 %, 15 % and 30 % CA/ SB incorporated formulations, and after one week | |

| | | |
|------------------|---|-----|
| | incubation in PBS..... | 118 |
| Table 4.7 | The data obtained from measuring tensile strength of the silicone elastomer strips by a Hounsfield Universal Tester. The experimental conditions involved; 0 %, 5 %, 15 % and 30 % CA/ SB incorporated formulations, and after one month incubation in PBS..... | 119 |
| Table 6.1 | Descriptive examples of liposome products currently available n the market with their indications..... | 134 |
| Table 6.2 | Summary of the range of liposomes formulations prepared in this study, the charge of the liposome, the total molar ratio and their corresponding molar ratios of the individual components... | 149 |
| Table 6.3 | The effect of various hydration media (PBS and d.H2O) on characteristics of the TG2 inhibitor integrated small unilamellar vesicles..... | 158 |

Acknowledgments

My heart felt gratitude goes to my supervisor, Professor Yvonne Perrie and my associate supervisor, Professor Martin Griffin for their valuable advice, expert guidance and encouragement throughout the period of my study.

Huge thanks to Dr. Russell Collighan who is a fountain of knowledge and without whom I would have been completely lost.

Many thanks to my entire research group for their marvellous support and enormous help.

I also extend special thanks to all the staff at Aston University including Jiteen Kansara and Chris Bache for their technical assistance in the lab.

Finally, I am indebted to my family for their tremendous moral and financial support, encouragement and ceaseless love all through this study.

Chapter 1:

Introduction

1.1 Introduction

In this thesis, the targeted delivery (locally and systemically) of a novel group of inhibitors of the enzyme transglutaminases (TGs) was investigated. Two types of delivery options were considered: 1) Factor XIIIa inhibitor was integrated into catheters as a new approach for the treatment of central venous catheter and other medical implant devices-associated thrombi and staphylococcal infections. 2) Tissue transglutaminase (TG2) inhibitor was incorporated into liposomes, with the aim of targeting the liver as a new approach to the treatment of liver fibrosis and its end stage disease liver cirrhosis. This chapter focuses on general background information regarding central venous catheters, liver fibrosis/cirrhosis, TGs and the TG inhibitors. Details of the delivery systems employed will be outlined in the respective chapters.

1.2 Central venous catheters

1.2.1 General introduction and background

Although the earliest use was noted in 1982, central venous catheters were not a usual part of medical therapy until 1945 when plastic catheters became available (Garg et al., 2004). Central venous catheters (CVCs) are defined by Morris et al. (2010) as long flexible catheters with single or multiple (2 - 5) lumens that enter central veins. These catheters are commonly introduced into the jugular, subclavian and less frequently the femoral veins (Figures 1.1 & 1.2). The use of CVCs allows the administration of fluids, blood products, medication, total parenteral nutrition and/or haemodynamic monitoring of critically ill patients. The application of long-term CVCs is of great importance for patients who require long-term medical therapy or multiple course of intermittent treatment (Xiang et al., 2001).

CVCs are being utilised with increasing frequency in the hospital and in the community. In spite of the extensive experience gained in their application, CVCs are related to the long-term risks of catheter sheath formation, infection and thrombosis (of the catheter or vessel itself) during catheterisation. Such CVCs related-complications (CRCs) are associated with increased morbidity, mortality, and duration of hospitalisation (Piozzi et al., 2004). Furthermore, these sequences could result in expensive interventions, loss of the access mechanism, or loss of access sites in a maximum of one-third of patients (Forauer & Theoharis, 2003).



Figure 1. 1 Multi-lumen Central Venous Catheter Systems (web image 1).

Figure 1. 2 Central venous catheter inserted into subclavian vein (web image 2).

1.2.2 Central venous catheter complications

1.2.2.1 Catheter sheath formation

The formation of a fibrin sheath around a catheter inserted into the subclavian vein was first reported by Motin et al (1964) and termed 'fibrin sleeve'. A fibrin sleeve has been regarded a general reaction between blood and catheter and could be developed within 24 hours following catheterization (Hoshal et al., 1971). Approximately all CVCs are coated with a fibrin sheath within days of insertion (Kutter, 2004). The reported incidence of a "fibrin sleeve" ranges from 42 % to 100 % with variable length (Brismar et al., 1981; Raad II et al., 1994). The sleeve itself generally does not cause clinical symptoms, nevertheless has been counted as the reason of several catheter-related complications such as thrombosis and infection (Xiang et al., 1998).

1.2.2.2 Catheter-related blood vessel thrombosis (DVT)

One of the major complications of CVCs is thrombosis (Figures 1.3 & 1.4). According to the German physician, Rudolf Virchow, thrombus formation requires three essential components; hypercoagulability, hemodynamic changes (stasis, turbulence) and endothelial injury/dysfunction (Armstrong et al., 2008). A foreign body in the bloodstream can activate coagulation at its surface. All central venous catheters are basically intravascular foreign bodies. Platelets and the complement coagulation pathways are activated at the focal site of injury where the catheter places the vein or potentially at any place all along the entire catheter length. Red blood cells, platelets, white blood cells, fibrinogen, and fibrin attach to a catheter surface. Thrombus formation associated with central venous catheters can form at the tip of a

catheter, along the entire intravascular catheter and also at the site of venous entry (Santilli, 2002).

The mural thrombi may partly or completely block the blood vessel and may involve 12 – 74 % of all CVCs (Kutter, 2004). This wide variability is due to the diagnostic methods used, the difficulties in interpretation of observations, the way thrombosis is defined and reported (Xiang et al., 2001), variation in catheter type, position, duration of insertion, and the underlying diseases (Kutter, 2004). Aside from reducing the function of the catheter the CV-related thrombi can cause postphlebitic syndrome in 15 – 30 % of cases and pulmonary embolism in 11 % of cases (only half of which are symptomatic) (Kutter, 2004).



Figure 1. 3 Taking out of the catheter with the surrounding fresh thrombus material with the help of a clamp (web image 3).

Figure 1. 4 Parts of Cava-fix catheter and covering thrombus surrounding it (inside), after removal from a patient (Figure 1.3) (web image 4).

1.2.2.3 Catheter-related infection

Infection is defined as a homeostatic imbalance between the host tissue and existence of microorganism (Zilberberman and Elsner, 2008). Nosocomial or hospital acquired infections are a major cause of morbidity and mortality among hospitalized patients. They concern 5 – 15 % of hospitalized patients and can lead to complications in 25 - 50 % of those admitted to intensive care units (ICUs) (Eggimann et al., 2004). Urinary tract and surgical site infections, followed by respiratory and bloodstream infections are the most frequent infections worldwide (Eggimann, & Pittet, 2001). Methicillin-resistant *Staphylococcus aureus* (MRSA) is the most common cause of nosocomial infections (Sisirak et al., 2010). The National Nosocomial Infection Surveillance

(NNIS) (2000) system reported that the majority of nosocomial bloodstream infections in ICUs are related with the utilisation of intravascular access and the infection rates are considerably higher among patients with central venous catheters than among those with peripheral lines.



Figure 1. 5 A tube-site infection. Most catheter-related infections involve local cellulitis, as shown here, with erythema and tenderness. These infections frequently respond to local wound care and oral antibiotics (web image 5).

Figure 1. 6 Appearance of a central venous catheter associated with bacteremia (web image 6).

CVC-related infection has been defined in various terms by the Centers for Disease Control, researchers, and authors. In general it consist of any of the following conditions: *“a catheter colonized with more than 15 colony-forming units, according to the Maki technique (1977), with symptoms of sepsis (hyperthermia, hypothermia, or hypotension); purulent drainage at the catheter site with or without bacteremia; symptoms of sepsis with or without bacteremia, unrelated to infection at another site, in the presence of an indwelling CVC; and bacteremia, unrelated to infection at another site, in the presence of an indwelling CVC”* (Hoppe, 1995).

Systemic and local infectious complications of CVCs include local site infection, catheter related blood stream infection (CRBSI), septic thrombophlebitis, endocarditis, and other metastatic infections such as lung abscess, brain abscess, osteomyelitis and endophthalmitis (O’Grady et al., 2002; Garg et al., 2004) (Figures 1.5 & 1.6). The American Centers for Disease Control and Prevention (CDC) defines CRBSI as the isolation of the same organism from the colonised catheter and

peripheral blood in a patient with clinical sepsis and no other apparent source of bloodstream infection (Garg et al, 2004). The most common pathogens isolated from hospital acquired CRBSI are coagulase negative *Staphylococcus* species, Gram-negative rods and *Staphylococcus aureus* (Garg et al., 2004).

It was first suggested by Press et al. in 1984 that thrombosis is a major risk factor for infection of CVCs by demonstrating that bacteremia was much more common in patients with documented CVCs thrombosis (Press et al., 1984). This could be due to the fact that all cannulated blood vessels comprise a fibrin sheath seeded with adherent cocci (Kutter, 2004). Figure 1.7 demonstrates the potential routes of catheter infection.



Figure 1. 7 Potential routes of catheter infection (web image 7).

There are two most general pathways identified in the development of catheter-related infections. Initially, colonization of the external surface begins with the colonization of the insertion site by microorganisms that may progressively move through the transcutaneous part of the dermal tunnel surrounding the catheter. Skin colonization is a strong indicator of catheter-related infection. Secondly, colonization of the internal surface may occur by colonization of the hub and intraluminal surface of the catheter during utilization and frequent opening of the hub. The third pathways could be haematogenous seeding of the catheter throughout blood stream infection.

Nevertheless, contamination of fluids or drugs intravenously administered could be responsible for catheter-related infections. As a consequence, a biofilm constituted of host glycoproteins including fibrinogen, fibronectin, collagen and laminin may be formed. This layer increases the adherence of bacteria, in particular *Staphylococcus aureus* and coagulase-negative *staphylococci* to the foreign material (Figure 1.7) (Eggimann et al., 2004). Contamination of intravenous fluid is the fourth potential source of CVC-related infection. This mechanism hardly ever results in bacteremia, however it has been associated with cases of epidemic nosocomial infections (Hoppe, 1995).

1.2.3 Epidemiology for CRBSI

It has been found that 2.8 – 18 % of CVC patients suffer from catheter-related infection (Mughal, 1989). In the United States, CRBSI occurs with 3 – 7 % of catheters and affects more than 200,000 patients per year with a mortality of 10 - 25 % and an extra cost to the health-care system of approximately \$ 25,000 per episode (O’Grady et al., 2002).

The epidemiology, clinical outcomes and costs associated with CRBSIs in four European countries (France, Germany, Italy and the UK) based on recent information are estimated in Table 1.1 & Figure 1.8. In the UK, approximately 6000 patients acquire catheter-related bloodstream infection annually with a considerable increase in the length of hospitalisation and medical care costs (Fletcher & Bodenham, 1999). The most recent CRBSI study in the UK was conducted by the Scottish Executive Health Department in 2005 in five hospitals in six intensive care units (ICUs). This pilot study using the Hospital in Europe Link for Infection Control through Surveillance definitions (HELICS) reported an estimate of 4.2 CRBSIs per 1000 catheter days (95 % CI: 1.4–9.8). Based on a study performed by Plowman et al (2001), it was estimated (through modeling) that CRBSIs might be accountable for an extra length of stay (LOS) of 4.0 days (1.9 days based on observed, not modeled, data). The extra LOS was regarded as low and related to the considerable use of medical resources. This translates into an estimate of 16 980 to 35 750 days caused by CRBSIs, i.e. 1.9–4 days extra LOS multiplied by the 8940 CRBSIs in the UK (Plowman et al., 2001; Tacconelli et al., 2009).

Mortality rates for CRBSI are complicated to calculate due to the presence of various confounding factors that were observed amongst patients. In a relatively recent study carried out by Tacconelli et al. (2009), no information was retrieved concerning CRBSI-related mortality in the UK. However, rates in France, Germany and Italy were reported (Table 1.1).

Table 1.1 Key results of a Medline literature review of published epidemiological studies, economic evaluations and cost studies in the field of CRBSIs. (taken from Tacconelli et al, 2009). ICU stands for intensive care unit; CRBSI stands for catheter-related bloodstream infections; LOS stands for length of stay.



The cost of a CRBSI episode can be determined by multiplying the extra LOS related to CRBSI by the daily ICU cost. Plowman et al. (2001) provided an estimation of additional costs per blood stream infection of ~ € 9,251 (£ 6,209) (exchange rate: £ 1 = € 1.49) when modeled versus € 4,392 (£ 2,949) when observed, whilst Tacconelli et al. (2009) expected that the costs for the National Health Service (NHS) could be between £ 19.1 and £ 36.2 million (€ 28.5 to € 53.9 million) (Figure 1.8). Another study at Blackpool Victoria Hospital, NHS Trust stated that the full cost of hospital acquired bacteremia in general surgical and the institutional technical unit (ITU) patients over a 12 month period was £ 491,984 (Garg et al., 2004). Presently this number is increasing rather than decreasing.



Figure 1. 8 Extra costs of catheter-related bloodstream infection (CRBSI) per implanted central venous catheter per country (France, Germany, Italy and the UK). Results present the minimum and maximum estimates per country for the additional costs of CRBSIs per implanted CVC (taken from Tacconelli et al., 2009).

1.2.3 Current treatment options for CRCs

Many approaches have been made to reduce the incident of catheter related complications including:

- Regular flushing with heparin and saline (Kutter, 2004).
- Administration of warfarin or low molecular weight heparin (LMWH).
- Use of antimicrobial coated catheters such as antiseptic coated catheters including: chlorhexidine/ silver sulphadiazine, benzalkonium chloride, platinum/ silver; antibiotic coated catheters including: minocycline/ rifampin or teicoplanin; bonding with cefazoline.
- Impregnation with extremely small silver particles throughout the polymer matrix has also been tried (Garg et al., 2004).

In spite of these options, prophylactic flushes with heparin or saline are insufficient to avoid blood vessel thrombosis (Kutter, 2004). The advantage of systemic prophylaxis with LMWH or warfarin has not been widely recognized. Low-dose warfarin prophylaxis remains debatable, although many earlier studies support the use of low-dose warfarin, most recent studies do not. There is also a major inconvenience of daily subcutaneous injections of standard heparin or LMWH. Even low prophylactic doses of LMWH may accumulate and lead to bleeding in the asthenic or elderly cancer patient with a reduced glomerular filtration rate. This effect is augmented in patients with reduced renal function due to disease or chemotherapy. Nevertheless, in patients with sufficient nutrition and hepatic function, the risks of this approach seem negligible (Kutter, 2004). There have been debates concerning the utilization of antibiotic-coated catheters and the increased risk for bacterial resistance and the possible ineffectiveness of these agents against antibiotic resistant nosocomial bacteria and fungi. To date, clinical trials have not overcome this problem (Darouiche et al., 1999; Hanna et al., 2003).

1.2.4 Transglutaminases (TGs): Nature's biological glues

The term transglutaminase (TGs) (EC2.3.2.13) was initially described by Clarke et al. in 1957, while observing the transamidating activity in guinea-pig liver. Subsequent studies conducted by Pisano et al. (1968) on the stabilization of fibrin monomers during blood clotting, demonstrated that transamidation is brought about by Ca^{2+} and thiol-dependant enzymes which cross-link proteins through an acyl-transfer reaction between the γ -carboxamide group of peptide-bound glutamine and the ϵ -amino group of peptide-bound lysine, resulting in a ϵ -(γ -glutamyl) lysine isopeptide bond (Griffin et al., 2002) (Figure 1.9).

The ϵ -(γ -glutamyl) lysine cross link is essentially an isopeptide bond, being found in a range of organisms from humans to bacteria and plasmodium (Peterson et al., 1983). The resultant bonds are covalent, stable, and resistant to proteolysis, thus enhancing the resistance of tissues to chemical, enzymatic, and physical degradation (Hiragi, 1999).



Figure 1. 9 Cross-linking reaction of transglutaminases. The enzyme forms covalent bonds between the γ - carboxamide group of a glutamine residue in one polypeptide chain and the ϵ -amino group of peptide-bound lysine in a second polypeptide chain with the subsequent release of ammonia (NH_3) (web image 8).

Eight distinct TGs isoenzymes have been identified at the genomic level in mammals (Grenard et al., 2001) (Table 1.2), however their function in a variety of physiological and pathological processes is still a matter of considerable research and dispute (Wodzinska, et al., 2005). These enzymes are dispersed in plasma, tissues, and extracellular fluids, transglutaminase modified proteins are manifest all through the body in the fibrin network of blood clots, cell membranes, extracellular matrix, features of the epidermis and its appendages (callus, hair, and nail) (Greenberg et al., 1991). They are also involved in many therapeutic applications including the use of FXIII substitutive therapy in a rare genetic defect due to the loss of plasma TGs, repair of surgical wounds, fractures and cartilage lesions, treatment of certain intestinal disease or reduction in tumor growth, in addition to commercial application of TGs in the pathogenesis of infectious diseases and in the development of novel strategies in vaccination for bacterial and viral infections. Nevertheless, deregulation of enzyme activity usually associated with main interruption in cellular homoeostatic mechanisms and has resulted in these enzymes contributing to various human diseases, including inflammatory disease, chronic neurodegenerative diseases (Alzheimer's and Huntington's disease), neoplastic diseases, autoimmune conditions, such as celiac disease, cancer, tissue fibrosis and diseases related to the epidermis of the skin (Griffin et al., 2002).

Table 1.2 Identified active types of TGs in mammals (taken from Griffin et al., 2002). They are distinguished from each other by their physical properties and distribution in the body.

"
"



1.2.5 Plasma factor XIII

Blood coagulation Factor XIII (FXIII), also known as fibrin-stabilizing factor (or fibrinoligase), is one of the best characterized transglutaminases, and its physiological role is well established (Figure 1.10). FXIII is a tetramer composed of two A subunits (FXIII A) and two B subunits (FXIII B) noncovalently associated (Iorand et al., 1986). The Factor XIII A-subunit gene belongs to the transglutaminase family (Ariens, et al., 2002). Dissimilar to many other TGs, it is a zymogen (proenzyme) that is converted into an active transglutaminase (FXIIIa) by the proteolytic action of thrombin and Ca^{2+} in the final phase of the coagulation cascade. Its main task is to crosslink α -, and γ -chains of fibrin and α 2-plasmin inhibitor to fibrin.



Figure 1. 10 Crystal structure of human Factor XIII (web image 9).

By this way FXIIIa strengthens fibrin and protects it from the prompt elimination by the fibrinolytic system (Ichinose et al., 1990). Cross-linking by FXIIIa improves the mechanical strength, rigidity and elasticity of the clot and increases its resistance to plasmin-mediated degradation (Ariens, 2002). Therefore, inhibition of FXIIIa activity

enhances fibrin degradation mediated by plasmin *in vitro* and accelerates thrombolysis in animal models of venous and arterial thrombosis and in experimental pulmonary embolism (Bereczky et al., 2003; 2004).

1.2.6 FXIIIa inhibitors: a new approach to the treatment of catheter-related infection and thrombosis

FXIIIa, the key enzyme of the normal blood clotting process in thrombus stabilisation could also be exploited by *Staphylococci* which then become permanently attached to the blood clot, thus shielding them from immune attack and the antibiotics used to eradicate them. The link between catheter-related thrombus formation and *Staphylococci* infection is the mechanism by which *Staphylococci aureus* colonise surfaces of medical devices by binding to the host proteins (fibrin/ fibrinogen and fibronectin). The interaction is mediated by the production of a number of microbial surface components recognizing adhesive matrix molecules; in *Staphylococci aureus* these include the fibrinogen-binding clumping factors A and B and the fibronectin-binding protein (FnB) (Foster et al., 1998). FnB is a substrate for FXIIIa and undergoes covalent cross linking to fibrinogen and fibronectin (Matsuka et al., 2003; Anderson et al., 2004). *Staphylococci aureus* becomes covalently cross-linked to fibrinogen and fibrin during deposition within the fibrin-platelet matrix of thrombi on the catheter surface; this prevents the release of bacteria into the blood during natural fibrinolysis and retaining the organisms in an environment protected from antibiotics action and host defenses (Griffin et al., 2004).

Incorporation of the FXIIIa inhibitors into catheter or other medical implant devices could be used as a new approach to reduce the incidence of catheter sheath formation, thrombotic occlusion and associated infection in CVCs (Griffin et al., 2004).

Recently, a novel group of transglutaminase inhibitors has been introduced by Griffin et al. (2004; 2008). These small, non-toxic inhibitors could prevent stabilisation of thrombi by FXIIIa and consequently increase the natural rate of thrombolysis. In addition they could reduce *staphylococcal* colonisation of catheters by inhibiting FXIIIa-mediated cross-linking of *staphylococci* to host proteins on the catheter surface (Griffin et al., 2004) (Figure 1.11, Lambert, 2007).

A major aim of this study was the integration of the fluorescent FXIIIa inhibitor into the polymeric coating of polyurethane central venous catheters or silicone central venous catheter, with the intent of producing CVCs with a lower incidence of thrombosis and related *staphylococcal* infections.



Figure 1. 11 Effect of the FXIIIa inhibitors (R281 & R283, excising inhibitors) on release of *Staphylococcus aureus* from human thrombi. The release of *Staphylococcus aureus* from human thrombi is increased in the presence of the FXIIIa inhibitors over time (Lambert, 2007).

As previously stated, TGs inhibitors could also be used for treating of liver fibrosis and its end stage disease cirrhosis.

1.3 Liver fibrosis/ Cirrhosis

1.3.1 General introduction and background

The term cirrhosis, derived from the Greek term *scirrhus*, meaning orange, was first introduced by Laennec in 1819 to describe the way that cirrhotic livers turn from yellowish to tan in colour. In general, cirrhosis is a chronic degeneration of an organ resulting in the replacement of healthy tissues with extensive



Figure 1. 12 A healthy liver in adults (left). A liver damaged by alcoholism shows a build up of fatty tissue (middle), and a liver with cirrhosis is enlarged and swollen (right) (web image 10).

fibrous connective tissue (Iredale, 2003). The term is most commonly used to depict a diseased state of the liver, the organ that is most frequently influenced by cirrhosis (Figure 1.12). Cirrhosis of the liver is the end stage of fibrous scarring and hepatocellular regeneration, distinguished by diffuse disorganization of the normal hepatic structure of regenerative nodules and fibrotic tissue (Ueki et al., 1999). Following chronic liver damage, inflammatory lymphocytes enter the hepatic parenchyma, some hepatocytes undergo apoptosis, and Kupffer cells become activated, and release fibrogenic mediators. Hepatic stellate cells (HSCs) proliferate, experience a substantial phenotypical activation and secrete a considerable amount of extracellular matrix proteins. Sinusoidal endothelial cells relinquish their fenestrations, and the tonic contraction of HSCs results in increased resistance to blood flow in the hepatic sinusoid (Figure 1.13) (Bataller and Brenner, 2005).



Figure 1. 13 Alterations in the hepatic structure in a fibrotic liver caused by accumulation of ECM proteins. Normal liver (A) and advanced hepatic fibrosis (B). Following chronic liver damage, inflammatory lymphocytes enter the hepatic parenchyma. Some hepatocytes undergo apoptosis. Kupffer cells activate, and release fibrogenic mediators. HSCs proliferate, experience a considerable phenotypical activation and secrete a significant amount of extracellular matrix proteins. Sinusoidal endothelial cells relinquish their fenestrations, and the tonic contraction of HSCs results in increased resistance to blood flow in the hepatic sinusoid (taken from Bataller and Brenner, 2005).

Liver cirrhosis is the end stage of liver fibrosis (Li and Wang, 2009). Therefore the prevention and inversion of liver fibrosis is the approach used to cure chronic hepatic diseases and to improve prognosis. Liver fibrosis, the extreme accumulation of extracellular matrix proteins such as collagen, is a result of the wound-healing response of the liver to recurring injury (Figure 1.13) (Friedman, 2003; Bataller and Brenner, 2005; Iredale, 2007).

1.3.2 Etiology of liver cirrhosis

The common causes of liver fibrosis and cirrhosis include hepatitis B, hepatitis C, alcohol, immune-mediated damage, genetic abnormalities, exposure to various drugs and toxic chemicals and non-alcoholic steatohepatitis, which is associated with diabetes and metabolic syndrome (Dufour et al., 1993; Day, 2002; Adrian et al., 2007). It is well known that alcohol consumption is a foremost contributor in deaths from cirrhosis and the related condition of alcoholic hepatitis (Mann et al., 2003).

1.3.3 Epidemiology of liver cirrhosis in European countries

A survey conducted by Leon (2007) between the periods 1987-1991 and 1997-2006, on two age groups (15-44 years old and 45-64 years) of men and women. The study shows that the cirrhosis mortality rate accelerated dramatically in Britain, whilst rates in most of Western Europe were declining, with Scotland having one of the fastest growing chronic liver disease and cirrhosis death rates in the world (Figure 1.14). Nevertheless, since the early 1950s, there has been a considerable increase in liver cirrhosis mortality rates in Scotland, England and Wales for both sexes. Since then there has been a steady increase that continued until the end of 1970, which became more dramatic in the 1980s, and again from 1990 to 1994, and continuing until today. Indeed rates in men increased five-fold in England and Wales, and six fold in Scotland, between the period of 1950-54 and that of 2000-2002, whilst in women there was a corresponding four-fold increase in mortality rates. The same pattern of increase was observed for both of the age groups, although the absolute rates in the older age-group of women were much higher. In contrast, mortality rates for both men and women in both age-groups rose sharply compared with the mean for other European countries from 1955 and peaked in the early 1970s. In Scotland, the mortality rates for both age groups and sexes are approximately twice that of other

European countries, while the mortality rate in England and Wales was equal to if not higher than the European average (Figure 1.14).



Figure 1. 14 Chronic liver disease and cirrhosis mortality rates per 100,000 populations, 1950-2006 (taken from Leon, 2007).

1.3.4 Epidemiology of liver cirrhosis in United States

In a surveillance report which was published by the National Institute on Alcohol Abuse and Alcoholism (NIAAA), trends in liver cirrhosis mortality in the United States were presented from 1970-2005. Accordingly, liver cirrhosis was considered to be one of the 12 major causes of death in the United States. Overall, cirrhosis mortality in the United States grew steadily following the end of Prohibition in 1933 until 1973, when the age-adjusted death rate (a rate that accounts for differences in mortality regardless of any difference in the age distribution between populations) reached a peak at 18.1 deaths per 100,000 of the population. Cirrhosis mortality then

began an almost steady decrease which continued until 2005, the most recent year for which data is available (Yoon et al., 2008).

1.3.5 Current options for treatment of liver fibrosis/ cirrhosis

Contrary to the conventional view that cirrhosis is an irreversible process, recent evidence shows that even advanced fibrosis is reversible (Friedman, 2000 ; Arthur, 2002 ; Bataller & Brenner, 2005). At present, there is no efficient pharmaceutical intervention to treat this fibrotic disease (Pinzani et al., 2005; Li & Wang, 2009). Currently, the cure for cirrhosis is limited to removing the underlying cause of the disease. The development of fibrosis can reduce after removal of the main cause of damage, nevertheless to accomplish complete treat of advanced liver fibrosis, medical intervention is required in most cases. Some of these interventions comprise eradicating viruses using interferon, ribavirin and nucleoside analogues in viral hepatitis and ultimately, liver transplantation which is a highly successful treatment for end stage cirrhosis (Iredale, 2003). Nevertheless, to date no effective treatment other than liver transplantation has been established (Adrian et al., 2007).

1.3.6 Problems of current interventions in treatment of liver fibrosis/ cirrhosis

The main problem with current antifibrotic drugs *in vivo* is that they are neither liver-specific nor fibrosis-specific. Accordingly, many drugs that demonstrate potent antifibrotic activity *in vitro* frequently demonstrate only slight effects *in vivo* due to inadequate concentrations of drugs around the target cell and adverse effects on non-target cells, particularly during chronic administration (Li & Wang, 2009).

Therefore, it can be concluded that targeting therapeutics to the relevant tissue or disease-associated cell has several advantages over non-targeted therapies. A lower concentration of the therapeutic agent is required to be delivered to the site of action to achieve a therapeutic effect. Furthermore, altered pharmacodynamics increases the possibility of specific action directed at the target tissue/cell and decrease the probabilities of adverse effects (Elrick et al., 2005).

1.3.7 Tissue transglutaminase (TG2) inhibitors: a new approach to the treatment of liver cirrhosis.

Tissue transglutaminase (TG2, transglutaminase 2, transglutaminase C, Gah) is the ubiquitous member of TGs and is also one of the most studied (Collighan & Griffin, 2009) (Figure 1.15). Recent evidence supports the view that the enzyme has a general protective and stabilizing role in cells and tissues. However, in a pathological environment, the uncontrolled activation of TG2 can alter its protective function into a pathological one (Fesus and Piacentini,

2002). TG2 is emerging as a well-characterized, multifunctional molecular agent in numerous diseases and processes (Aeschlimann et al., 2000) such as fibrosis and scarring (Johnson et al., 1999). Huntington's disease and Alzheimer's disease (Citron et al., 2001) coeliac disease (Marzari et al., 2001) thrombosis (Ariëns et al., 2002) and cancer (Mangala & Mehta, 2005).

The development of hepatic fibrosis reflects an alteration in the normally balanced processes of extracellular matrix production and degradation (Friedman, 2000). Liver fibrosis is characterised by increased synthesis and decreased degradation of the extracellular matrix (ECM) molecules (Sarem et al., 2006). Covalent cross-linking of collagen enhances its resistance to proteolytic degradation and excessive cross-linking may result in destructive loss of tissue functionality (Grenard et al, 2001).

Tissue transglutaminase catalysed cross-linking is a physiological mechanism for the stabilization of basement membranes and cartilage matrix (Aeschlimann et al., 1995). Transglutaminase-mediated covalent cross-linking has been implicated in the stabilization and accumulation of the ECM in number of fibrotic diseases (Griffin et al., 1979; Johnson et al., 1997, 1999; Mirza et al., 1997; Grenard et al., 2001; Skill et al., 2001) and in kidney fibrosis. In the latter, it has also been shown that in rats induced to undergo either renal scarring or development of diabetic nephropathy,



Figure 1. 15 Overall structure of a human tissue transglutaminase (TG) (web image 11).

treatment with the site directed TG inhibitors leads to up to 80 - 90 % reduction in kidney scarring with preservation of kidney function (Griffin et al., 2008; Huang et al., 2009). Shweke et al. (2008) demonstrated that TG2 knockout mice show a reduction of renal fibrosis induced by urethral obstruction.

Thus, it can be predicted that potent and selective TG2 inhibitors would have broad therapeutic potential in treatment of fibrotic diseases characterised by increased ECM deposition and cross linking (Griffin et al., 2008, Collighan & Griffin, 2009). The anti-fibrosis effect of the tissue transglutaminase non-specific inhibitor, cystamine, on liver fibrosis has been investigated by Qiu et al (2007). Cystamine ameliorates carbon tetrachloride (CCl₄) induced liver fibrosis via inhibition of TG2. The probable mechanism is linked with the reduced synthesis of the ECM caused by the inhibition of hepatic stellate cell activation and decreased expression of tissue inhibitor of metalloproteinases 1 (Qiu et al., 2007).

As TG2 is assumed to participate in many essential biological processes, a number of researchers challenge the above view (Nardacci et al., 2003), stating that TG2 plays a protective role in liver injury by enhancing tissue stability and repair, therefore pharmacological inhibition of TG2 may have undesirable side effects. This hypothesis presumes that a fraction of TG2 is constitutively active *in vivo*, and that this activity is essential under normal physiological condition. One objection to this argument is data supporting the view that a physiological role for the catalytic activity of TG2 is limited. Intracellular and extracellular TG2 is catalytically inactive under normal physiological conditions. Nevertheless, physical or certain types of chemical damage can lead to rapid enzymatic activation (Siegel et al., 2008). The normal development and normal phenotype of TG2 knockout mice along with the lack of toxicity observed in mice dosed chronically with dihydroisoxazole inhibitors indicate that TG2 activity is not essential for survival in a stress free environment (Nanda et al. 2001; De Laurenzi & Melino, 2001; Choi et al., 2005; Yuan, 2006; Strnad, 2006; Siegel et al., 2008). Consequently, it can be argued that on the one hand, the mammalian body requires a reasonably non-specific cross linking enzyme in approximately all the organs to assist rapid tissue growth and healing. On the other hand, considering the extreme stability of an isopeptide linkage, uncontrolled TG2 activity possibly yields to excessive scar tissue formation and the formation of

neoepitopes that could initiate an autoimmune response. Therefore, the catalytic activity of TG2 must be activated rapidly when required, and inactivated almost immediately following the completion of its task. Disruption of this sensitive balance may be the basis for a range of seemingly disparate diseases (Siegel et al., 2008).

Recently, a novel group of specific tissue transglutaminase inhibitors has been described which has the advantage of targeting TG2 in the extracellular environment this limiting cell toxicity (Griffin et al., 2004; 2008). These inhibitors have already shown themselves to be successful candidates in the treatment of kidney fibrosis in animal models (Griffin et al., 2008), where they were delivered directly to the kidney via an osmotic pump. Some of these inhibitors have been shown to be TG2 specific and subsequently have the advantage of exclusive inhibition of the tissue transglutaminase (TG2) enzyme rather than other extracellular transglutaminase enzymes Factor XIIIa. A major aim of this study was to investigate *in vivo* pharmacokinetics and tissue biodistribution of the TG2 inhibitor and develop an efficient drug delivery system for site specific delivery of the novel TG2 inhibitors into the liver with the aim of treating liver fibrosis and its end stage disease cirrhosis.

1.4 Aims and objectives

The aim of this thesis was to establish an efficient method of effective delivery of the TG inhibitors for their applications such as treatment of catheter-related complications and liver fibrosis.

The objective of this work is outlined below;

- Characterisation of fluorescent derivatives as potential probes for the novel TG inhibitors.
- Development of a controlled release polymer coats with incorporated FXIIIa inhibitor for polyurethane (PU) central venous catheters and quantifying the enzyme inhibitor release from the polymeric coating *in vitro*.

- Integration of the FXIIIa inhibitor into silicone elastomers for sustained drug release and measuring the amount of inhibitor release from the elastomers *in vitro*.
- Investigation of pharmacokinetics and biodistribution of the TG2 inhibitor *in vivo*.
- Development of an efficient drug delivery system for site specific delivery of the TG2 inhibitor into the liver.

Chapter 2:
**Characterisation of fluorescent derivatives as potential
probes for novel TG inhibitors**

2.1 Introduction

As detailed in chapter 1, transglutaminases (TG) are an extensively distributed group of enzymes that catalyze a calcium-dependent acryl transfer reaction between the γ -carboxamide group of a polypeptide bound lysine residue to form an ϵ -(γ -glutamyl) lysine isopeptide bond or the formation of (γ -glutamyl) polyamine bonds through catalyzing the incorporation of polyamines into peptide-bound glutamine (Griffin et al., 2002). Nevertheless, deregulation of enzyme activity usually associated with major disruption in cellular homoeostatic mechanisms has caused these enzymes contributing to a number of human diseases, such as chronic neurodegeneration, neoplastic diseases, autoimmune diseases, diseases involving progressive tissue fibrosis and diseases related to the epidermis of the skin (Griffin et al., 2002; Lorand & Graham 2003). Hence, it can be expected that potent and selective TG inhibitors would find wide therapeutic potential (Griffin et al., 2008).

Irreversible TG2 inhibitors (suicide inhibitors) prevent enzyme activity by covalently modifying the enzyme thereby preventing substrate binding. The majority of irreversible TG2 inhibitors are intended to target the active site cysteine of the TG enzyme, using chemical functional groups that are reactive in the presence of a nucleophilic atom. However, they form relatively stable chemical bonds following reacting (Siegel & Khosla, 2007). Several irreversible inhibitors of tissue transglutaminase (TG) have been published (Freund et al. 1994; Choi, et al., 2005; Pardin et al., 2006; Yuan et al., 2006; Siegel & Khosla, 2007).

Recently, a novel group of transglutaminase inhibitors has been introduced by Griffin et al. (2004; 2008). These inhibitors are specific and subsequently have the advantage of exclusive inhibition of FXIIIa and tissue transglutaminase rather than other transglutaminases enzymes. Different types of TG synthesized inhibitors are detailed below;

2.1.1 Irreversible non-fluorescent TG inhibitor (R281)

R281 (Figure 2.1) was one of the first site-directed TG inhibitors synthesized by Griffin, Saint and Coutts (2004). Despite its ability to act as an enzyme inhibitor, it is difficult to monitor if studies are undertaken on the compound as a potential drug. For

example it would be difficult to easily track and follow it inside the body or to detect it in buffer, blood plasma or body tissues, therefore marker options were investigated.

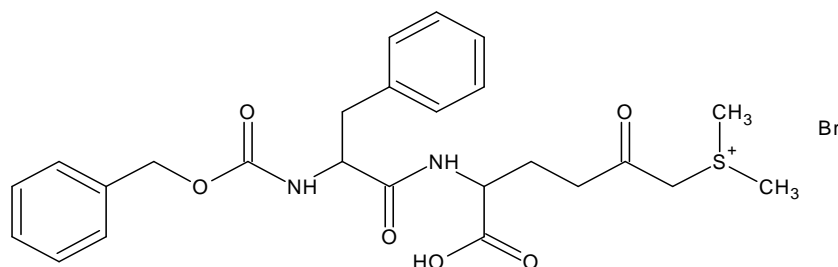


Figure 2.1 The schematic structure of irreversible non-fluorescent transglutaminase inhibitor (**R281**), with a dimethyl ulfonium group at one end and a carbobenzyloxy group (CBZ) at the N-terminus of the peptide-based inhibitor.

2.1.2 Irreversible fluorescent TG inhibitor

The novel fluorescent inhibitors of TG are essentially R281 with a fluorescent group attached and prepared within the chemistry department at Aston University by Dr. Alexandre Mongeot and Dr. Dan Rathbone. Synthesis was based on an existing irreversible non-fluorescent TG inhibitor (R281). To achieve this, a fluorescence group (pyrene or dansyl ring) was added to replace the CBZ group (carbobenzyloxy) at the N-terminus of the peptide-based inhibitor, whilst the dimethylsulfonium or tetramethylimidazolium group was a thiol reactive warhead. The TG inhibitors investigated in this study were R281 with a dimethylsulphonium warhead and a phenylalanine amino acid and its derivatives with a fluorescent pyrene group, a dimethylsulphonium warhead and a phenylalanine amino acid (AM1/99) or with a fluorescent dansyl group, a dimethylsulphonium warhead and a phenylalanine amino acid (AM1/107) or with a fluorescent dansyl group, a tetramethylimidazolium warhead and a phenylalanine amino acid (AM2/97) or with a fluorescent dansyl group, a dimethylsulphonium warhead and a proline amino acid (AM2/169) (Table 2.1). The recently described group of TG inhibitors offer potential advantages over existing inhibitors (monodansylcadaverine (MDC) and cystamine) due to their irreversible nature, improved tolerability (so far tested only in rats and mice), specificity and short half-life as will be discussed.

Drug product characterization is essential during the development of new drug substances. Appropriate characterisation enables discriminating formulations during

preliminary screening, monitoring drug consistency during processing, and essentially testing and releasing of the commercial product. Characterisation is also important for comparison of the drug product with other products. Therefore, in order to employ the fluorescent derivatives of the TG inhibitor as potential probes for novel TG inhibitors, physicochemical characteristics of the novel group of transglutaminase enzyme inhibitors were determined.

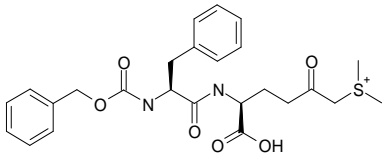
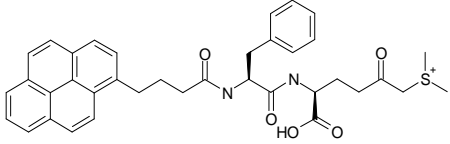
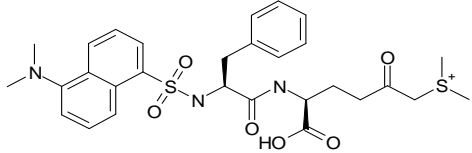
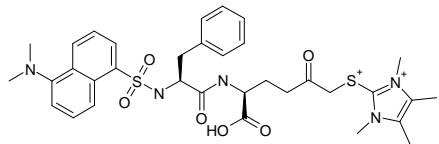
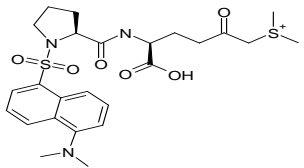
2.2 Aim and objectives

The aim of this study was physicochemical characterisation of the fluorescent derivatives of the TG inhibitor (R281) as potential probes for novel TG inhibitors.

The objectives of this work were;

- Determination of excitation/emission spectra of the fluorescent TG inhibitors.
- Quantification of the TG inhibitors, using either fluorescence spectrophotometry or high performance liquid chromatography.
- Verification of the relative efficacy of the TG inhibitors *in vitro*, using an enzyme linked sorbent assay.
- Cytotoxicity studies of the TG inhibitors, by measurement of mitochondrial dehydrogenase activity (XTT assay) and direct cell counting (Trypan blue test).

Table 2.1 The name, chemical structure, molecular weight and components of the fluorescent and non- fluorescent TG inhibitors investigated.

| Compound | Structure | Molecular weight (Dalton) | Amino acid | Protecting group | Warhead |
|----------------|---|---------------------------|---------------|------------------|------------------------|
| R281 |  | 567.5 | Phenylalanine | CBZ | Dimethylsulphonium |
| AM1/99 |  | 703.68 | Phenylalanine | Pyrene | Dimethylsulphonium |
| AM1/107 |  | 666.65 | Phenylalanine | Dansyl | Dimethylsulphonium |
| AM2/97 |  | 760.79 | Phenylalanine | Dansyl | tetramethylimidazolium |
| AM2/169 |  | 616.58 | Proline | Dansyl | Dimethylsulphonium |

2.3 Material

TG inhibitors were prepared within the chemistry department at Aston University by Dr. Alexandre Mongeot and Dr. Dan Rathbone as previously described (Griffin et al., 2008). Human tissue transglutaminase (hTG2) recombinant in E.coli and N-(Biotinyl)cadaverine hydrochloride were obtained from Zedira, Germany. Human coagulation factor XIII was from CSL Behring, UK. Phosphate buffered saline (PBS), ethylenediaminetetraacetic acid (EDTA), o-phenyldiamine (OPD), TRIS-HCL, ExtrAvidin-peroxidase, hydrogen peroxide and Dimethyl sulfoxide (DMSO) were purchased from Sigma-Aldrich, UK. Fetal bovine serum was obtained from Biosera, UK. Bovine serum albumin (BSA) and Dimethyl casein were procured from Calbiochem, UK. HPLC grade water, HPLC grade acetonitrile (ACN) were from Fisher Scientific, UK. Tween 20 and calcium chloride (CaCl_2) were acquired from Melford Laboratories Ltd, UK. Unless stated otherwise PBS was used at 0.01M, pH 7.4. Doubly distilled and filtered water was used in the preparation of all solutions.

Albino Swiss mouse embryo fibroblast (3T3 line) was obtained from American Type Culture Collection (ATCC, USA) and were routinely maintained in a Dulbecco's Modified Eagle's Medium (DMEM, Sigma-Aldrich, UK) supplemented with 10 % (v/v) heat inactivated fetal bovine serum (FBS, Sigma-Aldrich, UK), 2 mM glutamine (Sigma-Aldrich, UK), 1 % (v/v) nonessential amino acids (Sigma-Aldrich, UK) and 100 U/ml of penicillin and 100 $\mu\text{g}/\text{ml}$ of streptomycin and consistently cultured in a humidified atmosphere at 37 °C in a 5 % (v/v) CO_2 and 95 % (v/v) air.

2.4 Methods

2.4.1 Determination of excitation/emission spectra

Excitation and emission wavelengths for the TG inhibitors were determined using spectral scanning by a spectrofluorometer (Spectra Max Gemini XS, Molecular Devices). Initially, a stock solution of 0.1 M of the inhibitor was prepared, using DMSO (dimethyl sulphoxide) as a solvent. Subsequently, different concentrations (0, 1, 10, 100 μM) of the inhibitor solutions were prepared, using PBS (pH 7.5) as a diluent. Emission spectra were obtained through stepwise variation of the excitation wavelength from 250 to 350 nm with 10 nm intervals for each excitation wavelength. The emission wavelengths were always set at a minimum of 20 nm above the

excitation wavelength. The step increment was set to 2 nm. The emission wavelength was fixed subsequent to emission peak observation. The solutions were then excited at a point between 250 nm and 20 nm beneath the emission peak and the maximum excitation was measured. All measurements were carried out at 25 °C.

2.4.2 Analytical method for quantification of the TG inhibitors

The sensitivity of quantification of fluorescent TG inhibitors by fluorescence, via direct measurement or separation by reversed-phase chromatography with fluorescent detection, was applied to measure and model controlled release of the inhibitors from delivery systems.

2.4.2.1 Fluorescence spectrophotometry

To quantify the concentration of the TG inhibitors in buffer and to assess the amount of released drug from carrier systems, solutions were analyzed via fluorescence, using direct measurement and a drug calibration curve was obtained. First, from a stock solution of the inhibitors in DMSO (0.1 μM), a series of the inhibitor solutions in PBS were prepared. Subsequently, by setting the excitation and the emission spectrum at the corresponding wavelengths, the drug emission intensity within 200 μl aliquot of each solution was measured fluorometrically, on a 96 well microtiter plate. The calibration curve was then obtained by plotting the drug concentration (μM) along the x-axis and relative fluorescence unit (RFU) along the y-axis. Fluorescence is affected by temperature; consequently it was kept constant at 25 °C during each reading of the plate. In order to validate accuracy, precision (repeatability and reproducibility) and specificity of the analytical procedure, a minimum of 5 concentrations of each inhibitor in 3 replicate samples (15 determinations) were prepared and measured for 5 continuous days.

2.4.2.2 High performance liquid chromatography (HPLC)

Estimation of the drug in blood and tissues was performed by fluorimetric estimation using high performance liquid chromatography (HPLC). Reverse phase HPLC analysis of the inhibitor was performed on an AKTA Purifier (Amersham Biosciences) HPLC system, with a fluorescence detector (Cecil Instruments Limited, CE 4500 fluorescence detector) on a Bio-Rad Hi-Pore C4 HPLC column (250 X 4.6

mm) (Richmond, CA, U.S.A). A linear gradient elution of two solvent systems, solvent A and B, was optimised. Solvent A was composed of 1 % (trifluoroacetic acid) TFA in water; while solvent B was acetonitrile (ACN). The modified gradient procedure had a flow rate of 1 ml/min, a 20 μ L sample loop and the following gradient: 100 % A held for 6 minutes, 5 minutes linear gradient to 37.5 % B, 15 minute linear gradient to 45 % B, 5 minutes hold at 100 % B for a final time of 31 minutes (Table 2.2). Elution was monitored with an excitation and an emission wavelength of 330 and 570 nm, respectively. Under these analytical conditions the retention time for the inhibitor was about 7.30 minutes. Concentrations of the TG inhibitors in the samples were determined by reference to a calibration curve prepared from dilutions of a stock solution of the inhibitor.

Table 2.2 Parameters for the elution of the TG inhibitor from the RP-304 C4 column. Solvent A is 1 % TFA in water and solvent B is ACN. Elution was monitored at a constant flow rate of 1 ml/min and excitation/emission 330/570 nm.

| Time (min.) | % solvent A | % solvent B |
|-------------|-------------|-------------|
| 0 | 100 | 0 |
| 6 | 100 | 0 |
| 7 | 62.5 | 37.5 |
| 11 | 62.5 | 37.5 |
| 21 | 55 | 45 |
| 26 | 55 | 45 |
| 31 | 0 | 100 |

Afterwards, from a stock solution of the inhibitor in DMSO (0.1 μ M), a different series of solutions in PBS between 0 and 200 μ M were prepared (0, 25, 50, 100, 150 and 200 μ M). Subsequently, each sample was individually loaded into HPLC. The calibration curve was obtained by plotting the concentration of the inhibitor along the x-axis and the peak area along the y-axis.

2.4.3 Inhibition of TG activity: ELSA (enzyme linked sorbent assay)

The efficacy of the TG inhibitors as inhibitors of the enzyme TG was verified by studying the dose-dependency of their effect on the activity of human tissue transglutaminase (TG2) and human coagulation factor XIIIa (FXIIIa), using an enzyme-linked sorbent assay (ELSA) based on biotinylated cadaverine (BTC) incorporation into N, N'-dimethyl casein (DMC) as described previously (Slaughter et al., 1992). ELSA was performed as follows:

Initially, 96-well microtiter plates were coated with 100 μ l of 10 mg/ml DMC as a substrate for the enzyme in 10 mM Tris pH 7.4 overnight at 4 °C. The following day, the plates were washed twice with Tris-buffered saline Tween (TBS-Tween) pH 7.4 and once with Tris-buffered saline (TBS) pH 7.4. Then, a reaction mix was prepared that contained 5 mM calcium chloride (CaCl_2), as a cofactor for activating the enzyme, 5 mM dichloro-diphenyl-trichloroethane (DTT) as a reducing agent and 0.132 mM BTC as a substrate for the enzyme in 50 mM Tris pH 7.4. The TG inhibitors were initially prepared as 100 mM stock solution in DMSO and diluted to the appropriate final concentration in the same reaction solution. The mix was prepared so that the appropriate final concentrations would be achieved upon addition of 10 μ l of 200 μ g/ml TG to 990 μ l of mix to start the reaction. Following addition of TG, 100 μ l of the solution was pipetted into 8 replicate wells per sample, and the reaction was allowed to proceed for 1 hour at 37 °C. The reaction was terminated by removal of the solution and the addition of 100 μ l of 10 mM ethylenediaminetetraacetic (EDTA) in PBS pH 7.4 to stop the activity of the enzyme. Plates were then again washed twice with TBS-Tween pH 7.4, once with TBS pH 7.4 and blocked by incubation with 100 μ l per well of 3 % (w/v) bovine serum albumin (BSA) in PBS pH 7.4 for 1 hour at room temperature to occupy any remaining unbound sites. Incorporated BTC was detected by incubation with 100 μ l per well of extravidine peroxidase (EXAP) solution diluted 1 in 5000 in blocking buffer for 1 hour at 37 °C. Subsequently, the plates were washed as before and were pre incubated for 5 minutes in 0.05 M phosphate citrate buffer pH 5 containing 0.014 % (v/v) H_2O_2 . Later, the solution was removed and replaced with 100 μ l per well of distilled water containing o-phenyldiamine (OPD). The development reaction was terminated by the addition of 50 μ l of 1 N H_2SO_4 . Afterwards, the absorbance of the resulting colour which is directly proportional to TG activity was measured on a microtiter plate reader at 490 nm (Griffin et al., 2008).

2.4.4 Half maximal inhibitory concentration (IC_{50})

To measure and compare the potency of the TG inhibitors on the enzyme TG, the half maximal inhibitory concentration (IC_{50}) of the inhibitors was measured. The IC_{50} was expressed as the inhibitor concentration at which 50 % inhibition of TG activity *in vitro* was observed (Griffin et al., 2008).

2.4.5 Cell culture studies

Prior to any *in vivo* studies, preliminary *in vitro* investigations are required in order to determine the relative cytotoxicity and the rapid screening process of various formulations and compounds. To achieve this, external factors such as cell type, medium used and experimental protocol were kept constant throughout the study. Therefore, variation in cell viability and proliferation between formulations could be directly related to internal factors, such as substitution of the protecting group or warhead.

2.4.5.1 Thawing cells from storage

Vials of frozen cells were removed from liquid nitrogen and the cell suspension thawed quickly in a water bath at 37 °C. The cell suspension was carefully transferred to 15 ml tubes and 7 ml of serum supplemented growth medium was added drop-wise, mixing well after each addition. After that the cell suspension was centrifuged at 300 x g for 5 minutes to discard the freezing agent DMSO. After centrifugation the supernatant was carefully removed and the pellet was resuspended in 5 ml complete medium. The diluted cell suspension was then transferred into a tissue culture flask and the cells were incubated for 24 hours before changing the medium. Cells were passaged once before use in an experiment.

2.4.5.2 Passage of cells

Cells were passaged at approximately 95 % confluency. The monolayer of adherent cells was first rinsed with PBS (pH 7.4), followed by the addition of 0.25 % (w/v) trypsin/5 mM EDTA solution in PBS. The trypsinised cells were incubated at 37 °C for 2 minutes. After detaching all the cells, the trypsin was diluted and inactivated by adding Dulbecco's Modified Eagle's Medium (DMEM). After that, the cell suspension was collected and added to a centrifuge tube and subsequently centrifuged at 300 x g for 5 minutes prior to reseeding. After centrifugation, under sterile conditions, the supernatant was carefully removed and the pellet was resuspended in a complete medium, then aliquots of cell suspension were seeded to an appropriate cell culture flask containing DMEM or on a 96-well plate and incubated at 37 °C in a 5 % (v/v) CO₂ humidified atmosphere until cells reached confluence. In order to minimize the variation between formulations and obtain reproducible results, the adherent cells were evenly distributed between wells. If necessary, counting of cells was performed

using a haemocytometer and the required amount of cells seeded/used for the experiment.

2.4.5.3 Incubation of cells with the TG inhibitors

Adherent fibroblast cells were brought into suspension as previously described. Subsequently, the cells were seeded at a concentration of 5000 cells/well on a 96-well plate, flat bottom for XTT cell viability assay and incubated in a 5 % CO₂ incubator at 37 °C for 24 hours. All TG inhibitors were initially solubilized in DMSO. Then, a series of TG inhibitor solutions (0, 100, 200, 300, 400, 500 µM) were prepared in DMEM. Subsequently, the cell medium was removed and the adherent cells were treated with different concentrations of the TG inhibitors. Negative control was cells without treatment (cells and medium only). Positive control was inoculated cells with staurosporine (1 µM). Vehicle control was 0.5 % (v/v) DMSO. The treated cells were then incubated for 48 hours at 37 °C in a 5 % (v/v) CO₂ humidified atmosphere. Later on, the cells were examined under an inverted microscope prior to any cytotoxicity assay. The final volume of tissue culture medium in each well was 0.1 ml. All treatments were carried out in three replicates.

2.4.5.4 *In vitro* toxicological studies cytotoxicity studies

Cell proliferation was evaluated by two methods, measurement of mitochondrial dehydrogenase activity (XTT assay) and direct cell counting (Trypan blue test). XTT assay (Cell proliferation assay kit II, Roche) using sodium 3'-[1-(phenylaminocarbonyl)-3,4-tetrazolium]-bis (4-methoxy-6-nitro) benzene sulfonic acid hydrate (XTT) was performed according to the manufacturer's instructions. The XTT assay is based on the cleavage of the yellow tetrazolium salt XTT to form an orange formazan dye by metabolically active cells. Therefore, this conversion only occurs in viable cells. An increase in the number of living cells results in an increase in the overall activity of mitochondrial dehydrogenases in the sample, which directly correlates to the amount of orange formazan formed as monitored by the absorbance. To determine the number of dead cells, a Trypan Blue test was carried out. Trypan Blue is a vital dye. The reactivity of trypan blue is based on the fact that the chromophore is negatively charged and does not interact with the cell unless the membrane is damaged. Therefore, all the cells which exclude the dye are viable.

2.4.5.4.1 Cell proliferation assay with XTT reagent

To each well of 96-well plate containing treated fibroblast cells, 15 µl of XTT labeling mixture (XTT labeling reagent and electron coupling reagent) was added. The plate was shaken gently to evenly distribute the dye in the wells and then incubated at 37 °C, in a 5 % humid CO₂ atmosphere. After the incubation period, orange formazan solution was formed which can be spectrophotometrically quantified. In order to determine the optimal incubation period, the absorption was measured at different time points (1, 2, 3 and 4 hours) on a microplate reader at 490 nm and 750 nm (as the reference absorbance for non-specific readings).

2.4.5.4.2 Trypan blue cell viability test

Initially fibroblast cells were seeded on a 12-well tissue culture plate at a density of 100,000 cells/ well and incubated at 37 °C for 24 hours. After removing the medium, the cells were treated with 500 µM concentration of different types of the TG inhibitors. Positive control (1 µM staurosporine), negative control (cells and medium) and vehicle control (0.5 % DMSO) were also included. The plate was then incubated in a humid CO₂ atmosphere. After 48 hour incubation, adherent fibroblast cells were brought into suspension as previously described and centrifuged for 5 minutes at 2000 x g. The supernatant was discarded. Thereafter, 0.4 % Trypan Blue stain was added and gently mixed with the cell suspension (1:1 v/v). After standing for 3-5 minutes at room temperature, cell viability and cell counts were determined using a haemocytometer. To each side of the cover slip of the haemocytometer, 10 µl of the Trypan Blue cell suspension was added and viewed microscopically. The bright cells (viable cells) with intact cell membrane and stained blue cells (non viable cells) were counted. The average number of stained cells and unstained cells in each quadrant was calculated according to;

$$\text{Cells/ml} = \frac{\text{Counted number of cells} \times \text{Dilution factor}}{\text{mm}^2 \text{ of counted area} \times \text{Chamber Depth}}$$

and using a haemocytometer, with 0.1 mm chamber depth. The percentage of dead cells is the number of dead cells divided by the number of dead and viable cells (total cells), multiplied by 100 (Freshney, 1987).

2.5 Statistical analysis

For all experiments, means and standard deviations were calculated and represent one of at least three separate experiments undertaken in triplicate, unless stated otherwise. To determine statistical significance in resultant data, a one-way analysis of variance (ANOVA) was performed. Differences described as significant or extremely significant in the text correspond to $p < 0.05$ or $p < 0.001$ respectively. Tukey's post hoc test was conducted to determine which conditions differ significantly from each other.

2.6 Results and discussions

2.6.1 Determination of excitation/ emission spectra

Using spectrofluorometry, the excitation and emission spectra of the TG inhibitors with a fluorescent pyrene group (AM1/99) were determined to be 340 and 456 nm respectively. While the TG inhibitors with a fluorescent dansyl group (AM1/107, AM2/97 and AM2/169) were determined to be 330 nm and 570 nm respectively.

2.6.2 Construction of the calibration curve using spectrofluorometry

To quantify concentrations of the TG inhibitors in buffer, initially solutions were analyzed via fluorescence, using direct measurement.

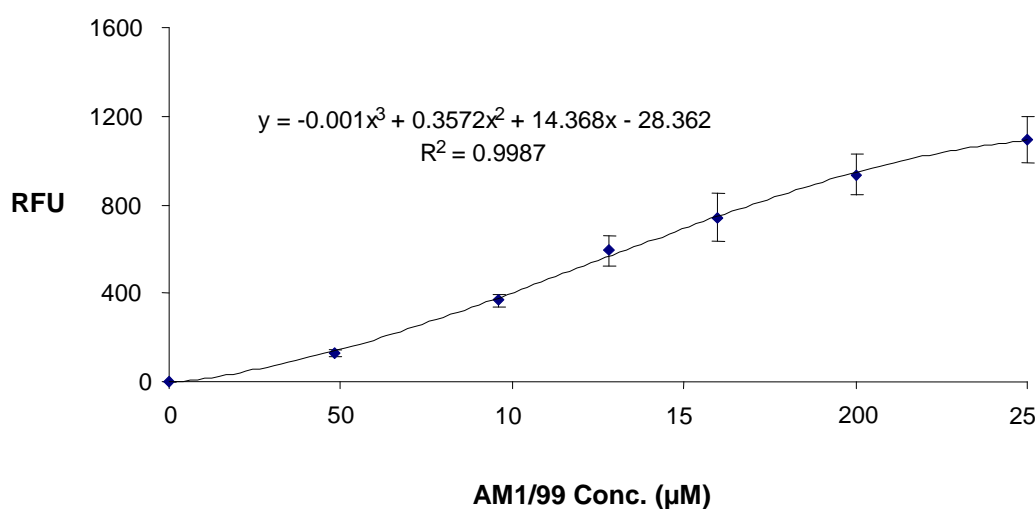


Figure 2. 2 Graphic representation of the calibration record of AM1/99. A series of the inhibitor in PBS (0 - 250 μM) from a stock solution of the inhibitors in DMSO (0.1 μM) were prepared. The drug emission intensity was measured fluorometrically with excitation at 340 nm and emission at 456 nm by a spectrofluorometer. Results denote mean \pm SD from 3 independently synthesized batches.

The results in Figure 2.2 indicate a non-linear, sigmoidal relationship between the inhibitor concentration and relative fluorescence unit, which may be due to the formation of fluorescence group-mediated dimers at higher concentrations of the inhibitor. To investigate this further, samples were measured at fixed excitation or fixed emission wavelengths (Figures 2.3 and 2.4).

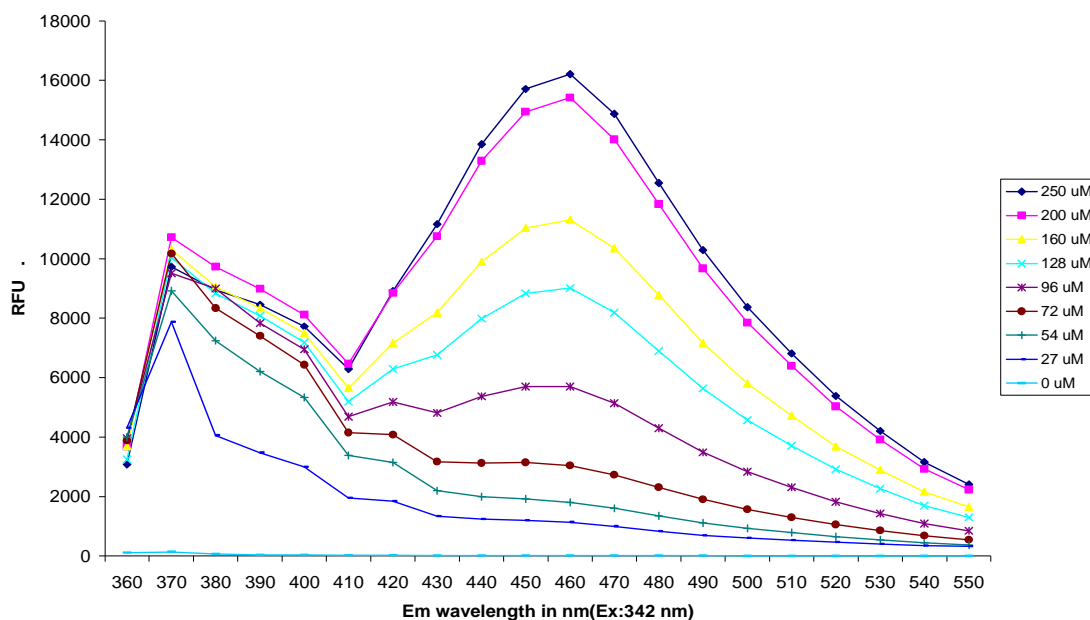


Figure 2.3 Scanning the emission wavelengths of different concentrations of AM1/99 (0-200 μM) in a fixed excitation wavelength (340 nm) using spectrofluorometry.

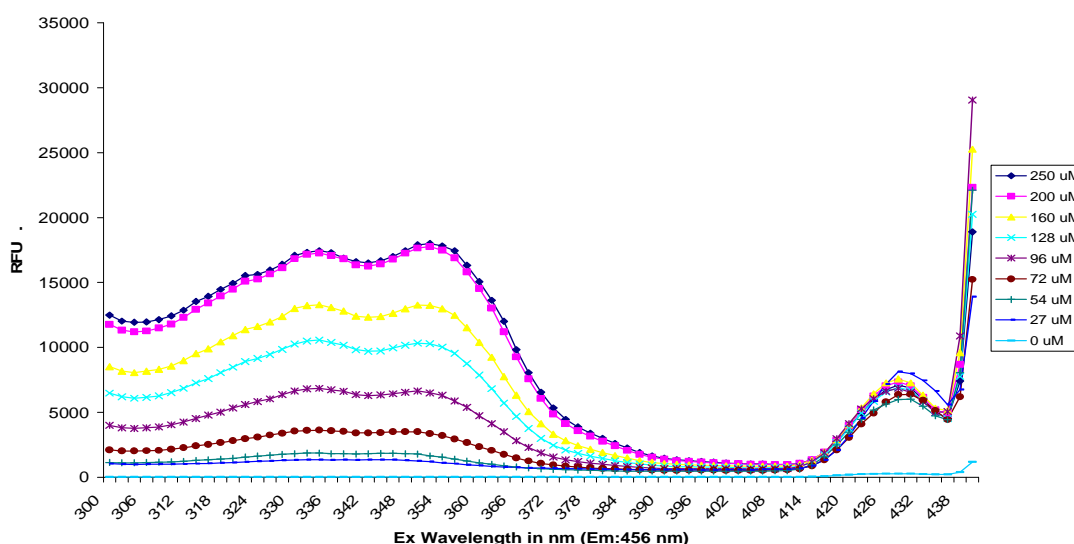


Figure 2.4 Scanning the excitation wavelengths of different concentrations (0-200 μM) of AM1/99 in a fixed emission wavelength (456 nm) using spectrofluorometry.

Figures 2.3 and 2.4 suggest that the fluorescence spectrum of the compound is composed of two bands, a structured band with peaks at 370 nm from uncomplexed excited pyrene (monomer) and an unsaturated band centered at 460 nm from an excited state pyrene dimer (eximer). Consequently, the results prove that the formation of dimers occurs at higher concentrations of the inhibitor, as pyrene rings are known to dimerise in solution at certain concentrations causing a change in the fluorescence emission wavelength (Föster et al., 1955).

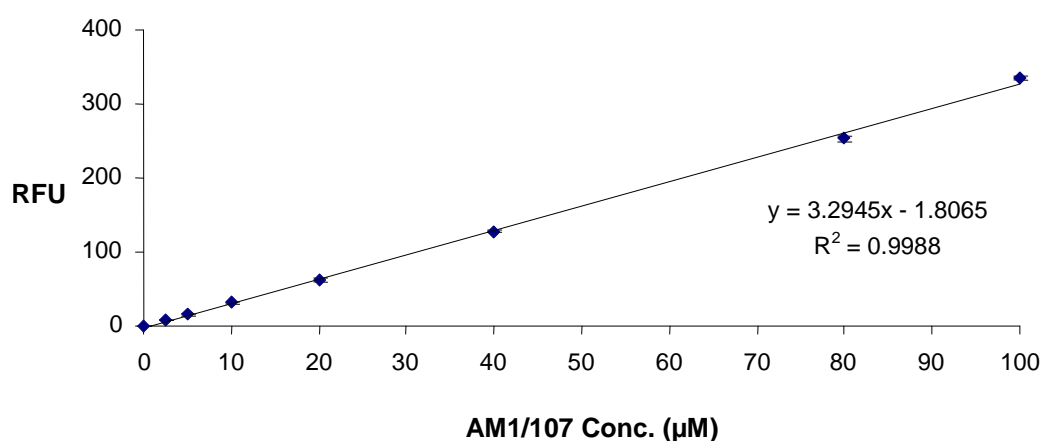


Figure 2. 5 Graphic representation of the calibration record of AM1/107. A series of the inhibitor solution in PBS (0-100 μM) from a stock solution of the inhibitors in DMSO (0.1 μM) were prepared. The drug emission intensity was measured fluorometrically with an excitation at 330 nm and emission at 570 nm by a spectrofluorometer. Results denote mean \pm SD from 3 independently synthesized batches.

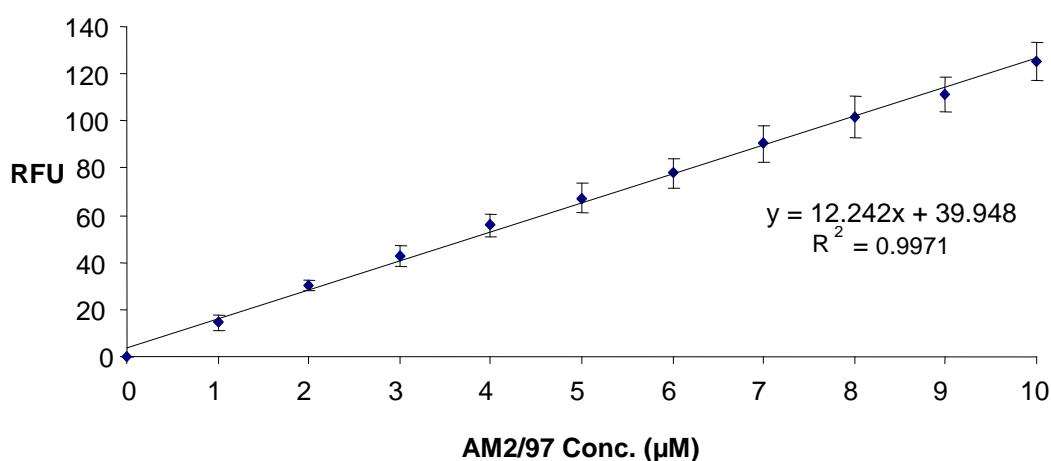


Figure 2. 6 Graphic representation of the calibration record of AM2/97. A series of the inhibitor solution in PBS (0-100 μM) from a stock solution of the inhibitors in DMSO (0.1 μM) were prepared. The drug emission intensity was measured fluorometrically with an excitation at 330 nm and emission at 570 nm by a spectrofluorometer. Results denote mean \pm SD from 3 independently synthesized batches.

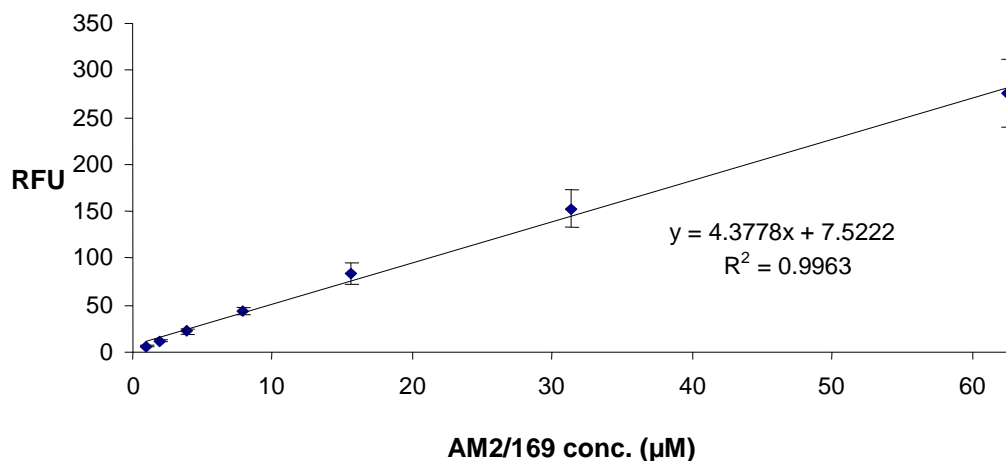


Figure 2. 7 Graphic representation of the calibration record of AM2/169. A series of the inhibitor solution in PBS (0- 60 μM) from a stock solution of the inhibitors in DMSO (0.1 μM) were prepared. The drug emission intensity was measured fluorometrically with an excitation at 330 nm and emission at 570 nm by a spectrofluorometer. Results denote mean \pm SD from 3 independently synthesized batches.

Figures 2.5, 2.6 and 2.7 demonstrate calibration of AM1/107, AM2/97 and AM1/169 concentration versus relative fluorescent unit (RFU). The linearity of a method is a measure of the range within which the observed detector response (y) are directly proportional to the analyte concentration (x) in samples within a given range (expressed as a linear regression equation: $y = a + bx$) (Cao et al., 2005). A straight line correlation was obtained between the inhibitor concentration and the RFU with a correlation coefficient (measuring the degree of correlation) of 0.99 in all cases. The fitting line of the calibration data for AM1/107, AM2/97 and AM1/169 was $y = 3.2945x - 1.8065$, $y = 12.242x + 39.948$ and $y = 4.3778x + 7.5222$ respectively, which was further applied to measure the amount of drug in buffer.

2.6.3 Construction of the calibration curve using HPLC

To allow for the quantification of the TG inhibitor (AM1/169) in blood serum and tissues, HPLC analysis was also undertaken and the drug concentration plotted against AUC (Figure 2.8).

Figure 2.8 indicates a linear relationship between the inhibitor concentration and the area under the curve (AUC) of the chromatogram peak with a correlation of 0.9984. The fitting line of the calibration data ($y = 4.4177x + 7.906$) was then further applied to measure the amount of drug in plasma and tissue

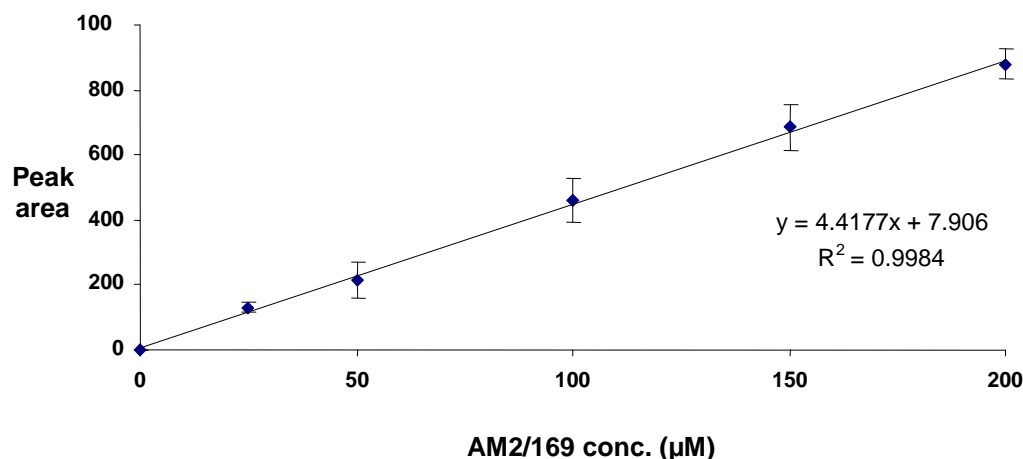


Figure 2. 8 Graphic representation of the calibration record of AM2/169. Reverse phase HPLC was used with a fluorescence detector on a RP-304 C4 column and a linear gradient of two solvents (0.1 % TFA in water and ACN) at a flow rate of 1 ml/minute. The elutes were monitored at an excitation and emission wavelengths of 330 and 570 nm respectively. Results denote mean \pm SD from 3 independently synthesized batches.

2.6.4 Inhibition of TG activity

To investigate the effectiveness of the TG inhibitors on the TG enzymes (FXIIIa and TG2), the activity of the enzyme inhibitor was determined by studying the dose-dependency of its effect on the activity of human FXIIIa and human tissue transglutaminase using ELSA as described previously.

Results in Figures 2.9-2.13 demonstrate the effect of the TG inhibitors on human FXIIIa and human tissue transglutaminase. Upon increasing the concentration of the inhibitor, the measured absorbance and consequently the activity of the enzyme TG decreases. Hence, the inhibitory action can be seen to be concentration dependent. The TG enzyme binds to the inhibitor via the formation of a covalent bond between the inhibitor and the active site cysteine, thus blocking irreversibly the action of this thiol dependent TG enzyme. Irreversible inhibition (inactivation) by covalent modification of the active site cysteine of TG is one of the approaches to enzyme inhibition. Several nonspecific thiol reactive reagents were established to inactivate TG2 and FXIIIa including iodoacetamide, α -halogenmethyl carbonyl compounds designed on a scaffold of amine pseudo-substrates were shown to inactivate FXIIIa in crude plasma fraction from bovine blood. Although their structure activity profile confirmed previously learned lessons about the enzyme active site architecture; however, high

intrinsic activity of these compounds towards thiol and thiol dependant enzymes is at the root of their toxicity and lack of potential therapeutic utility (Wodzinska, 2005).

Therefore, it can be deduced that the tested TG inhibitors can act as an enzyme inhibitor for the TG enzyme (FXIIIa and TG2) in a concentration dependent manner. To compare the potency of the TG inhibitors tested; the half maximal inhibitory concentration (IC_{50}) of the TG inhibitors was measured.

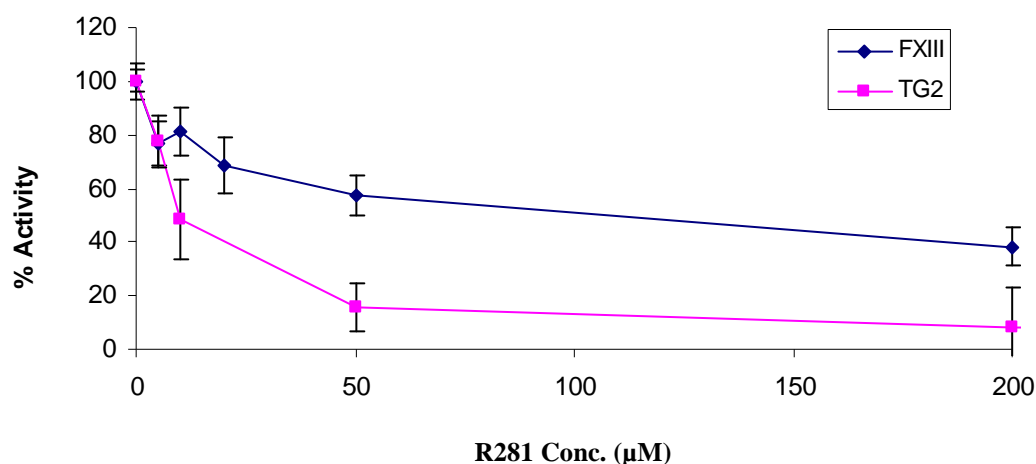
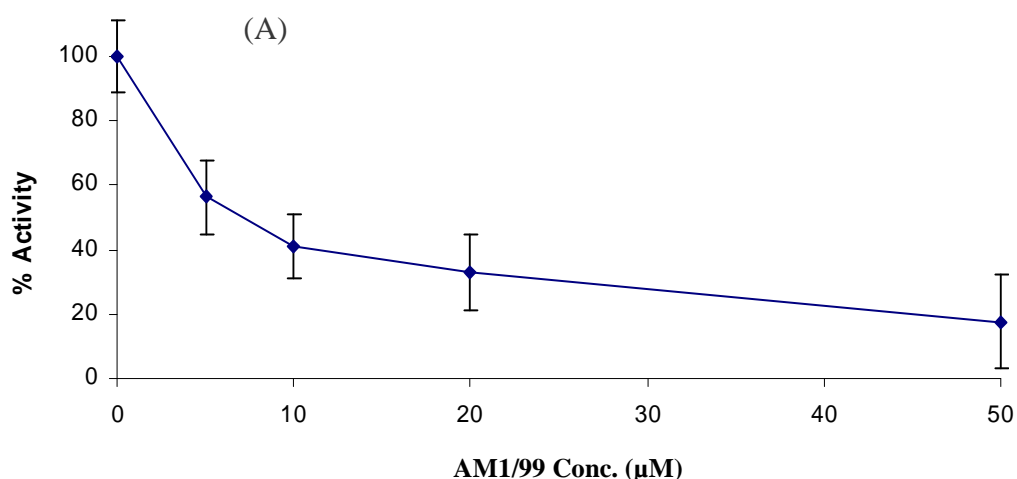


Figure 2. 9 The inhibition of FXIIIa and TG2 by R281. The activity of the enzyme inhibitor was determined by studying the dose-dependency of its effect on the activity of human FXIIIa and human tissue transglutaminase using an enzyme linked sorbent assay (ELSA) based on biotinylated cadaverine (BTC) incorporation into N, N'-dimethyl casein (DMC). The results represent mean \pm SD. n = 8.



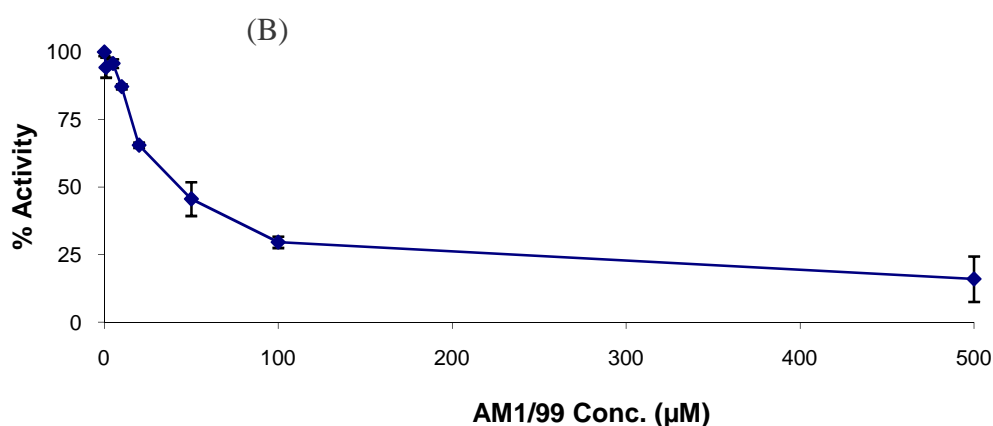


Figure 2.10 The inhibition of FXIIIa and TG2 by AM1/99. The activity of the enzyme inhibitor was determined by studying the dose-dependency of its effect on the activity of human tissue transglutaminase (A) and human FXIIIa (B) using an enzyme linked sorbent assay (ELSA) based on biotinylated cadaverine (BTC) incorporation into N, N'-dimethyl casein (DMC). The results represent mean \pm SD. n = 8.

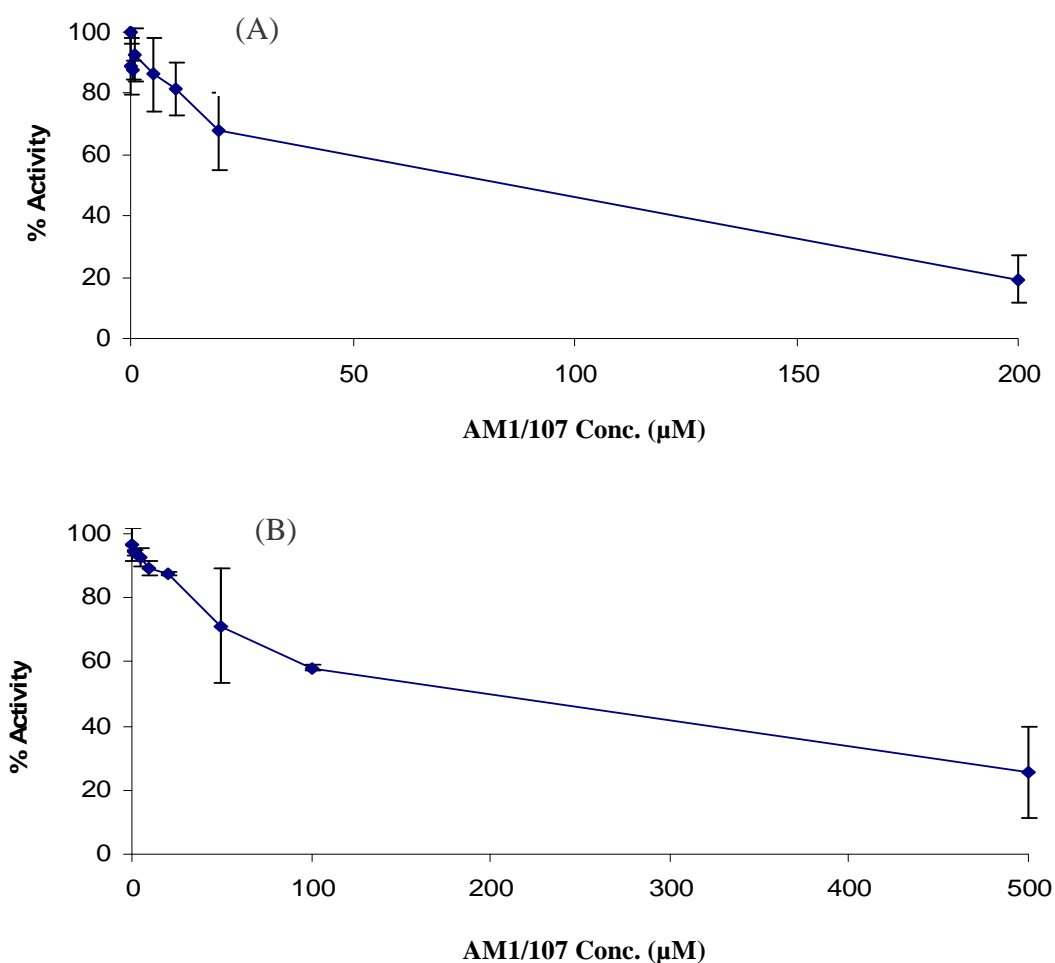


Figure 2.11 The inhibition of FXIIIa and TG2 by AM1/107. The activity of the enzyme inhibitor was determined by studying the dose-dependency of its effect on the activity of human tissue transglutaminase (A) and human FXIIIa (B) using an enzyme linked sorbent assay (ELSA) based on biotinylated cadaverine (BTC) incorporation into N, N'-dimethyl casein (DMC). The results represent mean \pm SD. n = 8.

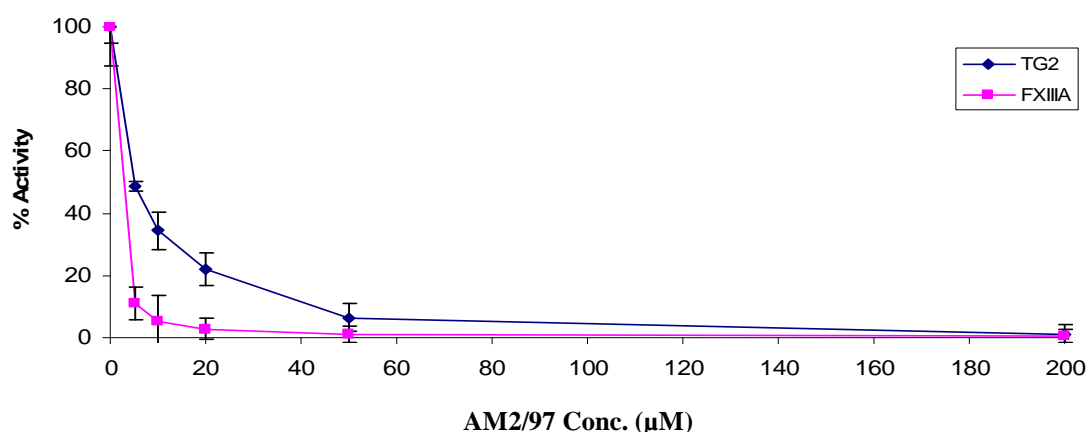


Figure 2.12 The inhibition of FXIIIa and TG2 by AM2/97. The activity of the enzyme inhibitor was determined by studying the dose-dependency of its effect on the activity of human FXIIIa and human tissue transglutaminase using an enzyme linked sorbent assay (ELSA) based on biotinylated cadaverine (BTC) incorporation into N, N'-dimethyl casein (DMC). The results represent mean \pm SD. n = 8.

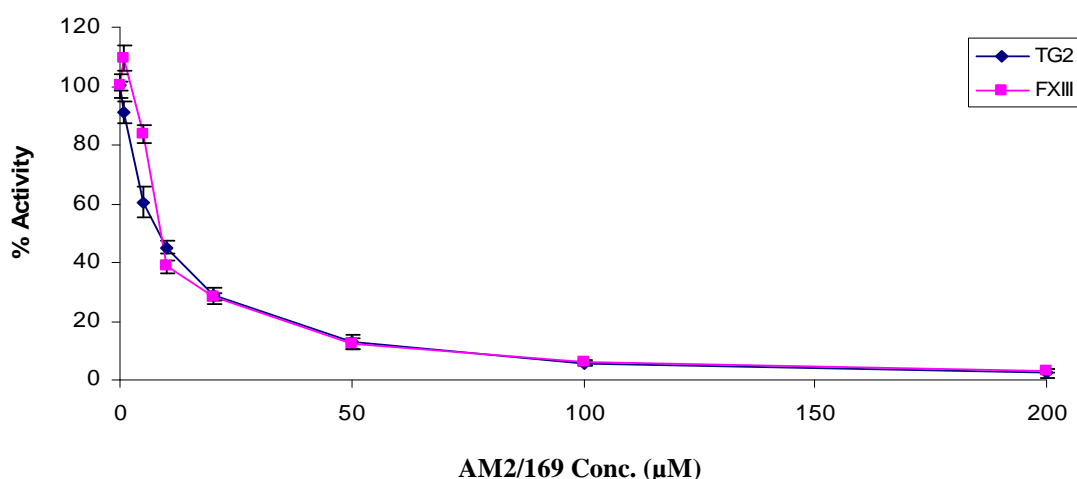


Figure 2.13 The inhibition of FXIIIa and TG2 by AM2/169. The activity of the enzyme inhibitor was determined by studying the dose-dependency of its effect on the activity of human FXIIIa and human tissue transglutaminase using an enzyme linked sorbent assay (ELSA) based on biotinylated cadaverine (BTC) incorporation into N, N'-dimethyl casein (DMC). The results represent mean \pm SD. n = 8.

2.6.5 Determination of the half maximal inhibitory concentration (IC_{50}) of the TG inhibitors

The IC_{50} of the TG inhibitors for the two types of the enzyme TG (TG2 and FXIIIa) was calculated in order to measure and compare the potency of the inhibitors tested on the enzyme TG. IC_{50} is the required concentration of the inhibitor for 50 % inhibition of the TG enzyme.

Table 2.3 IC₅₀ values of the TG inhibitors on the two types of the enzyme TG (TG2 and FXIIIa)

| Compound | TG2 IC ₅₀ (μM) | FXIIIa IC ₅₀ (μM) |
|----------------|---------------------------|------------------------------|
| R281 | 10 ± 2 | 105 ± 20 |
| AM1/99 | 7 ± 3 | 40 ± 10 |
| AM1/107 | 85 ± 20 | 195 ± 25 |
| AM2/97 | 6 ± 3 | 2 ± 3 |
| AM2/169 | 8 ± 2 | 9 ± 3 |

Table 2.3 indicates that R281 and its fluorescent versions (AM1/99, AM1/107, AM2/97 and AM2/169) can act as an enzyme inhibitor for the TG. In general, the lower the IC₅₀, the greater the potency of the inhibitor, and the lower the concentration of the drug that is required to inhibit the enzyme. While, AM1/99, AM2/97 and AM2/169 demonstrate lower IC₅₀ and consequently more inhibition activity for FXIIIa and TG2 compared with R281, AM1/107 shows a higher IC₅₀ and less inhibitory activity for both TG enzymes. This suggests that the addition of the dansyl group to replace the CBZ group (carbobenzyloxy) at the N-terminus of the peptide-based inhibitor reduces the activity of the inhibitor and increases the IC₅₀ from ~ 10 μM to ~ 85 μM for TG2 and from ~ 105 μM to ~ 195 μM for FXIIIa; conversely, the addition of the pyrene group (AM1/99) enhances the activity of the enzyme inhibitor by approximately 2 fold for both the enzymes and decreases the IC₅₀ from ~ 10 μM to ~ 7 μM for TG2 and from ~ 105 μM to ~ 40 μM for FXIIIa. Furthermore, the substitution of the CBZ group with the dansyl group, as well as the substitution of dimethylsulphonium warhead with tetramethylimidazolium warhead (AM2/97) dramatically decrease the IC₅₀ value from ~ 105 μM to ~ 2 μM and therefore augment the activity of the enzyme inhibitor for FXIIIa by approximately 52.5 folds. However, upon the exchange of the CBZ group with the dansyl group and the exchange of dimethylsulphonium warhead with tetramethylimidazolium warhead (AM2/169), there was no a significant difference in the IC₅₀ value for TG2 (from ~ 10 μM to ~ 8 μM). In summary, AM2/97 and AM2/169 demonstrate a greater effectiveness in terms of inhibiting FXIIIa and TG2 respectively amongst all the TG inhibitors tested.

2.6.6 XTT cell proliferation assay

To investigate the cytotoxicity of the novel group of TG inhibitors, the proliferation of fibroblast cells was assessed by XTT-based colorimetric cellular cytotoxicity assay.

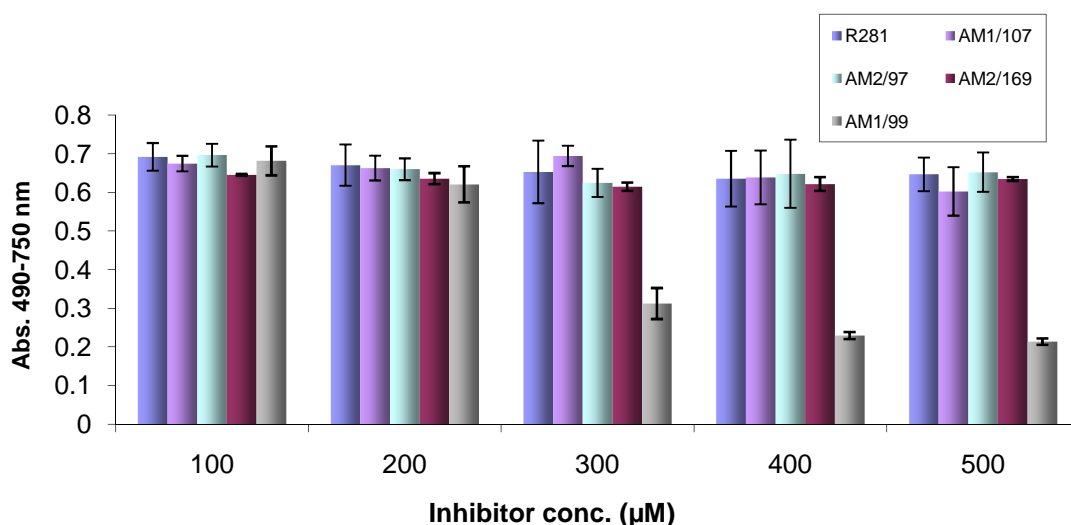


Figure 2.14 Effect of different concentrations of the TG inhibitors on fibroblast cell viability. The cytotoxicity of a wide range (100-500 μM) of the TG inhibitors (R281, AM1/99, AM1/107, AM2/97 and AM2/169) was determined using XTT cell proliferation assay. The viability of the cells remained constant within the range of the concentration tested (100-500 μM) of R281, AM1/107, AM2/97 and AM2/169. Additionally, there was no a considerable variation in terms of cell viability amongst the four types of the TG inhibitors tested. On the contrary, the viability of the cells decreased considerably (~ 50 %) for very high concentrations (300 - 500 μM) of AM1/99. The results from three independent experiments denote mean ± SD absorbance at 490-750 nm, n=3.

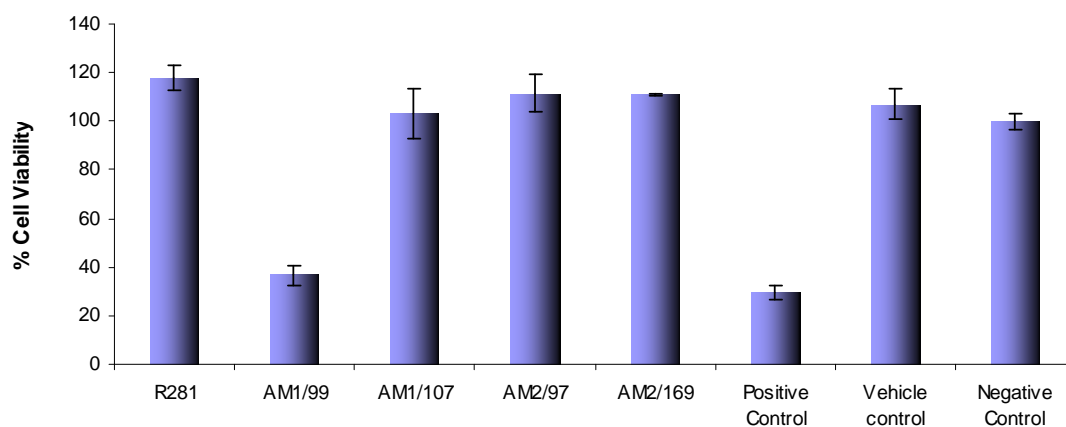


Figure 2.15 Cytotoxicity of various TG inhibitors to fibroblast cells. The *in vitro* toxicity of 500μM of the TG inhibitors (R281, AM1/99, AM1/107, AM2/97 and AM2/169) was assessed by XTT based colorimetric cellular cytotoxicity assay. Results are expressed as a percentage of negative control (without treatment: cells and medium only). Positive control includes cells incubated with 1 μM staurosporine. Vehicle control was 0.5 % (v/v) DMSO. Aside from AM1/99, there was no significant disparity in the percentage of the viability of R281, AM1/107, AM2/97 incubated cells when compared with negative control. The results from three independent experiments denote mean ± SD, n=3.

According to Figures 2.14 and 2.15, the viability of the fibroblast cells remained constant within the range of the concentration tested (100-500 μM) for R281, AM1/107, AM2/97 and AM2/169. Additionally, there was no significant variation (ANOVA, $p > 0.05$) in terms of cell viability amongst the four types of the TG inhibitors tested. Furthermore, there was no a significant disparity (ANOVA, $p > 0.05$) in the percentage of the viability of R281, AM1/107, AM2/97 incubated cells when compared to negative control ($\sim 100\%$). However, the viability of the cells decreased considerably ($\sim 50\%$) for very high concentrations (300 - 500 μM) of AM1/99 (0.35 g/L) (ANOVA, $p < 0.001$). Across all the tested concentration, each inhibitor was shown to have a significant cellular viability when compared to positive control (ANOVA, $p < 0.001$). Using 0.5 % (v/v) DMSO as a vehicle control had no effect on the viability of the cells in the tested concentration range; however the toxicity of higher concentration of DMSO (1 % (v/v)) has been reported to decrease cell viability, increase cellular apoptosis, and up regulate Bax in human lens epithelial cells (Cao et al., 2007).

These results suggest that while replacing the CBZ group at the N-terminus of R281 with the fluorescent dansyl group does not interfere with the proliferation of the cells, replacing the CBZ group with the pyrene group could result a decrease in cell proliferation. Pyrene is a polycyclic aromatic hydrocarbon (PAH) consisting of four fused benzene rings. A large amount of literature exists for the toxicity and carcinogenicity of PAHs, but toxicity data for pyrene is very limited. As a result, the United States Environmental Protection Agency classified pyrene in Group D (not classifiable as to human carcinogenicity) as there was no human data and inadequate data from animal bioassays (U.S. EPA, 1993 a and b).

The measured IC_{50} of AM1/99, AM1/107 and AM2/97 for FXIIIa was 40, 2 and 195 μM respectively. Therefore, it can be concluded that AM1/107 and AM2/97 were not toxic to the cells up to 500 μM which is respectively ~ 3 and ~ 250 fold higher than their recorded efficacy. Regarding AM1/99, there was no significant difference in the viability of the cells at concentrations ~ 7 fold higher (up to 300 μM). However at concentrations of 500 μM the viability decreases by 50 % compared to negative control, R281 and the other dansyl compounds. Therefore, it can be concluded that in

contrast to AM1/99 (pyrene compound) neither R281 nor the dansyl compounds are toxic to the cells at the tested concentrations (100 - 500 μ M).

2.6.7 Trypan Blue test

To investigate the cytotoxicity of the novel group of inhibitors of TG, the proliferation of fibroblast cells was assessed by direct cell counting using a trypan blue test.

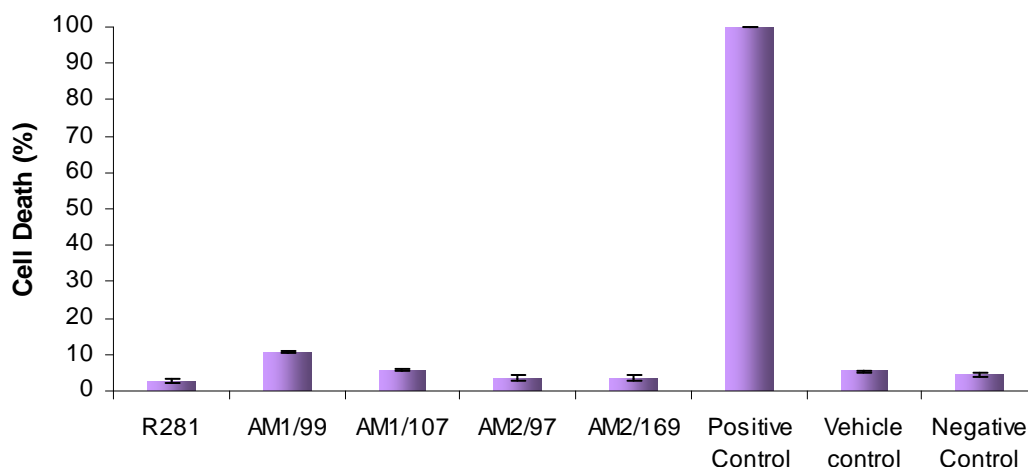


Figure 2.16 Effect of the TG inhibitors on fibroblast cell death. The Percentage of cell death after 48 hour incubation with different types of TG inhibitors (R281, AM1/99, AM1/107, AM2/97 and AM2/169) was measured using a Trypan blue test. Trypan blue is a diazo dye which is unable to cross intact plasma membranes, and so only labels dead cells. Positive control includes cells incubated with 1 μ M staurosporine. Vehicle control was 0.5 % (v/v) DMSO. Results denote mean \pm SD from three independent experiments, n=3.

The percentage of dead cells for R281 (500 μ M), AM1/107 (500 μ M), AM2/97 (500 μ M), AM2/169 (500 μ M), negative control, vehicle control (0.5 % DMSO) and positive control (1 μ M staurosporine) was 2.3 %, 10 %, 6 %, 3.7 %, 5 %, 6 %, 5 % and 100 % respectively (Figure 2.16). The percentage difference could be attributed to the external factors rather than the formulation of inhibitors. Aside from AM1/99, cell viability remained above 95 % of control across all the inhibitors tested, indicating that all the inhibitors were non toxic to the cells at the studied concentration. However, treated cells with 500 μ M of AM1/99 decreased dramatically (by about 50 %) in viability and proliferation of the cells with 10 % of dead cells. These results are in clear agreement with the previous XTT cell proliferation study and confirm the potential cytotoxicity of the pyrene compound previously shown in Figures 2.14 and 2.15 earlier.

2.7 Conclusion

All the tested TG inhibitors were found to be effective on the activity of the TG enzyme. With the exception of AM1/99, all the inhibitors deemed to have a linear relationship between the inhibitor concentration and either the area under the curve or relative fluorescence unit. Regarding the cytotoxicity test, high concentration (500 μ M) of AM1/99 (the fluorescent inhibitor with pyrene group) reduced cell viability and consequently increased cell toxicity and this needs to be taken into account by any further studies. On the other hand, the rest of the inhibitors tested (AM1/107, AM2/97 and AM2/169) appeared to be suitable for future investigations as they have not indicated any sign of toxicity to the cells at the concentration ranges tested. AM2/97 appeared to be more appropriate for inhibiting FXIIIa enzyme as it demonstrated the lowest IC_{50} and consequently more inhibition activity for FXIIIa amongst the TG inhibitors tested. Furthermore, the tetramethylimidazolium warhead makes the inhibitor more stable than the dimethylsulphonium warhead at the N-terminus of the peptide based inhibitor. Therefore, it was selected as the inhibitor of choice to coat or to be integrated into catheters or other implant devices, with the aim of reducing the incidence of catheter sheath formation, thrombotic occlusion and associated infection in central venous catheters (CVCs). AM2/169, with one of the lowest IC_{50} for TG2, is the favoured inhibitor for targeting the liver with the aim of treating liver fibrosis and its end stage disease liver cirrhosis. Moreover, the proline amino acid in the structure of AM2/169 results in a more stable compound than the other inhibitors investigated for bio-distribution studies.

Chapter 3:
Controlled release of FXIIIa inhibitor from
polyurethane catheters

3.1 Introduction

Catheters are used widely for a variety of therapeutic purposes in modern medical practice.

3.1.1 Catheter requirements

The British standard states the specifications, to which all catheter devices and materials must conform (British Standard EN 30993, 1992). These requirements were listed below;

3.1.1.1 Biocompatibility

All biomaterials are required to possess suitable properties, in particular good biocompatibility. British Standards for catheter materials are outlined so as to ensure appropriate quality and diminish toxicity to tissues. The importance of such standards is emphasised by a research study (Salama, 1993), which found that four out of seven commercially existing urethral catheters demonstrated considerable cytotoxicity with severe urethral strictures in patients for urinary catheters. It was then concluded that the international standards for urethral catheter toxicity, in addition to quality controls for the devices were inadequate (British Standard EN 30993, Lawrence & Turner, 2005), suggesting that further development of such systems are required.

3.1.1.2 Physical and mechanical properties

An appropriate combination of physical and mechanical properties is of great importance for a catheter to be efficacious in its application (Lawrence & Turner, 2005). These properties include smooth surface finish, flexibility and strength.

3.1.1.2.1 Smooth surface finish

A catheter needs to have a smooth surface finish and a low coefficient of friction, once manufactured and ready for application. This is specified in the British standard EN 1616:1997 as, ‘shall appear free from extraneous matter’. This applies to the shaft, tip, balloon and eyes of the device, and examination is to be conducted using a magnification of $2.5 \times$ (British Standard EN 1616, 1997). This yields to a minimum mechanical trauma and shear forces at the biomaterial–tissue interface, enhancing ease of insertion and removal, which also improves patient comfort (Denstedt et al., 1998; Lawrence & Turner, 2005).

3.1.1.2.2 Flexibility

The flexibility of the catheter material is also imperative. A smooth and pliable catheter tips reduce the occurrence of venous perforation during insertion (Lawrence & Turner, 2005).

3.1.1.2.3 Strength and elastic recovery

Strength is also essential in terms of device integrity. Whilst flexible, a catheter must also be strong enough to avoid kinking or collapse (Cox et al., 1987). Catheters can be exposed to considerable tensile force upon removal from the patient which must not lead to damage or dislodging of the shaft from the balloon as occurs with the Foley catheter, or in the separation of the device into two or more parts. Therefore, the elastic recovery of the constituent biomaterial is a necessary property that must be considered when manufacturing catheters (British Standard EN 1618, 1997; Lowthian, 1998; Lawrence & Turner, 2005).

3.1.2 Types of polymeric coatings

The choice of coating material depends on the device material, its application and other processing requirements. Table 3.1 outlines some of the key characteristics of the most commonly applied coatings for catheters such as silicone and hydrogel (Polymer coatings for powder-free medical gloves, 1999; Lawrence & Turner, 2005).

A number of researchers suggested that polyurethane catheters might be a better alternative to silicone catheters for long term venous access and polyurethane catheters should have a lower thrombogenicity than silicone elastomer catheters (Pottecher et al., 1984; Curelaru et al., 1983; Wheeler et al., 1992). However in a comparative study of polyurethane and silicone cuffed-catheters in long-term home total parenteral nutrition patients (TPN), Beau and Matrat (1999) demonstrated that both silicone and polyurethane catheters enable safe, long-term venous access and usually prevent inadvertent catheter dislodgement. Therefore, there is little evidence to support the hypothesis that polyurethane catheters offer more security than silicone catheters in home TPN adult patients.

In this chapter, hydrogel-coated polyurethane catheters will be discussed, whilst silicone catheters will be detailed in chapter 4.

Table 3.1 Comparison of properties of common coating substances (hydrogel and silicone)

| Property | Hydrogel | Silicone |
|--------------------------------------|----------|----------|
| Tensile strength | Low | Low |
| Adhesion to natural rubber | Low | Moderate |
| Elongation | Low | Moderate |
| Puncture resistance | Low | Low |
| Abrasion resistance | Low | Moderate |
| Oil resistance | Moderate | Low |
| Swelling on exposure to water | High | Low |
| Integrity after stretch | Low | Low |
| Hydration/water swelling | High | Low |
| Allergic reaction | No | No |

3.1.3 Hydrogels: General introduction and background

Introduced to the medical device industry in the early 1960s (Wichterle & Lim, 1960), hydrogels are three-dimensional, hydrophilic, polymeric networks which are able to imbibe large quantities of biological fluids while remaining insoluble in aqueous solutions (Peppas et al., 2000). Since the establishment of the first synthetic hydrogels by Wichterle and Lim in 1954 (Wichterle & Lim, 1960), the growth of hydrogel technologies has advanced many fields ranging from food additives to pharmaceuticals to biomedical implants. Among these applications, hydrogel-based drug delivery devices represent a major area of research interest with several commercial products already developed (Lin & Metters, 2006). Hydrogels demonstrate many physicochemical attributes that make them beneficial for application as biomaterials; they are soft and pliable (Huang, 2003) and do not dissolve while holding a large quantity of water within their structure, on account of physical and chemical cross-linkage of hydrophilic polymer chains. This results in the formation of a thin water film on the contacting surface, thus improving its smoothness and lubricity (Lawrence and Turner, 2005). Hydrogels mirror natural

living tissue more than any other class of synthetic biomaterials, due to their high water content and soft consistency which is similar to natural tissue, which contributes to their biocompatibility (Peppas, 2000). As a result, hydrogels are particularly useful in biomedical and pharmaceutical applications.

Hydrogels can be prepared from natural or synthetic polymers. Although hydrogels made from natural polymers may not offer adequate mechanical properties and may contain pathogens or engender immune responses, they do provide some advantages such as inherent biocompatibility, biodegradability, and biological recognised moieties that support several cellular activities. Synthetic polymers do not manifest these innate bioactive properties; however their well defined structures can be altered to yield tailorable degradability and functionality. Chitosan, alginate, fibrin, collagen, gelatin, hyaluronic acid and dextran are the examples of natural hydrogels, while *N*-(2-hydroxypropyl) methacrylate (HPMA), *N*-vinyl-2-pyrrolidone (NVP), *N*-isopropyl acrylamide (NIPAAm), vinyl acetate (VAc), acrylic acid (AA), methacrylic acid (MAA), polyethylene glycol, acrylate/methacrylate (PEGA/PEGMA), polyethylene glycol and diacrylate/dimethacrylate (PEGDA/PEGDMA) are examples of the synthetic ones (Lin & Metters, 2006).

3.1.4 Hydrogel coating

Hydrogel coatings are used on medical products such as catheters, angioplasty balloons, introducers, contact lenses and other indwelling medical devices, to enhance surface lubricity (Ikada & Uyama, 1993). This could be attributed to the nature of the soft and slippery surface of hydrogels upon hydration (Park et al., 2002). In spite of technological advances, studies and trials of hydrogel-coated catheters have been controversial. On the one hand, some researchers have indicated that there is promising potential for these catheters. Talja et al. (1990) claimed that a hydrogel-coated catheter was less prone to encrustation compared to full silicone or siliconized catheters. A similar encrustation trend on various indwelling double-J stents was also observed by Cormio et al. (1995). On the other hand, others have raised doubts and concerns over their usage (Liedberg et al., 1990; Bologna et al., 1999; Ahearn and Grace, 2000). For instance, research has indicated that despite the fact that hydrogel catheters had been designed to resist bacterial contamination and subsequent encrustation, they were amongst some of the most rapid to block (Morris et al., 1997;

Lawrence and Turner, 2005). Other trials (Cox et al., 1988; 1989; Thibon et al., 2000) also demonstrated no statistical difference between the incidence of infection in patients treated with a hydrogel catheter and a standard all-silicone device. The possibility of higher encrustation on hydrogel surfaces than on other surfaces has also been suggested (Tunney et al., 1996; Desgrandchamps, 1997). Consequently, it was concluded that there was insufficient evidence to support or recommend the widespread use of such modified catheters (Lawrence and Turner, 2005).

In terms of bacterial infection, once again, results have been varied. Some researchers have reported positive findings where bacterial adherence to hydrogel-coated catheters was notably lower than on standard devices. On the contrary, some other reports have stated that there was no significant difference between the rate and incidence of bacterial infection in hydrogel-coated and standard catheters and concluded that there was insufficient data to prove any clinical benefits from using these devices (Monson et al., 1974; Chene et al., 1990; Liedberg et al., 1990; Lawrence and Turner, 2005).

3.2 Aim and objectives

This present research is aimed at the incorporating of the fluorescent FXIIIa enzyme inhibitor (AM2/97) into the polymeric coatings of polyurethane (PU) central venous catheters (CVCs) and other medical implant devices. The sustained release of biologically active compound from the catheters could reduce the incidence of catheter sheath formation, thrombotic occlusion and associated infection in CVCs (Griffin et al., 2004; Lambert et al., 2007).

The objectives of this work were:

- Defining the key characteristics for an effective polymeric-coating such as drying time, flexibility, uniformity and consistency of finish and thickness of the coated PU strips.
- Ascertaining the most suitable polymer for coating of the PU strips according to predefined key characteristics for an effective coating.
- Determining the most appropriate solvent which is compatible with the enzyme inhibitor, the PU strips and the polymer of choice.

- Producing a polymeric coating on the PU strips for the incorporation of the enzyme inhibitor.
- Quantifying the enzyme inhibitor release from the PU strips *in vitro*.

3.3 Materials

Phosphate buffered saline (PBS), polyethylene oxide (PEO) with molecular weight 1000000 and 5000000; polyethylene glycol (PEG) with molecular weight 8000, 4600 and 2000; polyvinylpolypyrrolidone (PVP) with the molecular weight 360000, 10000 and 40000, poly(D,L-lactide-co-glycolide) (PLGA) with a lactide/glycolide ratio 50:50 and 85:15 were supplied by Sigma-Aldrich (Dorset, England). Polyethylene oxide with molecular weight 300,000 was purchased from Fisher Scientific (Loughborough, UK). Poly(L-lactic acid) (PLA) with molecular weight 2000, 50000 and 300000 were obtained from Polysciences, Inc. (Eppelheim, Germany). The polyurethane (PU) sheets with a hardness of 85 A°, thickness of 1 mm and dimensions of 3 m x 700 mm were ordered from PPL Polyurethane Products Ltd (Reforfd, Nottinghamshire, UK). Unless stated otherwise PBS was used at 0.01 M, pH 7.4. Doubly distilled and filtered water was used in the preparation of all solutions. AM2/97 (fluorescent-labeled FXIIIa inhibitor) was prepared within the chemistry department of Aston University by Dr. Alexandre Mongeot and Dr. Dan Rathbone as previously described (Griffin et al., 2008).

3.4 Methods

3.4.1 Polyurethane sheet

The intravascular guiding catheters are extensively used in clinics at the present time and polyurethanes (PU) are extensively selected as the matrix material (Wang et al., 2001). For preliminary studies, the polyurethane sheets (Figure 3.1) cut into equal strips to a size of 5 x 1 cm².



Figure 3. 1 Polyurethane sheet

3.4.2 Cleaning

As with any coating procedure, surface cleanliness is essential prior to dipping to ensure successful adhesion between the polymer and the substrate. Common

contaminants are finger oils, dust, and it is critical that these are removed prior to coating. Thus, a variety of cleaning methods have been successfully employed, including washing with alkaline detergent and soaking in solvents such as isopropanol (IPA) or ethanol (Reitman & McPeak, 2005).

3.4.3 Key requirements for an effective polymer coating

For an effective coating of the polyurethane strips, 4 key characteristics were defined and investigated.

- Drying time
- Flexibility
- Smoothness and consistency of finish
- Thickness

3.4.3.1 Drying time

The first feature examined was drying time of the PU strips subsequent to coating. The strips were dip-coated 1-5 times in a selection of polymer solutions at intervals. The drying process of the coated strips was conducted by hanging them from a stand in a vertical position at room temperature (Figure 3.2) and once dried the same procedure was repeated. The time of drying for each coated strip was measured by a stopwatch.



Figure 3. 2 The polymer-coated strips were hung from a stand in a vertical position and dried at room temperature subsequent to coating.

3.4.3.2 Flexibility

As discussed in 3.1.1.2.2, capability of being twisted devoid of breaking, cracks or delamination of the PU strips after the polymeric coating was qualitatively assessed.

3.4.3.3 Smoothness and consistency of finish

The smoothness and consistency of finish is detailed in 3.1.1.2.1 and visually analysed, following the polymeric-coating of the PU strips.

3.4.3.4 Thickness of the PU strips

3.4.3.4.1 Scanning electron microscopy (SEM)

The thickness of the polymer-coated PU strips was determined using scanning electron microscopy (SEM). At the outset, specimens were thoroughly dried and gold coated by a gold sputter coater (Emscope SC500 Sputter coater, Ashford, Kent, Great Britain). The thickness of the strips was then measured by a scanning electron microscope (Cambridge Instruments, Stereoscan 90) at six points and the average was used. The experimental conditions involved the PU strips coated in 5 % (w/v) polymer in DCM, 1-5 times.

3.4.3.4.2 Epifluorescent microscopy

The thickness of the inhibitor-and polymer-coated strips was measured using epifluorescent microscopy by an AxioCam HRC camera mounted on a Zeiss Axioskop microscope with AxioVision version 3.1 software and a Achromplan 4x/ 0.10 objective. Layers were recorded using a Zeiss filter set giving excitation at 365 nm, and emission at 420 nm. The experimental conditions were the PU strips coated using a solution composed of 5 % (w/v) polymer and 0.25 % (w/v) AM2/97 in DCM, 2-4 times.

3.4.4 Choice of polymer

As per the criteria defined above, and based on preliminary studies (appendix 1), polyvinylpyrrolidone (PVP) with 40 k molecular weight and poly (lactic-co-glycolic acid) (PLGA) with a lactide/glycolide ratio 85:15 appeared to fulfil the features mentioned for having an effective coating.

3.4.5 Choice of solvent

To investigate the most appropriate solvent which is compatible with the enzyme inhibitor, polyurethane and the polymer (PVP or PLGA), a different range of solvents such as PBS, acetone, methanol, ethanol, dimethyl sulfoxide (DMSO), chloroform and dichloromethane (DCM) were examined. DCM appeared to be the optimum

solvent; it evaporated fast and had no effect on the polyurethane strips. Furthermore, it was a good solvent for both the polymer and inhibitor. Acetone fades the colour of the PU strips, whilst methanol dissolves it. PBS and DMSO do not evaporate fast.

3.4.6 Dip-coating method

The polyurethane strips were coated using dip-coating method (Jones, 2000). Initially, the polymer was dissolved in the appropriate solvent at a desired concentration, in a suitable tank. To create a local drug delivery system, a requisite amount of the enzyme inhibitor was also added to the polymer solution. The coating solution was maintained on dry ice to avoid evaporation of the organic solvent and a consequent increase in the polymer concentration. The polyurethane strips were inserted vertically into the container containing the coating material and the inhibitor and then taken out and force dried. The strips were coated by a two, three and four times dip-coating procedure to achieve a dense and regular polymer coating. The coated polyurethane strips were dried at room temperature, allowing the solvent to evaporate completely. To obtain reproducible and consistent coatings, attempts were made to ensure that the strips were immersed in and removed from the coating solution at the same rate. The benefits of this technique include simplicity, low cost, ease of control, good coverage and consistency (Jones, 2000). The coating process was followed by measurement of weight alterations after each coating layer. The schematic of the dip coating process is illustrated in Figure 3.3.

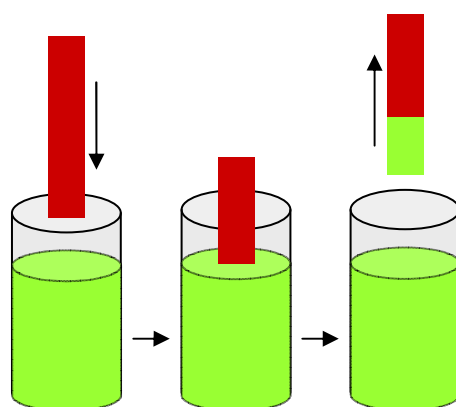


Figure 3. 3 The schematic of dip-coating of the polyurethane strips in the polymer solution containing the fluorescent inhibitor

Given that the fluorescent compounds are highly photosensitive, precaution was taken to protect them from light, using aluminium foil to cover the drug solution throughout the duration of the experiment.

3.4.7 *in vitro* release study of FXIIIa inhibitor

To study the drug release from the inhibitor and polymer coated polyurethane strips (2 x 1 x 0.1 cm³), each of the strips was placed in a 50 ml universal tube containing 10 ml of 0.01 M of phosphate buffer saline pH 7.4 (Figure 3.4). The universal tubes were then put in a shaking water bath set at 80 rpm and 37 °C. The release medium was sampled and replaced constantly (to promote sink condition). The amount of relative fluorescent unit (RFU) within the release media was measured using 200 µl aliquots taken at pre-determined time points and measured spectrofluorimetrically with an excitation maximum at 330 nm and emission peak at 570 nm (Spectra Max Gemini XPS, Molecular Probes), to quantify the amount of inhibitor release from the coated polyurethane strips.

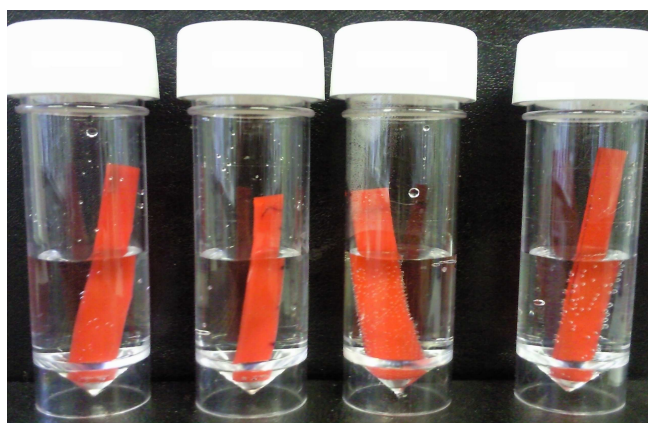


Figure 3. 4 The inhibitor-and polymer-coated polyurethane strips placed in PBS

Accordingly the concentration of the inhibitor released within the media was calculated using a drug calibration curve which was formerly prepared from a set of standard samples of known concentration. The results were then reported as cumulative drug release, which corresponds to accumulation of the drug within the release media from time zero up to the measured time point, expressed as percentage (%) of total drug added and concentration (µmole/ ml) of the inhibitor released. Estimation of the amount of the inhibitor entrapped within the coatings was calculated by measuring the density of the coating solution and weight changes of the solution

subsequent to each coating, which was followed by calculating the number of moles of the inhibitor incorporated per coating.

3.5 Results and Discussion

3.5.1 Drying time

The PU strips were repeatedly dip-coated using the polymer solutions with various concentrations at room temperature. The coating formulation was incorporating 5 %, 10 % and 20 % (w/v) PVP or PLGA in DCM.

Regarding Figure 3.5, the drying time was lengthened correspondingly with the number of coatings from 1 to 5 times, and the concentration of the polymer from 5 % to 20 % (w/v).

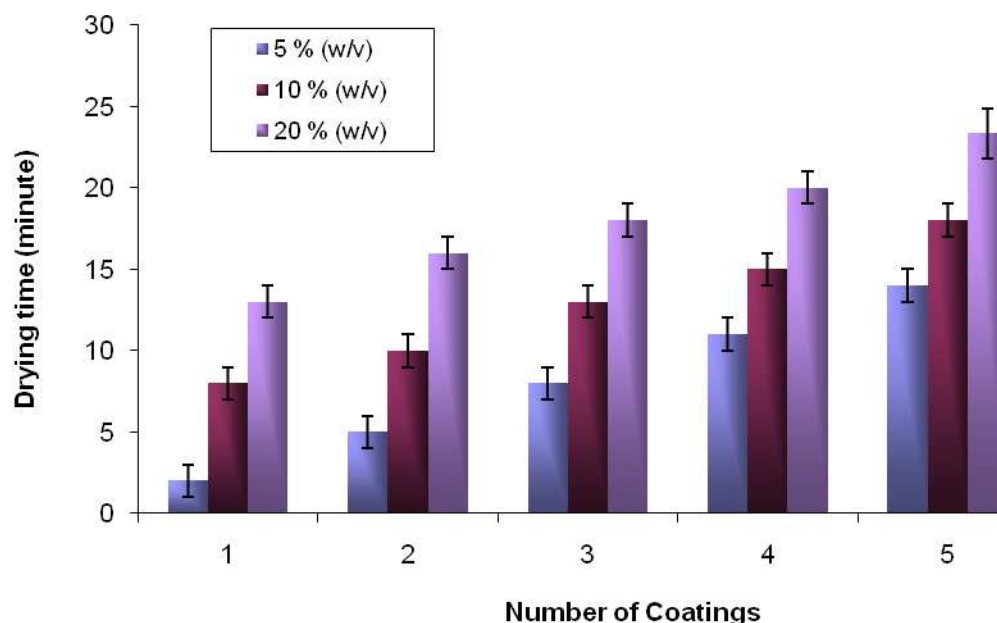


Figure 3. 5 Drying time (minute) of the PU strips at different concentrations of the polymeric-coating solution. The coating formulation was incorporating 5 %, 10 % and 20 % (w/v) PVP or PLGA in DCM. The drying time was augmented correspondingly with the number of coatings and the concentration of polymers. Results denote mean \pm SD from 3 independently synthesized batches.

As the number of coatings and consequently the thickness of the strips was increased, the drying time was raised from ~ 2 minutes to ~ 15 minutes for 5 % (w/v) polymer solution, from ~ 7 minutes to ~ 17 minutes for 10 % (w/v) polymer solution and finally from ~ 15 minutes to ~ 25 minutes for 20 % (w/v) polymer solution. Drying is a complex procedure which involves simultaneous heat and mass transfer phenomena. The phenomena which must be considered in convective air drying of solids are the

moisture diffusion in the solid toward its external surface, the vaporization and convective transfer of the vapour into the air stream, the conductive heat transfer within the solid mass and the convective heat transfer from the air to the solid's surface (Catalano, 2008).

These results could be explained using Fick's Law of diffusion, the equation describing the rate at which diffusion occurs (equation 3.1). J_x (the flux density) is the amount of species x crossing a certain area per unit time. The diffusion rate is directly proportional to the difference in concentration, dc , and the cross-sectional area, A , across which the molecules are diffusing and inversely proportional to the distance, dx , through which the molecules diffuse or in other words the thickness. The diffusion coefficient (D), has units of m^2/s . The negative sign indicates that the direction of flow is from high to low concentration.

$$J_x = -DA \frac{dc}{dx} \quad (\text{Equation 3.1})$$

According to Fick's law, a longer time is required for the moisture diffusion in the solid towards its external surface in a thicker layer than in the thinner one. Therefore, a consequent increase of coating thickness results in an increase in drying time.

Furthermore, an approximate dependence of the diffusion coefficient on temperature can often be found using the Stokes-Einstein equation, which predicts that:

$$\frac{DT_1}{DT_2} = \frac{T_1 \mu T_2}{T_2 \mu T_1} \quad (\text{Equation 3.2})$$

T_1 and T_2 denote temperatures 1 and 2, respectively, D is the diffusion coefficient (m^2/s), T is the absolute temperature and μ is the dynamic viscosity of the solvent ($Pa \cdot s$).

In accordance with Stokes-Einstein equation, the diffusion rate is directly proportional to the temperature. Therefore, as temperature and consequently the diffusion rate increases, the drying time decreases. Thus, an attempt was made to conduct the experiment for all the specimens at the same temperature.

3.5.2 Flexibility, Smoothness and consistency of finish

It is essential that the polymer coating adheres well to the underlying substrate, providing integrity during performance. Hence, a number of techniques have been established to ensure this, such as treating the substrate with an acidic solution or a polymeric adhesion layer prior to application of the hydrogel (Allegiance Research & Technology, 1999). Nevertheless, due to a significant difference between the elastic modulus of hydrogels and that of substrate, the hydrogel coatings tend to crack throughout device manufacture and use. If the adhesion of the coating to the rubber is poor, the coating flakes off from the substrate. This can result in problems including particulate debris and the formation of adherence sites for bacteria. Furthermore, in terms of physical properties, tensile strength and puncture resistance are typically low in hydrogel coating (Young et al., 1998; Allegiance Research & Technology, 1999; Lawrence and Turner, 2005).



Figure 3. 6 Partial delamination of the polymeric coating of the PU strips



Figure 3. 7 The polymeric coating of the PU strips with partial delamination and cracks



Figure 3. 8 Complete delamination of the polymeric coating of the PU strips

Cracking, partial or complete delaminating was observed subsequent to coating of a quantity of the PU strips with the various polymer solutions. Some others exhibited

irregular and inconsistent surface finish (Figures 3.6-3.8, additional details have been presented in appendix 1).

PVP and PLGA demonstrated optimum coating amongst the entire range of polymers tested, in terms of flexibility and smooth surface finish (appendix 1). The coating had the ability to withstand the compressive and tensile strains imparted and was devoid of cracking or delamination during the expansion process. Moreover, the coatings were consistent, unvaried in texture and free from extraneous matter.

3.5.3 Thickness

3.5.3.1 Scanning electron microscopy

To determine the thickness of the polymer-coated strip, scanning electron microscopy was performed. The coating formulation was incorporating 5 % (w/v) PVP or PLGA in DCM.

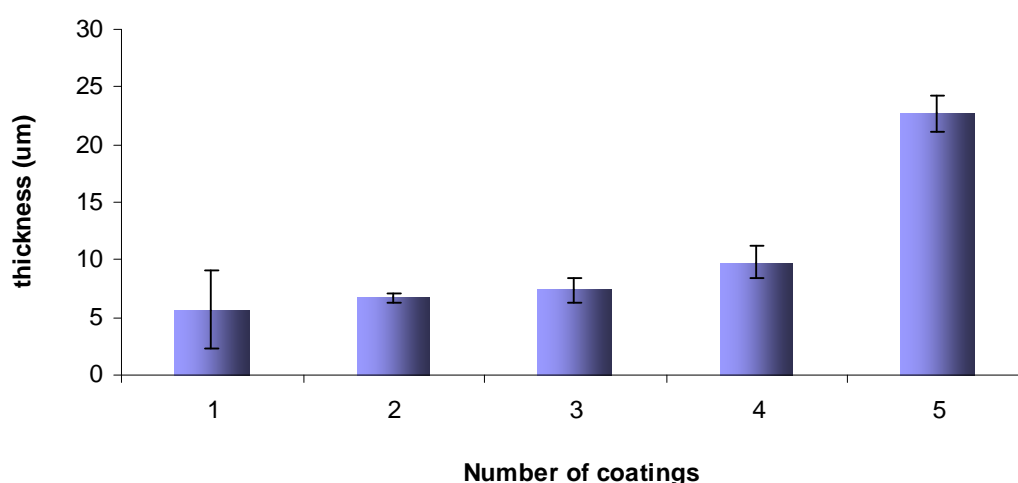


Figure 3. 9 The thickness of the polymer-coated polyurethane strips, using SEM. The coating formulation was incorporating 5 % (w/v) PVP or PLGA in DCM. The thickness was measured at six points and the average was used. There was a steady increase in the thickness of the PU strips with increasing the number of coatings. Results denote mean \pm SD from 3 independently synthesized batches.

As shown in Figure 3.9, there was a steady increase in the thickness of the PU strips from about 5 μm to around 25 μm , with increasing the number of coatings from 1 layer to 5 layers. Insufficient information is available on the commercial application of the coatings; however they are commonly believed to be in the order of 50 μm in thickness (Lawrance and Turner, 2005).

3.5.3.2 Epifluorescent microscopy

To confirm the integration of the enzyme inhibitor throughout the coating of the PU strips and to certify the coating thickness of the inhibitor-and polymer-coated PU strips, epifluorescent microscopy was achieved. The coating formulation was incorporating 5 % (w/v) PVP or PLGA and 0.25 % AM2/97 in DCM.

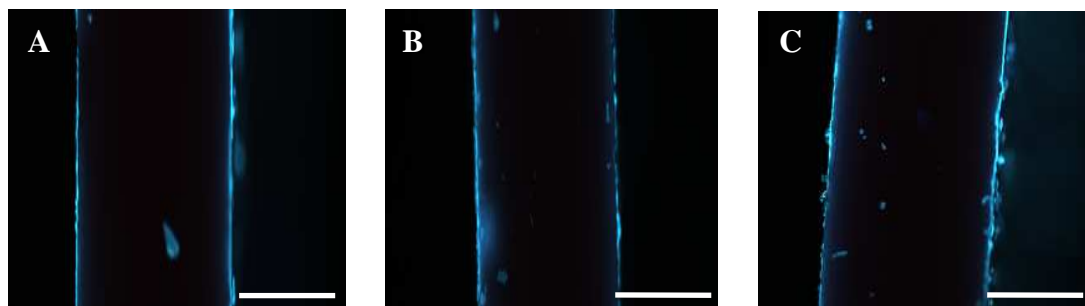


Figure 3. 10 A-C epifluorescent microscope images of the 2, 3 and 4 times inhibitor-and polymer-coated polyurethane strips, using 4 x objectives. The coating formulation was incorporating 5 % (w/v) PVP or PLGA and 0.25 % AM2/97 in DCM. The thickness of the coatings augmented with the number of the coatings. Bar indicates 100 μm .

The thickness of the coated PU strips was measured by an epifluorescent microscope. The epifluorescent microscope images from the strips confirmed the integration of the enzyme inhibitor throughout the coating of the strips. As was expected, the thickness of the coatings augmented with the number of the coatings. The PU strips coated 2, 3 and 4 times, demonstrated an average thickness of about 5.5 μm , 8.5 μm and 15 μm respectively (Figures 3.10). These results were in agreement with the findings from SEM previously reported.

The coatings of the strips were performed manually; this would result in different withdrawal velocity which could affect the thickness of coatings and consequently the quantity of the integrated polymer into the PU strips. The increase of withdrawal velocity results in the increase of film thickness at the moderately low withdrawal velocity regime. Nevertheless, it was noted that the layer thickness begins to decrease with increasing withdrawal velocity, at the relatively high withdrawal velocity regime of the dip-coating process (Fang, 2008). Consequently, attempts were made to ensure that the strips were immersed in and removed from the coating solution at the same rate.

3.5.4 Rate-controlled release in drug delivery and targeting

The mechanisms controlling the rate of drug release from a delivery system are;

- Diffusion-controlled release mechanism
- Dissolution-controlled release mechanism
- Osmosis-controlled release mechanism
- Mechanical-controlled release mechanism
- Bio-responsive controlled release mechanism

Diffusion-controlled release mechanism

Diffusion-controlled release mechanism is briefly described here and is further detailed in chapter 4. In this case, the drug must diffuse either through the macromolecular mesh or the water-filled pores of the reservoir device or matrix system in order to be released.

Dissolution-controlled release mechanism

There are two major types of dissolution-controlled systems; reservoir device or matrix system. In dissolution-controlled release devices, drug release is controlled by dissolution rate of an employed polymer. Since the dissolution of polymeric material is the key to this mechanism, the polymer must be water-soluble or degradable in water (Hillery et al., 2001). The dissolution process includes two steps; initial dissolution and detachment of drug molecules from the surface of their solid structure to the adjacent liquid interface, followed by diffusion of the solvated molecules from the interface into the bulk liquid medium. It is generally believed that the first step is much faster than the second step. This procedure could be manipulated to create controlled release delivery systems with desired profiles and a favourite rate of release (Wang & Shmeis, 2005).

The rate of dissolution, the amount of dissolved solid per unit time, can be calculated by the Noyes-Whitney equation which relates the rate of dissolution of solids to the properties of the solid and the dissolution medium and written as:

$$\frac{dM}{dt} = A \times \frac{D}{h} (C_s - C_b) \quad (\text{Equation 3.2})$$

Where M = mass, t = time, A = surface area of the solid, D = diffusion coefficient, h = thickness of diffusion layer, C_s = concentration of the solid in the diffusion layer surrounding the solid, C_b = concentration of the solid in bulk dissolution medium.

Alteration of the thermal and spatial aspects of drug release using coatings involves applying a layer or layers of retardant material between the drug and the elution/dissolution medium. When a coated system is made of water-soluble constituents, the rate limiting step leading the release of drug from the system is the dissolution rate of polymer coating over time. Once the polymeric membrane has dissolved by gentle disentanglement of the polymer chain, the drug inside the membrane is instantaneously available for dissolution and absorption. At this stage, release is depending on the core properties (drug and excipients) including porosity, drug solubility and dissolution rate in the dissolution medium. Cores can be immediate release systems or controlled release matrix system (Wang & Shmeis, 2005).

3.5.4.1 Initial burst drug release from the PU strips

Poly vinyl pyrrolidone (PVP) was the first polymer which was selected for coating of the PU strips and studying *in vitro* drug release. PVP is a water-soluble polymer made from the monomer *N*-vinylpyrrolidone (Haaf et al., 1985) and a typical example of hydrogel polymers that have been utilised in indwelling medical device surface modifications (Huang, 2003; Shintani, 2004). PVP is a hydrophilic hydrogel which adsorbs water on contact with the blood and produces an extremely smooth surface. As well as improved haemocompatibility, the hydrogel significantly reduces bacterial adhesion in *in vitro* assays (John, 1996). Therefore, the chosen PVP coating enables the possibility of covering medical implants with biodegradable and biocompatible surface coating. The release pattern of the enzyme inhibitor into the medium was represented by plotting the cumulative drug release ($\mu\text{mole/ml}$) and the cumulative percent (%) drug released against time. The coating formulation of the PU strips was incorporating 5 % (w/v) PVP and 0.25 % (w/v) AM2/97 in DCM (Figures 3.11 & 3.12).

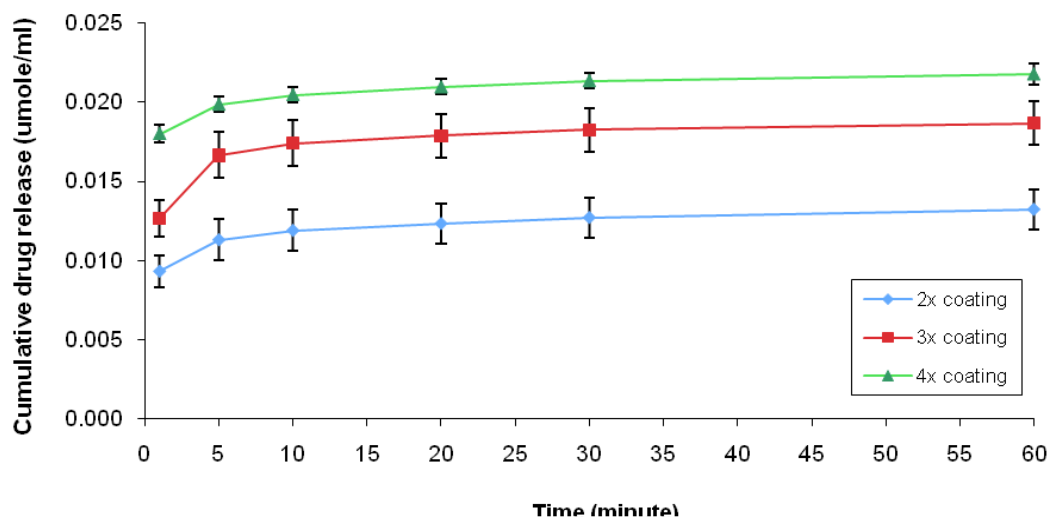


Figure 3. 11 Cumulative releases ($\mu\text{mole/ml}$) of the fluorescent FXIIIa inhibitor (AM2/97) into 10 ml PBS from the individually coated polyurethane strips over 60 minutes under sink condition. The formulation was incorporating 5 % (w/v) PVP and 0.25 % (w/v) AM2/97 in DCM. Cumulative drug release corresponds to accumulation of the drug within the release media from time zero up to the measured time point, expressed as concentration ($\mu\text{mole/ml}$) of the inhibitor released. Results denote mean \pm SD from 3 independently synthesized batches.

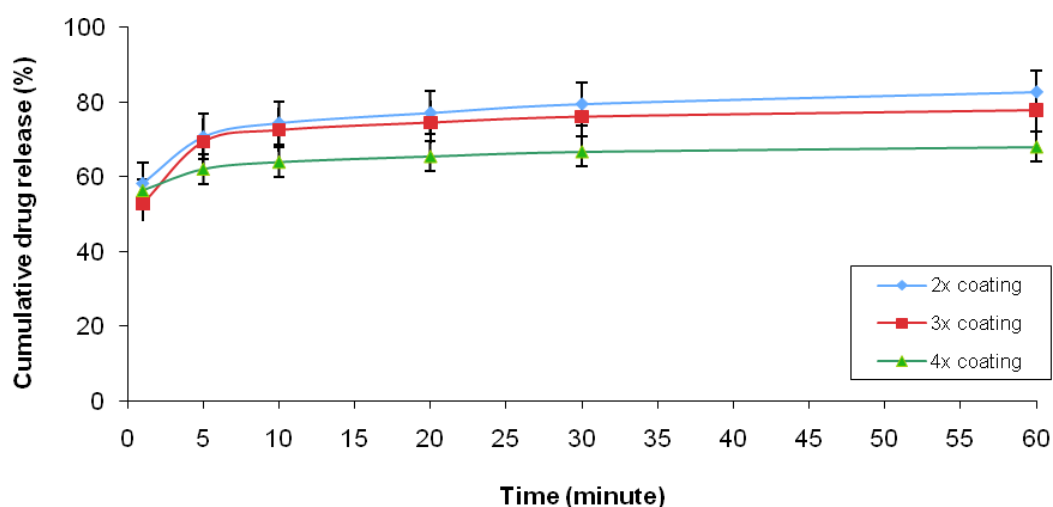


Figure 3. 12 Cumulative percentage release of the fluorescent FXIIIa inhibitor (AM2/97) into 10 ml PBS from the individually coated polyurethane strips over 60 minutes under sink condition. The formulation was incorporating 5 % (w/v) PVP and 0.25 % (w/v) AM2/97 in DCM. Cumulative drug release corresponds to accumulation of the drug within the release media from time zero up to the measured time point, expressed as percentage (%) of total drug added. Results denote mean \pm SD from 3 independently synthesized batches.

With regards to Figures 3.11 and 3.12, an initial burst release of the integrated inhibitor (0.09 - 0.17 $\mu\text{mole/ml}$) was obtained within the first minute for all the coatings tested ($\sim 50\%$). The 2, 3 and 4 times PVP coatings, demonstrated 80 %, 75 % and 60 % cumulative percent drug release and 0.011, 0.017 and 0.020 $\mu\text{mole/ml}$ total cumulative drug release subsequent to 10 minutes respectively, thereafter the

drug release was insignificant. In this case, the drug release was controlled by the dissolution rate of polymer coating over time. Upon contact of the polymer coating of the PU strips with PBS, a rapid release of the incorporated inhibitor from the surface on hydration and consequently dissolution of the biodegradable polymer was achieved. Increasing the number of coatings had no affect on the release time; however it affected the concentration of drug released into the media, due to the higher total concentrations within the coat. Unlike some diffusion-controlled release coated systems, release profile from dissolution-controlled release coated systems do not follow zero-order kinetic (Wang & Shmeis, 2005).

To investigate the drug concentration-effect on release behaviour, the percentage of the integrated drug in the formulation was incorporated from 0.25 % to 0.5 % (w/v). The coating formulation of the PU strips incorporated 5 % (w/v) PLGA and 0.5 % (w/v) AM2/97 in DCM.

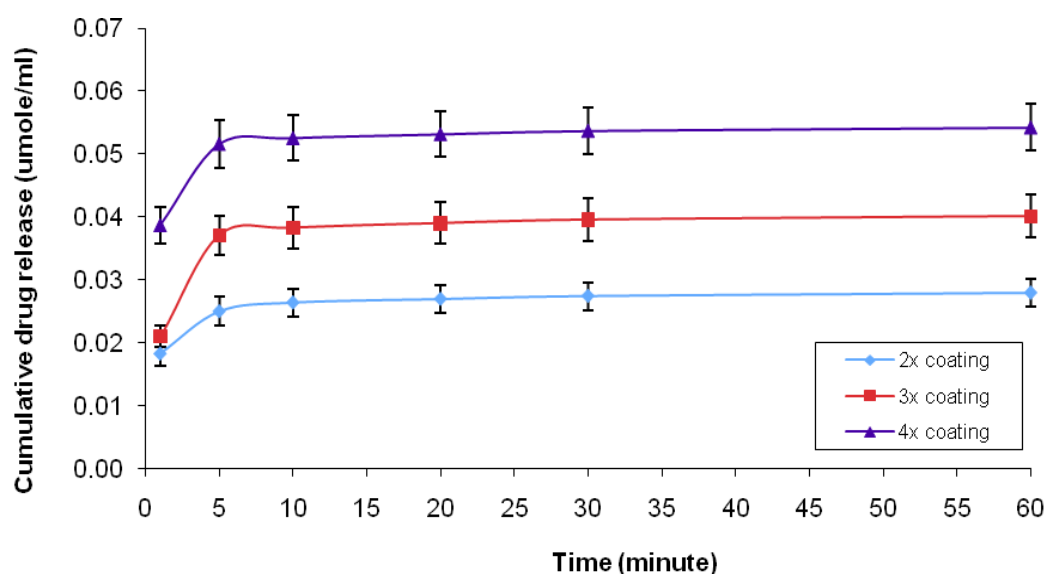


Figure 3. 13 Cumulative releases ($\mu\text{mole/ml}$) of the fluorescent FXIIIa inhibitor (AM2/97) into 10 ml PBS from the individually coated polyurethane strips over 60 minutes under sink condition. The formulation was incorporating 5 % (w/v) PVP and 0.5 % (w/v) AM2/97 in DCM. Cumulative drug release corresponds to accumulation of the drug within the release media from day zero up to the measured time point, expressed as concentration ($\mu\text{mole/ml}$) of the inhibitor released. Results denote mean \pm SD from 3 independently synthesized batches.

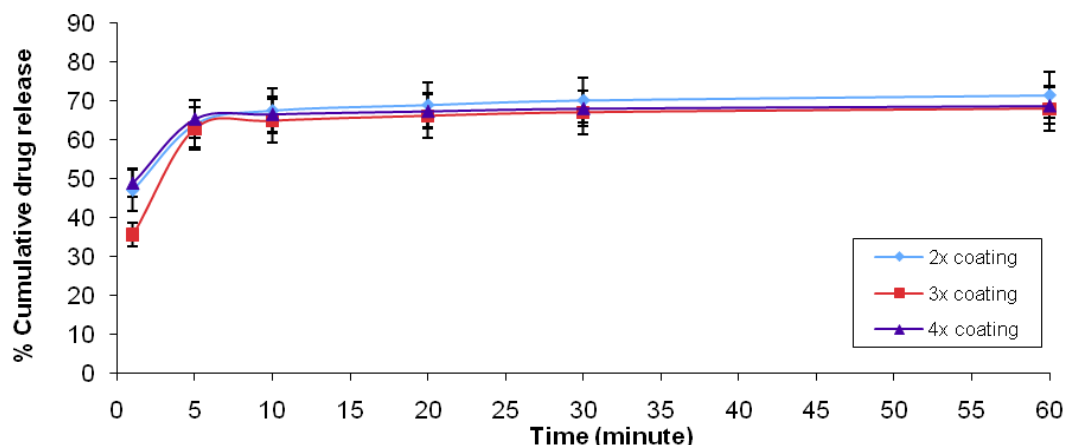


Figure 3. 14 Cumulative percentage release of the fluorescent FXIIIa inhibitor (AM2/97) into 10 ml PBS from the individually coated polyurethane strips over 60 minutes under sink condition. The formulation was incorporating 5 % (w/v) PLGA and 0.5 % (w/v) AM2/97 in DCM. Cumulative drug release corresponds to accumulation of the drug within the release media from day zero up to the measured time point, expressed as percentage (%) of total drug added. Results denote mean \pm SD from 3 independently synthesized batches.

Upon doubling the amount of the incorporated inhibitor, the same trend was observed as in Figure 3.12, in terms of the total cumulative drug release. Nevertheless, the total amount of drug release augmented from ~ 0.011 to ~ 0.025 $\mu\text{mol/ml}$ for 2 times coating, from ~ 0.017 to ~ 0.035 $\mu\text{mol/ml}$ for 3 times coating and from ~ 0.020 to ~ 0.050 $\mu\text{mol/ml}$ for 4 times coating, at the end of 5 minutes (Figure 3.13). Afterwards the drug release was insignificant for all tested coatings. The cumulative percentage drug release was virtually the same for all the tested coatings with no significant difference, reaching a maximum of ~ 65 % after 5 minutes (Figure 3.14). A higher drug incorporation results in a greater amount of the drug being present on the surface or proximal to the surface which leads to a greater initial and ultimate drug release. Thus, it can be concluded that a twofold increase in the amount of the integrated inhibitor, approximately twice the total amount of drug release from the PU strips, however it does not influence the release time.

3.5.4.2 Delayed drug release from the PU strips

To improve the drug release profile, a hydrophobic co-polymer such as PLGA with a lactide/glycolide ratio 85:15 was selected as the polymer of choice for coating of the PU strips. The coating formulation was incorporating 5 % (w/v) PLGA and 0.25 % (w/v) AM2/97 in DCM (Figures 3.15 & 3.16).

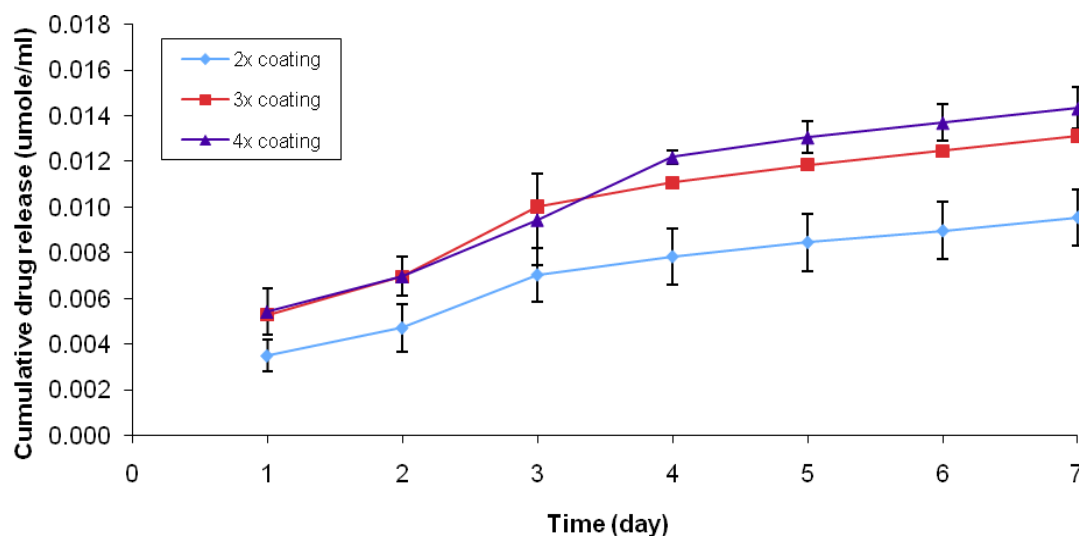


Figure 3. 15 Cumulative releases (μmole/ ml) of the fluorescent FXIIIa inhibitor (AM2/97) into 10 ml PBS from the individually coated polyurethane strips over 7 days under sink condition. The formulation was incorporating 5 % (w/v) PLGA and 0.25 % (w/v) AM2/97 in DCM. Cumulative drug release corresponds to accumulation of the drug within the release media from day zero up to the measured time point, expressed as concentration (μmole/ ml) of the inhibitor released. Results denote mean \pm SD from 3 independently synthesized batches.

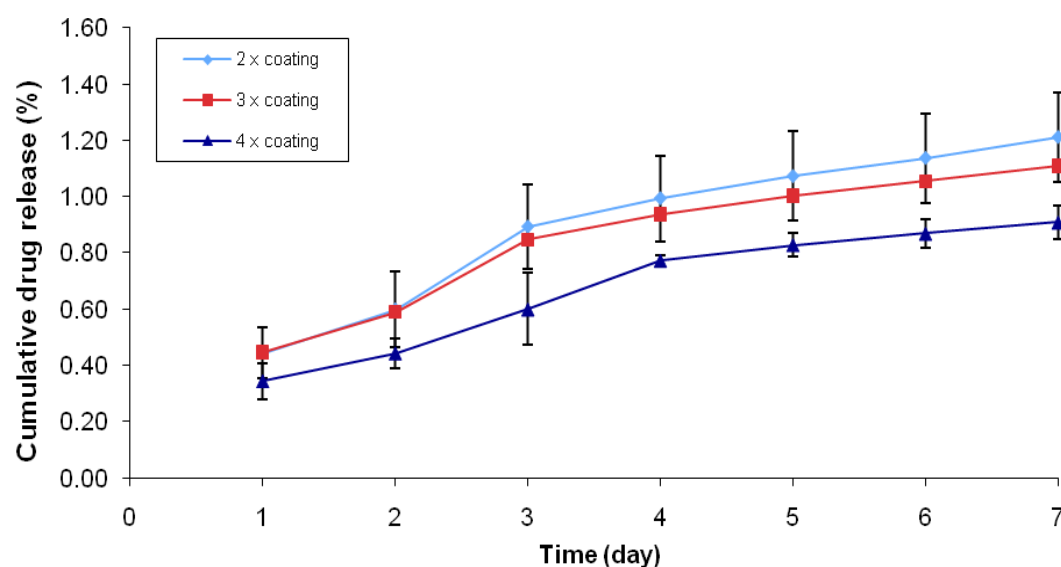


Figure 3. 16 Cumulative percentage release of the fluorescent FXIIIa inhibitor (AM2/97) into 10 ml PBS from the individually coated polyurethane strips over 7 days under sink condition. The formulation was incorporating 5 % (w/v) PLGA and 0.25 % (w/v) AM2/97 in DCM. Cumulative drug release corresponds to accumulation of the drug within the release media from day zero up to the measured time point, expressed as percentage (%) of total drug added. Results denote mean \pm SD from 3 independently synthesized batches.

PLGA is a synthetic copolymer of lactic acid (α -hydroxy propanoic acid) and glycolic acid (hydroxy acetic acid) (Avgoustakis, 2005). Indeed, it has been established that PLGA has desirable characteristics such as good biocompatibility and biodegradation. It has been utilised extensively for a variety of applications, including the design and

properties of the controlled-release systems for pharmaceutical agents. In recent years, PLGA has been broadly investigated for usage as implantable biodegradable carriers for controlled release of drugs. Using PLGA as drug carrier for medical implants coating could overcome the side effects of non biodegradable polymers (Gombotz & Pettit, 1995; Pan et al., 2007; Zheng et al., 2006).

The Figures 3.15 and 3.16 demonstrate that the cumulative drug release for the 2 times coating was $\sim 0.009 \mu\text{mole/ml}$, which is significantly lower than the cumulative drug release for 3 and 4 times coating (~ 0.013 and $\sim 0.14 \mu\text{mole/ml}$ respectively), whereas the cumulative percent drug release for the same layers of coatings is approximately between 0.80 % and 1.20 %, at the end of 7 days. These values are extremely low when compared to the other polymer used former in this study. This could be attributed to the poor solubility of the drug, as will be detailed in chapter 4. Briefly, lipophilic drugs are solubilised in matrix system, diffuse, and are released. Water-soluble drugs neither dissolve nor diffuse in a matrix system. Initially, water-soluble drugs existing on the surface, and subsequently the ones near the surface dissolve into water. Repetition of these procedures results in channel formation, allowing water-soluble drugs to be released in bulk. However water-insoluble drugs neither dissolve nor diffuse in a matrix system; they are not released since channels are not formed because of their insolubility in water. Hence, the release of the insoluble drugs from matrix system has long been considered challenging (Kajihara, 2003).

3.5.4.3 Sustained drug release from the PU strips

To provide a sustained release profile over a longer time for the enzyme inhibitor, a polymer blend of PVP (hydrophilic) and PLGA (hydrophobic) was utilised in order to release the active drug continuously at a moderate rate to grant a long-term therapeutic effect. The coating formulation integrated 2.5 % (w/v) PVP, 5 % (w/v) PLGA and 0.25 % (w/v) AM2/97 in DCM (Figures 3.17 & 3.18).

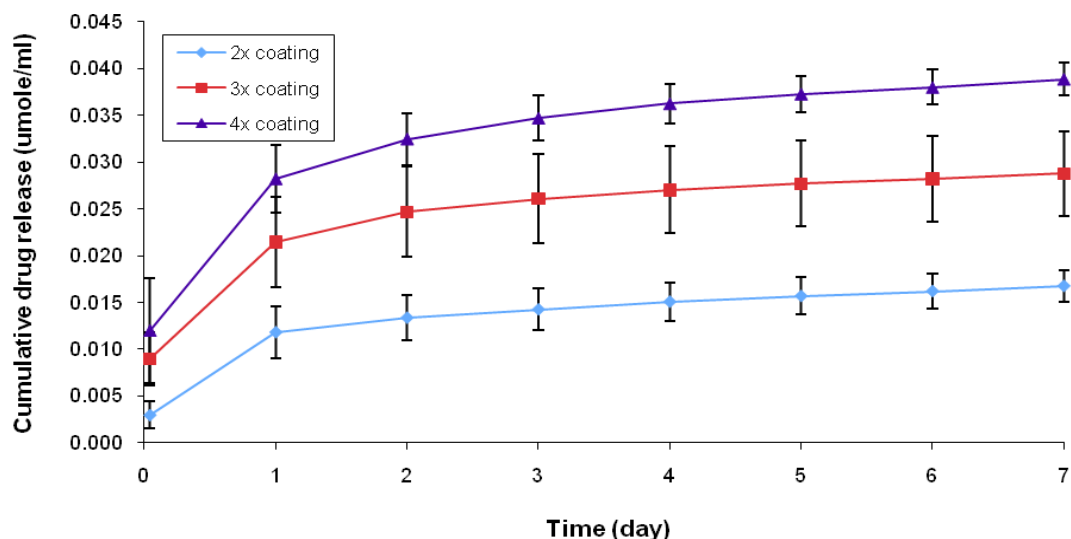


Figure 3. 17 Cumulative releases ($\mu\text{mole/ml}$) of the fluorescent FXIIIa inhibitor (AM2/97) into 10 ml PBS, from the individually coated polyurethane strips over 7 days under sink condition. The formulation was incorporating 2.5 % (w/v) PVP, 5 % (w/v) PLGA and 0.25 % (w/v) AM2/97 in DCM. Cumulative drug release corresponds to accumulation of the drug within the release media from day zero up to the measured time point, expressed as concentration ($\mu\text{mole/ml}$) of the inhibitor released. Results denote mean \pm SD from 3 independently synthesized batches.

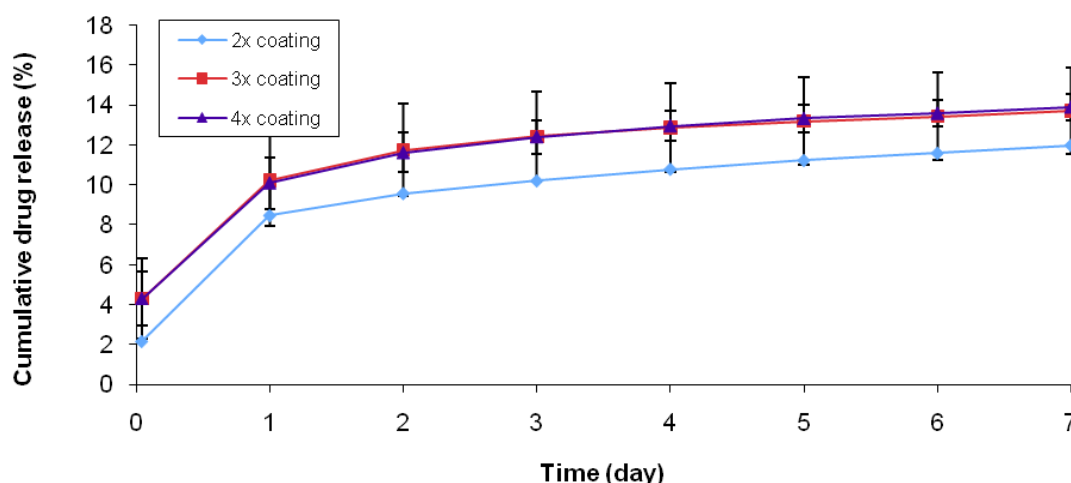


Figure 3. 18 Cumulative percentage release of the fluorescent FXIIIa inhibitor (AM2/97) into 10 ml PBS from the individually coated polyurethane strips over 7 days under sink condition. The formulation was incorporating 2.5 % (w/v) PVP, 5 % (w/v) PLGA and 0.25 % (w/v) AM2/97 in DCM. Cumulative drug release corresponds to accumulation of the drug within the release media from day zero up to the measured time point, expressed as percentage (%) of total drug added. Results denote mean \pm SD from 3 independently synthesized batches.

The cumulative percent drug release was in the proximity of 0.015, 0.025 and 0.037 $\mu\text{mole/ml}$ for 2, 3 and 4 times coating respectively (Figure 3.17), whilst the cumulative percentage of drug release for all the three coatings was approximately between 11 % and 14 % at the end of 7 days with no significant difference (Figure 3.18). It was deemed that utilization of the polymer blend for coating of the PU strips

increased the amount of drug release significantly. PVP, being a hydrophilic polymer undergoes dissolution and dissolves instantly. This process leads to the formation of channels in the PLGA-coating layers and eventually leads to drug release, which was not initially possible due to PLGA's hydrophobic nature (Kajihara, 2003).

To investigate the release profiles in a more potentially relevant media, fetal bovine serum (FBS) and PBS 50:50 (v/v) was utilised as the release medium in replacement of PBS, where the formulation of coating was amalgamating 2.5 % (w/v) PVP, 5 % (w/v) PLGA and 0.25 % (w/v) AM2/97 in DCM (Figures 3.19 & 3.20).

According to Figures 3.19 & 3.20 the cumulative percentage of drug release was measured from 11 – 14 % to 35 – 50 % for 2.5 % (w/v) PVP, 5 % (w/v) PLGA and 0.25 % (w/v) AM2/97 coated PU strips. The cumulative drug release was measured at around 0.05, 0.08 and 0.13 $\mu\text{mole/ml}$ for the PU strips coated 2, 3 and 4 times, by the end of 14 days. It was found that upon the substitution of the release medium, there was a substantial increase in the amount and duration of drug release.

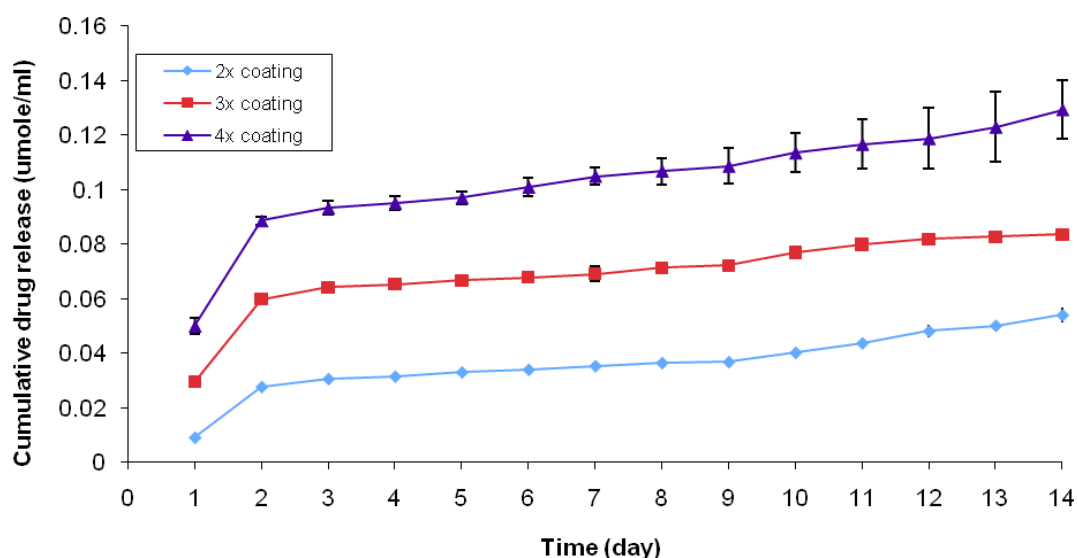


Figure 3. 19 Cumulative releases ($\mu\text{mole/ml}$) of the fluorescent FXIIIa inhibitor (AM2/97) into PBS: FBS 50:50 (v/v) from the individually coated polyurethane strips over 14 days under sink condition. The formulation was incorporating 2.5 % (w/v) PVP, 5 % (w/v) PLGA and 0.25 % (w/v) AM2/97 in DCM. Cumulative drug release corresponds to accumulation of the drug within the release media from day zero up to the measured time point, expressed as concentration ($\mu\text{mole/ml}$) of the inhibitor released. Results denote mean \pm SD from 3 independently synthesized batches.

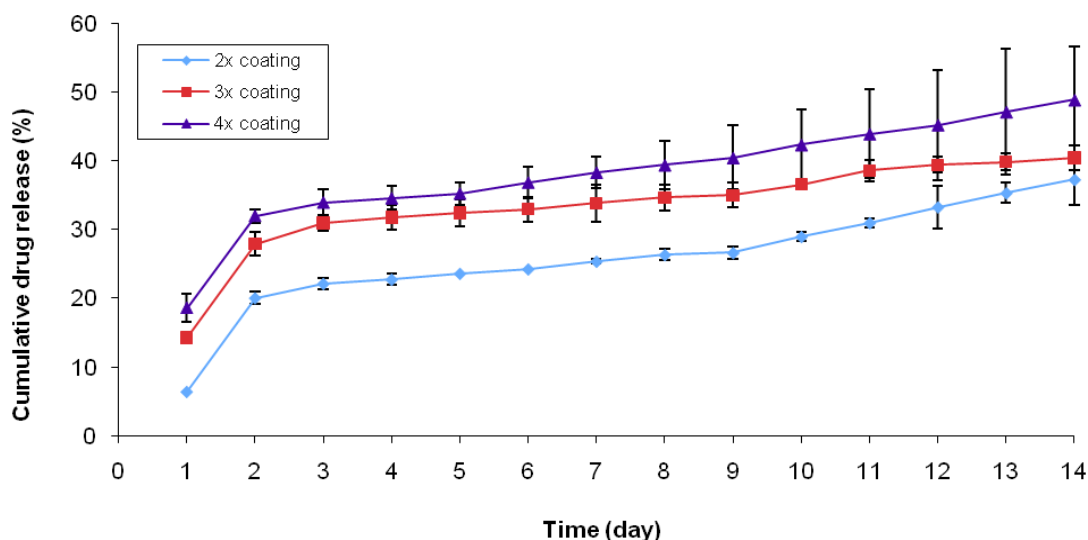


Figure 3. 20 Cumulative percentage release of the fluorescent FXIIIa inhibitor (AM2/97) into 10 ml PBS: FBS 50:50 (v/v) from the individually coated polyurethane strips over 14 days under sink condition. The formulation was incorporating 2.5 % (w/v) PVP, 5 % (w/v) PLGA and 0.25 % (w/v) AM2/97 in DCM. Cumulative drug release corresponds to accumulation of the drug within the release media from day zero up to the measured time point, expressed as percentage (%) of total drug added. Results denote mean \pm SD from 3 independently synthesized batches.

In an attempt to further enhance the total amount and duration of the enzyme inhibitor release, the percentage of incorporated PVP in the formulation was increased from 2.5 % to 5 % (w/v). The coating formulation was incorporating 5 % (w/v) PVP, 5 % (w/v) PLGA and 0.25 % (w/v) AM2/97 in DCM (Figures 3.21 and 3.22).

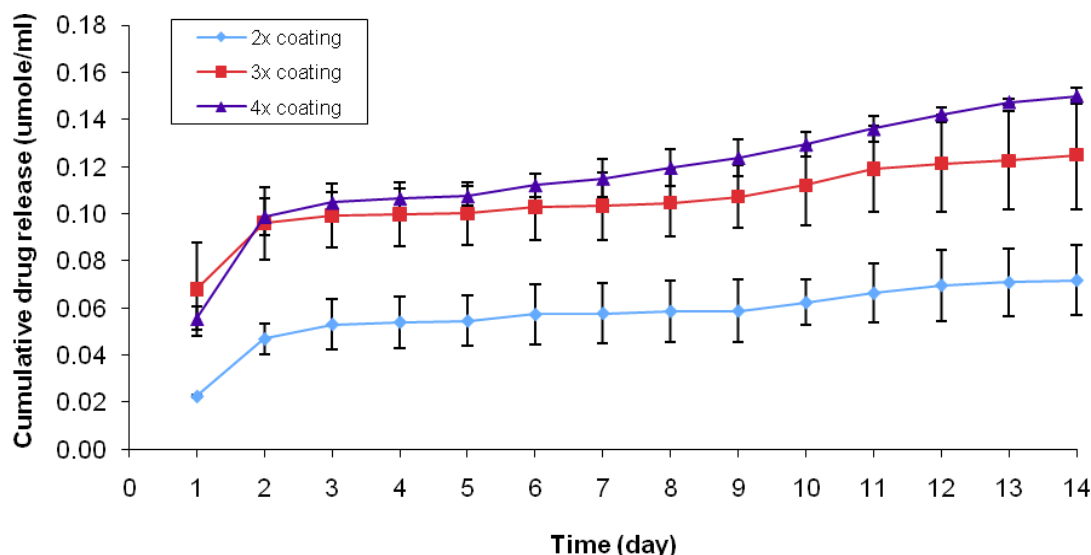


Figure 3. 21 Cumulative releases ($\mu\text{mole/ml}$) of the fluorescent FXIIIa inhibitor (AM2/97) into PBS: FBS 50:50 (v/v) from the individually coated polyurethane strips over 14 days under sink condition. The formulation was incorporating 5 % (w/v) PVP, 5 % (w/v) PLGA and 0.25 % (w/v) AM2/97 in DCM. Cumulative drug release corresponds to accumulation of the drug within the release media from day zero up to the measured time point, expressed as concentration ($\mu\text{mole/ml}$) of the inhibitor released. Results denote mean \pm SD from 3 independently synthesized batches.

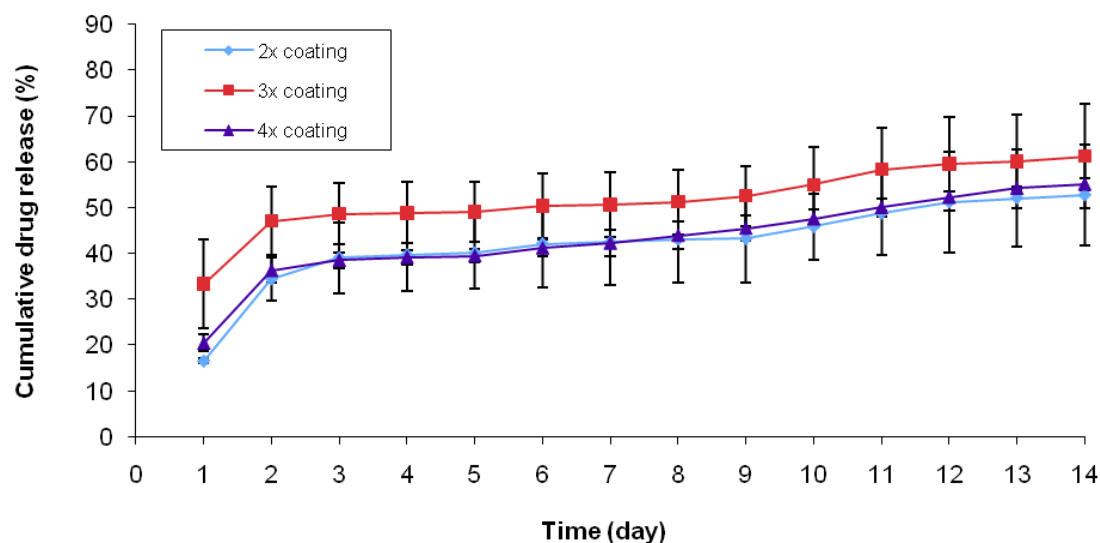


Figure 3. 22 Cumulative percentage release of the fluorescent FXIIIa inhibitor (AM2/97) into PBS: FBS 50:50 (v/v) from the individually coated polyurethane strips over 14 days under sink condition. The formulation was incorporating 5 % (w/v) PVP, 5 % (w/v) PLGA and 0.25 % (w/v) AM2/97 in DCM. Cumulative drug release corresponds to accumulation of the drug within the release media from day zero up to the measured time point, expressed as percentage (%) of total drug added. Results denote mean \pm SD from 3 independently synthesized batches.

Subsequent to increasing the quantity of incorporated PVP in the formulation, there was a significant increase in the cumulative percentage of drug release from 35 – 50 % to 50 – 70 %, and in the total cumulative drug release from ~ 0.05 - 0.13 $\mu\text{mole/ml}$ to ~ 0.07 – 0.15 $\mu\text{mole/ml}$ for 2, 3 and 4 times coating by the end of 14 days (Figures 3.21 & 3.22). This could be due to the formation of more channels in the coating of the PU strips upon the increasing of the percentage of incorporated PVP which eventually leads to sustained release of the larger amount of the enzyme inhibitor. The greater total cumulative drug release for 4 times coating in all the cases could be attributed to the higher amount of drug loading.

3.6 Conclusion

Within this study, various polymers according to the predefined test criteria were investigated; PVP & PLGA were selected as the most suitable polymers for dip-coating of the PU strips and further *in vitro* studies. The epifluorescent microscope images from the inhibitor-and polymer-coated PU strips confirmed the integration of the enzyme inhibitor throughout the coating of the strips. Upon incubation of the inhibitor-and polymer-coated strips in PBS, the PVP-coating was dissolved instantly, generating fast and significant drug release, whilst the PLGA-coating did not dissolve, yielding a slow and an insufficient amount of drug release. Nevertheless, the drug

release profile was enhanced upon employing a blend solution of PVP and PLGA for the coating.

| POLYMER | PERCENT SOLUTION (w/v) | The solubility and coating quality of the polymer within a range of solvents | | | | | | | | | | | | | | | | |
|--|---------------------------|--|---|-----------------------------------|---------|---|------------------------------------|---------|---|------------------------------------|------------|---|--|-----|---|-----------------------------------|---|--------------------|
| | | Methanol | | comments | Ethanol | | comments | Acetone | | comments | Chloroform | | comments | DCM | | comments | | |
| Polythylene-glycol | | S | C | Poor quality coating was observed | S | C | Polymer aggregates in ethanol | S | C | Polymer aggregates in acetone | S | C | Poor quality coating Insoluble solution | S | C | Polymer aggregates in DMC | | |
| H(OCH ₂ CH ₂) _n OH | 2% | √ | X | | X | - | | X | - | | √ | X | | X | - | | | |
| MW:8000 | 5% | √ | X | | X | - | | X | - | | X | - | | X | - | | | |
| | 10% | √ | X | | X | - | | X | - | | X | - | | X | - | | | |
| Polythylene-glycol | 2% | √ | X | Same as above | X | - | Same as above | X | - | Same as above | X | - | A thick white precipitate was observed | √ | X | Poor quality coating was observed | | |
| H(OCH ₂ CH ₂) _n OH | 5% | √ | X | | X | - | | X | - | | X | - | | X | - | X | - | Insoluble solution |
| MW:4600 | 10% | √ | X | | X | - | | X | - | | X | - | | X | - | X | - | |
| Polythylene-glycol | 2% | √ | X | Same as above | √ | X | Poor quality coating was observed. | √ | X | Poor quality coating was observed. | √ | X | yPoor quality coating was observed. | √ | X | Poor quality coating was observed | | |
| H(OCH ₂ CH ₂) _n OH | 5% | √ | X | | √ | X | | √ | X | | √ | X | | √ | X | | | |
| MW:2000 | 10% | √ | X | | √ | X | | √ | X | | √ | X | | √ | X | | | |

Table 1 The solubility and coating quality of polyethylene-glycol of various molecular weights within a range of solvents. S = the solubility of the polymer in the solvent, C = the coating of the PU strips, √ = good, √√ = very good and X= analysis not applicable.

| POLYMER | PERCENT SOLUTION (w/v) | The solubility and coating quality of the polymer within a range of solvents | | | | | | | | | | | | | | |
|---|---------------------------|--|---|----------|---------|---|----------|---------|---|----------|------------|---|----------|-----|---|---------------------------------|
| | | Methanol | | comments | Ethanol | | comments | Acetone | | comments | Chloroform | | comments | DCM | | comments |
| Polyethylene oxide -(CH ₂ -CH ₂ -O-) _n MW:1000,000 | | S | C | | S | C | | S | C | | S | C | | S | C | |
| | 2% | X | - | | X | - | | X | - | | X | - | | X | - | |
| | 5% | X | - | | X | - | | X | - | | X | - | | X | - | |
| | 10% | X | - | | X | - | | X | - | | X | - | | X | - | |
| Polyethylene oxide -(CH ₂ -CH ₂ -O-) _n MW:300,000 | 2% | X | - | | X | - | | X | - | | X | - | | √ | √ | A fragile coating was observed. |
| | 5% | X | - | | X | - | | X | - | | X | - | | √ | √ | |
| | 10% | X | - | | X | - | | X | - | | X | - | | X | - | |
| Polyethylene oxide -(CH ₂ -CH ₂ -O-) _n MW:5000,000 | 2% | X | - | | X | - | | X | - | | X | - | | X | X | |
| | 5% | X | - | | X | - | | X | - | | X | - | | X | - | |
| | 10% | X | - | | X | - | | X | - | | X | - | | X | - | |

Table 2 The solubility and coating quality of polyethylene oxide of various molecular weights within a range of solvents. S = the solubility of the polymer in the solvent, C = the coating of the PU strips, √ = good, √√ = very good and X= analysis not applicable.

| POLYMER | PERCENT SOLUTION (w/v) | The solubility and coating quality of the polymer within a range of solvents | | | | | | | | | | | | | | |
|--|------------------------|--|---|----------------------------|---------|---|-----------------------------------|---------|---|--------------------|------------|---|---|-----|---|--------------------------------------|
| | | Methanol | | comments | Ethanol | | comments | Acetone | | comments | Chloroform | | comments | DCM | | comments |
| Polyvinylpolypyrrolidone MW:360,000 | | S | C | A flimsy coat was observed | S | C | | S | C | | S | C | | S | C | |
| | 2% | √ | X | | √ | X | Not good coating | X | - | Insoluble solution | X | - | A milky white aggregate of the polymer was observed | √ | X | Poor quality coating was observed |
| | 5% | √ | X | | √ | √ | The coat splintered on drying. | X | - | | X | - | | X | - | Insoluble solution was observed |
| | 10% | √ | X | | √ | √ | coat dissolved in PBS | X | - | | X | - | | X | - | |
| Polyvinylpolypyrrolidone MW:10,000 | 2% | √ | X | Same as above | √ | X | Same as above | X | - | Same as above | √ | √ | The coat uncoupled when dried | √ | X | Poor quality coating was observed |
| | 5% | √ | X | | √ | √ | | X | - | | √ | √ | | √ | X | |
| | 10% | √ | X | | √ | √ | | X | - | | X | - | Insoluble | √ | √ | Coat dissol - ved in PBS |
| Polyvinylpolypyrrolidone MW:40,000 | 2% | √ | X | Same as above | √ | X | Poor quality coating was observed | X | - | Same as above | √ | √ | A good quality coating was obtained | √ | X | Poor quality coating was observed |
| | 5% | √ | X | | √ | | The coat splintered on drying. | X | - | | √ | √ | | √ | √ | A good quality coating was obtained. |
| | 10% | √ | X | | √ | √ | | X | - | | √ | √ | | √ | √ | |

Table 3 The solubility and coating quality of polyvinylpolypyrrolidone of various molecular weights within a range of solvents. S = the solubility of the polymer in the solvent, C = the coating of the PU strips, √ = good, √√ = very good and X= analysis not applicable

| POLYMER | PERCENT SOLUTION (w/v) | The solubility and coating quality of the polymer within a range of solvents | | | | | | | | | | | | | | |
|---------------------------------------|---------------------------|--|---|--------------------|---------|---|--------------------|---------|---|--------------------|------------|----|-----------------------------------|-----------------------------------|----|-----------------------------------|
| | | Methanol | | comments | Ethanol | | comments | Acetone | | comments | Chloroform | | comments | DCM | | comments |
| Poly(L-lactic acid) MW:300,000 | | S | C | | S | C | | S | C | | S | C | | S | C | |
| | 2% | X | - | Insoluble solution | X | - | Insoluble solution | X | - | Insoluble solution | √ | X | Poor quality coating was observed | √ | X | Poor quality coating was observed |
| | 5% | X | - | | X | - | | X | - | | √ | X | | √ | X | |
| | 10% | X | - | | X | - | | X | - | | X | - | Highly viscous solution | X | - | Highly viscous solution |
| Poly(L-lactic acid) MW:50,000 | 2% | X | - | Same as above | X | - | Same as above | X | - | Same as above | √ | X | Poor quality coating was observed | √ | X | Poor quality coating was observed |
| | 5% | X | - | | X | - | | X | - | | √ | √√ | | | √ | |
| | 10% | X | - | | X | - | | X | - | | √ | √√ | | √ | √√ | |
| Poly(L-lactic acid) MW:2000 | 2% | X | - | Same as above | X | - | Same as above | X | - | Same as above | √ | √ | Coat dissol-ves in PBS | X | √ | Coat dissolves in PBS |
| | 5% | X | - | | X | - | | X | - | | √ | X | | Poor quality coating was observed | X | |
| | 10% | X | - | | X | | | X | - | | √ | X | X | | X | |

Table 4 The solubility and coating quality of poly(L-lactic acid) of various molecular weights within a range of solvents. S = the solubility of the polymer in the solvent, C = the coating of the PU strips, √ = good, √√ = very good and X= analysis not applicable.

| POLYMER | PERCENT SOLUTION (w/v) | The solubility and coating quality of the polymer within a range of solvents | | | | | | | | | | | | | | |
|---|---------------------------|--|---|--------------------|---------|---|--------------------|---------|---|--|------------|----|--|-----|----|-----------------------|
| | | Methanol | | comments | Ethanol | | comments | Acetone | | comments | Chloroform | | comments | DCM | | comments |
| Poly(D,L-lactide-co-glycolide) 50:50 | | S | C | | S | C | | S | C | | S | C | | S | C | |
| | 2% | X | - | Insoluble solution | X | - | Insoluble solution | X | - | Insoluble solution | √ | √ | Good coating | √ | X | Coat dissolved in PBS |
| | 5% | X | - | | X | - | | X | - | | √ | √ | | X | X | |
| | 10% | X | - | | X | - | | X | - | | √ | √ | | X | - | Insoluble solution |
| Poly(D,L-lactide-co-glycolide) 85:15 | 2% | X | - | Same as above | X | - | Same as above | √ | √ | Good coating but the coat dissolved in PLA | √ | √ | A very good quality coating was observed | √ | √ | |
| | 5% | X | - | | X | - | | √ | √ | | √ | √√ | | √ | √√ | |
| | 10% | X | - | | X | - | | √ | √ | | √ | √√ | | √ | √√ | |

Table 5 The solubility and coating quality of poly(D, L-lactic-co-glycoside) of various molecular weights within a range of solvents. S = the solubility of the polymer in the solvent, C = the coating of the PU strips, √ = good, √√ = very good and X= analysis not applicable

Chapter 4:
**Controlled release of FXIIIa inhibitor from silicone
elasotomers**

4.1 Introduction

Silicones $[R_2SiO]_n$ are a large family of organic silicon polymer products which consist of a main chain of alternating silicon and oxygen atoms (...-Si-O-Si-O-Si-O-...) with four-coordinate organic side groups attached to the silicon atoms. The basic repeating unit is known as silicone and typically each silicon in the chain carries two organic groups mainly methyl groups (CH₃).

The most common silicone is called poly (dimethylsiloxane) abbreviated to PDMS (Bondurant et al, 2000). This is the basic characteristic of compounds with the name silicones, assigned by Kipping (Kipping, 1904) based on their similarity with ketones, since there is on average

one silicon atom for one oxygen and two methyl groups in most cases. Silicone polymers can be simply transformed into a three-dimensional network a cross linking reaction, which allows the arrangement of chemical bonds between adjacent chains that form silicone elastomers (Figure 4.1).

Silicone is one of the most common forms of polymeric biomaterials and has been employed in the manufacture of catheters, stents, cardiac leads, respiratory aids and similar medical devices (Malcolm et al., 2004). Although, numerous recent studies have focused on biodegradable implantable materials (Commandeur et al., 2006), certain advantages are acquired from non-degradable biomaterials, including their ready removal due to adverse effects which arise from the drug (Brooke et al., 2008). The silicone-based devices have been reported to possess several desirable features, such as biostability, non-irritancy, non-toxicity, non-carcinogenicity, non-allergic, good moisture resistance, biocompatibility, thermal stability, mechanical flexibility, excellent UV resistance, good chemical resistance, moderate adherence and non-biodegradability during an optimal treatment period (Huie et al., 1985; Lee et al., 1997; Kajihar et al., 2003; Maeda et al., 2003; Lawrence and Turner, 2005; Mashak, 2008). Moreover, all-silicone apparatus can



Figure 4. 1 The 3-D polymer structure of silicone elastomer. Silicone elastomers are cross linked linear silicone fluids or gums with a three-dimensional structure (web image 12).

be produced with a relatively thin wall which creates a large drainage lumen in relation to external diameter, causing a longer time to encrust and block. This is an important factor to consider when conducting any comparative tests with other catheter types (Lawrence and Turner, 2005). Additionally, some cases, such as children with high risk malignancies receive silicone CVCs at the initiation of chemotherapy, leaving their peripheral veins in good condition (Haire et al., 1990), while insertion of non-tunneled polyurethane CVCs which are often used for continuous blood flow in adults (Johansson et al., 1999), may cause local vessel damage because of the stiffness of the material, with subsequent local thrombosis and infectious complications (Madero et al., 1997; Hahn et al., 1995).

Even though silicone elastomers are one of the widespread biomaterials utilised in medical device production, they have a relatively high coefficient of friction and the resulting lack of inherent lubricity leads to pain and tissue damage on device insertion and removal (Woolfson et al., 2003; Malcolm et al., 2004). Furthermore as with all biomaterials, silicone is also prone to surface formation of a drug-resistant microbial biofilm (Tunney et al., 1996; Marion-Ferey et al., 2003), leading to device-related infections and device blockage (Gorman and Tunney 1997; Haire et al., 1990; Malcolm et al., 2004). To reduce the risk of occlusion, different anticoagulation regimens including oral acetylsalicylic acid, minocycline, rifampin and heparin flushing or continuous heparin infusion have been described as detailed in chapter 1 (Stephens et al., 1993; Lawrence and Turner, 2005). Moreover, to overcome the problem of microbial biofilm formation *in vivo*, a variety of antimicrobial agents have been employed.

In spite of this, there are no definitive studies to support the claims by manufacturers that their products showed improvements over the standard catheters. A number of researchers have reported that silicone coated and all-silicone devices, as well as all other currently available devices, are unable of resisting biofilm growth or encrustation and so far no single material has been established to be significantly superior in decreasing catheter-associated complications (Lawrence and Turner, 2005).

4.2 Aim and objectives

The present study was to incorporate the novel group of the inhibitors of the enzyme Factor XIII (FXIII) into a lubricious silicone elastomer and subsequent polymeric coating of the produced elastomer in order to generate an optimized drug delivery system whereby a secondary sustained drug release profile occurs following an initial burst release for catheters and other medical devices.

It was proposed that impregnation of the FXIIIa inhibitors into the lubricious silicone elastomer would produce an optimized drug delivery system in preventing both catheter associated staphylococcal infection and a lower incidence of thrombotic occlusion. Furthermore, the new technique could be used as a local delivery system for extended release with an immediate onset of action for other poorly soluble compounds.

The objectives of this work were;

- Preparation of the silicone elastomer strips.
- Incorporation of the FXIIIa inhibitor into the silicone elastomer strips for sustained drug release.
- Quantification of the amount of the FXIIIa inhibitor release from the silicone elastomer strips *in vitro*.
- Determination of the biological activity of the released inhibitor from the silicone elastomer strips.
- Production of a smart polymeric coating on the silicone strips for initial immediate drug release.
- Morphological analysis of the silicone strips such as scanning electron microscopy, digital images and optical microscopy.
- Investigation of the mechanical properties of the silicone elastomer strips such as tensile strength and Young's modulus.

4.3 Materials and methods

4.3.1 Materials

MED5-6382 medical grade silicone elastomer (three component silicone: Base, cross-linker and catalyst) was obtained from Nusil Technology (Carpinteria, USA). Sodium bicarbonate and phosphate buffered saline were acquired from Sigma-Aldrich (Dorset, England). Citric acid was purchased from VWR international Ltd. Spacer palates were procured from Bio-Rad Laboratories, Inc. Unless stated otherwise PBS was used at 0.01 M, pH 7.4. Doubly distilled and filtered water was used in the preparation of all solutions. The silicone elastomers used in this study were manufactured by linear, hydroxy-terminated poly(dimethylsiloxane) macromolecules crosslinked with a low molecular weight tetraalkoxysilane crosslinking agent (TPOS), derived from propanol, in the presence of stannous octoate as a catalyst, via a condensation cure mechanism. AM2/97 (fluorescent-labeled FXIIIa inhibitor) was prepared within the chemistry department of Aston University by Dr. Alexandre Mongeot and Dr. Dan Rathbone as previously described (Griffin et al., 2008).

4.3.2 Preparation of silicone elastomer strips integrated the FXIIIa inhibitor: sustained drug release

As described in Figure 4.2, medical grade condensation cure silicone elastomers are conventionally manufactured by the cross linking of α,ω -hydroxyl functionalised poly(dimethylsiloxane) with a tetra-functional tetraalkoxysilane (tetrapropoxysilane) (tetrapropyl orthosilicate) (tetrapropyl silicate) (TPOS). TPOS is renowned as the standard crosslinking agent in the commercial manufacturing of medical grade silicone elastomers (Etienne et al., 1990; Qusseume et al., 1994; Woolfson et al., 2003). TPOS-cured silicone elastomers generate propan-1-ol as a by-product of the crosslinking reaction that forms the elastomer. The evaporation of a volatile substance such as propan-1-ol from a homogeneous polymeric material includes dissolution of the permeant in the matrix, its diffusion through the matrix, and subsequent evaporation from the surface of the polymer (Watson and Payne, 1990). Hence, propan-1-ol is lost from the surface of the elastomer rapidly (Woolfson et al., 2003). Such elastomers are nowadays regularly

utilised in drug delivery applications from silicone devices (Woolfson et al., 1999; 2003; Malcolm et al., 2003).

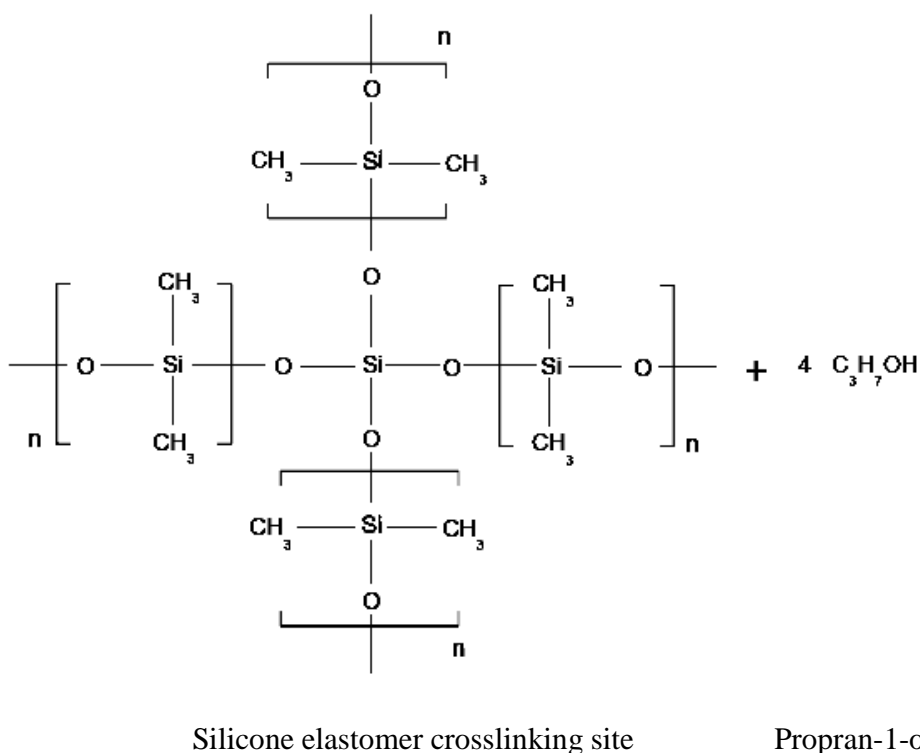
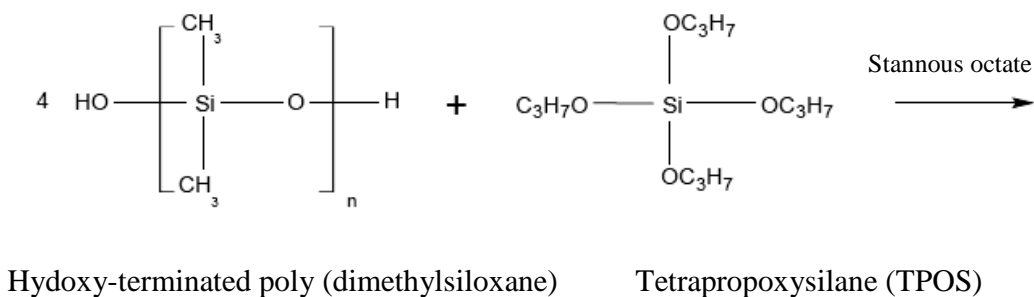


Figure 4. 2 Cross-linking chemistry between hydroxy-terminated poly(dimethylsiloxane) and tetrapropoxysilane (TPOS) in the production of condensation cured silicone elastomer (-drawn using Chemska software).

The conventional silicone elastomer mix was prepared by thoroughly mixing 2.5 parts by weight of TPOS as cross-linker, 97 parts of MED5-6382 silicone elastomer as base and 0.5 parts of stannous octate as catalyst for two minutes. Different percentages of citric acid (CA) and sodium bicarbonate (SB) (0 % (blank), 5 %, 15 %, 30 % and 40 % w/w) in

a ratio of 1:3 as additives, together with the FXIIIa inhibitor (AM2/97) (0.5 % and 1 % w/w) were incorporated into the mixture. The formulations prepared are listed in Table 4.1.

Table 4.1 Composition of silicone elastomer formulations

| Drug Powder | | Formulation |
|-------------|-------------|-----------------------|
| Drug | Content (%) | Additives (%) |
| AM2/97 | 0.5 % w/w | CA:SB = 1:3, 0 % w/w |
| AM2/97 | 0.5 % w/w | CA:SB = 1:3, 5 % w/w |
| AM2/97 | 0.5 % w/w | CA:SB = 1:3, 15 % w/w |
| AM2/97 | 0.5 % w/w | CA:SB = 1:3, 30 % w/w |
| AM2/97 | 0.5 % w/w | CA:SB = 1:3, 40 % w/w |
| AM2/97 | 1 % w/w | CA:SB = 1:3, 30 % w/w |

The silicone elastomer mixture was then placed between one spacer plate with 1.0 mm integrated spacers, with a size of 10.1 x 7.3 cm, and a short plate, with a size of 10.1 x 7.3 cm. The glass plates were left overnight at room temperature to de-aerate. The glass plates used were initially treated with an anti-static foam cleanser and a supergliss spray as a lubricant to avoid adherence of silicone mixture. The elastomeric silicone sheets thus produced were cut into strips of dimensions 10 × 30 mm using a scalpel and subsequently weighed (mean weight = 0.42 ± 0.08 g, mean surface area = 3.00 cm²).

4.3.3 Production of a smart polymeric coating on the silicone strips: initial immediate drug release

In order to obtain an immediate onset of action of drug, the silicone elastomer strips were then dip-coated with Poly-vinyl-pyrrolidone (PVP) as described in chapter 3. In brief, the polymer was dissolved in chloroform at a concentration of 5 % (w/w). Afterwards, 0.25 % (w/w) of the enzyme inhibitor was added to the polymer solution. The coating solution was kept on dry ice to prevent evaporation of the organic solvent and a subsequent increase in the polymer concentration. Subsequently, the silicone strips were vertically dip-coated in the polymer solution containing the inhibitor and withdrawn three times. The strips were coated using a two, three and four times dip-coating procedure to achieve a dense and regular polymer coating. The invariableness of the lifting velocity and

coating times was confirmed to yield approximately the same coating thickness. The coated silicone strips were dried at room temperature to allow the solvent to evaporate completely.

4.3.4 FXIIIa inhibitor release from the silicone elastomer strips *In vitro*

Each of the silicone strips was placed in a 50 ml universal tube containing 10 ml of 0.01 M of phosphate buffer saline (PBS, pH 7.4). The universal tubes were then put in a shaking water bath set at 80 rpm and 37 °C. The release medium was sampled and replaced every 24 hour (to promote sink condition) over a period of 30 or 40 days. The amount of relative fluorescent unit (RFU) within the release media was quantified using 200 µl aliquots taken every 24 hours and measured spectrofluorimetrically with an excitation maximum at 330 nm and emission peak at 570 nm (Spectra Max Gemini XPS, Molecular Probes). Accordingly the concentration of the inhibitor released within the media was calculated using a drug calibration curve which was previously prepared from a set of standard samples of known concentration. The results were then reported as cumulative drug release, which corresponds to accumulation of the drug within the release media from time zero up to the measured time point, expressed as percentage (%) of total drug added and concentration (µmole/ ml) of the inhibitor released. Estimation of the amount of the inhibitor entrapped within the coatings through dip-coating method was calculated by measuring the density of the coating solution and weight changes of the solution subsequent to each coating, which was followed by calculating the number of moles of the inhibitor incorporated per coating.

4.3.5 Biological activity of the released FXIIIa inhibitor

The biological activity of the released inhibitor from the silicone strips as inhibition of human FXIII was verified by applying ELSA as previously described, using aliquots of 200 µl which were collected from the release medium at preset incubation time points (one day, and one, two, three and four weeks). The results were then expressed as a percentage of FXIII activity compared to negative control (without the inhibitor).

4.3.6 Morphological analysis

4.3.6.1 Scanning electron microscopy (SEM)

The specimens were thoroughly dried and gold coated by a gold sputter coater (Emscope SC500 Sputter coater, Ashford, Kent, Great Britain) prior to SEM. Cross-sectional SEM images from silicone elastomer formulations were captured by a scanning electron microscope (Cambridge Instruments, Stereoscan 90) at 29 x, 49 x and 103 x magnification. The experimental conditions involved 0 %, 5 %, 15 % and 30 % (w/w) CA/ SB incorporated formulations, and before and subsequent to incubation (1 day, 1 week and 1 month time points) in PBS.

4.3.6.2 Digital images

The appearance of the silicone strips was examined by a JVC KY-F1030 digital camera fitted with a zoom lens (18-108 / 2.5, Japan, NO-5019055) for 0 %, 5 %, 15 % and 30 % (w/w) CA/ SB integrated formulations, prior to and after one month incubation in PBS.

4.3.6.3 Optical microscopy

Optical images were obtained from the surface of the silicone elastomer specimen, using a Reichert-Jung Polyvar MET optical microscope with a JVC KY-F75 digital camera, at 25 x and 50 x magnification. This was conducted in set conditions previously mentioned in section 4.3.6.1.

4.3.7 Swelling studies

The weight dimensions (width, length and thickness) and volume of silicone elastomer strips prior to and subsequent to incubation (1 day, 1 week and 1 month time points) in PBS (pH 7.4, 37 °C) were measured by a digital caliper. Accordingly, the swelling (alteration in the volume) of each strip after the preset time points was calculated. The results were then reported as percent change in the volume.

4.3.8 Mechanical properties

4.3.8.1 Tensile strength

Tensile properties were measured by a Hounsfield Universal Tester S Series H10KS-0393 (Figure 4.3). The Hounsfield S Series was supplied by Tinius Olsen Ltd (Surrey, UK) with Q-Mat 2.18 software including Test Generator, Testzone and File examination. The crosshead was able to move at jog speeds of 0.001 to 1000 mm/min, with an extension accuracy of ± 0.01 mm and a speed accuracy of ± 0.05 % of the set speed. The experimental set up is presented in Table 4.2.

Stretching apparatus:

The tensile strength (MPa) of the silicone strips was measured to investigate the greatest lengthwise stress the strips could withstand without breaking. While the Hounsfield universal tester (Figure 4.3) loads the strip, it measures the applied force and the elongation of the specimen over some distance. The amount of applied force and consequently stress on the strip is continuously increased until the rupture of the specimen (Figure 4.4). The level of exerted force required to pull the strip to the point where it breaks is directly proportional to the amount of tensile strength. The amount of force exerted on the specimen (Newton) (N) divided by the cross-sectional area (A) (m^2) (mm^2) of the strip, yields the stress experienced by the sample and the stress needed to break the strip is the tensile strength of the sample which is expressed as Pa or MPa.

$$\text{TS} = \text{Force (N)} / \text{cross-sectional area (Equation 4.1)}$$

In the SI system, the unit of measurement of tensile strength is the Newton per square meter (N/m^2), also known as the Pascal (Pa), where $1\text{MPa} = 1\text{ N/mm}^2$



Figure 4. 3 Hounsfield H10KS Universal Testing Machine

Table 4.2 Experimental setup of Hounsfield Universal Tester for measuring the tensile strength of the silicone strips.

| | Setup | Range available |
|--------------------------------|--------------|------------------------|
| Load Range (N) | 5000 | [50-5000] |
| Extension Range (mm) | 2000 | [0.1-2000] |
| Speed (mm/min) | 50 | [0.01-1000] |
| Gauge Length (mm) | 20 | [1-1000] |
| Approach Speed (mm/min) | 50 | [0.0005-1000] |
| Preload (N) | 0 | [0-500] |

4.3.8.2 Force-extension curve

The Force-extension curves are a graphical representation of the relationship between force and extension. The curves were obtained by plotting the force which was derived from measuring the load on a silicone strip along the x-axis and extension which was derived from measuring the elongation of the strip before the break along the y-axis.

4.3.8.3 Young's modulus (modulus of elasticity) (elastic modulus) (Tensile modulus)

Young's modulus (E) was measured by plotting the amount of applied stress on the silicone strip versus elongation which were previously obtained during tensile tests conducted on silicone strips. The height of the curve when the strip breaks is the tensile strength and the Young's modulus is the slope of this plot. Therefore, the modulus of elasticity was calculated easily by dividing the tensile strength at break by the strain at break (Woolfson et al., 2003).

$$E = \text{Stress/Strain} = (F/A) / (L_i/L_o) = (F \cdot L_o) / (A \cdot L_i) \text{ (Equation 4.2)}$$

Where E is Young's modulus, F is the force applied, A is the cross sectional area of the object, L_o is the original length, and L_i is the alteration in length. The Young's modulus is expressed in units such as the Pascal, Newton per square meter or MPa.

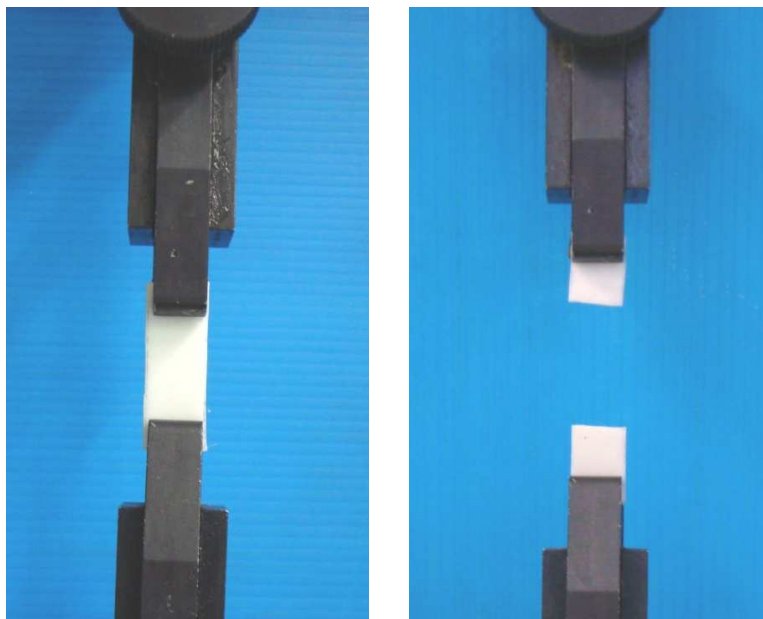


Figure 4. 4 Measuring the tensile strength and Young's modulus of the silicone strips by a Hounsfield Universal Tester. The silicone strip was held between upper and lower clamps and then the crosshead moved upwards. Subsequently, the amount of applied force continued to increase till the strip was broken.

4.3.9 Statistical analysis

For all experiments, means and standard deviations were calculated and represent one of at least three separate experiments undertaken in triplicate, unless stated otherwise. To determine statistical significance in resultant data, a one-way analysis of variance (ANOVA) was performed. Differences described as significant or extremely significant in the text correspond to $p < 0.05$ or $p < 0.001$ respectively. Tukey's post hoc test was conducted to determine which conditions differ significantly from each other.

4.4 Results and discussions

4.4.1 Drug release mechanism

Diffusion can be defined '*as a process by which molecules transfer spontaneously from one region to another in such a way as to equalise chemical potential or thermodynamic activity*' (Liu, 2001). Diffusion-controlled release is one of the few mechanisms by which drug release rate is controlled. Generally, in diffusion-controlled release mechanisms, the drug must diffuse through either a polymeric membrane or a polymeric or lipid matrix in order to be released. The rate of diffusion of drug molecule through the membrane can be described by classical Fick's law of diffusion (Kim, 2000; Fan and Singh, 1989) and is

thus dependant on the partition and diffusion coefficient of the drug in the membrane, the available surface area, the membrane thickness and the drug concentration gradient (Figure 4.5).

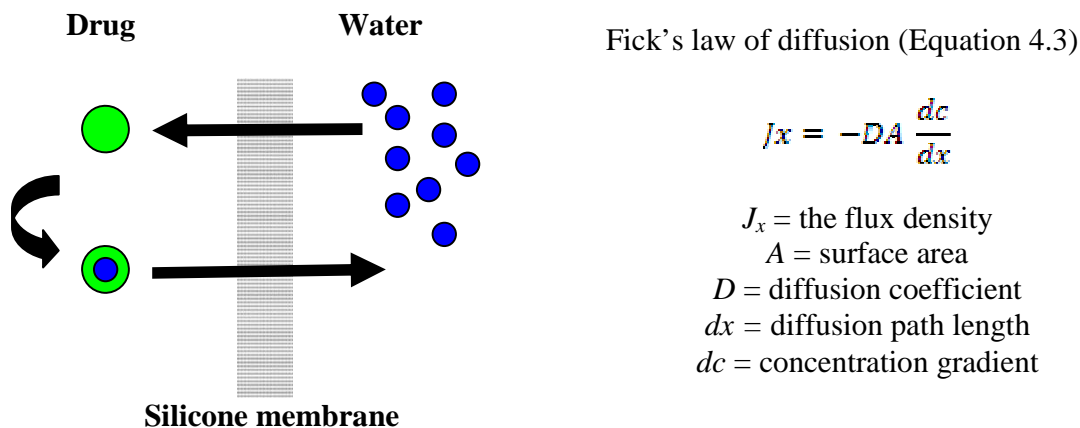


Figure 4. 5 Fick's law of diffusion in diffusion controlled devices. Fick's law of diffusion describes the rate at which diffusion occurs, where J_x (the flux density) is the amount of species x crossing a certain area per unit time and is typically expressed in units such as moles of particles per m^2 per second. D is the diffusion coefficient of species x . The term dc/dx represents the concentration gradient of species x and is the driving force that leads to molecular movement. The negative sign indicates that the direction of flow is from high to low concentration.

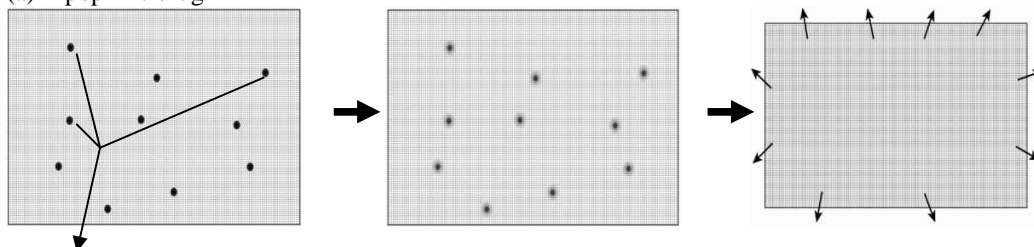
During preliminary studies, no drug release was observed from the silicone elastomer preparations after incubation in PBS. To overcome this problem, different alternatives were applied such as;

1. Changing the release media (PBS, distilled H_2O)
2. Reducing the particle size of the inhibitor by milling and using different mesh sizes (100-300 μm)
3. Reducing the percentage of cross linker in the formulations (from 2.5 % down to 1.25 %)

In spite of these approaches, the percentage of drug release from silicone carriers did not alter substantially. This could be due to poor solubility of the enzyme inhibitor. The release characteristics of drugs from diffusion-controlled polymeric delivery systems are largely determined by the solubility and diffusivity of the drug within the cross-linked polymer network (Chien et al., 1992). Therefore, the drug release mechanism from a silicone carrier differs depending on the physiochemical properties of the drugs (Figure 4.6); lipophilic drugs are solubilized in silicone, diffuse, and are released (Figure 4.6a).

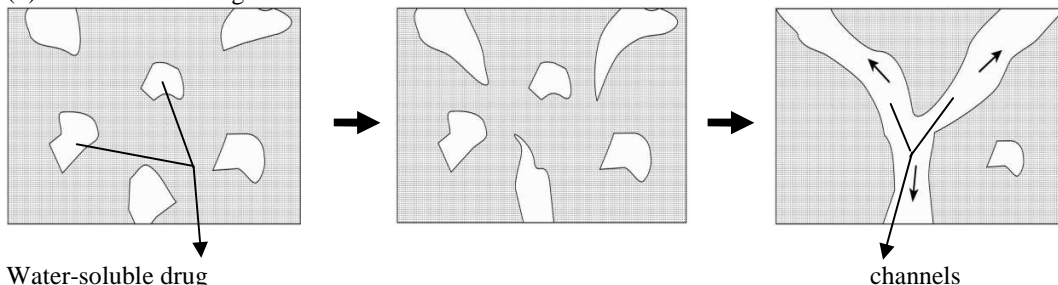
Water-soluble drugs neither dissolve nor diffuse in silicone (Figure 4.6b). At the outset, water-soluble drugs existing on the surface, and subsequently the ones in the near-surface area dissolve into water. Recurrence of these processes leads to channel formation, allowing water-soluble drugs in the bulk to be released. Conversely water insoluble drugs neither dissolve nor diffuse in silicone (Figure 4.6c), they are not released since channels are not formed because of insolubility in water. Therefore, their release from silicone has long been considered challenging (Kajihara, 2003).

(a) Lipophilic drug



Lipophilic drug

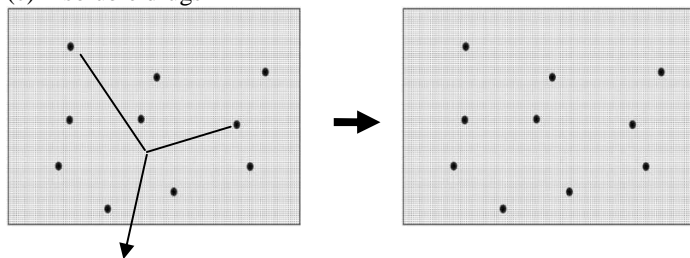
(b) Water-soluble drug



Water-soluble drug

channels

(c) Insoluble drugs



Insoluble drugs

Figure 4. 6 Release mechanisms of drugs with different physiochemical properties from a silicone carrier. Lipophilic drugs are solubilized in silicone, diffuse, and eventually are released (Figure 4.6a). Water soluble drugs neither dissolve nor diffuse in silicone (Figure 4.6b). Water-soluble drugs exist on the surface area, and then, those existing in the near-surface area dissolve into water. Recurrence of these sequences lead to channel formation, allowing water-soluble drugs in the bulk to be released. On the contrary, insoluble drugs neither dissolve nor diffuse in silicone (Figure 4.6c), they are not released as channels are not formed due to insolubility in water (Kajihara, 2003).

4.4.2 Influence of additives on release behaviour

4.4.2.1 Sustained drug release from the silicone elastomer strips

Given the poor release of the FXIIIa inhibitors outlined already, a second approach was adopted. The release of insoluble or poorly soluble drugs from silicone carriers can be enhanced by employing additives. Accordingly, sodium bicarbonate (SB) and citric acid (CA) were added as additives to the silicone formulations. The fluorescent FXIIIa inhibitor as a poorly soluble drug was not released from the silicone carrier when it was dispersed in the silicone devoid of additives (0 % (w/w) CA and SB). However, the release of the enzyme inhibitor increased correspondingly with incorporation of CA and SB in the silicone strips (Figures 4.7 and 4.8).

The results in Figures 4.7 and 4.8 indicate that the silicone preparations released the inhibitor in the rate depending on the concentrations of CA and SB (0 %, 5 %, 15 % and 30 % (w/w)). The amount (and percentage) of the inhibitor release from all the preparations tested was enhanced by increasing CA and SB content. The amount (and percentage) of released inhibitor from the formulations containing 30 % (w/w) CA and SB powders was greater than the amount (and percentage) released from the preparations containing 15 % and 5 % (w/w) CA and SB powders, respectively. Similarly, the level and percentage of release from formulations containing 15 % (w/w) CA and SB powders was more than that of 5 % (w/w) formulation ($P < 0.05$, ANOVA). For example after 1 day, 0.007 and 0.012 $\mu\text{mol/ml}$ of drug was released from silicone formulations containing 5 % and 15 % (w/w) of CA and SB respectively, whilst significantly higher amounts (0.032 $\mu\text{mol/ml}$) were released from silicone preparations containing 30% of the additives. By day 7, the release rates from the silicone preparations were leveling out at approximately 0.098 $\mu\text{mole/ml}$, which was about 5-fold higher than the amount released by preparations containing 5 % and about 3-fold higher than those containing 15 % of the additives. For each of the four preparations (0 %, 5 %, 15 % and 30 % (w/w) CA and SB) the maximum released after 30 days was 0, 0.043, 0.087 and 0.147 $\mu\text{mole/ml}$ respectively. These data as a percentage of initial amounts loaded are illustrated in Figure 4.8. Water-soluble CA and SB forms channels and pores in and on the specimen and react upon mixing to generate carbon dioxide in the channels. The gaseous carbon

dioxide as a driving force accelerates the release of the inhibitor (Figure 4.9). A faster release was attained by altering the quantity of carbonate and acid in the formulations from 0 % to 30 %, thus generating a larger amount of carbon dioxide (Kajihara, 2003).

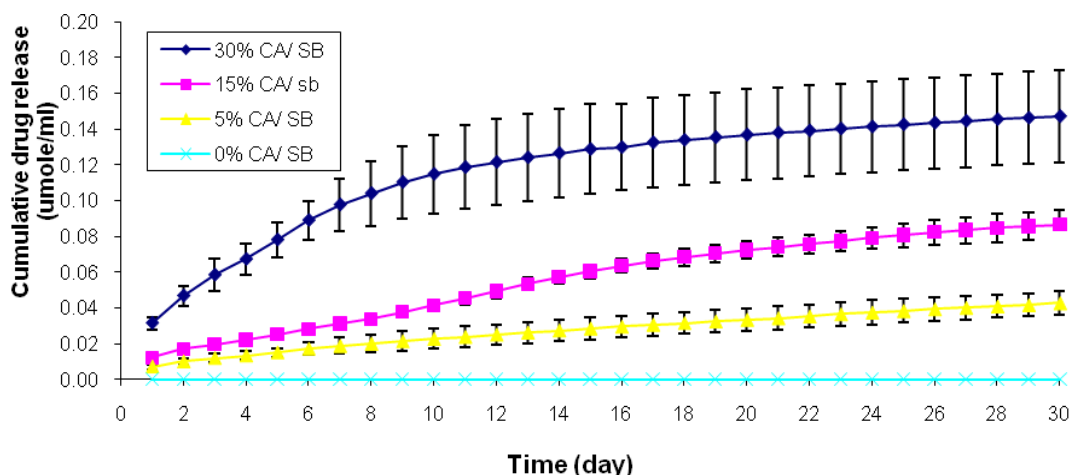


Figure 4. 7 Cumulative releases ($\mu\text{mole/ml}$) of the fluorescent FXIIIa inhibitor (AM2/97) into 10 ml PBS from the silicone elastomer strips over 30 days under sink condition. The formulations incorporated 0 %, 5 %, 15 %, 30 % (w/w) CA: SB, and 0.5 % (w/w) AM2/97. Cumulative drug release corresponds to accumulation of the drug within the release media from day zero up to the measured time point, expressed as concentration ($\mu\text{mole/ml}$) of the inhibitor released. No release was observed from the silicone carriers when it was dispersed inside the silicone devoid of additives (0 % CA: SB). The amount of drug release increased significantly when the percentage of acid and carbonate was raised. Results denote mean \pm SD from 3 independently synthesized batches.

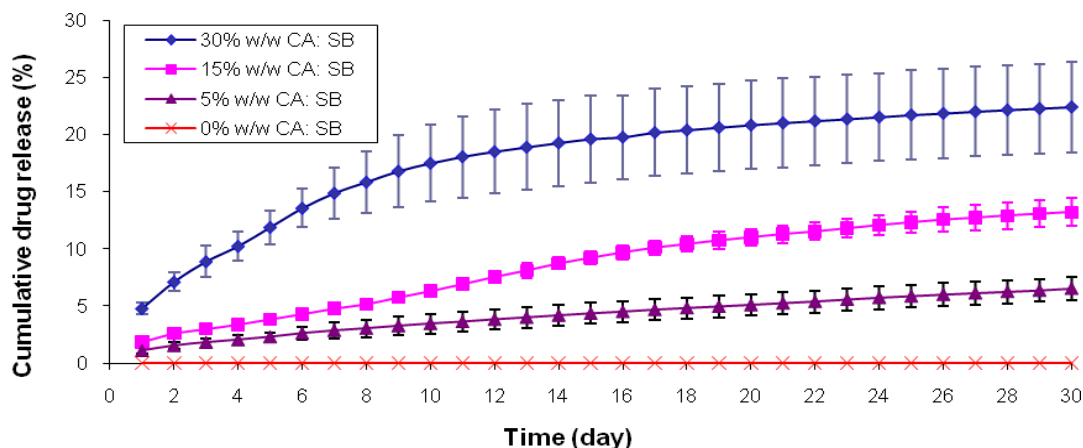


Figure 4. 8 Cumulative percentage release of the fluorescent FXIIIa inhibitor (AM2/97) into 10 ml PBS from the silicone elastomer strips over 30 days under sink condition. The formulations incorporated 0 %, 5 %, 15 %, 30 % (w/w) CA: SB, and 0.5 % (w/w) AM2/97. Cumulative drug release corresponds to accumulation of the drug within the release media from day zero up to the measured time point, expressed as percentage (%) of total drug added. No release was observed from the silicone carriers devoid of additives (0 % CA: SB). The amount of drug release increased significantly when the percentage of acid and carbonate was raised. Results denote mean \pm SD from 3 independently synthesized batches.

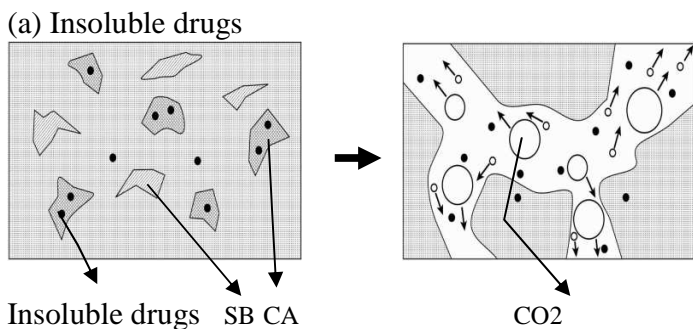


Figure 4. 9 Diagrams demonstrating the process of drug release from a silicone carrier. Insoluble drugs can be released from the strips by gas generation using sodium bicarbonate and citric acid as additives (Kajihara, 2003).

Nevertheless further increase in the content of sodium bicarbonate and citric acid was not achieved as silicone elastomers could not be formed with the formulation incorporating 40 % (w/w) CA and SB, as a result of the high powder content in the specimen. This prevented the process whereby polymers become interlinked to form a solid, three-dimensional matrix.

Additionally, increasing the amount of drug loaded in the preparation (from 0.5 % to 1 %) at 30 % (w/w) CA and SB improved significantly the duration of release from 30 days to 40 days and also total amount of release from 0.173 to 0.286 $\mu\text{mol/ml}$, but caused a decline in the percentage of drug release from 26.27 % to 21.75 %, after 40 days (Figures 4.10 & 4.11). This could be due to the low solubility of the inhibitor.

Furthermore with regard to Figures 4.7 – 4.11, the rate of drug release decreased regularly for the first 14 days. Afterwards, a slow and constant drug release could be observed for the rest of the time points for all formulations incorporating acid and carbonate powders. If the drug concentration gradient remains constant, for instance where solid drug particles are present and constant dissolution maintains the concentrations of the drug in solution, the rate of drug release does not vary with time and zero-order controlled release is attained. However, in the present study, regardless of the drug's physical state in the polymeric matrix, this device does not provide zero-order drug release properties. This is because as the drug molecules at the surface of the device are released, those in the center of the device have to migrate a longer distance to be

released. This increased diffusion time results in a decrease in the release rate from the device with time (Hillery, 2001).

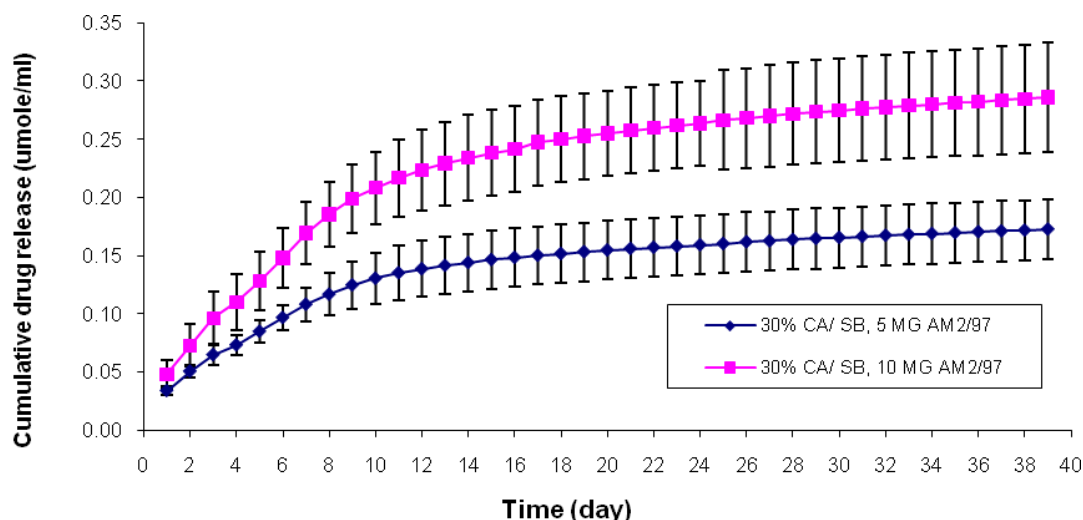


Figure 4. 10 Cumulative releases ($\mu\text{mole/ml}$) of the fluorescent FXIIIa inhibitor (AM2/97) into 10 ml PBS from the silicone elastomer strips over 40 days under sink condition. The formulations were incorporating 30 % (w/w) CA: SB, 0.5 % and 1 % (w/w) AM2/97. Cumulative drug release corresponds to accumulation of the drug within the release media from day zero up to the measured time point, expressed as concentration ($\mu\text{mole/ml}$) of the inhibitor released. Augmenting the amount of inhibitor in formulations is increasing the amount of cumulative release. Results denote mean \pm SD from 3 independently synthesized batches.

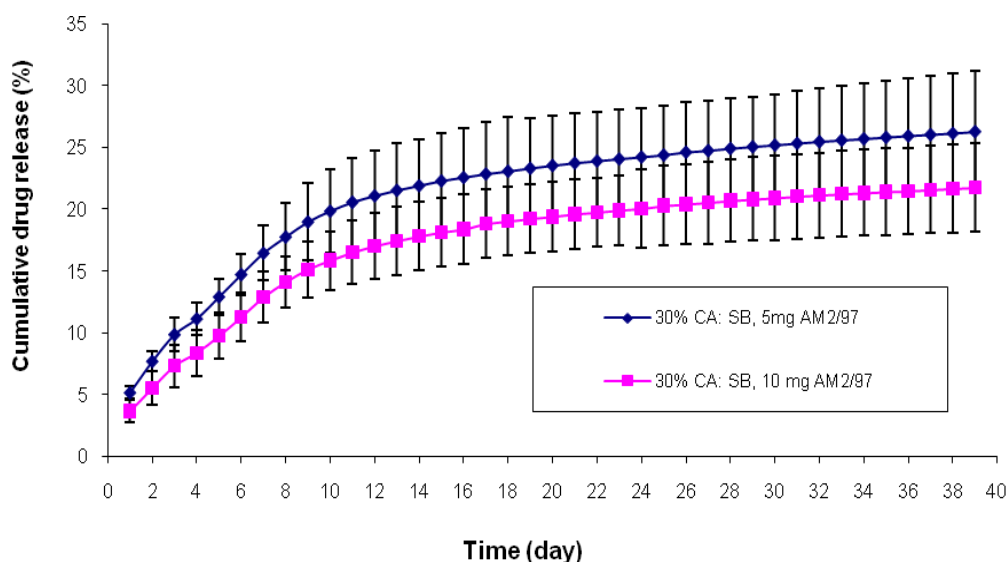


Figure 4. 11 Cumulative percentage release of the fluorescent FXIIIa inhibitor (AM2/97) into 10 ml PBS from the silicone elastomer strips over 40 days under sink condition. The formulations were incorporating 30 % (w/w) CA: SB, 0.5 % and 1 % (w/w) AM2/97. Cumulative drug release corresponds to accumulation of the drug within the release media from day zero up to the measured time point, expressed as percentage (%) of total drug added. Augmenting the amount of inhibitor in formulations is decreasing the percentage of release. Results denote mean \pm SD from 3 independently synthesized batches.

4.4.2.2 Initial immediate drug release

In some cases an initial burst release of drug followed by a secondary sustained drug release is favoured. To investigate the potential of this, after manufacturing, the silicone elastomer strips was dip-coated with a hydrophilic polymer such as PVP by a solvent casting technique as described previously in chapter 3.

The incorporated inhibitor demonstrated an immediate drug release within the first 5 minutes of much of the loaded drug (Figure 4.12 & 4.13). For those systems coated twice with the PVP coating, 100 % release was achieved within 30 minutes, whilst maximum amounts of released drug were around 80 % and 70 %, respectively, for 3 x and 4 x PVP coating. Initially, the drug release may be controlled by the dissolution rate of polymer coating over time. Upon contact of the polymer coating of the silicone strips with PBS, a rapid release of the incorporated inhibitor from the surface on hydration and consequently dissolution of the biodegradable polymer was achieved. Furthermore, it can be concluded that increasing the number of coatings does not affect the release time but affects the concentration of drug released into the media, due to the higher total concentrations within the coat.

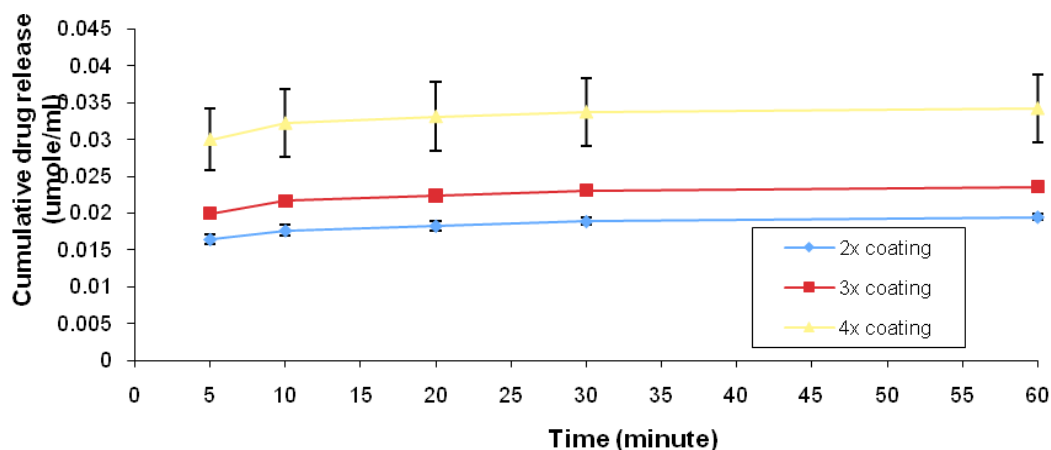


Figure 4. 12 Cumulative release ($\mu\text{mole/ml}$) of the fluorescent FXIIIa inhibitor (AM2/97) into 10 ml PBS from the silicone elastomer strips with 2, 3 and 4x PVP coatings over 60 minute under sink condition. The formulations contained 5 % (w/w) PVP and 2.5 % (w/w) AM2/97. Cumulative drug release corresponds to accumulation of the drug within the release media from day zero up to the measured time point, expressed as concentration ($\mu\text{mole/ml}$) of the inhibitor released. The incorporated inhibitors showed an immediate release within the first 5 minutes of much of the loaded drug. Results denote mean \pm SD from 3 independently synthesized batches.

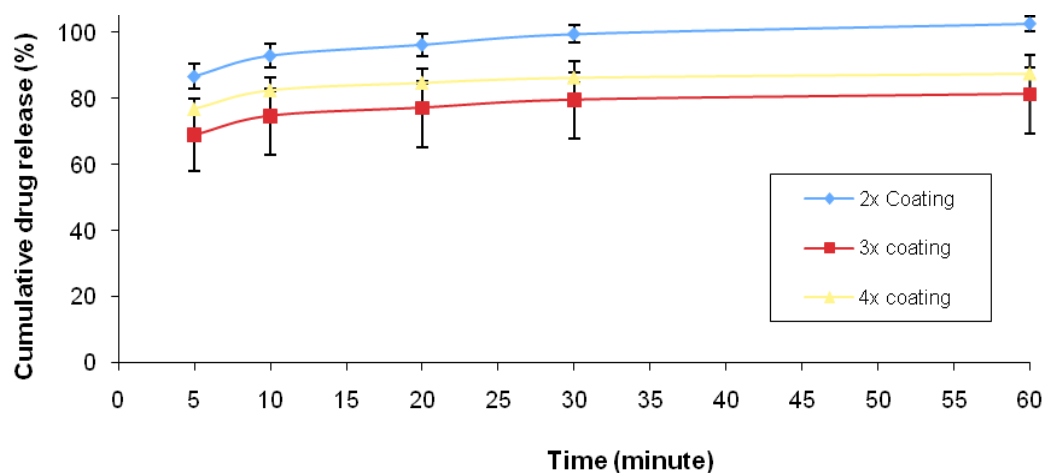


Figure 4. 13 Cumulative percentage release of the fluorescent FXIIIa inhibitor (AM2/97) into 10 ml PBS from the silicone strips with 2, 3 and 4x PVP coatings over 60 minutes under sink condition. The formulations contained 5 % (w/w) PVP and 2.5 % (w/w) AM2/97. Cumulative drug release corresponds to accumulation of the drug within the release media from day zero up to the measured time point, expressed as percentage (%) of total drug added. The incorporated inhibitors showed an immediate release within the first 5 minutes of much of the loaded drug. Results denote mean \pm SD from 3 independently synthesized batches.

4.4.3 Biological activity of the released inhibitors

The biological activity of the released inhibitor from the silicone elastomer strips in inhibition of human FXIIIa for a period of one month was then investigated by applying ELSA.

Table 4.3 Measurement of biological activity of the released inhibitors, using an enzyme linked sorbent assay. The results were expressed as a percentage activity of TG compared to positive control (without the inhibitor). Results denote mean \pm SD from 3 independently synthesized batches.

| Inhibitor (w/w) | % activity of TG | | % reduction in activity of TG | |
|-----------------|------------------|-------|-------------------------------|-------|
| | 1 % | 0.5 % | 1 % | 0.5 % |
| time | | | | |
| 1 Day | 9.12 | 16.06 | 90.88 | 83.94 |
| 1 week | 6.55 | 12.06 | 93.45 | 87.94 |
| 2 week | 54.34 | 57.90 | 45.66 | 42.10 |
| 3 week | 46.16 | 50.23 | 53.84 | 49.77 |
| 4 week | 78.30 | 82.20 | 21.70 | 17.80 |

Results in Table 4.3 indicates that biological activity of the released inhibitor was gradually reduced and consequently the activity of TG was increased as the amount of inhibitor released from the silicone strips decreased over a one month period. Therefore,

it can be concluded that the inhibitor is still biologically active after the release from the silicone elastomer strips; however the inhibitory activity decreases as the amount of released inhibitor decreases.

4.4.4 Scanning electron microscopy

To investigate the morphology of the silicone strips before and subsequent to immersion in PBS, SEM analysis of the strips was performed. Cross sectional SEM images (Figures 4.14 - 4.17) captured from the silicone elastomer strips containing 5 %, 10 % and 30 % (w/w) CA/ SB prior to and after to incubation in PBS (37 °C, pH 7.4) confirmed the formation of channels and cracks inside the specimens. As the percentage of incorporated CA/ SB was raised, the number and size of pores and channels generated as a result of generating a larger amount of carbon dioxide was increased. The amount of channels and pores at 30 % (w/w) CA/ SB integrated preparations was considerably higher than that of formulations containing 0 %, 5 % and 15 % (w/w) CA/ SB. In contrast, in 0 % incorporated CA/ SB (blank), no channels or pores were observed. As previously stated, SB and CA might create channels and pores upon mixing and the high pressure caused by the consequent production of carbon dioxide eventually leads to sustained release of the inhibitor.

Similarly, the production of pores and channels in specimens was found to be directly proportional to the length of incubation time. As a consequence, there is a greater amount of pores and channels in the one-month incubated strips as opposed to the one-day and one-week incubated specimens, for all the formulations tested. This could be attributed to the creation of more and larger channels and cracks over time (Figures 4.14 to Figures 4.17).

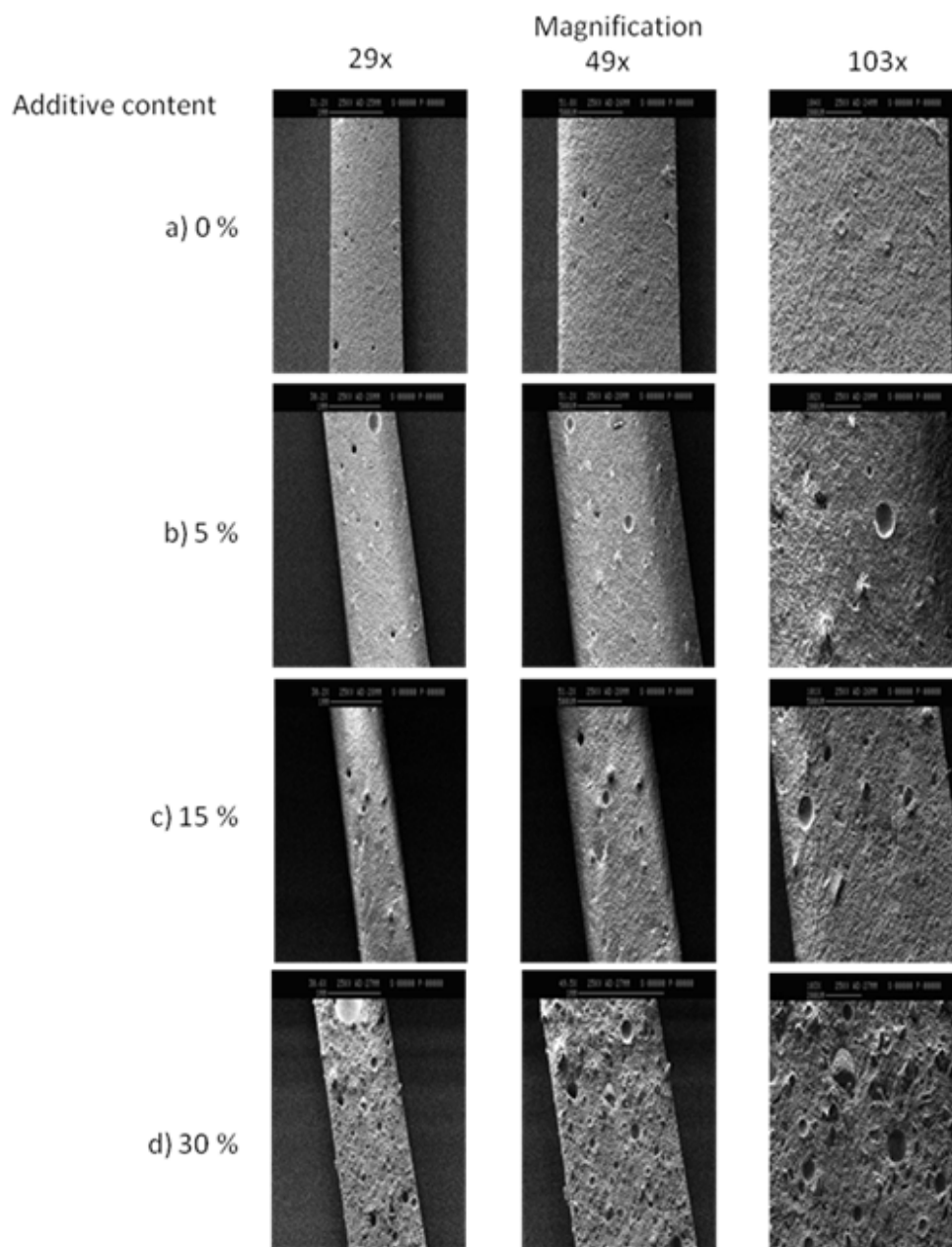


Figure 4. 14 Cross sectional SEM images from the silicone elastomer strips containing 0% to 30% (w/w) CA: SB (a to d), prior to incubation in PBS at 29 x, 49 x and 103x magnification respectively.

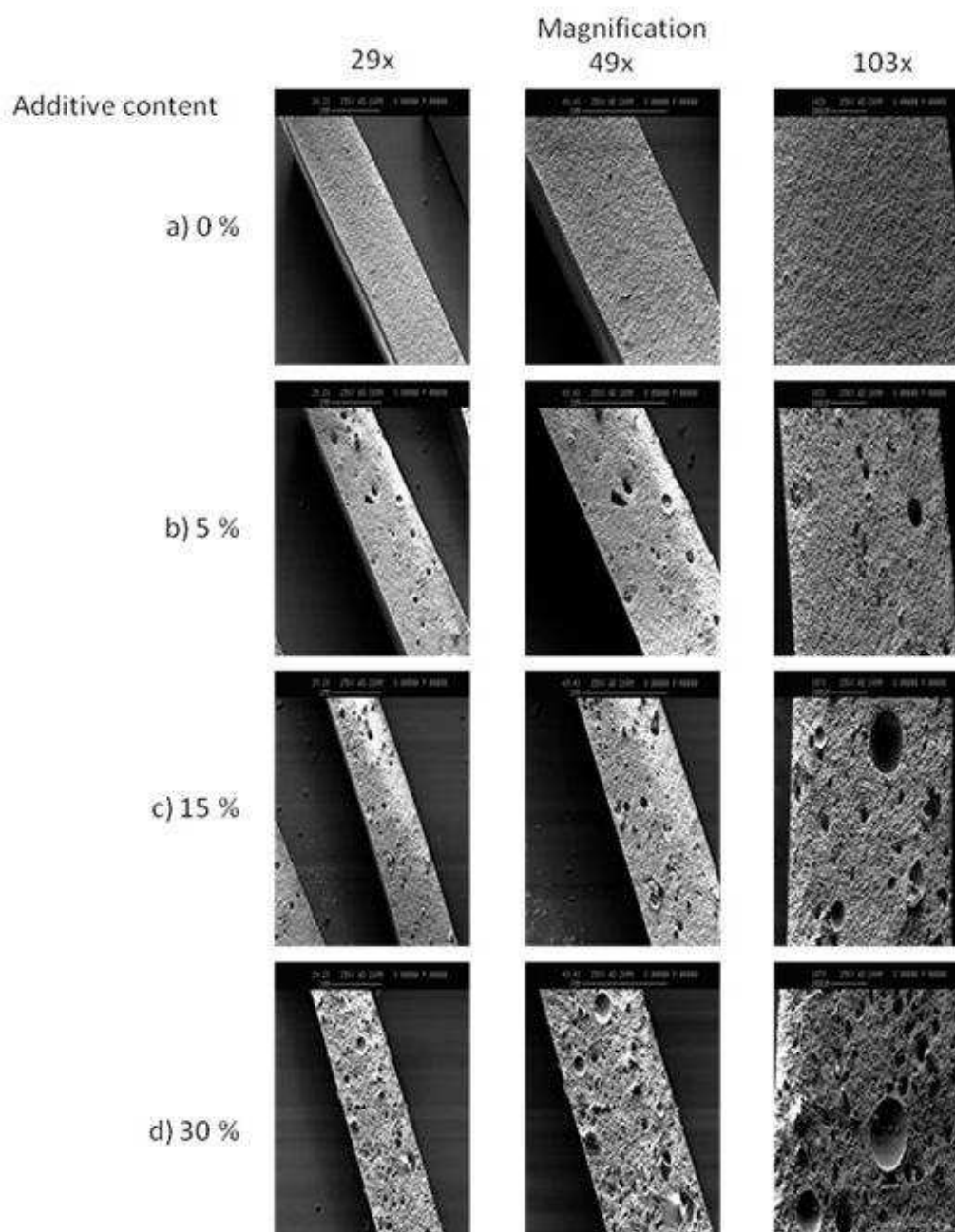


Figure 4. 15 Cross sectional SEM images from the silicone elastomer strips containing 0 % to 30 % (w/w) CA: SB (a to d), subsequent to 1 day incubation in PBS at 29 x, 49 x and 103 x magnification respectively.

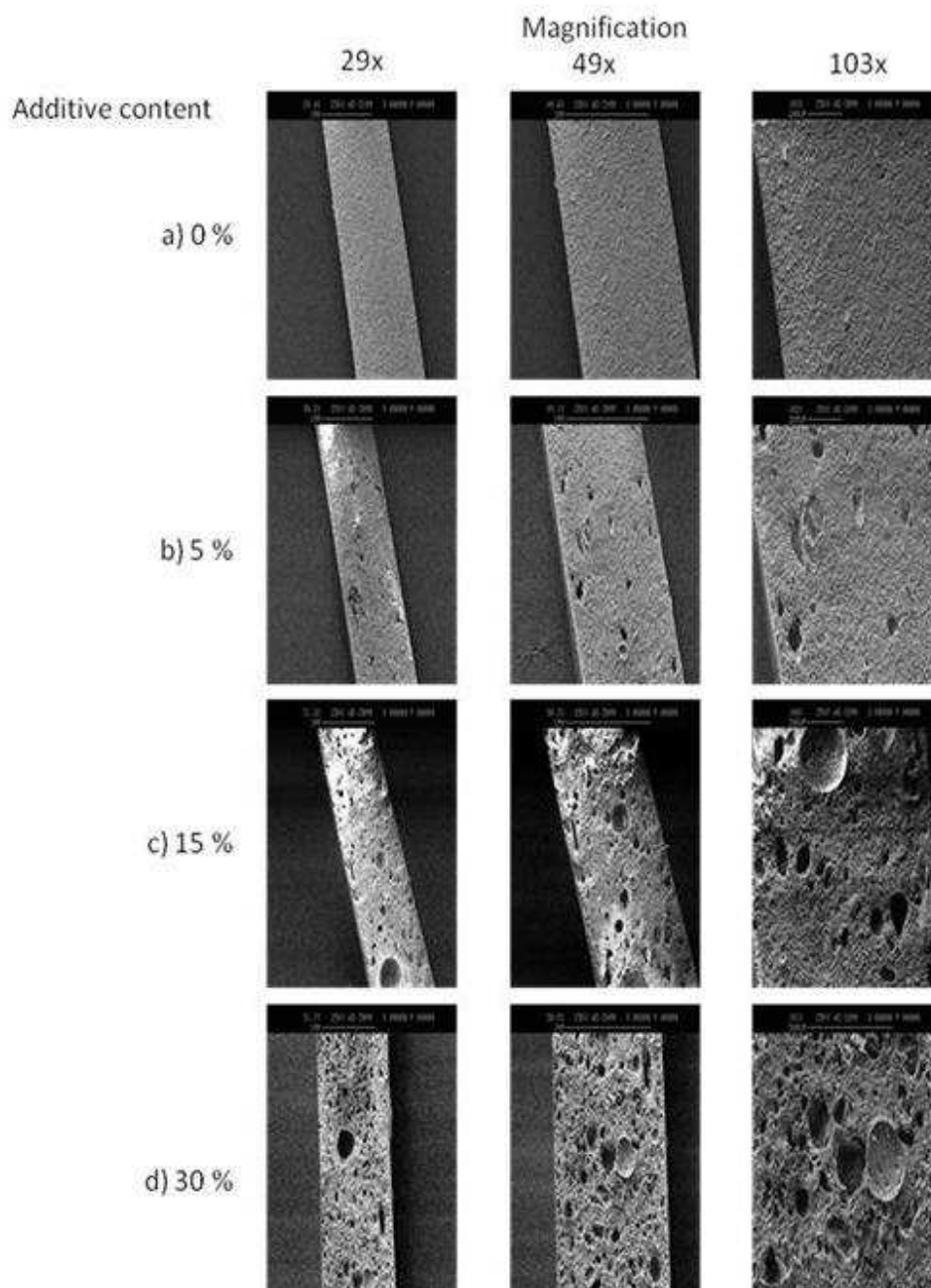


Figure 4. 16 Cross sectional SEM images from the silicone elastomer strips containing 0 % to 30 % (w/w) CA: SB (a to d), subsequent to 1 week incubation in PBS at 29 x, 49 x and 103 x magnification respectively.

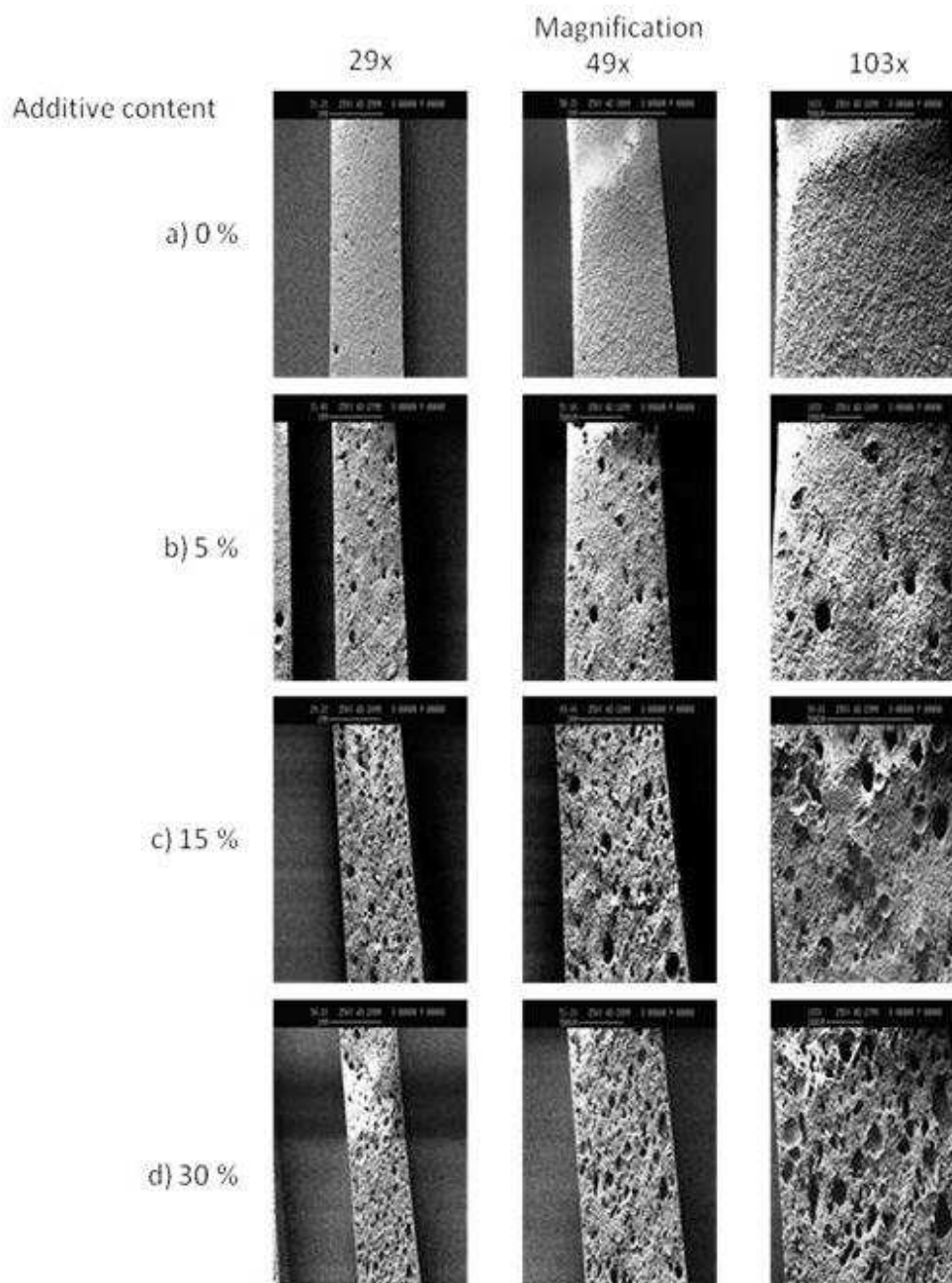


Figure 4. 17 Cross sectional SEM images from the silicone elastomer strips containing 0 % to 30 % (w/w) CA: SB (a to d), subsequent to 1 month incubation in PBS at 29 x, 49 x and 103 x magnification respectively.

4.4.5 Macroscopic morphology

Macroscopic photographs of the silicone elastomer strips containing 0 %, 5 %, 10 % and 30 % (w/w) CA/ SB were obtained prior to and after one month incubation in PBS (37 °C, pH 7.4). Across all the formulations tested (Figure 4.18; a, b, c and d), there was no major difference in the macroscopic appearance of the strips prior to the incubation. However, after one-month immersion in PBS, the CA/ SB incorporated strips (Figure 4.18; b', c' and d') gently swelled, while retaining the initial shape. As the amount of amalgamated CA/ SB in the silicone matrix was increased from 5 % to 30 %, the strips were more swollen and expanded. The significant expansion of strips incorporating 30 % (w/w) CA/ SB compared to the other formulations and blank (0 % CA/ SB) was also visible to the naked eye. These results confirm the absorption of water by the strips integrating CA/ SB as a consequence of the creation of channels and pores during CO₂ production. In spite of this, the appearance of the silicone elastomer strips containing 0 % (w/w) CA/ SB (Figure 4.18; a') after one month immersion in PBS, portrayed no noticeable alteration or swelling, indicating that channels and cracks were not created under these conditions.

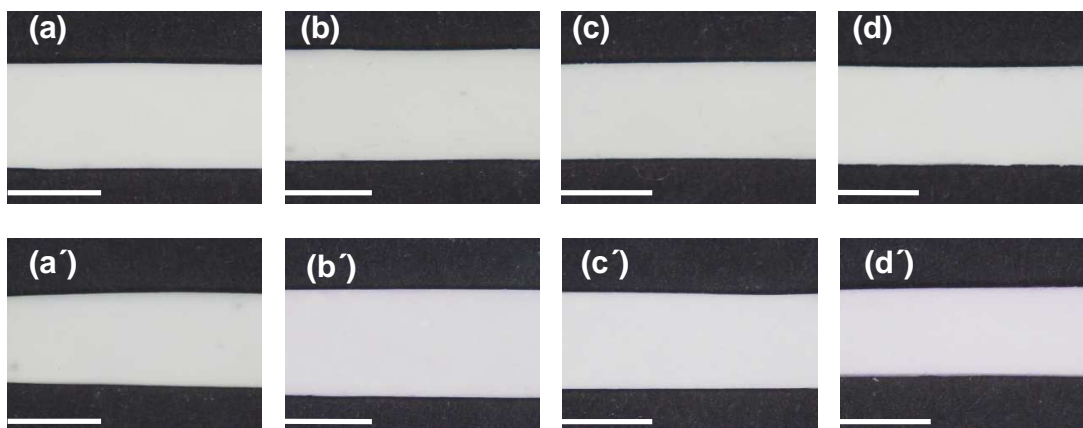


Figure 4. 18 Macroscopic photographs of the silicone elastomer strips before and after one-month incubation in PBS. a, b, c and d images represent silicone strips incorporating 0 %, 5 %, 15 % and 30 % (w/w) CA/ SB respectively, before incubation. a', b', c' and d' represent the same strips after one-month immersion in PBS (pH 7.4). Across all the formulations tested (a, b, c and d), there was no major difference in the appearance of the strips before the incubation. However, after one-month immersion in PBS, the CA/ SB incorporated strips (b', c' and d') gently swelled, while retaining the initial shape. In spite of this, the appearance of the silicone elastomer strips containing 0 % CA/ SB (a') after one month immersion in PBS, portrayed no noticeable alteration or swelling. All bars = 1cm.

4.4.6 Optical microscopy

To study the topography of the silicone elastomer strips' surface, optical images of each of the strips prior to and after incubation were captured. Silicone prepared without the addition of CA and SB (0 % (w/w) CA and SB) had a smooth topography (Figure 4.19a), however as the quantities of CA and SB increased within the preparations from 5 % to 30 % (Figure 4.19 b to d respectively), the exterior of silicone strips became less smooth and more 'pitted'.

For all the formulations tested, the surface of the silicone strips became irregular in nature with small apertures following one-day incubation in PBS (Figure 4.20 a to d). Subsequent to one-week incubation in PBS (Figure 4.21 a to d), the number and size of the apertures and pores increased. The surface of the strips subsequent to one-month incubation demonstrated more apertures and minute openings when compared to strips which had been incubated for one week (Figure 4.22 a to d). Particularly where CA and SB were present in the silicone mixes, pores and channels were visible with the porous nature increasing with the increased percentage of CA and SB contained within the preparations from 5 % to 30 %.

Overall it can be seen that the quantity of channels and pores increased both with the amount of integrated CA and SB in the tested preparations and with longer incubation periods, confirming the formation of openings and pores on the surface and within the silicone strips structure with incorporated additives over incubation time.

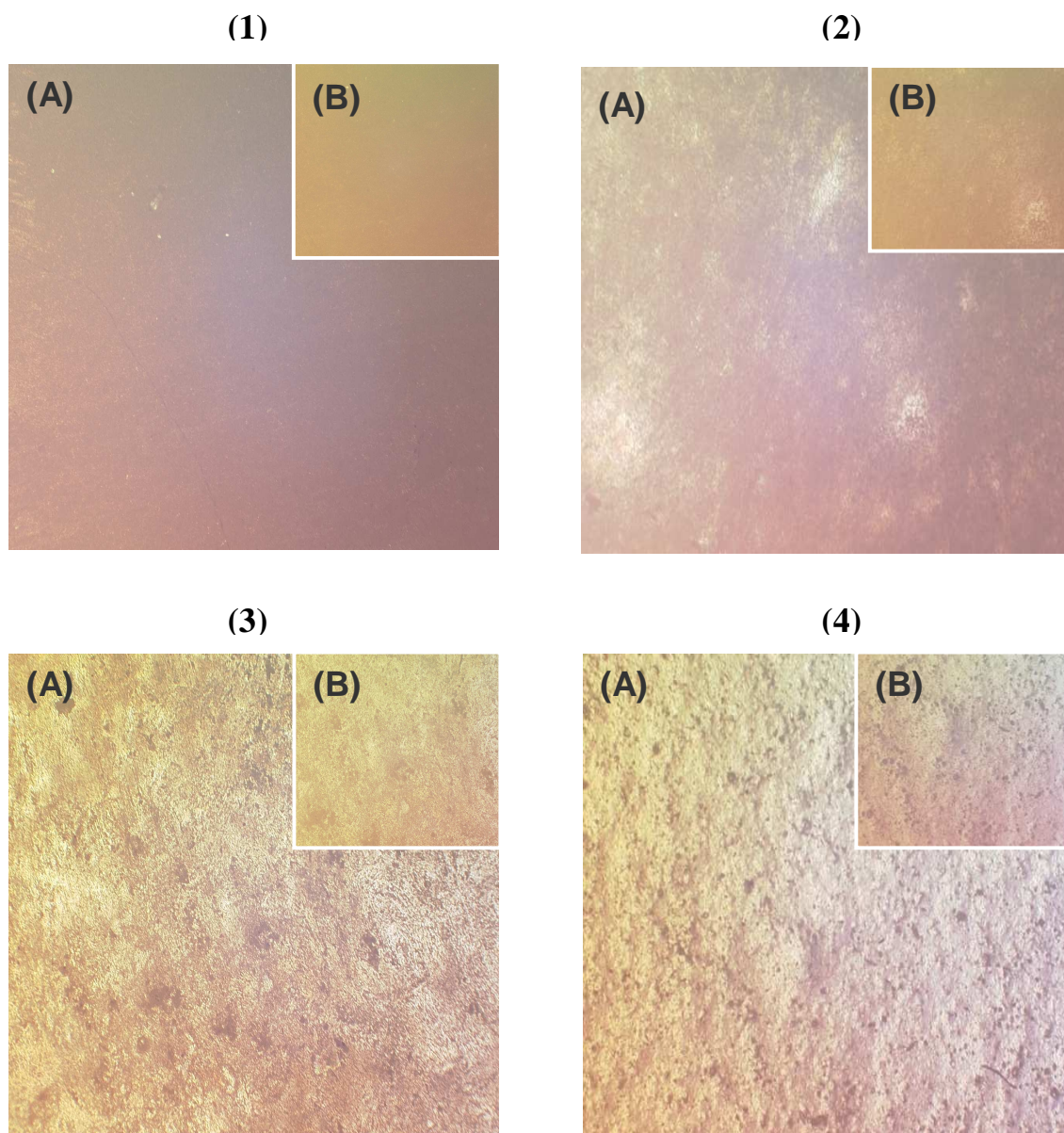


Figure 4. 19 a-d Optical images from the surface of the silicone elastomer strips containing 0 % (1), 5 % (2), 15 % (3) and 30 % (4) (w/w) CA: SB, prior to incubation in PBS at 25x (A) and 50x (B) magnifications respectively, using a Reichert-Jung Polyvar microscope. Silicone prepared without the addition of CA and SB (0 % CA: SB) had a smooth topography (Figure 4.19a), however as the quantities of CA and SB increased within the preparations from 5 % to 30 % (Figure 4.19 b to d respectively), the exterior of silicone strips became less smooth and more ‘pitted’.

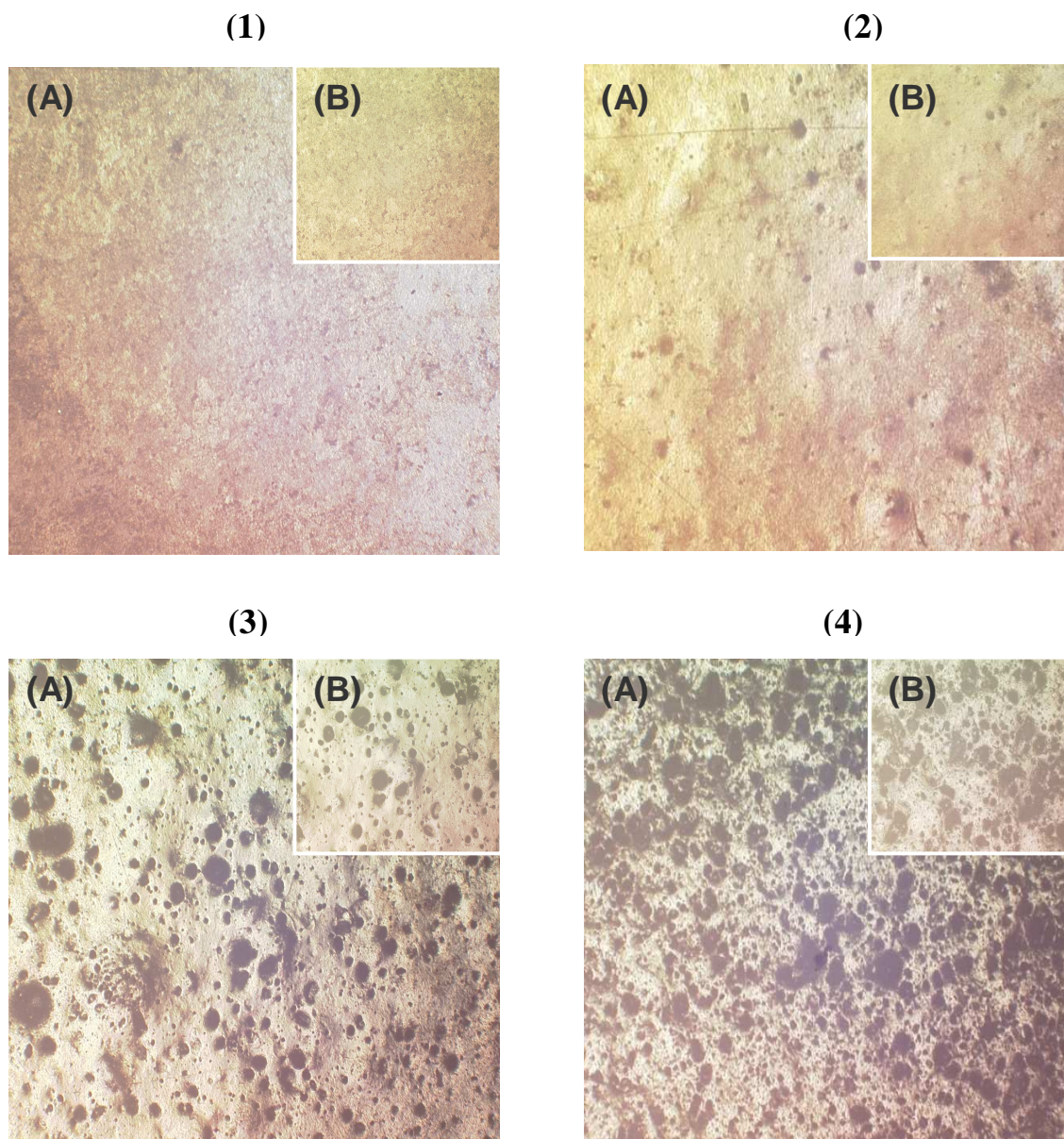


Figure 4. 20 a-d Optical images from the surface of the silicone elastomer strips containing 0 % (1), 5 % (2), 15 % (3) and 30 % (4) (w/w) CA: SB, after 1 day incubation in PBS (37 °C) at 25x (A) and 50x (B) magnifications respectively, using a Reichert-Jung Polyvar microscope. For all the formulations tested, the surface of the silicone strips became irregular in nature with small apertures following 1 day's incubation in PBS. Particularly where CA and SB were present in the silicone mixes, pores and channels were visible with the porous nature increasing with the increased percentage of CA and SB contained within the preparations from 5 % to 30 %.

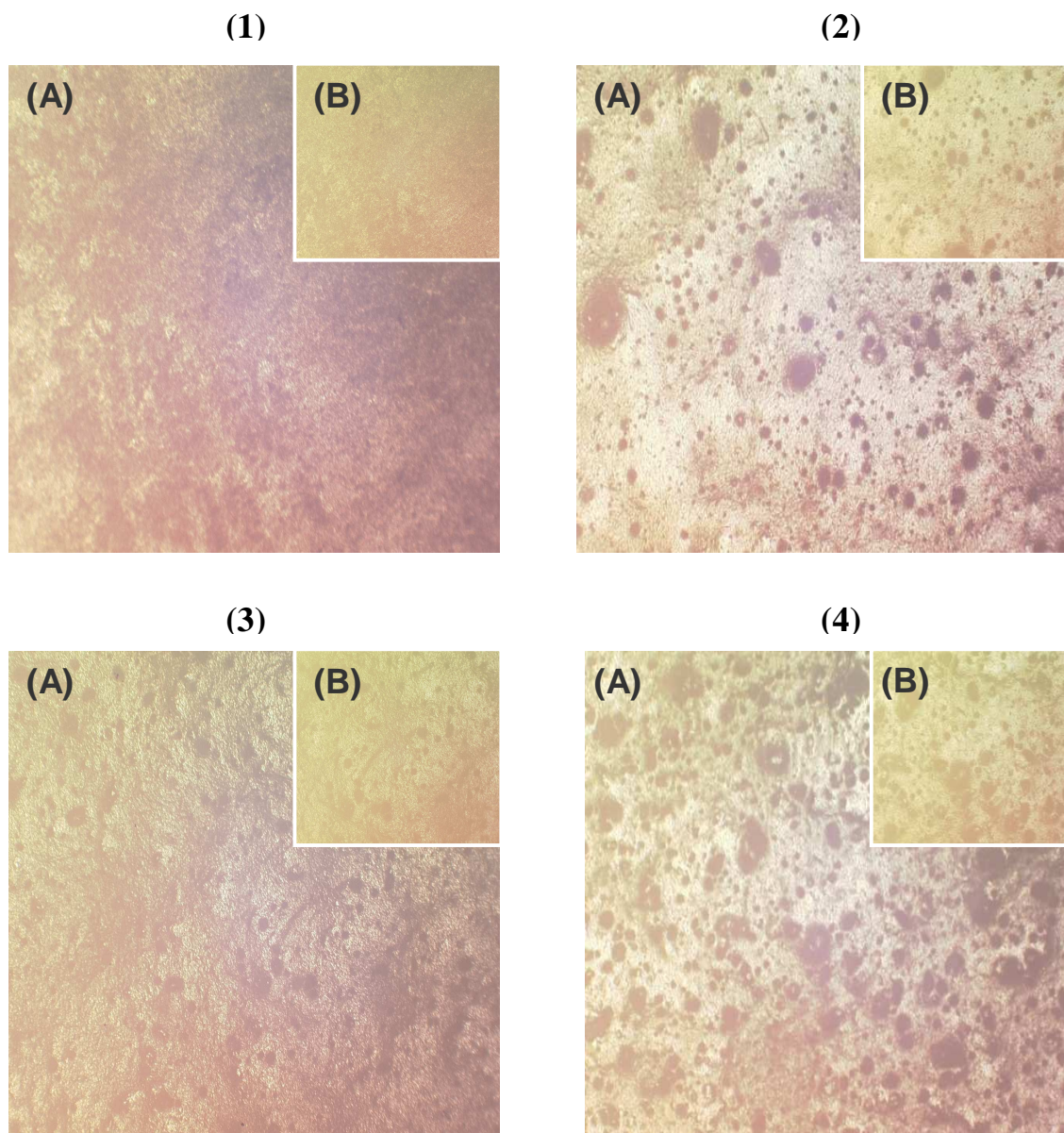


Figure 4. 21 a-d Optical images from the surface of the silicone elastomer strips containing 0 % (1), 5 % (2), 15 % (3) and 30 % (4) (w/w) CA: SB, after 1 week incubation in PBS (37 °C) at 25x (A) and 50x (B) magnifications respectively, using a Reichert-Jung Polyvar microscope. Subsequent to one week's incubation in PBS (Figure 4.21 a to d), the number and size of the apertures and pores increased, for all the formulations tested. Particularly where CA and SB were present in the silicone mixes, pores and channels were visible with the porous nature increasing with the increased percentage of CA and SB contained within the preparations from 5 % to 30 %.

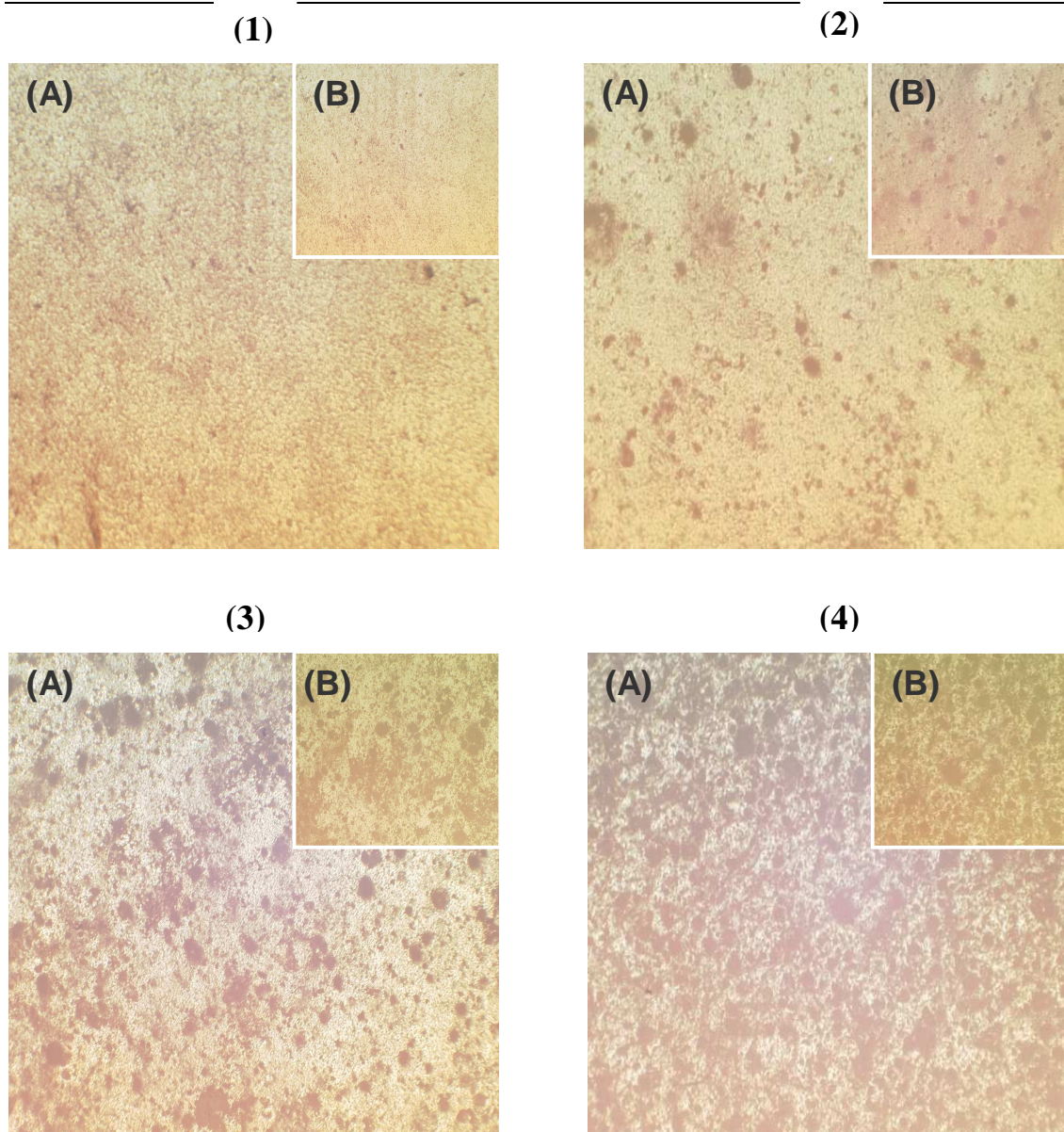


Figure 4. 22 a-d Optical images from the surface of the silicone elastomer strips containing 0 % (1), 5 % (2), 15 % (3) and 30 % (4) (w/w) CA: SB, after 1 month incubation in PBS (37 °C) at 25x (A) and 50x (B) magnifications respectively, using a Reichert-Jung Polyvar microscope. For all the formulations tested, the surface of the strips after one month incubation demonstrated more apertures and minute openings when compared to strips which had been incubated for one week (Figure 4.22 a to d). Particularly where CA and SB were present in the silicone mixes, pores and channels were visible with the porous nature increasing with the increased percentage of CA and SB contained within the preparations from 5 % to 30 %.

4.4.7 Swelling studies

To study the swelling properties of the silicone elastomer strips in buffer solution upon addition of CA and SB, the weight, dimensions (width, length and thickness) and corresponding volume of strips prior to and subsequent to incubation (1 day, 1 week and 1 month time points) in PBS (pH 7.4, 37 °C) were measured. Swelling of the strips was investigated by monitoring the percent change in the volume of each strip for the pre-set time points.

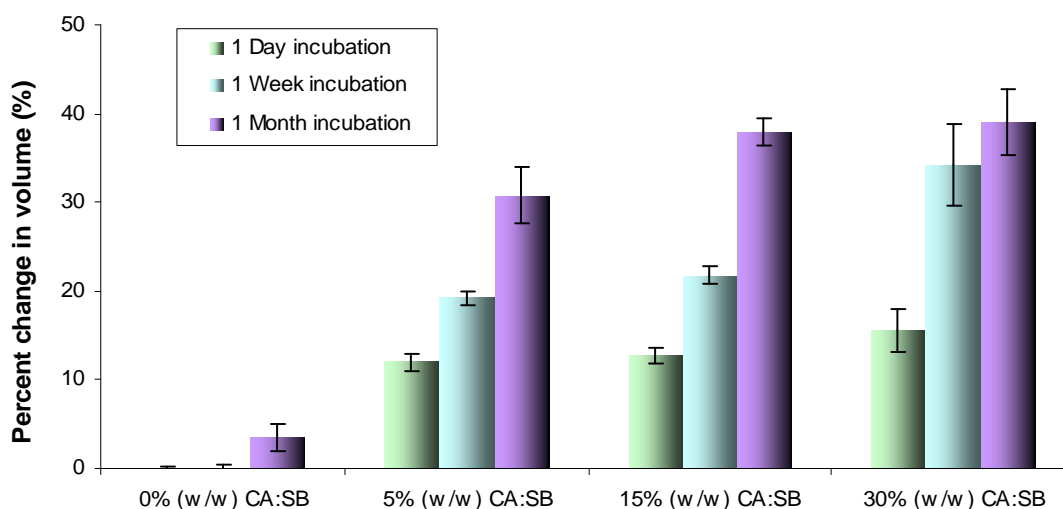


Figure 4. 23 Percent change in volume (%) of the silicone elastomer strips integrating 0 %, 5 %, 15 % and 30 % CA: SB after incubation (1 day, 1 week and 1 month) in PBS (pH 7.4, 37 °C). For all the formulations integrating CA and SB, the alteration in volume of the strips was found to increase with the incubation period. The maximum volume for all preparations was seen after one month of incubation in PBS. Furthermore, as the amount of integrated CA and SB in preparations rose, the volume change increased. Results denote mean \pm SD from 3 independently synthesized batches.

As shown in Figure 4.23, alterations in the volume of the strips across all of the measured time points for strips containing 0 % (w/w) CA and SB were minimal (< 5 %) amongst all the preparations tested. For the formulations integrating CA and SB, the alteration in volume of the strips was found to increase with the incubation period and the amount of integrated CA and SB in the preparations. The maximum volume for all the preparations tested was seen following one month of incubation in PBS with the modification in volume at 30 % (w/w) CA and SB being the highest for all the tested formulations (45 fold). For the same time point, the formulations containing 5 % (w/w) CA and SB

demonstrated a 15-fold increase in volume, whereas those containing 15 % demonstrated a 35 fold increase. As previously discussed inclusion of more CA and SB in formulations, increases the creation of pores and channels, which results in absorbing more PBS over time, and eventually swelling and expanding of the strips. This is in line with the systems initially proposed by Kajihara (2003), demonstrating again the presence of CA and SB was able to suitably modify the morphology of the silicone strips, thereby supporting the proposed mechanism of drug release.

4.4.8 Mechanical properties of silicone strips

Mechanical characteristics of the silicone strips were measured to reveal the reaction of the silicone elastomer strips to an applied external force, thereby indicating their suitability for mechanical applications such as Young' modulus and tensile strength.

4.4.8.1 Tensile strength

As mentioned earlier in chapter 1, catheters can be exposed to significant tensile force upon removal from the patient which might result in destruction or detachment of the shaft from the balloon in the case of Foley catheters or in the separation of the catheter into two or more parts. Consequently, the elastic recovery of the constituent biomaterial is a necessary property that must be considered when manufacturing catheters (British Standard EN 30993, 1992; Lowthian, 1998; Lawrence and Turner, 2005). Tensile strength (MPa) is the resistance of a material to longitudinal stress, measured by the minimum amount of longitudinal stress required to rupture the material. It is expressed as the minimum tensile stress (force per unit area) needed to split the material apart. The tensile strength of each strip prepared in these studies was measured after initial preparation in PBS at 37 °C (Figure 4.24) to investigate the greatest lengthwise stress that the silicone strips could withstand without breaking.

According to Figure 4.24, there was no a considerable variation (ANOVA, $P > 0.05$) in terms of tensile strength amongst the blank formulations (0 % (w/w) CA/ SB) within the range of time points measured (approximately 5 MPa). For the rest of the formulations tested, a common trend apparent is that with an increase in percentage of incorporated

CA/ SB, the maximum force required to break the strips and hence the tensile strength was reduced. Across all the time points, the specimens incorporating 30 % (w/w) CA/ SB demonstrated the lowest tensile strength, whereas the ones with 0 % represented the highest. From these findings it could be suggested that incorporation of more acid and carbonate powders in the formulations results in the weakening of intermolecular, secondary forces (Van der Waals' forces) in the polymer structure due to the presence of the pockets of CA/ SB which subsequently form channel and pores in the silicone strips.

Moreover, all the silicone elastomer strips illustrated a greater tensile strength prior to incubation than after incubation in PBS. As the incubation period for the formulations amalgamated with CA/ SB increased from one day to one month period the tensile strength decreased. For the preparations incorporating 5 % and 15 % (w/w) CA/ SB, there was a downward trend in the tensile strength from 4.75 to 2.45 MPa and from 3.88 to 1.76 MPa respectively over the entire incubation period. The greatest reduction in the amount of tensile strength at 30 % (w/w) CA/ SB was on the first day (from 3.33 to 1.32 MPa), after which it remained constant. Again this would be consistent as a consequence of the formation of holes and pores, as a result of gas generation upon the mixing of carbonate and acid powders. Hence, the longer the period of time that the specimens were maintained in PBS, the greater number of pores and channels were formed. Commonly, silicone has a tensile strength of 2.4 - 7 MPa and an elongation of 350-600 % (Lawrence and Turner, 2005). These results are in conjunction with the results obtained in this study (Figure 4.24).

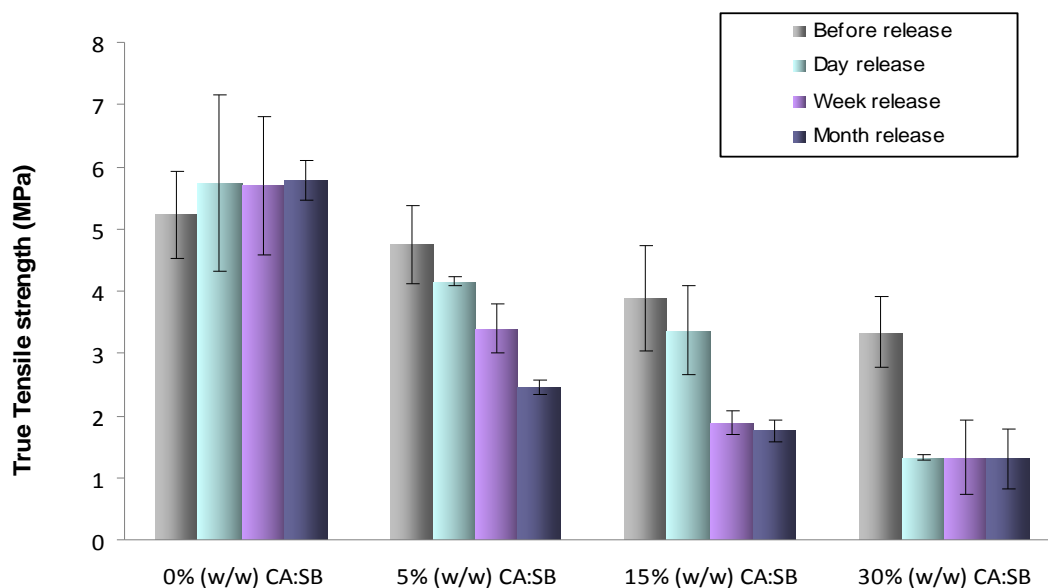


Figure 4. 24 The true tensile strength of the silicone elastomer strips incorporating 0 %, 5 %, 15 % and 30 % CA: SB previous to and after incubation (1 day, 1 week and 1 month) in PBS (pH 7.4, 37 °C). It was apparent that with a rise in the percentage of incorporated CA and SB and incubation period, the maximum force required to break the strips and consequently the tensile strength was decreased. In all of the formulations, the specimen containing 30 % CA/ SB showed the lowest tensile strength, whereas, the ones with 0 % CA/ SB demonstrated the highest. Furthermore, all the silicone elastomer strips exhibited a greater tensile strength prior to incubation than after incubation in PBS. As the incubation period for formulation amalgamated with CA/ SB increased from one day to one month period, the tensile strength decreased. Results denote mean \pm SD from 3 independently synthesized batches.

4.4.8.2 Force-extension curve

The major product of a tensile test is a load versus elongation curve. Force-extension graphs were plotted in order to display the silicone strips deformation under a load. As the force was applied to the strips, the specimen began to stretch or extend. The force was applied at a constant rate and readings of force and extension were recorded until the specimen broke. These readings could be plotted on a graph to display the overall performance of the specimen. The shape of the graph is imperative in predicting how the material would react under different loading conditions. In the elastic region, the graph is a straight line; this means that the material stretches under the load in proportion to applied stress, however when the load is removed, it returns to its original length. The graph becomes non-linear beyond the elastic region, as Hooke's Law is not obeyed and force is not proportional to extension. The line in the linear region of the curve obeys the

relationship defined as Hooke's Law where the ratio of force to elongation is a constant. The elongation of the strip is directly proportional to the tensile force and the length of the strip and inversely proportional to the cross-sectional area and the modulus of elasticity.

Hooke's experimental law;

$$\delta = \frac{P \ell}{AE} \text{ (Equation 4.4)}$$

δ = Tensile strength

P = Force producing extension of bar (lbf)

ℓ = Length of bar (in)

A = Cross-sectional area of bar (in²)

d = Total elongation of bar (in)

E = Elastic constant of the material, called the Modulus of Elasticity, or Young's Modulus (lbf/in²)

Figures 4.25 - 4.28 below illustrate the force-extension curves of a silicone elastomer strip containing 0 %, 5 %, 15 % and 30 % (w/w) CA/ SB, prior to and subsequent to incubation in buffer (1 day, 1 week and 1 month). As can be seen, the amount of exerted force increases proportionally to the amount of extension of the strips. A sheer and short slope indicates that more fore is required for deformation of polymer strips. On the other hand, a slight and long slope implies the conversely. Similarly, if the slope is steep, the sample has a high tensile modulus, which means it resists deformation. On the contrary, if the slope is gentle, then the sample has a low tensile modulus, which means it is easily deformed. Accordingly, CA/ SB integrated specimen curves have a gentler slope than the ones devoid of CA/ SB powders. By augmenting the amount of incorporated CA/ SB in the formulations from 5 % to 30 %, a gradual diminishing effect of the slope of the curves could be observed, suggesting that less strength is mandatory to break the strips. Correspondingly, a decrease in the slope of the curves is directly associated with an increase in incubation time. The one-month incubated strips appear to break more effortlessly than their one-day and one-week counterparts. This could be due to the formation of more holes and pores throughout the incubation period.

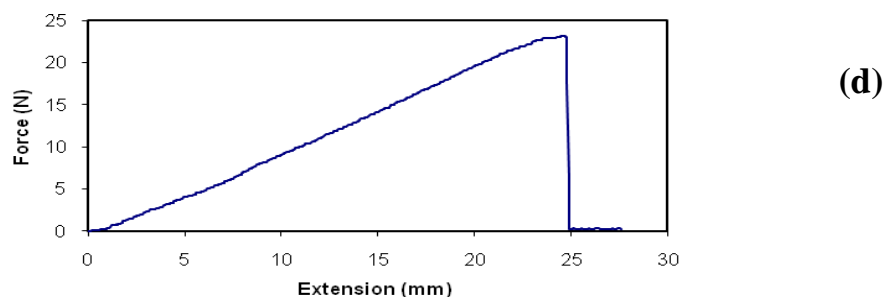
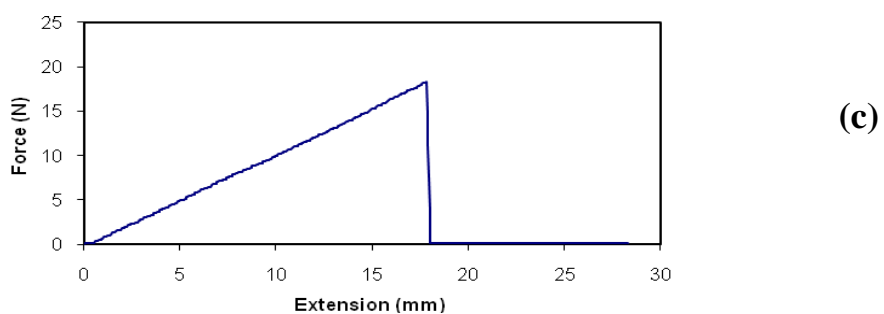
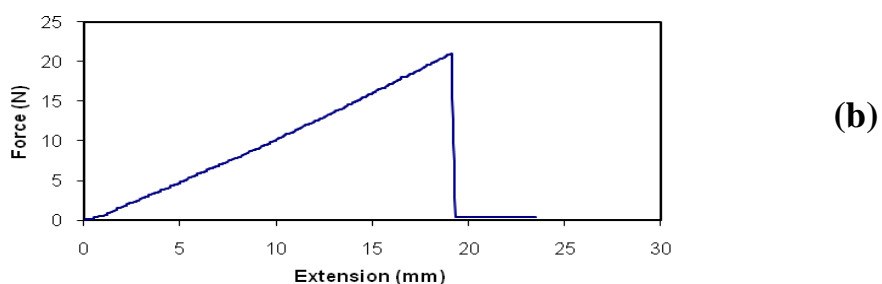
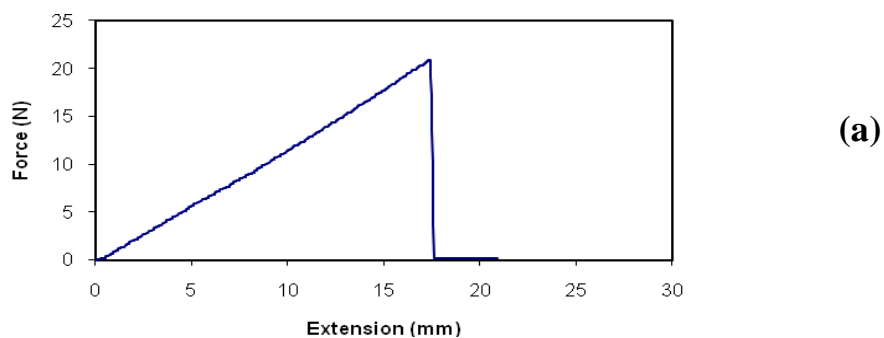


Figure 4. 25 a-d Force-extension curve of the silicone elastomer strip containing 0 % (w/w) CA: SB, prior to incubation in PBS (1) and after 1 day (2) 1 week (3) and 1 month (4) incubation in PBS (pH 7.4, 37 °C). The curve is a graphical representation of the relationship between force, derived from measuring the load applied on the silicone strip and extension derived from measuring the elongation of the strip before the break.

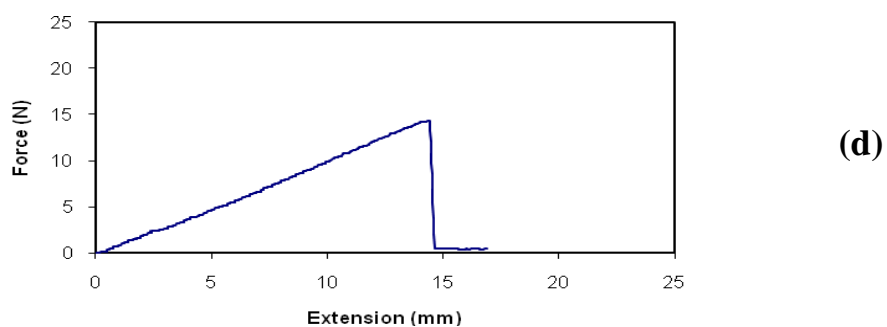
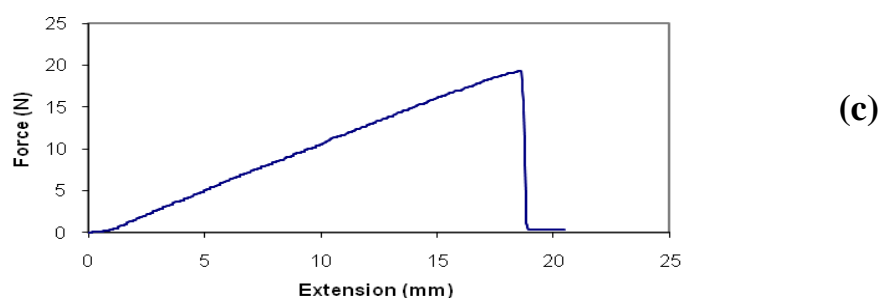
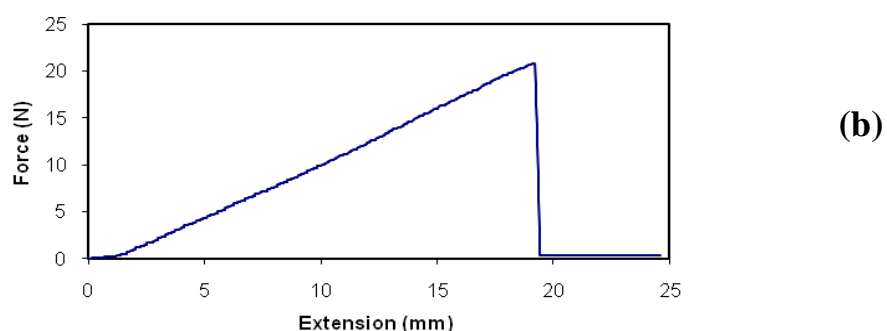
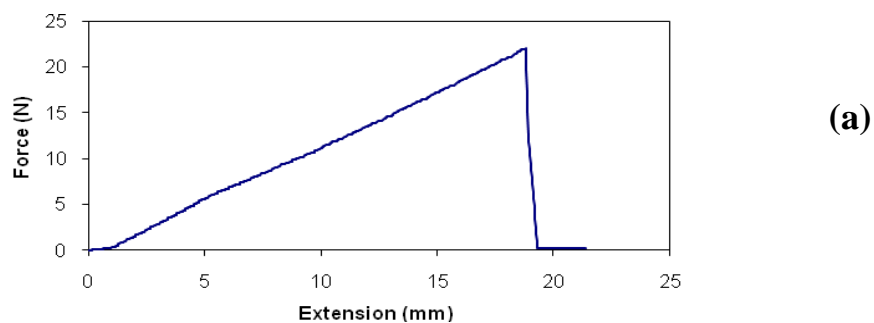
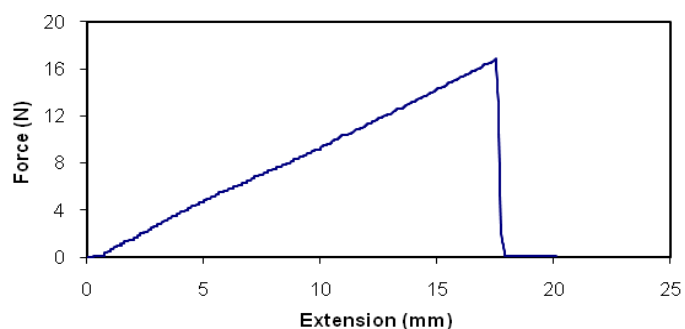
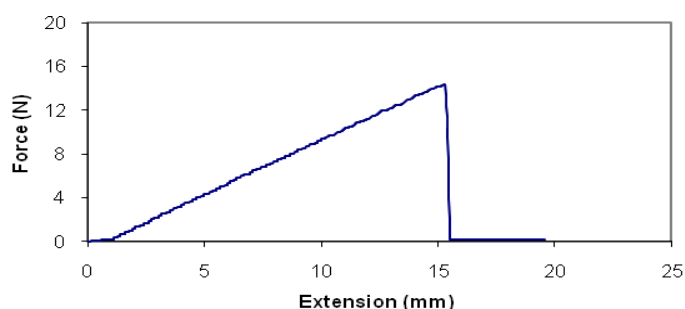


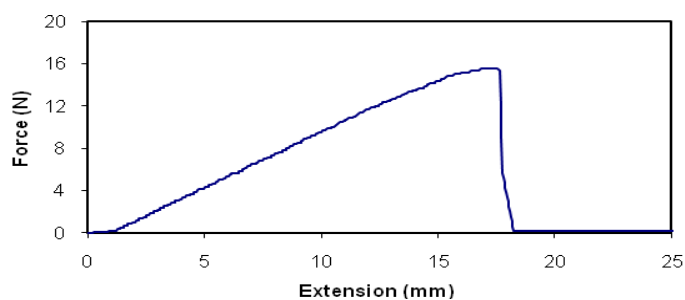
Figure 4. 26 a-d Force-extension curve of the silicone elastomer strip containing 5 % (w/w) CA: SB, prior to incubation in PBS (1) and after 1 day (2) 1 week (3) and 1 month (4) incubation in PBS (pH 7.4, 37 °C). The curve is a graphical representation of the relationship between force, derived from measuring the load applied on the silicone strip and extension derived from measuring the elongation of the strip before the break.



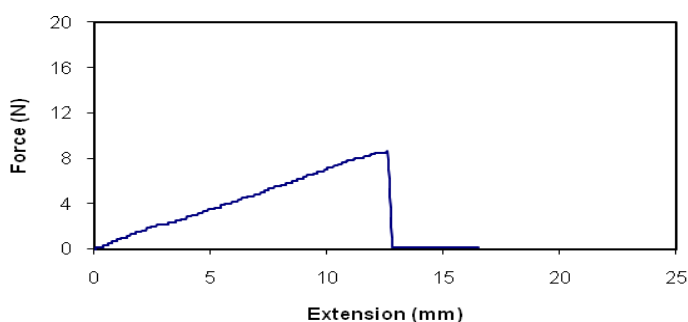
(a)



(b)



(c)



(d)

Figure 4. 27 a-d Force-extension curve of the silicone elastomer strip containing 15 % (w/w) CA: SB, prior to incubation in PBS (1) and after 1 day (2) 1 week (3) and 1 month (4) incubation in PBS (pH 7.4, 37 °C). The curve is a graphical representation of the relationship between force, derived from measuring the load applied on the silicone strip and extension derived from measuring the elongation of the strip before the break.

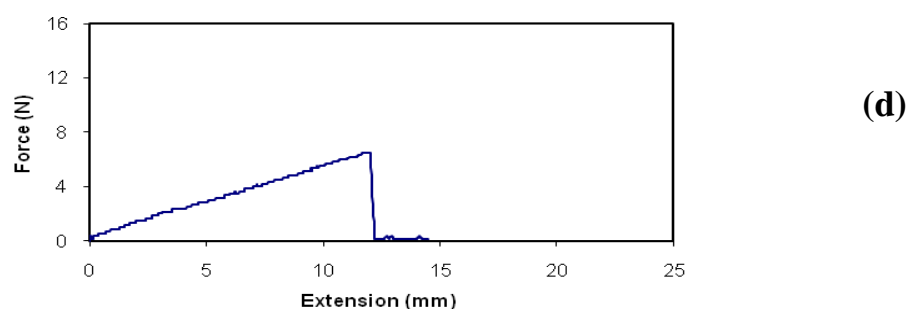
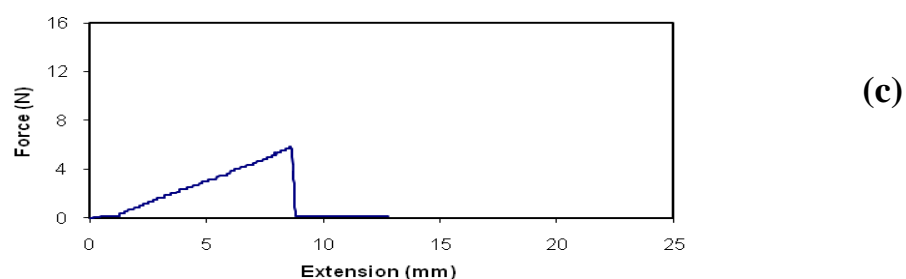
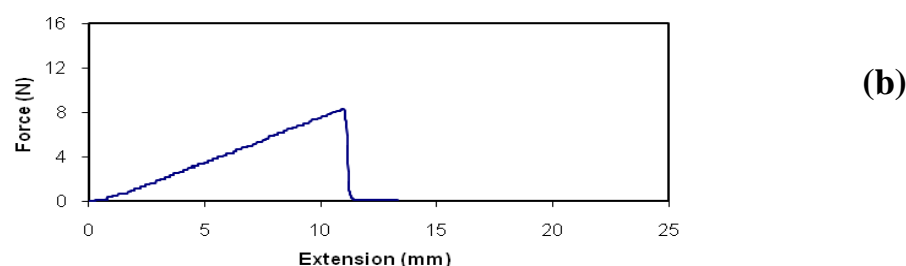
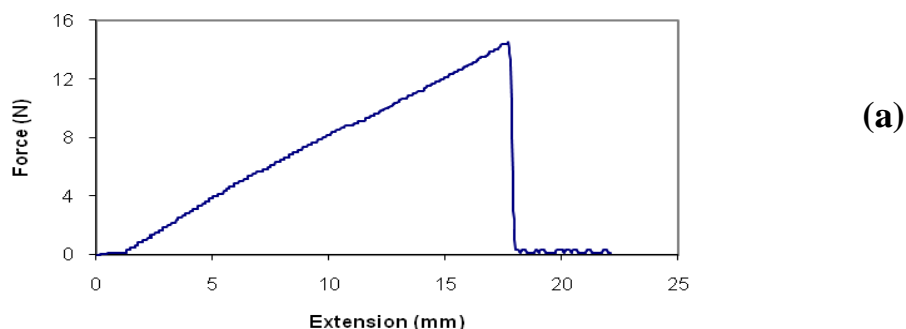


Figure 4. 28 a-d Force-extension curve of the silicone elastomer strip containing 30 % (w/w) CA: SB, prior to incubation in PBS (1) and after 1 day (2) 1 week (3) and 1 month (4) incubation in PBS (pH 7.4, 37 °C). The curve is a graphical representation of the relationship between force, derived from measuring the load applied on the silicone strip and extension derived from measuring the elongation of the strip before the break.

4.4.8.3 Young's modulus (modulus of elasticity) (elastic modulus) (Tensile modulus)

To quantify the elasticity or stiffness of the silicone elastomers, the Young's modulus (E) of each silicone strips was measured (Figure 4.29).

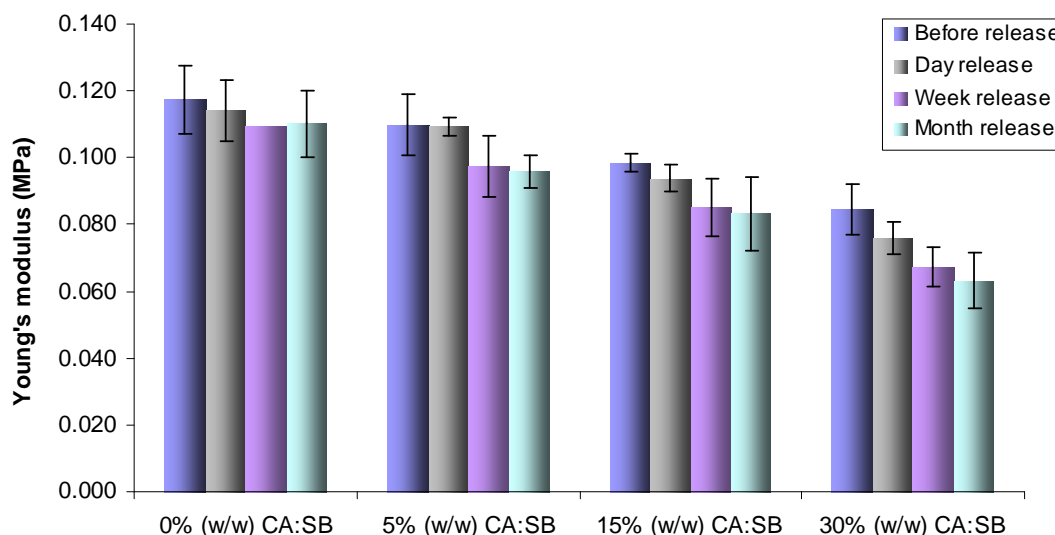


Figure 4. 29 Young's modulus of the silicone elastomer strips incorporating 0 %, 5 %, 15 % and 30 % CA: SB previous to and after incubation (1 day, 1 week and 1 month) in PBS (pH 7.4, 37 °C). A common trend apparent is that with an increase in the percentage of incorporated CA and SB and the incubation period Young's Modulus and consequently the elasticity of silicone elastomer strips decreased. Results denote mean \pm SD from 3 independently synthesized batches.

As illustrated in Figure 4.29, Young's modulus and consequently the elasticity of the silicone elastomer strips declined steadily, with an increase in the amount of incorporated CA/ SB in the formulations from 0 % to 30 %. The highest modulus, ~ 0.110 MPa, was measured in the preparations incorporating 0 % (w/w) CA/ SB which were the most elastic and the least stiff of all the specimens. Conversely, the smallest modulus, 0.06 - 0.08 MPa, was measured in 30 % (w/w) CA/ SB integrated formulations, indicating the lowest elasticity and highest stiffness among the formulations.

There was no considerable disparity (ANOVA, $P > 0.05$) in the Young's modulus measured in all the preparations devoid of CA/ SB (0 %), prior to and subsequent to incubation in PBS (~ 0.110 MPa). For the rest of the formulations (5 %, 15 % and 30 %

(w/w) CA/ SB), the amount of applied force and stress which was required to break the strips, in addition to Young's modulus, declined slowly with increased incubation time from one day to one month. Particularly at 30 % CA/ SB (w/w), where the Young's modulus measured declined gradually from 0.085 MPa to 0.063 MPa. However, when comparing the time point prior to release with that after one-day release, the alteration in the Young's modulus was insignificant (ANOVA, $P > 0.05$), for both 5 % and 15 % (w/w) CA/ SB incorporated formulations. Similar results were also observed when comparing the time point after one-week release with that after one-month release. The creation of channels and pores in the CA/ SB amalgamated preparations during the suspension of strips in PBS weakens the intermolecular forces that act between molecules or between functional groups of macromolecules, in turn lessening the elastic properties of the strips and enhancing stiffness.

In a similar study conducted by Wolfson et al. (2003), the tensile strength of the silicone strips measured from 1.46 – 3.37 MPa and the Young's modulus measured from 0.68 – 2.26 MPa. The resultant tensile strength was in accordance with the experimental results obtained from Figure 4.23, while the elastic modulus was greater than the comparative study conducted in this chapter (Figure 4.29). This could be attributed to the incorporation of CA/ SB in the formulations as earlier discussed.

4.4.9 Summary

Characteristics of different strips are summarised in the four tables below (Table 4.4 to 4.7); these high-light the differences in material characteristics in terms of increasing the CA/SB content, resulting in reduced tensile strength and Young's modulus.

Table 4.4 The data obtained from measuring tensile strength of the silicone elastomer strips by a Hounsfield Universal Tester. The experimental conditions involved; 0 %, 5 %, 15 % and 30 % CA/ SB incorporated formulations, and prior to incubation in PBS.

| | Blank | 5 % (w/w) | 15 % (w/w) | 30 % (w/w) |
|-----------------------|----------------|----------------|----------------|---------------|
| Tensile (MPa) | 2.45 ± 0.33 | 2.31 ± 0.44 | 1.96 ± 0.34 | 1.76 ± 0.21 |
| Max Force (N) | 24.58 ± 3.31 | 23.16 ± 4.41 | 19.63 ± 3.4 | 17.65 ± 2.12 |
| Elong at Max % | 103.24 ± 10.51 | 105.85 ± 12.45 | 108.13 ± 19.92 | 105.25 ± 4.59 |
| Break (Mpa) | 0.08 ± 0.17 | 0.01 ± 0 | 0.34 ± 0.4 | 0.12 ± 0.12 |
| Break (N) | 0.88 ± 1.7 | 0.15 ± 0 | 3.45 ± 4.02 | 1.25 ± 1.27 |
| Elongation% | 375.9 ± 537.35 | 124.5 ± 11.73 | 116 ± 24.07 | 112.5 ± 2.82 |

Table 4.5 The data obtained from measuring tensile strength of the silicone elastomer strips by a Hounsfield Universal Tester. The experimental conditions involved; 0 %, 5 %, 15 % and 30 % CA/ SB incorporated formulations, and after one day incubation in PBS.

| | Blank | 5 % (w/w) | 15 % (w/w) | 30 % (w/w) |
|-----------------------|----------------|----------------|----------------|---------------|
| Tensile (MPa) | 2.51 ± 0.52 | 2.01 ± 0.39 | 1.87 ± 0.41 | 0.93 ± 0.19 |
| Max Force (N) | 25.15 ± 5.23 | 20.16 ± 3.94 | 18.72 ± 4.14 | 9.33 ± 1.95 |
| Elong at Max % | 115.56 ± 17.52 | 92.83 ± 19.34 | 95.84 ± 18.86 | 64.59 ± 17.57 |
| Break (Mpa) | 0.28 ± 0.61 | 0.05 ± 0.04 | 0.04 ± 0.06 | 0.04 ± 0.05 |
| Break (N) | 2.8 ± 6.13 | 0.5 ± 0.44 | 0.41 ± 0.65 | 0.44 ± 0.52 |
| Elongation% | 147.14 ± 35.27 | 123.46 ± 38.83 | 182.5 ± 183.33 | 78.75 ± 14.13 |

Table 4.6 The data obtained from measuring tensile strength of the silicone elastomer strips by a Hounsfield Universal Tester. The experimental conditions involved; 0 %, 5 %, 15 % and 30 % CA/ SB incorporated formulations, and after one week incubation in PBS.

| | Blank | 5 % (w/w) | 15 % (w/w) | 30 % (w/w) |
|-----------------------|----------------|----------------|--------------|---------------|
| Tensile (MPa) | 2.64 ± 0.3 | 1.78 ± 0.13 | 1.24 ± 0.21 | 0.92 ± 0.31 |
| Max Force (N) | 26.49 ± 3.02 | 17.83 ± 1.31 | 12.42 ± 2.13 | 9.26 ± 3.16 |
| Elong at Max % | 130.9 ± 16.86 | 79.33 ± 11.47 | 63.11 ± 4.36 | 57.78 ± 13.59 |
| Break (Mpa) | 0.02 ± 0.01 | 0.02 ± 0.01 | 0.1 ± 0.14 | 0.12 ± 0.15 |
| Break (N) | 0.2 ± 0.1 | 0.28 ± 0.11 | 1 ± 1.43 | 1.28 ± 1.57 |
| Elongation % | 149.35 ± 12.55 | 112.03 ± 26.13 | 76.51 ± 9.33 | 67.87 ± 15.12 |

Table 4.7 The data obtained from measuring tensile strength of the silicone elastomer strips by a Hounsfield Universal Tester. The experimental conditions involved; 0 %, 5 %, 15 % and 30 % CA/ SB incorporated formulations, and after one month incubation in PBS.

| | Blank | 5 % (w/w) | 15 % (w/w) | 30 % (w/w) |
|-----------------------|----------------|-----------------|---------------|---------------|
| Tensile (MPa) | 2.42 ± 0.47 | 1.41 ± 0.25 | 1.14 ± 0.24 | 0.92 ± 0.21 |
| Max Force (N) | 24.26 ± 4.76 | 14.1 ± 2.58 | 11.46 ± 2.45 | 9.23 ± 2.13 |
| Elong at Max % | 121.92 ± 16.76 | 70.91 ± 12.24 | 67.77 ± 13.99 | 68.92 ± 12.97 |
| Break (Mpa) | 0.22 ± 0.48 | 0.06 ± 0.11 | 0.14 ± 0.22 | 0.17 ± 0.22 |
| Break (N) | 2.21 ± 4.85 | 0.64 ± 1.19 | 1.4 ± 2.24 | 1.76 ± 2.28 |
| Elongation % | 141.03 ± 18.03 | 138.64 ± 122.64 | 85.83 ± 25.6 | 82.95 ± 22.66 |

4.4.10 Conclusion

The results presented within this chapter demonstrate that the incorporated FXIIIa inhibitor as a poorly soluble drug was not released from the silicone carrier when it was dispersed devoid of additives; however its release profile was improved by using CA and SB as additives. CA and SB as water-soluble compounds form channels and pores upon dissolution and generate gaseous carbon dioxide as a driving force to accelerate the release of the inhibitor. The drug release rate could be controlled by the amount of CA and SB incorporated in the silicone matrix. A common trend apparent was that with an increase in the percentage of incorporated CA and SB, the consequent drug release also increased. Thus, the amount of the inhibitor released at 30 % CA and SB is the most amongst the formulations and approximately 30 folds higher when compared to the blank. Morphological analysis confirmed the formation of channels and cracks inside the specimens upon the addition of CA and SB. Furthermore, it was found that the inhibitor was still biologically active subsequent to being released from the silicone elastomer strips. However, the tensile strength, in addition to Young's modulus of silicone elastomer strips, decreased constantly with an increasing amount of amalgamated CA/ SB in the formulations. According to these studies, FXIIIa inhibitor incorporating catheters and other medical devices could offer new perspectives on preventing bio-material associated infections and thrombosis.

Chapter 5:
Biodistribution and pharmacokinetic studies of the
TG2 inhibitor

5.1 Introduction

As detailed in chapter 1, liver fibrosis and its end stage disease cirrhosis are a major cause of mortality and morbidity around the world. There is no effective pharmaceutical intervention for liver fibrosis at present. Liver fibrosis is characterized by increased synthesis and decreased degradation of the extracellular matrix (ECM). Increase in TG2 activity has been linked to an increase in the deposition of extracellular matrix proteins in fibrotic conditions. It can therefore be predicted that TG2 inhibitors could be used for the cure of fibrotic diseases characterised by increased ECM deposition and cross linking.

5.2 Aim

In the development of new drugs, pharmacokinetic data is essential. In contrast to *in vitro* studies, animal models allow the estimation of many variables, such as absorption, distribution, clearance, drug interactions and toxicity by reproducing the host immune defects and systemic infections. The aim of this study was to examine *in vivo* pharmacokinetics and tissue biodistribution of the TG2 inhibitor (AM2/169) subsequent to intraperitoneal (IP) administration in rats. The inhibitor concentrations in major organs and plasma were quantitatively analysed using a high performance liquid chromatography-fluorescence assay. Pharmacokinetic parameters were calculated based on plasma concentration-time profiles of AM2/169.

5.3 Animals

All animal experimentation strictly adhered to the 1986 Scientific Procedures Act and to the Guidance on the Operation of Animals (Scientific Procedures) Act, as outlined by the Home Office in the UK and adopted by the ethics committee on animal experimentation within the research establishment. All protocols were subject to stringent ethical review and were carried out in a designated establishment. All animals were kept in a typical laboratory environment: four or five per cage with an air filter cover under light (12 hour light/ 12 hour dark cycles) and temperature-control (19 ± 23 °C), a relative humidity of 55 ± 15 %, and were observed daily for any signs of distress.

5.4 Study design, drug administration and sample collection

The study design in this chapter was initially based on the work of previous researchers specific to this field of research (Choi et al 2005; Strnad et al, 2006). Biodistribution studies were carried out in Wistar rats at different time intervals after parenteral administration of the fluorescent drug ($n = 5$ rats per time point). Initially, a total of twenty male Wistar rats, with an average bodyweight of 95 gram were injected with 50 mg/kg of 10 mg/ml AM2/169 in 50 % DMSO/PBS intraperitoneally (IP). At each time point (0.083, 0.33, 0.5, 1, 2, 4, 12 and 24 hours) five rats were anesthetized with isoflurane (4-5 %). Subsequently, the blood samples were collected at various time intervals using different techniques. At 0.083 and 0.33 hours, blood samples were collected by cannulation of the jugular vein, by cardiac puncture at 0.5, 1, 4 and 24 hours time points and from tail vein at 0.5, 2 and 12 hours time points. After predetermined time intervals (0.33, 1, 4 and 24 hours time points) the rats were terminated and organs such as the liver, lungs, kidneys, brain and spleen were removed and kept in autoclaved PBS for further analysis.

Blood plasma was collected after centrifugation of whole blood at 10000 g for 10 minutes at room temperature on a table-top centrifuge. The plasma was then separated and transferred to micro centrifuge tubes. The amount of inhibitor in the plasma was determined fluorometrically using HPLC as described in chapter 2.

Extraction of the TG2 inhibitor from the organs was performed on 250 mg of each organ. To each weighted organ 0.5 ml of methanol (40 % v/v) was added and homogenized for several minutes using a tissue homogenizer, which was carefully cleaned and disinfected with 70 % ethanol after each homogenization. The homogenate was centrifuged at 10000 g for 10 minutes, after which the supernatant was collected and read by fluorimetric estimation using HPLC. All harvested samples were stored at -80°C and analyzed within one month.

5.5 Results and discussions

5.5.1 Biodistribution and pharmacokinetic of the TG2 inhibitor

To investigate the biodistribution and pharmacokinetic of the TG2 inhibitor, the plasma concentration of AM2/169 following IP administration in rats was measured at various time points (Figures 5.1a, 5.1b and 5.1c). Figure 5.1a represents a linear plot of the

decline in the mean plasma concentration of AM2/169 following an IP dose of 50 mg/kg to a group of male Wistar rats. The time scale is from a 0.083 hour time point (the time the drug has reached the blood stream) to a 2 hour time point (the time the drug has completely cleared from the blood stream). Figure 5.1b demonstrates a semi logarithmic plot of the data shown in Figure 5.1a. The time scale is the same as in Figure 5.1a (0.083 to 2 hours time points), although the ordinate (concentration) scale is logarithmic. Figure 5.1c shows the same data as Figure 5.1b, but with a time scale from a 0.33 hour time point (the time the drug has reached the maximum blood concentration) to a 2 hour time point (the time the drug has completely cleared from the blood stream).

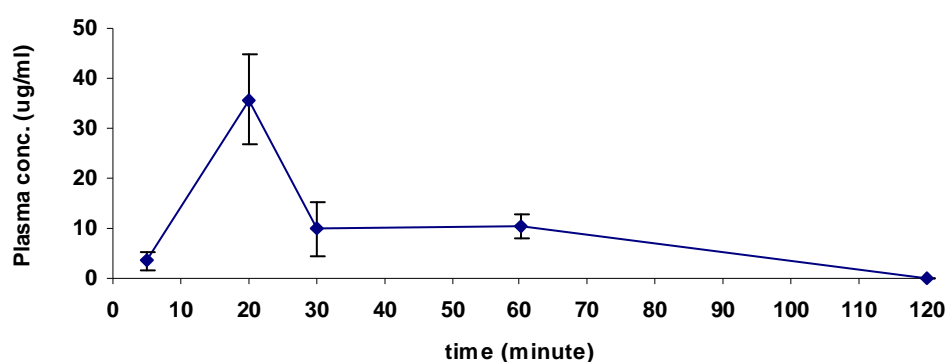


Figure 5. 1a A linear plot of the decline in the mean plasma concentration of AM2/169 following an IP dose of 50 mg/kg to a group of male Wistar rats. The time scale is from a 0.083 hour time point (the time the drug has reached the blood stream) to a 2 hour time point (the time the drug has completely cleared from the blood stream). The area under the curve (AUC) represents total systemic exposure to the drug. Values denote mean \pm SD (n=3).

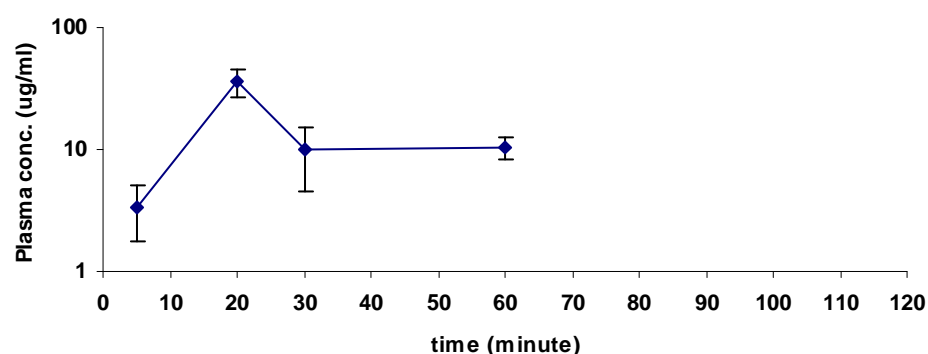


Figure 5. 1b A semi logarithmic plot of the decline in the mean plasma concentration of AM2/169 following an IP dose of 50 mg/kg to a group of male Wistar rats. The time scale is the same as Figure 5.1a (0.083 to 2 hours time points), however the ordinate (concentration) scale is logarithmic. Values denote mean \pm SD (n=3).

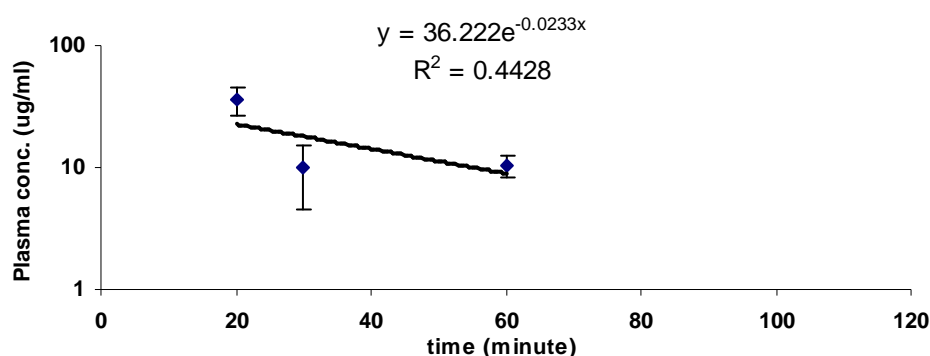


Figure 5. 1c A semi logarithmic plot of the decline in the mean plasma concentration of AM2/169 following an IP dose of 50 mg/kg to a group of male Wistar rats. The time scale is from a 0.33 hour time point (the time the drug has reached the maximum blood concentration) to a 2 hour time point (the time the drug has completely cleared from the blood stream). Values denote mean \pm SD (n=3).

Based on the time-points measured, the inhibitor reached the blood circulation after 5 minutes subsequent to intraperitoneal injection (absorption phase). The maximum plasma concentration (C_{\max}) of the drug was measured after 20 minutes (t_{\max}) at 35.74 $\mu\text{g/ml}$ with rapid clearance thereafter. Two hours after the injection, the inhibitor had been eliminated from the systematic circulation and entered the body tissues (elimination phase). Thus, the area under the curve (AUC) represents total systemic exposure to the drug. The area under the curve up to the time of the peak concentration is a measure of early exposure to the drug. The concentration profile before the peak is a function of how quickly the drug enters the systemic circulation (Figure 5.1a).

Accordingly, based on Figures 5.1b and 5.1c, the elimination half-life ($t_{1/2}$), volume of distribution (V_d) and clearance (CL) of the inhibitor were calculated.

Commonly, the kinetics of a drug is characterised by its half-life ($t_{1/2}$). The elimination half life is the time taken for the plasma concentration of the drug to fall by one half.

$$t_{1/2} = \frac{0.693}{k_e}$$

k_e is the elimination rate constant and presented by the slope of the line of the logarithmic plasma concentration versus time. K_e was calculated to be equal to 0.0233 min^{-1} . Thus;

$t_{1/2}$ was calculated to be 29.74 minutes.

For drugs that are hydrophobic (as in this case), comparatively little of the dose remains in the circulation to be measured; hence, plasma concentration is low and volume of distribution is high (Tozer & Rowland, 2006).

In order to quantify the distribution of the drug between the plasma and the rest of the body after parenteral dosing, the volume of distribution (apparent volume of distribution) and blood volume (BV) was measured. When the logarithm of drug concentration was plotted against time a straight line resulted (Figure 5.1c). If this is extrapolated back to time zero it gives the blood drug concentration before any drug is eliminated, i.e. when the whole dose (4.75 mg, $t = 0$) is still in the body. In this case, the extrapolated concentration at time zero is 36.22 mg/L and the V_d is 0.131 L.

$$V_d = \frac{\text{Amount of drug in the body}}{\text{Plasma drug concentration}} = \frac{4.75 \text{ mg}}{36.22 \text{ mg/L}} = 0.131 \text{ L} = 131 \text{ ml}$$

Blood volume was calculated by (Lee, 1985):

$$BV \text{ (ml)} = 0.06 \times BW \text{ (body weight)} + 0.77 \text{ (} r = 0.99, n = 70, p < 0.00 \text{)}$$

which was equal to 6.47 ml.

As expected, the volume of distribution for the inhibitor is significantly high. This could be attributed to the hydrophobicity of the drug. Lipid-soluble drugs would usually be absorbed via transcellular passive diffusion through the lipid membrane barrier. Therefore, they concentrate more in peripheral tissues or organs rather than plasma itself. Furthermore, one of the major determinants that quantify the distribution of the drug between the plasma and the rest of the body after parenteral administration is the relative avidity of the drug for tissue components as compared with blood. If a drug is very tightly bound by tissues and not by blood, most of the drug in the body will be held in the tissues and very little in the plasma, so that the drug will appear to be dissolved in a large volume and V_d will be large (in this case). Conversely, if the drug is tightly bound to plasma proteins and not to tissues, V_d can be very close to blood volume.

Clearance or rate of elimination is the single most important factor determining drug concentrations within the body and is influenced by dose, blood flow and intrinsic

function of the liver or kidneys. However, plasma protein binding may lead to false interpretation of drug clearance. In the data shown in the above graphs (Figure 5.1b and 5.1c), it can be seen that the drug is eliminated over a period of time as expected, as the rate of drug elimination is directly proportional to the concentrations of drug in the blood. To measure the rate at which the active drug is removed from the body, the rate of elimination (CL) was calculated as follows;

$$CL = \frac{k_e}{V_d} = 0.0233 \times 0.131 = 3 \text{ ml min}^{-1}$$

Furthermore, as there is a straight line on the logarithmic concentration plot (Figure 5.1c), it can be concluded that the reaction is first order and the rate of reaction is directly proportional to the concentration of the drug. In fact, first order kinetics reactions follow a natural logarithmic degradation. When absorption occurs through a first-order process, the rate of absorption is proportional to the amount of drug remaining to be absorbed. Therefore, as the drug is absorbed, its rate of absorption decreases and its rate of elimination increases. Consequently, the difference between the two rates diminishes. As long as the rate of absorption exceeds that of elimination the concentration in the blood continues to rise. Eventually, a time, t_{\max} , is reached when the rate of elimination exceeds the rate of absorption (20 minutes, in this case); the concentration is then at a maximum, C_{\max} (35.74 $\mu\text{g/ml}$). Subsequently, the rate of elimination exceeds the rate of absorption and the concentration declines (Figure 5.1a).

When a drug enters the systemic circulation, the drug molecules are distributed via the blood flow to the body's tissues. The drug is carried not only to the site of action, but also carried to other tissues including: skin, fat, muscle and eliminating organs (liver and kidney). The pattern of drug distribution in body tissues is determined by a number of factors such as the physicochemical properties of the drug (lipid solubility, molecular size and the degree of ionisation), the rate of blood flow to tissues (tissues with the highest blood flow receive the drug in a greater proportion), tissue mass, protein binding (lipophilic drugs are usually largely protein bound) and properties of the membrane. In order for a drug to be distributed to the site of action it must cross one or usually more membranes. Since for the majority of drug molecules, crossing of

the membrane occurs by simple diffusion, and given the largely lipophilic nature of the membrane, the prime determinant of the rate of absorption is the lipophilicity of drug molecules. As a result, lipophilic drugs penetrate cellular barriers and enter most tissues of the body.

Figure 5.2 demonstrates the concentration (μM) of the inhibitor in 1 mg of lung, kidney, liver and spleen at the indicated time points (0.33, 1 and 24 hours) following IP injection.

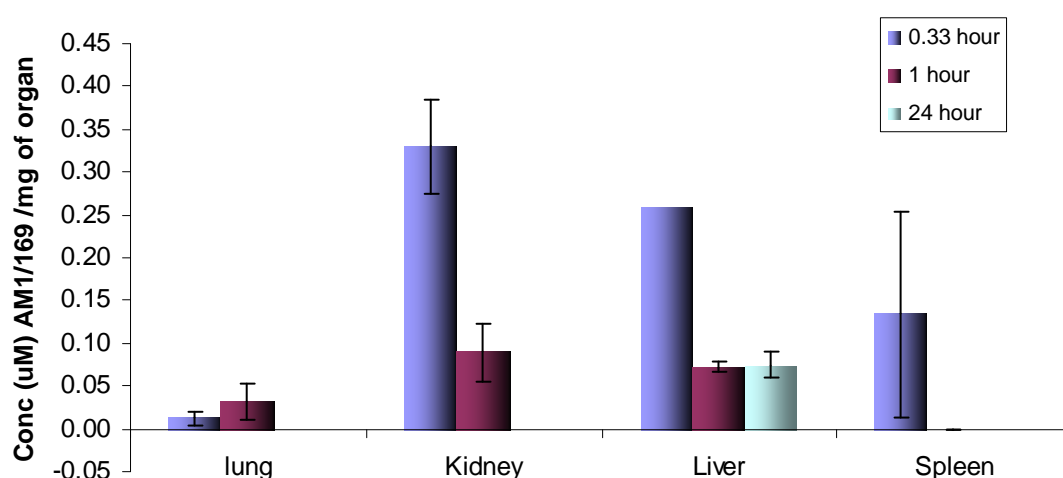


Figure 5. 2 Bio-distribution of AM2/169 in Wistar rats. The values represent the concentration (μM) of the inhibitor in 1 mg of each organ at the indicated time point. On a per organ basis, the distribution of the inhibitor is higher in the kidney and liver compared with other organs at all measured time points. Values denote mean \pm SD (n=3).

The distribution of AM2/169 in tissues was rapid and substantial. The distribution of drug into tissues primarily determines the early rapid decline in plasma concentration. As a result, the distribution of the enzyme inhibitor in tissues was significantly higher than the corresponding levels in serum.

On a per organ basis, the distribution of the inhibitor is higher in the kidney and liver compared with other organs at all measured time points. Initially, the drug concentration in the kidney and the liver was about 0.30 and 0.25 μM per mg of each organ at 0.33 hours. The concentration of the enzyme inhibitor reduced significantly at a 1 hour time point (~ 0.08 μM per mg of each organ) in both organs. No drug was detected in the kidney at a 24 hour time point, nevertheless for the same time point a

substantial amount of the drug was found in the liver; the level was roughly the same as that at the 1 hour time point.

The liver and kidneys are the two principal organs of elimination; kidneys are the primary organs for excretion of the chemically unaltered or unchanged drug, while the liver is the main organ for drug metabolism. Therefore, the distribution of the inhibitor in the kidney and liver is higher than the other organs. Furthermore, the drug stayed for a longer period in the liver (24 hours), suggesting that the preferred site of drug accumulation is the liver. This can be affected by the intrinsic lipophilicity of the drug. The initial concentration of the drug in the spleen was quite substantial and about 0.13 μM per mg of the organ; however no drug was detected after 0.33 hours in the spleen. There was also a small amount of drug distribution in the lungs at the primarily measured time points ($\sim 0.03 \mu\text{M}$ per mg of each lung); nonetheless subsequent to 24 hours, the drug was cleared from the lungs. The fastest drug clearance was in the spleen (after 0.33 hours). It can also be concluded that this drug has a very short journey within the body and after 24 hours time it has been eliminated entirely.

5.6 Conclusion

The novel inhibitor investigated has a rapid clearance and short half life in rats (20 minutes). Therefore an appropriate carrier system is required to enhance targeting of the inhibitor into the liver. Liposomes have been previously shown to be effective drug delivery systems for site specific delivery to the liver and could be similarly employed for the targeting of the novel group of inhibitors of enzyme transglutaminase into the liver. Integrating TG2 inhibitors into liposomes as a potential carrier system and subsequently targeting liposomes into the liver could reduce the large drug distribution, increase half life and eliminate the potential side effects of the drug.

Chapter 6:

**Transglutaminase inhibitor loaded liposomes: a new
approach to the treatment of liver fibrosis**

6.1 Targeted delivery of the TG2 inhibitors into the liver

There has been tremendous activity in the field of drug development and testing for hepatic fibrosis. Nevertheless as previously stated, thus far no drugs have been approved as antifibrotic agents in humans. A successful approach for the cure of hepatic disease should be based on the application of nontoxic drugs with a high therapeutic index and safety profile along with selective targeting. To accomplish these goals, several biological and synthetic carriers with a wide range of chemical and physical properties have been formulated (Di Campli et al., 1999).

As detailed in chapter 1 & 5, the application of transglutaminase inhibitors (TG2) in the treatment of tissue fibrosis shows great promise as a therapeutic strategy where increased ECM deposition and accumulation is involved. However, without effective delivery systems to the target organ, these novel peptide-based inhibitors are prone to rapid degradation or widespread biodistribution which may lead to adverse side effects. Therefore an appropriate carrier system is required to improve delivery and targeting of the inhibitor to the required site of action, in this case the liver. The open and relatively large fenestrations of the endothelial lining of the sinusoids makes the liver an ideal candidate for particulate targeting and uptake, this allows the greater possibility of particle extravasation, compared to the capillary bed of most other organ systems (Longmuir et al., 2006). Liposomes can be used as an efficient drug delivery system for site specific delivery of these site-directed inhibitors of transglutaminase into the liver.

Liposomes have been extensively evaluated as a potential drug delivery system for therapeutic applications due to their ability to alter the pharmacokinetics and diminish the toxicity of their associated drugs (Hwang, 1987; Allen and Hansen, 1991), relative ease of preparation, ability to protect effector molecules from degradation, and specific targetability. More significantly, liposomal drugs have established their efficacy and safety in humans with products such as Caelyx® and AmBiosome® which have already been clinically used (Allen and Cullis, 2004; Perrie, & Rades, 2009). Liposomes, depending on their formulation can be prepared to be nontoxic, non-immunogenic, biodegradable and can have a high loading capacity for a variety of drugs. Furthermore, fluorescent markers or radiolabels could be simply integrated into the liposomes; this

incorporation of marker molecules can provide precious information about the site and distribution of the injected agent (Yao et al., 1995). Despite many of these valuable properties, liposome application for the delivery of drugs by injection into the blood stream has been restricted by the rapid removal of liposomes subsequent to injection by the mononuclear phagocyte system (MRS), also called the reticuloendothelial system (RES), of which the liver and spleen are the main organs (Jones, 1995). Nevertheless, while the inherent affinity of liposomes for the liver has been the primary weakness and flaw in liposomal therapy for other researchers, it would prove to be an advantage for drug targeting to the liver with the aim of curing liver diseases (Yao et al., 1995). Therefore, liposomes can be selected as a potential vehicle for delivery of the TG2 inhibitors into the liver.

6.2 Liposomes

6.2.1 General background and application

In the early 1960s, Alec Bangham and his collaborators at Cambridge University observed under an electron microscope that purified phospholipids dispersed in water spontaneously formed multilayered vesicles (Bangham and Horne, 1964) which their colleague Gerald Weissman named liposomes (Bangham, 1992). They demonstrated that each layer was a bimolecular lipid membrane, and that the layers enclosed internal aqueous compartments. Liposomes as drug delivery vehicles were initially proposed by Gregoriadis and Ryman in 1971 as a carrier of enzymes in the treatment of lysosomal storage disease (Gregoriadis et al., 1971). Since then, the application of liposomes has been extended to a variety of drugs such as antineoplastic agents, antimicrobial compounds, immunomodulators, chelating agents, steroids, vaccines and genetic material (Gregoriadis and Florance, 1993).



Figure 6. 1 Diagrammatic representation of a liposome and its bi-layer forming lipid molecule in an aqueous medium (web image 13).

6.2.2 Liposomes (micro-particulate vesicular carrier)

Liposomes are micro-particulate or colloidal carriers which form spontaneously upon hydration of certain lipids in aqueous media (Bangham and Horne, 1964) (Figure 6.1). They range from 50 nm to 10 μ m diameter (Crommelin et al., 2002) and consists of an aqueous volume entrapped by one or more bi-layers of natural and/or synthetic lipids (phospho and sphingo-lipids), and may also contains cholesterol or other hydrophilic polymer conjugate lipids.

6.2.3 Why liposomes are formed?

Lipids could form liposomes or other colloidal structures display a dual chemical nature; the head groups are hydrophilic (water loving) and the fatty acyl chains are hydrophobic (water hating) (Weiner et al., 1989). When the lipid molecules are dispersed within an aqueous medium, such as water, the polar part of the phospholipid interacts with the water and the non-polar part of the molecule avoids the water. In order to accomplish this, the phospholipids align themselves side-by-side with their non-polar portions orienting themselves towards each other as shown in cross-section in the middle Figure 6.2. This structure is known as a phospholipid bi-layer. This bi-layer extends itself in water to form sheets which then curls into liposomes (Figure 6.2). The large free energy change between water and a hydrophobic environment (15.3 Kcal/mole for dipalmitoylphosphatidylcholine and 13.0 Kcal/mole for dimyristoylphosphatidylcholine) illustrates the natural preference of typical lipids for assembly in bi-layer structures excluding water as much as possible from the structure to reach the lowest free energy level and thus the maximum stability for the aggregate structure. It is also evident from these thermodynamic considerations that bi-layer structures do not form as such in the absence of water, since it is water that acts as the driving force for lipid molecules to assume a bi-layer arrangement (Weiner et al., 1989).

Drugs with extensively varying lipophilicities could be encapsulated, in the phospholipid bi-layer (lipophilic drugs), in the entrapped aqueous volume (hydrophilic drugs) or at the bi-layer interface (interface-associated drug) in liposomes (Sharma and Sharma, 1997).



Figure 6. 2 Diagrammatic illustration of a phospholipid molecule with a polar (water soluble) and a non polar group (oil like), a phospholipid bi-layer and a self-assembled liposome. When the lipid molecules dispersed within an aqueous medium, such as water, the polar part of the phospholipid interacts with the water and the non-polar part of the molecule avoids the water. In order to accomplish this, the phospholipids align themselves side-by-side with their non-polar portions orienting themselves towards each other as shown in cross-section in the middle figure above. This structure is known as a phospholipid bi-layer. This bi-layer extends itself in water to form a sheet which then curls into a liposome (web image 14).

6.2.4 Advantages of liposomes for drug delivery

Liposomes can be formulated in various sizes, compositions, surface charges. Thus, they could be formulated to present the most appropriate properties for the drug and the target site (Goyal et al., 2005). Upon injection into the systemic circulation, drugs incorporated within liposomes will remain with the carrier systems and have their pharmacokinetic distribution dictated by the liposomal carrier rather than the properties of the drug. Entrapped drugs are also physically separated from the environment, and are, therefore, protected against degradative enzymes (Chaize et al., 2004). These factors combined with their innate ability to passively target the MPS, sites of inflammation and tumor sites result in their capacity to enhance the drug therapeutic profile, by increasing the quantity of drug reaching the site of action whilst reducing general drug distribution and associated toxicity issues (Storm & Crommelin, 1998).

6.2.5 Manufacturing problems and limitations

As described above, liposomes have a great potential in the area of drug delivery. However, the number of liposome based therapies remains limited (Table 6.1).



Illustrations removed for copyright restrictions

The limitations to their application have been to find a way to manufacture a discrete liposomal formulation using a fully reproducible method, in large quantities and to guarantee a long shelf-life. To accomplish this, problems regarding stability, sterility, scale up and shelf life of the liposomes/liposomal preparations must be overcome. To solve each of these problems extensive work is needed to find appropriate conditions, firstly for stable liposomal systems. Secondly, the whole manufacturing process should be performed in a sterile condition. In terms of large scale preparations, a number of techniques exist, such as high pressure homogenization, injection method and detergent dialysis. Finally, freeze-drying of the liposomal formulation subsequent to preparation and storage of the liposome preparations at low temperature are two ways to slow down the diffusion process during shelf life (Massing and Fuxius, 2000).

6.2.6 Classification of liposomes

At a New York Academy of Sciences meeting in 1978 (Papahadjopoulos, 1978) liposomes were classified using several three letter acronyms as follows:

6.2.6.1 Multilamellar vesicles (MLV)

Multilamellar vesicles (MLV) are widely studied and are characterized by the presence of multiple lamellae with a volume diameter, ranging from as little as 100 nm to 10 microns in size (Ahl et al, 1994) (Figure 6.3). MLV can be prepared using a thin-film hydration method or hydration of lipids in the presence of an organic solvent Vemuri and Rhodes, 1995.



Figure 6. 3 Multilamellar vesicle (MLV) (web image 15).

6.2.6.2 Unilamellar vesicles of small size (SUV)

MLV can be sonicated or extruded through polycarbonate filters to produce a small and more uniformly sized population (Saunders et al., 1962). Small unilamellar vesicles (SUV) (Figure 6.4) have a volume diameter equal and are under approximately 0.1 μm in diameter (Gregoriadis, 1990).

6.2.6.3 Large unilamellar vesicles (LUV)

Large unilamellar vesicles (LUV) (Figure 6.5) are characterized by diameters in excess of 100 nm and are comprised of a solitary bilayer of lipids. LUV encapsulate a larger quantity of drug for a given concentration of lipid and thus have higher encapsulation efficiency compared with SUV (Liu et al., 2001). Nonetheless, the absence of multiple lamellae renders the vesicle more fragile compared with MLV (Kirby and Gregoriadis, 1999).



Figure 6. 4 Small unilamellar vesicles (SUV)
(web image 16).

Figure 6. 5 Large unilamellar vesicles (LUV)
(web image 17).

6.2.6.4 Reverse phase evaporation vesicles (REV)

Reverse phase evaporation vesicles (REV) are unilamellar vesicles and have a size range of 150-450 nm and are produced from an aqueous-organic emulsion by evaporation of the organic phase (Szoka and Papahadjopoulos, 1978).

6.2.6.5 Vesicles produced using the extrusion technique (VET)

VET are unilamellar with a size range from 50 to 180 nm and are produced by extruding MLV through controlled pore filters under high pressure (Mayer et al., 1986).

6.2.6.6 Dehydration-rehydration vesicles (DRV)

Dehydration-rehydration method was developed by Kirby and Gregoriadis (1984) to enhance the efficacy of drug incorporation within the liposomes. Dehydration-rehydration vesicles (DRV) are produced from dehydrated dispersions using a rehydration technique which enables relatively large quantities of materials to be entrapped.

6.2.7 Parameters which influence *in vivo* behavior of liposomes

Liposomal formulations of various drugs can be optimized in terms of drug content, stability, desirable bio-distribution patterns, and cellular affinity and in terms of the organ disposition of liposomes by altering their physicochemical parameters. These parameters include fluidity of the bi-layer membrane, surface charge density, surface hydration, particle size and method of preparation (Juliano and Stamp, 1975; Sharma and Sharma, 1997; Fraley et al., 1981; Gabizon and Papahadjopoulos, 1988; Liu et al., 1992; Straubinger et al., 1993; Yu and Lin, 1997). The effects of some of these parameters on the physical and biological properties of liposomes are detailed below.

6.2.7.1 Bi-layer fluidity

Lipids have a characteristic phase transition temperature (T_c). They exist in a rigid well-ordered arrangement below the T_c , and a liquid crystalline phase above the T_c (Weiner et al., 1989). The physical state of the bi-layer affects the permeability, leakage and overall stability of the liposomes. Accordingly, phospholipid liposomes must be produced at temperatures above the chain-melting temperature of the phospholipid, in order that the bi-layers be in the liquid-crystalline state. The chain-melting temperature of a phospholipid is verified by the head group type, the alkyl chain length and nature (saturated and non-saturated) of the fatty acid chain (Jones et al., 1995; Sharma and Sharma, 1997). Using phospholipids with a phase transition temperature higher than body temperature (e.g. distearoyl phosphatidylcholine (DSPC) with a T_c of above 55 °C) makes the liposome bi-layer membrane less fluid, consequently less leaky and more stable at physiological fluid; it could also diminish the extent of MPS uptake (Gabizon and Papahadjopoulos, 1988) and overcome the problem of liposome destabilization induced by plasma high-density lipoproteins (HDL) (Gregoriadis, 1995; Yu and Lin, 1997).

6.2.7.2 Surface charge

Surface charge is one of the main parameters which influence vesicle stability, the mechanism and extent of liposome-cell interaction and the *in vivo* fate of liposomes. Neutral liposomes show more aggregation and less stability compared to charged

liposomes (Weiner et al., 1989). The surface charge of liposomes has also a crucial role in cellular uptake and blood distribution of liposomes and it can be controlled by the type of lipid used. Neutral liposomes have less interaction with cells than charged liposomes. However, negatively charged liposomes are mainly taken up by cells through coated-pit endocytosis due to the high electrostatic surface charge which could promote the extent of liposome-cell interaction (Sharma and Sharma, 1997; Gabizon et al., 1990). Therefore, the inclusion of negatively charged lipids in liposome formulations accelerates the process of opsonization and subsequently the rate of hepatic uptake, resulting in rapid elimination of the liposomes from blood circulation following systematic administrations (Kamps et al., 1999, Huong et al., 2001; Massing and Fuxius 2000). Apparently, the exposure of negatively charged lipid serves as a signal for the removal of the liposomes (Liu et al., 1995). Some studies have even reported that the phosphatidyl serine-negatively charged liposomes were taken up by the liver to a 10-fold higher extent than the neutral ones (Rothkopt et al., 2005). As a consequence, negatively charged liposomes may be more appropriate than neutral or positively charged liposomes as an intrahepatocyte delivery vehicle since the cellular uptake of negatively charged liposomes is higher than positively charged or neutral liposomes (Yu and Lin, 1997). Furthermore, previous investigations revealed that the presence of negatively charged lipids, phosphatidyl serine (PS), phosphatidyl inositol (PI), or phosphatidyl glycerol (PG) or positively charged detergents such as stearylamine in liposome formulations reduces the likelihood of aggregation subsequent to the formation of vesicles. Furthermore, it leads to a greater overall entrapped volume; due to increase of the intercellular distance between successive bi-layers in the MLV structure (Weiner et al. 1989).

6.2.7.3 Liposome size

The average size of liposomes and size distribution are also main factors which verify the fraction cleared by MPS (Harashima et al., 1994) with the rate of liposome clearance increasing with greater vesicle size. Large liposomes ($\geq 0.1 \mu\text{m}$) are more prone to opsinization, thus clear more quickly and to a higher extent by the MPS when compared to small liposomes of the same composition ($\leq 0.1 \mu\text{m}$) (Sharma and Sharma 1997; Huong et al., 2001). Therefore, the size of liposomes is one of the physical properties

which can influence liposome targetability to the liver. Indeed it has been stated that an efficient liposome size for liver targeting is approximately 100 nm. At this size, the vast majority of liposomes deliver their contents to Kupffer cells as evidenced by fluorescence and EM studies (Yao et al., 1995).

6.2.8 Optimization of liposome composition

It has been shown that the membrane composition of liposomes is essential for its targeting and function. Liposome membranes consisting of glycerophospholipids with long hydrogenated fatty acid esters (e.g. synthetic phospholipids such as distearoylphosphatidylcholine (DSPC)) are more rigid than membranes consisting of glycerophospholipids composed of fatty acids of different length and saturation (e.g. egg lecithin, soya lecithin) (Patel, 1992; Devine et al., 1994). Thus, these liposome membranes are more stable against lipid exchange by serum proteins (e.g. high density lipoprotein (HDL)). Furthermore, increasing the hydrocarbon chain length of the fatty acid part of the phospholipid, results in a tighter film packing. A rigid membrane decreases the efflux of drugs from liposomes and stabilizes the liposomes themselves. In contrast, increasing the degree of unsaturation of the hydrocarbon chain of the phospholipid chain, the branching of the hydrocarbon chain of the phospholipid, or increasing the temperature of the system, yields to a looser film packaging (Massing and Fuxius, 2000).

Cholesterol also improves the fluidity of the bi-layer membrane, decreases the permeability of water soluble molecules through the membrane, and enhances the stability of the bi-layer membrane in the presence of biological fluids such as blood/plasma. Liposomes devoid of cholesterol have a propensity to react with the blood proteins such as albumin, m-transferrin, and macroglobulin which have a susceptibility to destabilize the liposomes and diminish the utility of liposomes as drug delivery systems (Kirby et al., 1980; Damen et al., 1981; Vemuri and Rhodes, 1995).

6.3 Aim and objectives

The work in this chapter focuses on the development of a liposome-based drug delivery system for site specific delivery of a novel group of inhibitors of the enzyme TG2 into the liver. The ultimate aim of the work is to develop a drug delivery system which can be applied in the delivery of site directed irreversible transglutaminase inhibitors to the liver which can then be further studied for the treatment of liver fibrosis in animal models. Integrating of the TG2 inhibitors into liposomes as a potential carrier system and subsequent passive targeting of vesicles into the liver could focus drug distribution, increase half life and eliminate the potential side effects of the drug.

The objectives of this work were,

- Preparation of multilamellar vesicle incorporating the TG2 inhibitor
- Preparation of small unilamellar vesicles incorporating the TG2 inhibitor
- Separation of non-incorporated drug from liposome suspension
- Characterising the TG2 incorporated liposomes in terms of liposome size, polydispersity, zeta potential and drug entrapment efficiency
- Investigating the effect of salt on the physico-chemical properties of the TG2 incorporated liposomes
- Stability studies in buffer and serum, in terms of drug retention, particle size and zeta potential.
- Bio-distribution study of the TG2 incorporated liposomes in mice

6.4 Materials

Egg phosphatidylcholine, distearoyl phosphatidylcholine and phosphatidylserin lipids were purchased from Avanti Polar Lipids, Inc. (Alabaster, AL, USA) and were used devoid of any further purification. Phosphate buffered saline (PBS) and cholesterol were acquired from Sigma-Aldrich (Dorset, England). Cholesterol, [1,2-³H(N)]-, 1mCi (37 MBq) and Ultima GoldTM scintillation fluid were obtained from PerkinElmer (Waltham, MA, USA). Fetal bovine serum was purchased from Biosera (East Sussex, England). AM2/169 (TG2 inhibitor) was prepared within the chemistry department of Aston

University by Dr. Alexandre Mongeot and Dr. Dan Rathbone as previously described (Griffin et al., 2008). Male Outbred mice were obtained from Charles River UK Ltd (Kent, England). Unless stated otherwise PBS was used at 0.01 M, pH 7.4. Doubly distilled and filtered water was used in the preparation of all solutions.

6.5 Methods

6.5.1 Liposome production

6.5.1.1 Production of multilamellar vesicle incorporating the TG2 inhibitor

Multilamellar vesicles (MLV) were prepared using a technique based on the established film method, the assembly of phospholipids into closed lipid bilayers within excess water as described by Bangham (1965). Initially, phosphatidylcholine (PC), 1,2-distearoyl-L-3-glycerol-phosphatidylcholine (DSPC), phosphatidylserin (PS) and cholesterol (Chol) were dissolved in a solvent mixture of chloroform and methanol (9:1 v/v) and subsequently mixed at the required composition and molar ratios, with(out) a requisite amount of the enzyme inhibitor. Phospholipids were dissolved in organic solvents in order to avoid oxidation of lipids during storage, assist uniform distribution of lipids in the lipid bi-layer and attain molecular mixture of various lipids amongst themselves (Vemuri and Rhodes, 1995). The required lipid solutions, at the desired concentrations, were then placed in a round-bottom spherical Quick-fit® flask. Thereafter, the solvents were evaporated on a rotary evaporator (Buchi Rotavapor-R) at about 37 °C to yield a dry lipid film on the inner wall of the flask. The thin lipid film on the wall of the flask was flushed with oxygen-free nitrogen in order to ensure complete removal of all solvent traces, since the residual quantity of solvents left in the final preparation could pose health hazards to the end user (Vemuri and Rhodes, 1995). The dry lipid film was hydrated through addition of an aqueous medium (PBS or distilled H₂O) and vortexed until the thin lipid film was transformed into a milky suspension. The hydration of the thin lipid film was maintained above the gel-liquid crystal transition temperature (T_c) of the phospholipids ($>T_c$). PC has a T_c of 0 °C and DSPC has a T_c above 55 °C, thus the aqueous medium added to hydrate DSPC was pre-warmed to a temperature above 55 °C. The preparations were left to stand above the T_c for 30 minutes during which time the vesicles formed and stabilized (Figure 6.6).

6.5.1.2 Production of small unilamellar vesicles incorporating the TG2 inhibitor

Sonication is one of the common methods of producing homogenous liposomes of specific sizes. To generate small unilamellar vesicles (SUV), the MLV suspension (prepared as detailed in section 6.5.1.1) was sonicated above T_c using a probe sonicator (Soniprep 150, MSE, England) with a titanium probe (exponential micro-probe and diameter 3 mm) and frequent intervals of rest (to prevent overheating), The tip of the sonicator was slightly immersed in the suspension for a few minutes at an amplitude of 5 microns to yield a clear suspension of small unilamellar vesicles (Figure 6.7). The amount of time required for sonication, varies depending on the lipid composition (approximately 2-5 minutes). Subsequent to sonication, the preparations were left to stand above the T_c for 30 minutes.



Figure 6. 6 Schematic representation of the preparation of MLV by ‘hand-shaking’ method. Lipids and drugs were dissolved in the organic solvents (A) and then evaporated (B); thereafter, dried lipid film was hydrated in the aqueous medium (PBS or d.H₂O) (C) and finally left to stand for 30 minutes to yield vesicles (D).



Figure 6. 7 Preperation of small unilamellar vesicles by sonication of MLV suspension. To generate SUV, MLV entrapped with the drug were sonicated at above T_c with frequent intervals of rest using an ultrasound probe sonicator. Sonication is one of the common methods of producing homogenous liposomes of specific sizes.

6.5.2 Separation of non-incorporated drug from liposome suspension

In order to utilize liposomes as a controlled release or pharmaceutical dosage form, the complete removal of the non-incorporated drug is essential. Various approaches have

been taken to remove the non-incorporated drug molecule in a laboratory setting. Centrifugation and size exclusion chromatography were applied to separate vesicles from the freely floating drug and to quantify the entrapped enzyme inhibitor of liposomes.

6.5.2.1 Size-exclusion chromatography

Size-exclusion chromatography is a chromatographic method that separates liposomes from the free drug molecules due to differences in the molecular weight and shapes of drug molecules and vesicles. Size-exclusion chromatography was performed on the AKTA Purifier (Amersham Biosciences) FPLC system, with a fluorescent detector (Cecil Instruments Limited, CE 4500 fluorescence detector) on a Superdex™ 200 10/300 GL column from GE Healthcare. PBS was used as the buffer and elution was monitored at excitation and emission wavelength 330 and 570 nm. Initially, the column was equilibrated with a buffer of the same osmolarity as the medium in which the liposomes were prepared and an aliquot of the liposomes was applied to the column. The column was eluted with the same buffer and fractions were collected (Weiner et al., 1989). The pores of support were of such a range as to allow only some of the molecules to enter. As shown in Figure 6.8, while the liposome preparation flows down the column, vesicles incorporating fluorescent enzyme inhibitor (red balls), are unable to enter any of the pores of the gel due to the large size and are therefore totally excluded and eluted first. The free drug (green balls), which is smaller in size, is held back as a consequence of permeating the particle pores and elutes in reverse order of size (Vemuri and Rhodes, 1995).

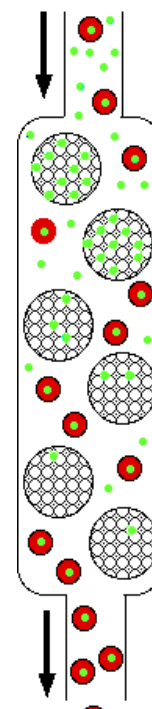


Figure 6. 8 Schematic representation of size-exclusion chromatography. As the liposome suspension flows down the column, vesicles incorporating fluorescent enzyme inhibitor (red balls), are not capable to penetrate the gel pores due to the large size and are therefore entirely excluded and eluted foremost. The free drug (green balls), which is smaller in size, is held back as an outcome of permeating the particle pores and elutes in reverse order of size.

Injection of MLV into the chromatographer was not possible due to the large size of the liposomes; therefore another approach was applied to effect the separation of the non-incorporated drug from the liposome mixture.

6.5.2.2 Centrifugation

Centrifugation technique applies centrifugal force to separate the liposome mixture. Liposomes sediment when subjected to a centrifugal force at a rate that is dependent on their density. More-dense components of the mixture (liposomes) move away from the axis of the centrifuge and precipitate, whilst less-dense components of the mixture (free drug) move towards the axis. Large liposomes composed of neutral lipids such as PC can be simply pelleted at fairly low g forces in a conventional centrifuge (Weiner et al., 1989).

Accordingly, subsequent to the preparation of MLV incorporating enzyme inhibitor, each sample was examined by retaining small unwashed aliquot and washing the non-incorporated drug from the liposome suspension by two times centrifugation at 14000 rpm in a Beckman model J2-21 centrifuge (JA-20 rotor), for 30 minutes at 4 °C following centrifugation, the supernatants (containing the free drug) were carefully removed and the pellets (containing entrapped or associated drug) were suspended to the required volume within the aqueous medium. The same cycle was repeated once more to ensure maximum separation of non-incorporated drug from liposome suspension. Liposomes were then ruptured by adding isopropanolol (1:1 v/v) to the pellets and mixed through vigorous shaking. The mixture incubated for 2-5 minutes at room temperature. The drug content in the liposome and supernatant was then analyzed by spectrofluorimetry at the corresponding wavelengths (excitation/emission 330/570 nm) as previously described.

6.5.3 Characterisation of liposomes

Methods of characterisation of liposomes instantaneously following production and upon storage are required for sufficient quality control of the product. The methods have to be reproducible, precise, and rapid in their application in an industrial setting (Vemuri and Rhodes, 1995).

6.5.3.1 Determination of the liposome size and polydispersity

The volume mean diameter (VMD) for all MLV formulations and preparations was determined by light scattering based on laser diffraction spectroscopy using Sympatec

Helos Compact laser diffraction analyzer (GmbH, Clausthal-Zellerfeld, Germany). An appropriate dilution of the sample was made in double-distilled water. Particle size distribution (PSD) is presented as X_{10} , X_{50} and X_{90} -values derived from the cumulative volume distribution curves as a function of the particle diameter. These diameters correspond to 10 %, 50 % and 90 % of total volume from cumulative percentage undersize curves. All measurements were performed at ambient temperature.

The z-average diameter and polydispersity for all SUV formulations and preparations, was determined by photon correlation spectroscopy on a ZetaPlus (Brookhaven Instrument Corporation, USA) at 25 °C and for the viscosity and refractive index the value of pure water was used (0.89 Cp and 1.0, respectively). Liposome samples (50 μ l) were diluted to 2 ml with 0.001M PBS to maintain optimal vesicle count rate and concentration. The reported measurements were the average of ten readings.

6.5.3.2 Measuring zeta potential

Zeta potential which is an indirect measurement of vesicle surface charge (Perrie et al., 2004) for all liposome formulations and preparations was measured on a ZetaPlus (Brookhaven Instrument Corporation, USA) at 25 °C. The technique used was microelectrophoresis, where the measured velocity of a particle is said to be proportional to the applied electric field. Liposome samples (50 μ l) were diluted to 2 ml with 0.001M PBS. The zeta potential results were mean averages taken from ten readings made for each formulation in triplicate. Control and transfer standard readings were regularly taken and logged for particle size (499 ± 5 nm, Brookhaven) and zeta potential (-68 mV \pm 6.8, Malvern) for the ZetaPlus Brookhaven Instrument.

6.5.3.3 Drug encapsulation studies

Percent encapsulation is typically defined as the total amount of encapsulant encapsulated vesicles versus the total initial input of encapsulant (Edwards and Baeumner 2006; Terzano et al., 2005). The extent of drug entrapped in vesicles can be determined using the column chromatography technique or other methods such as centrifugation. As mentioned previously, the liposome preparations are a mixture of

encapsulated and unencapsulated drug fractions (free drug). Therefore, to assess the free drug concentration as a first experimental step, the free and encapsulated drug fractions were separated.

6.5.3.3.1 Determination of drug entrapment efficiency by column chromatography

When a separation technique such as size-exclusion chromatography was applied (6.5.2.1), the percent encapsulation was described as the ratio of the unencapsulated peak area to that of a reference standard of the same initial concentration (Edwards and Baeumner, 2006).

6.5.3.3.2 Determination of drug entrapment by centrifugation

Subsequent to preparation of MLV incorporating enzyme inhibitor and the separation of the capsulated and unencapsulated drug by centrifugation, the pellet which contained the drug encapsulated liposomes was diluted with the required amount of aqueous medium. The encapsulated fraction of the drug was then treated with a detergent (isopropanolol 1:1 molar ratio), vigorously shaken and incubated for a period at room temperature to lyse the liposomes and to completely discharge the drug from the liposomes into the surrounding aqueous media. Thus the exposed drug was assayed using spectrofluorometry. The drug entrapment was then calculated based on fluorometric/spectrometric analysis on a 96 well microtiter plate, using spectrofluorometer (Spectra Max Gemini XS) with an excitation maximum of 335 nm and an emission peak of 560 nm. Entrapment values of the enzyme inhibitor within liposomes were then calculated using the following equations (including any dilutions):

$$\% \text{ Entrapment} = \frac{\text{Fluorescence of washed sample}}{\text{Fluorescence of unwashed sample}} \times 100$$

To ensure reliability of entrapment values, the total recovery of drug was also calculated using the following equation (including any dilutions):

$$\% \text{ Recovery} = \frac{\text{Fluorescence of washed sample} + \text{Fluorescence of supernatant}}{\text{Fluorescence of unwashed sample}} \times 100$$

6.5.4 The effect of salt on the physico-chemical properties of liposomes

In order to investigate the effect of salt on the physico-chemical properties of liposomes, liposomes composed of DSPC: chol: PS in a molar ratio of 12:1:4 or 16:1:0 were formed and rehydrated in phosphate buffered saline (pH 7.4), an isotonic buffer often used for *in vivo* studies and sized by sonication method. Their characteristics in terms of size and surface charge were measured by photon correlation spectroscopy as previously described.

6.5.5 Stability studies in buffer and serum

The stability of the prepared liposomes was investigated in terms of drug retention, particle size and zeta potential.

6.5.5.1 Drug retention

A principal feature of a successful drug delivery system is that liposomes quantitatively maintain their load while circulating (Gregoriadis, 1995). Accordingly, drug entrapment within liposome formulations, DSPC: chol: PS in molar ratios of 16:1:0 and 12:1:4, was measured as detailed previously. Following separation of the non-incorporated drug from the liposome suspension by size-exclusion chromatography, the release rate of the drug was determined by incubating drug-incorporated liposomes in PBS: FBS 50:50 (v/v) composition at 37 °C in a shaking (constant) water bath (80 rpm) at pre-set time intervals (0, 30, 60 and 120 minutes). At each time point, the amount of drug released was subsequently quantified by removing the required quantity of sample, diluting it with PBS as appropriate and loading it on to the column. The results were reported as the percentage of drug leakage from vesicles following 2 hour incubation in PBS (37 °C, pH 7.4).

6.5.5.2 Liposome stability: Particle size and zeta potential

Liposome formulations were prepared as detailed in section 6.4.1 and incubated in PBS or PBS: FBS 50:50 (v/v) composition in a gently shaking water bath (37 °C, 80 rpm). At various time points (0, 30, 60 and 120 minutes), the required quantity of sample was removed and subsequently the average diameter and surface charge of the liposomes were measured via the technique of dynamic light scattering using a ZetaPlus analyzer.

6.5.6 Bio-distribution of liposomes loaded with the enzyme inhibitor in mice

Bio-distribution of liposome-encapsulated enzyme inhibitor was monitored using H^3 labelled cholesterol in the formulations as a marker. SUV were prepared using the lipid-film hydration method previously described. In brief, weighed amounts of DSPC, cholesterol and PS in molar ratios of 16:1:0 or 12:1:4, in addition to the TG2 inhibitor (60 $\mu\text{g/ml}$) and the required amount of H^3 labelled cholesterol were dissolved in chloroform/methanol (9:1, by volume). To avoid the self-association of cholesterol in aqueous medium, the concentration of cholesterol was kept under the critical micelle concentration (25 - 40 nM at 25°) (Haberland and Reynolds, 1973). The organic solvent was then removed by a roto-evaporator followed by flushing with N_2 to form a thin lipid film on the bottom of a round-bottomed flask. The lipid film was then hydrated in PBS (pH 7.4). The size of produced MLVs was reduced by sonication for about 30 second or 5 minutes. The diameter of the liposome preparations used was approximately 100 nm with a polydispersity coefficient of not larger than 0.2 for neutral and anionic liposomes, or 500 nm with a polydispersity coefficient of not larger than 0.3 for anionic liposomes. The liposomal surface was not modified in any way, hence relying on the inherent affinity of PC and DSPC for the liver.

Experimentation strictly adhered to the 1986 Scientific Procedures Act (UK). All protocols have been subject to ethical review and were performed in a designated establishment. All the animals were housed appropriately and given a standard mouse diet ad-libitum.

Male Outbred mice with an average body weight of 40 grams were kept one to each cage. They were housed in an animal room with a 12 hour light/ 12 hour dark cycle, a temperature $19 \pm 23^\circ\text{C}$, and a relative humidity of $55 \pm 15\%$. A dose of the liposomes incorporating drug was given by intravenous injection (I.V.) into the tail vein of 3 mice in each group at preset time intervals (10, 30, 60 and 120 minutes). The volume of substance injected was 100 μl , containing 0.4 μmole of lipid and 200 kBq radioactivity (52 ng cholesterol). Blood samples were collected via cardiac puncture. The mice were then humanely terminated and organs including the liver, lungs, kidneys and spleen were

removed for further investigation. All of the samples were weighed into plastic scintillation vials, to which one and a half milliliter SOLVABLE™ (solubilising agent) was added. The vials were heated to 50 °C with frequent agitation of the tubes to enhance Solvable™ tissues penetration. Completely digested tissue samples were then bleached using 200 µl hydrogen peroxide followed by the addition of 10 ml Ultima Gold for H³ quantification and the radioactivities were determined in a Packard Tri-Carb model 1600 TR liquid scintillation counter (Packard Instrument Co., Meriden, CT).

6.6 Results and discussion

6.6.1 Liposomal characteristics

Manipulation of liposomal physical and chemical characteristics may cause alterations in cellular affinity and in the organ disposition of liposomes. Therefore, the characteristics of liposomes in terms of size, surface charge and drug loading were initially investigated in order to determine the most suitable formulations that would provide the optimal mixture of properties for liver targeting. The range of liposome formulations prepared in this study is summarized in Table 6.2.

Table 6.2 Summary of the range of liposomes formulations prepared in this study, the charge of the liposome, the total molar ratio and their corresponding molar ratios of the individual components.

| Formulation | Liposome charge | The total molar ratio | PC (µmole) | DSPC (µmole) | PS (µmole) | Chol (µmole) |
|-----------------------|-----------------|-----------------------|------------|--------------|------------|--------------|
| PC: chol | Neutral | 17 | 16 | - | - | 1 |
| DSPC: chol | Neutral | 17 | 16 | - | - | 1 |
| PC: chol: PS | Anionic | 17 | 12 | - | 4 | 1 |
| DSPC: chol: PS | Anionic | 17 | - | 12 | 4 | 1 |
| PC: chol: PS | Anionic | 17 | 8 | - | 8 | 1 |
| DSPC: chol: PS | Anionic | 17 | - | 8 | 8 | 1 |

6.6.1.1 Characteristics of the TG2 inhibitor incorporated multi-lamellar vesicles

The average size and size distribution of liposomes are essential parameters when the liposomes are intended for therapeutic use, particularly if they are administered by inhalation or the parenteral route (Vemuri et al., 1990). Moreover, a major physical characteristic of liposomes concerns the polydispersity of the suspensions (Grabielle-Madlmont et al., 2003). Therefore, the series of liposome formulations prepared were

initially characterised in terms of volume mean diameter (VMD) and particle size distribution (PSD). The PSDs are presented as X_{10} , X_{50} and X_{90} -values from cumulative undersize curves.

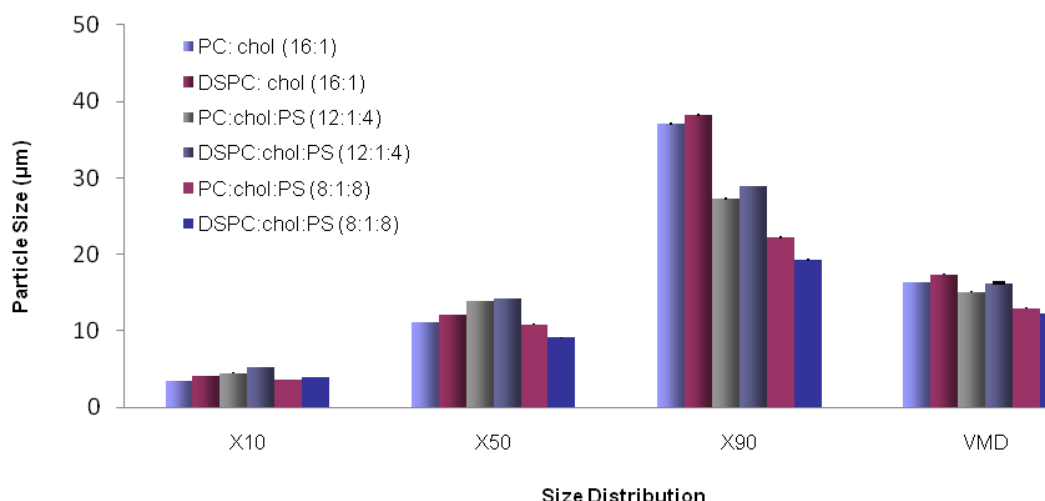


Figure 6. 9 Volume mean diameter (VMD) and particle size distributions (PSD) of various TG2 incorporated multi-lamellar vesicle formulations. The vesicles were prepared in d.H₂O and analysed prior to centrifugation, at 25 °C using a Sympatec Helos. The particle size distributions are presented as X_{10} , X_{50} and X_{90} -values from cumulative undersize curves. Upon the incorporation of the charged lipid, there was a slight decrease in the z-average diameter of the liposomes. A two fold increase in the amount of charged lipids in the formulation resulted in a further decrease in the surface charge of anionic liposomes. Values denote mean \pm SD from three experiments.

As is evident from Figure 6.9, there was no significant difference between the X_{10} of all the formulations (~ 3 -5 μm). The X_{50} of the anionic formulations with 12:1:4 molar ratio were slightly higher when compared to the X_{50} of the neutral preparations (with 16:1 molar ratio) and the anionic formulations containing higher level of PS (PC: chol: PS and DSPC: chol: PS 8:1:8). However this trend changed when considering the X_{90} with the neutral formulations, being significantly larger in size compared to anionic formulations ($P \leq 0.05$, ANOVA).

All vesicles had a volume mean diameter (VMD) in the range of about 12-17 μm . There was no considerable disparity ($P \geq 0.05$, ANOVA) when the VMD was considered amongst the anionic formulations with the same molar ratio or between the two neutral formulations with the same molar ratio, regardless of the lipid type and the lipid concentration used, suggesting that the substitution of PC lipid with DSPC lipid (a longer

alkyl chain lipid) had no major effect on the size of multi lamellar vesicles for all the formulations tested (Figure 6.9). However, there was a trend of reduction in the VMD of the liposomes, upon the incorporation of PS to the formulations. The inclusion of small quantity of a negatively charged lipid such as PS in the formulation may be due to the PS reducing the probability of vesicular aggregation following the formation of vesicles leading to a reduction in the size of charged vesicles (Weiner et al., 1989; Vemuri and Rhodes, 1995). This is supported by the major reduction in the X_{90} particle sizes measured with the anionic formulations. For the same reason, a two fold increase in the amount of charged lipids in the formulation resulted in a further decrease in the surface charge of anionic liposomes ($P \leq 0.05$, ANOVA).

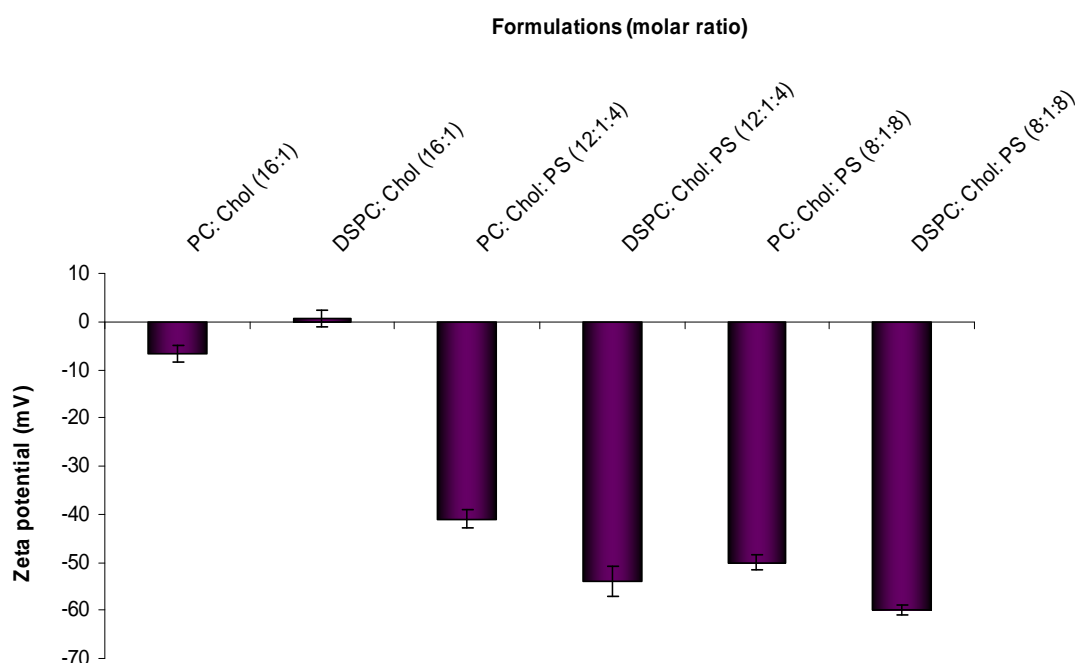


Figure 6. 10 Zeta potential (mV) of various TG2 incorporated multi-lamellar vesicle formulations. The vesicles prepared in d.H₂O and analysed prior to centrifugation, at 25 °C using a Brookhaven ZetaPlus. The inclusion of a charged lipid (PS) into the formulations has a remarkable effect on zeta potential values. In consequence, the surface charge was dropped significantly. Values denote mean \pm SD from three experiments.

With regard to the neutral liposomes, the formulation containing PC had a zeta potential in the range of $-6.6 \text{ mV} \pm 1.78$. Replacement of PC lipid with DSPC lipid yielded a slight increase in the zeta potential values of the liposomes ($0.64 \text{ mV} \pm 1.69$) (Figure 6.10). However, regarding the anionic liposomes, all the formulations containing DSPC

demonstrated a greater negative surface charge when compared to the liposomes containing PC with the same molar ratio. The inclusion of 4 μmole PS, significantly ($P \leq 0.01$, ANOVA) reduced the zeta potential as expected due to its anionic nature. An additional increase in the amount of charged lipids in the formulation by 2-fold resulted in a further decrease in the measured zeta potential of anionic liposomes ($P \leq 0.05$, ANOVA) as would be expected.

6.6.1.2 Characteristics of the TG2 inhibitor incorporated small unilamellar vesicles

6.6.1.2.1 Particle size and zeta potential of SUV

The influence of lipid alkyl chain length and charged liposomes on z-average diameter and zeta potential of various formulations of SUV was investigated. The findings in terms of the resultant liposomes size, polydispersity and zeta potential are shown in Figures 6.11 and 6.12.

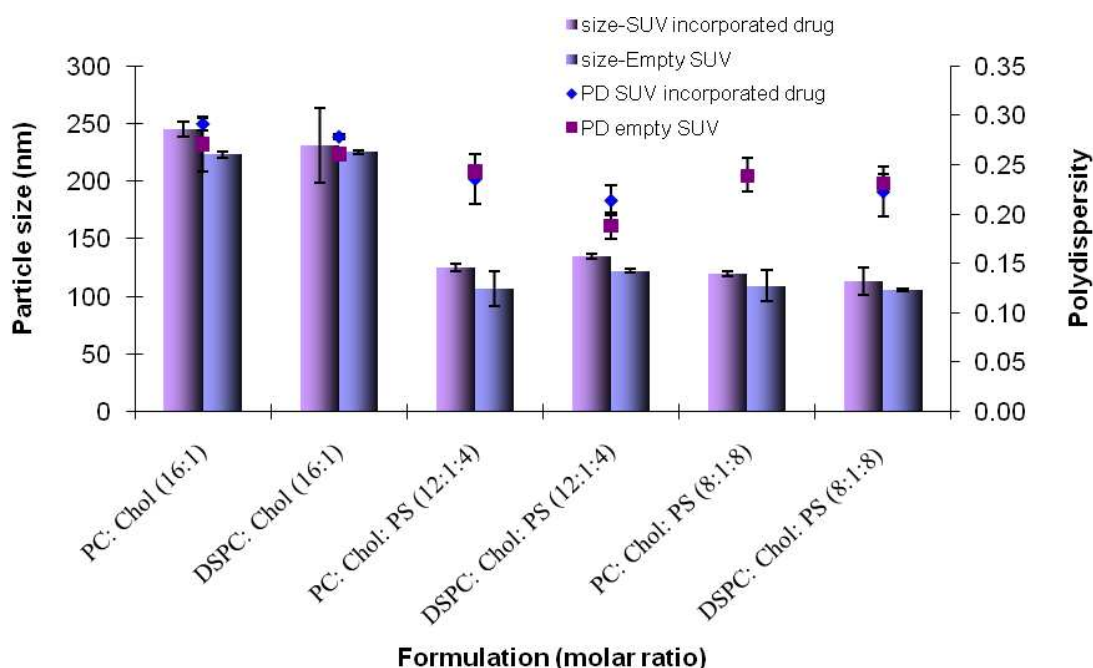


Figure 6. 11 Particle size (nm) and polydispersity of various small unilamellar vesicle formulations. Particle size distribution was measured following 2 minutes sonication in d.H₂O, at 25 °C using a Brookhaven ZetaPlus. The integration of a negatively charged lipid such as PS into the formulations has a significant effect on the vesicle size of liposomes. The substitution of PC lipid by a longer alkyl chain lipid such as DSPC in the anionic and neutral preparations had no substantial effect on the size of vesicles. The polydispersity index for the size distribution of the entire neutral and anionic vesicle was consistently in the proximity of 0.2. The addition of the TG2 inhibitor into the formulations, the average size of the vesicles and the zeta potential decrease marginally, conversely the polydispersity index remained approximately the same. The data are expressed as means \pm standard deviation of three independent experiments.

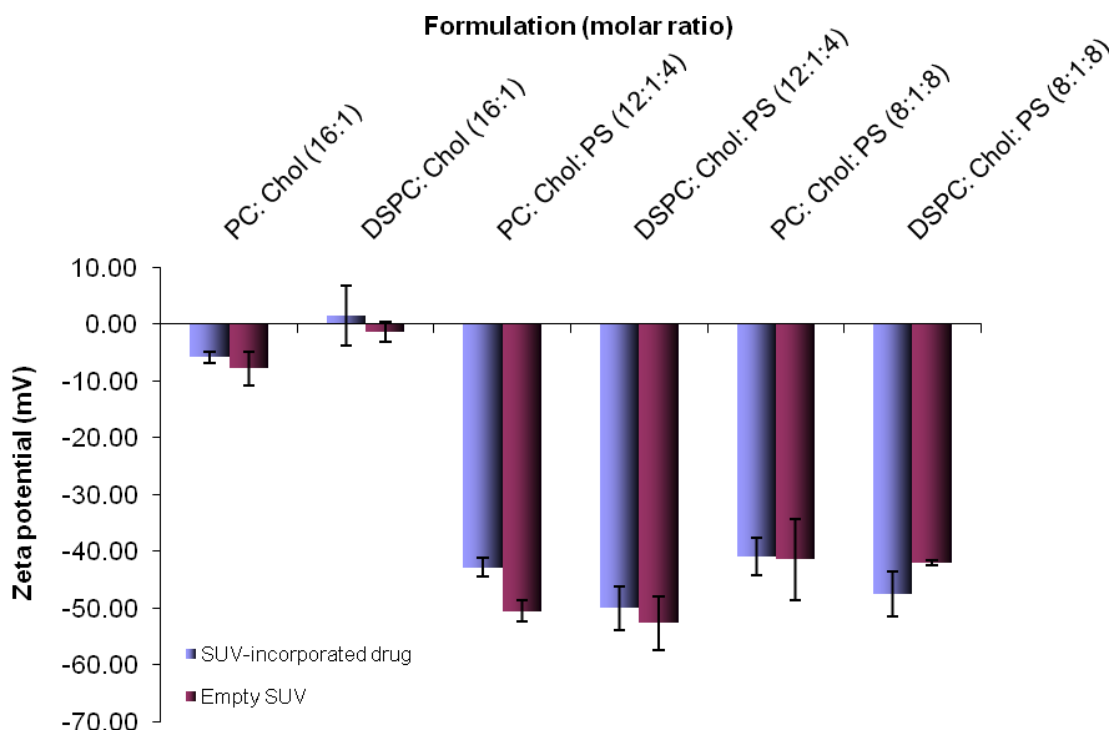


Figure 6. 12 Zeta potential (mV) of various small unilamellar vesicles formulations. Particle size distribution was measured following 2 minutes sonication in d.H₂O, at 25 °C using a Brookhaven ZetaPlus. The integration of a negatively charged lipid such as PS into the formulations has a significant effect on the surface charge of liposomes. The zeta potential of the anionic formulations incorporating DSPC lipid was slightly lower than their PC counterparts which can be due to the slightly negative nature of DSPC lipid. The data are expressed as means \pm standard deviation of three independent experiments.

According to Figures 6.11 and 6.12, the neutral liposomes exhibited an average particle size of ~ 200 nm and an average zeta potential of ~ -5 to $+5$ mV, whereas the anionic liposomes showed an average size of ~ 100 nm and an average zeta potential from ~ -40 to -50 mV. The polydispersity index (the measurement of homogeneity of dispersion) for the size distribution of the entire neutral and anionic vesicle was consistently in the proximity of 0.2.

In general, there was no significant difference ($P \geq 0.05$, ANOVA) in the size of SUV when comparing between the four anionic formulations or between the two zwitterionic formulations (Figure 6.11). Hence the substitution of PC lipid with a longer alkyl chain lipid such as DSPC (C_{18} alkyl chain length) in any of the formulations tested had no significant effect on the size or polydispersity of vesicles.

Similarly, there was no difference in zeta potential between the zwitterionic formulations or between the various anionic formulations with all formulations containing PS being negatively charged. However, the difference in the zeta potential between the anionic and neutral liposomes was highly significant ($P \leq 0.01$, ANOVA) (Figure 6.12) as would be expected. These findings confirmed the results obtained upon measuring the zeta potential of MLV integrating the TG2 inhibitor, which was approximately the same as the TG2 inhibitor integrated SUV. Consequently, sonication time does not have any impact on the surface charge of vesicles (Labhasetwar et al., 1994).

Upon the incorporation of PS lipid into the formulations (4 μ mole), there was a major decrease in the vesicle size (from a range of 200 nm to a range of 100 nm), and a substantial decline in the zeta potential as would be expected (from 1.51 ± 5.20 mV to $\sim 48.74 \pm 1.76$ mV for DSPC incorporated liposomes and from -5.82 ± 0.92 mV to 41.85 ± 1.32 mV for PC incorporated liposomes). These results confirm that the integration of a negatively charged lipid (PS) into the SUV formulations similar to the MLV formulations has a significant effect on both the size and zeta potential of the SUV liposomes. It can be concluded that regardless of liposome preparation, neutral liposomes produced larger complexes than anionic liposomes and the difference between the two was extremely significant ($P \leq 0.01$, ANOVA). However increasing the amount of PS added has no significant impact when considering the concentrations tested: increasing the PS content two-fold only slightly decreased vesicle sizes (from 135.13 ± 2.14 nm to 112.84 ± 11.67 nm for the liposomes incorporating DSPC and from 124.73 ± 3.08 nm to 119.43 ± 2.11 nm for the liposomes incorporating PC) and did not significantly influence the zeta potential of the formulations. This may be an outcome of the presence of a charged moiety in the lipid formulation which reduces the probability of vesicular aggregation following the formation of vesicles, thus leading to a reduction in the size of the charged vesicles.

The addition of the TG2 inhibitor made no significant difference to the size or zeta potential of the formulations tested (Figure 6.11 & 6.12). The TG2 inhibitor investigated in this study was neutral in charge. As a result, it can be stated that the integration of

AM2/169 into the liposome formulations had no substantial effect on the physico-chemical property of the liposomes.

Previous studies have reported that the incorporation of charged lipids in the liposome formulation resulted in an increase in drug loading and the size of vesicles. The rise in vesicle size may be attributed to the increased drug loading in response to the presence of a charged lipid rather than a direct outcome of the presence of charged lipid within the liposome formulation alone (Mohammed et al., 2004).

6.6.1.2.2 Encapsulation efficiency

Liposomal encapsulation has been shown to have a considerable effect on the pharmacokinetics and tissue distribution of the administered drugs (Ranade, 1989). Therefore, drug entrapment within the system is a key consideration. Consequently, the percent encapsulation of the enzyme inhibitor in SUV was investigated and the effect of lipid alkyl chain length and charged liposomes on the enzyme inhibitor encapsulation was studied on various liposomal formulations.

As shown in Figure 6.13, the measured entrapment efficiency was ~ 70 % for the neutral formulations with no significant difference between the PC and DSPC formulations (PC: Chol vs DSPC: Chol). The integration of 4 μ Moles PS, into the liposome preparations made no significant changes to the formulations containing DSPC. However, the drug entrapment reduced significantly from 75 % to 45 % for the formulations containing PC. Upon a two-fold increase in the amount of PS (to 8 μ Moles), there was no significant further reduction for PC and DSPC composing liposomes on the TG2 inhibitor incorporation. The presence of negatively charged lipids such as PS, PI, or PG has a tendency to increase the interlamellar distance between successive bi-layers and thus enhance the encapsulation efficiency (Vemuri and Rhodes, 1995). However given that the TG2 inhibitor should be incorporated within the bilayer it is unlikely this would have an effect on its incorporation. It has also been previously shown by other researchers that (Gregoriadis et al., 1973; Mohammed et al., 2004) longer alkyl chain lipids such as DSPC

could augment the drug loading due to the increased hydrophobic area within the liposome bi-layer.

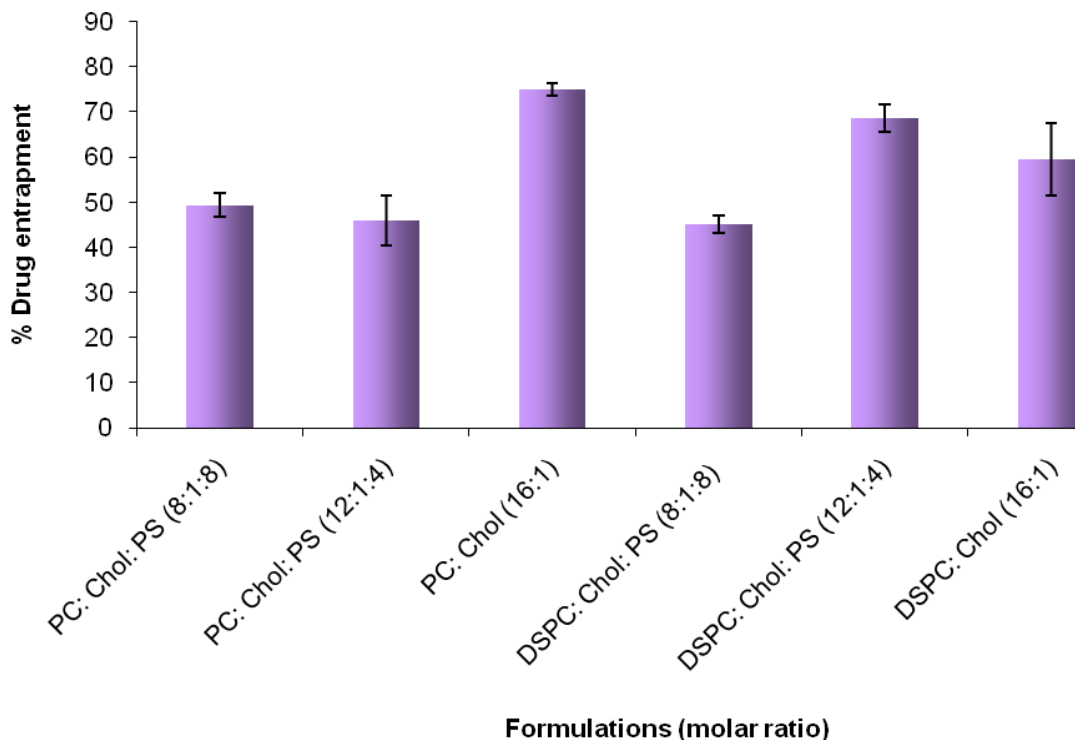


Figure 6. 13 Percentage of drug entrapment for various liposomal formulations using size-exclusion chromatography. The highest percentage of entrapment efficiency was ~70 % for the formulation amalgamating DSPC, cholesterol and PS lipid at a molar ratio of 12:1:4. The data are expressed as means \pm standard deviation of three independent experiments.

6.6.2 The formulation of choice for further *in vivo* studies

In view of the micro-anatomy of the liver and previous work by other researchers, the liposomes selected for the bio-distribution studies were of small unilamellar vesicles and negatively charged to allow free passage through the endothelial fenestrations and fast removal. As discussed earlier, it has been established that liposome membranes consisting of phospholipids with long hydrogenated fatty acid esters such as DSPC are more rigid and display a tighter film packing compared to membranes consisting of phospholipids composed of fatty acids of different length and saturation such as PC. Thus, these liposome membranes are more stable resisting lipid exchange by serum proteins such as HDL. Additionally, using phospholipids such as DSPC with a phase transition temperature higher than body temperature (55 °C) makes the liposome bi-layer

membrane less fluid and consequently less leaky and more stable in physiological fluid (37°C) (Gregoriadis, 1995; Gabizon and Papahadjopoulos, 1988; Patel, 1992; Devine et al., 1994; Yu and Lin, 1997). The drug loading studies in Figure 6.14 also demonstrate that the substitution of PC with DSPC produced drug loading equal to or higher than PC, thus taken together, these results indicated that DSPC could be a more effective lipid than PC within the liposome formulations for *in vivo* studies. Therefore, DSPC: Chol (16:1) and DSPC: Chol: PS (12:1:4) were selected as formulations of choice for further bio-distribution investigations.

6.6.3 The effect of salt on the physico-chemical properties of liposome

In bio-distribution research, buffer solutions are utilised to keep pH at a nearly constant value. Furthermore, the osmolarity and ion concentrations of the solution usually match those of the human body (isotonic). Accordingly, phosphate buffer solution (PBS) was selected as the buffer of choice to proceed with.

To investigate the effect of salts on physico-chemical properties of anionic and neutral liposomes, formulations were produced in PBS (often used as isotonic buffer for *in vivo* studies). Comparisons were then made against the previously obtained results from section 6.6.1.2.1. Regardless of the liposome surface charge, the rehydration media (PBS or d.H₂O) was shown to influence both the size and zeta potential of all the formulations tested. Rehydration in PBS resulted in a slightly decreased zeta potential compared to d.H₂O, decreasing from 1.51 ± 5.20 mV to -6.48 ± 3.52 mV for neutral liposomes and slightly increased from -49.99 ± 3.86 mV to -44.13 ± 2.35 mV for anionic liposomes (Table 6.3). This could be attributed to an increase in electrolyte concentration resulting in condensation of the double layer.

In terms of the particle size, formulations in PBS yielded notably greater size than those produced in d.H₂O ($P \leq 0.05$, ANOVA), irrespective of the liposome charge. There was about two-fold rise for the neutral formulation and about three-fold rise for the anionic ones.

Furthermore, the polydispersity index (the measurement of homogeneity of dispersion) for the size distribution of liposomal formulations rehydrated in PBS (~ 0.3) was considerably higher than that of the formulations hydrated in distilled H₂O (~ 0.2), suggesting that the substitution of PBS with d.H₂O as rehydration media produces a less homogenous liposome suspension (Table 6.3).

Table 6.3 The effect of various hydration media (PBS and d.H₂O) on characteristics of the TG2 inhibitor integrated small unilamellar vesicles (neutral and anionic) on the physicochemical characteristics. The data are expressed as means \pm standard deviation of three independent experiments.

| Formulation | PBS | | | d.H ₂ O | | |
|--------------------------------|--------------------|-----------------|------------------------------|--------------------|-----------------|------------------------------|
| | Size (nm) \pm SD | PD \pm SD | Zeta potential (mV) \pm SD | Size (nm) \pm SD | PD \pm SD | Zeta potential (mV) \pm SD |
| DSPC: Chol (16:1) | 524.7 \pm 65.8 | 0.38 \pm 0.01 | -6.48 \pm 3.52 | 231.25 \pm 32.31 | 0.28 \pm 0.00 | 1.51 \pm 5.20 |
| DSPC: Chol: PS (12:1:4) | 418.5 \pm 33.4 | 0.30 \pm 0.02 | -44.13 \pm 2.35 | 139.88 \pm 3.68 | 0.22 \pm 0.02 | -49.99 \pm 3.86 |

6.6.4 The influence of sonication time on physico-chemical characteristics of neutral and anionic liposomes

The influence of sonication time on z-average diameter, polydispersity and zeta potential of neutral and anionic liposomes within DSPC based SUV prepared in PBS was also investigated. Liposomes were formulated using DSPC (12 μ mol or 16 μ mole), cholesterol (1 μ mol) and with or devoid of 4 μ mol of the negatively charged PS.

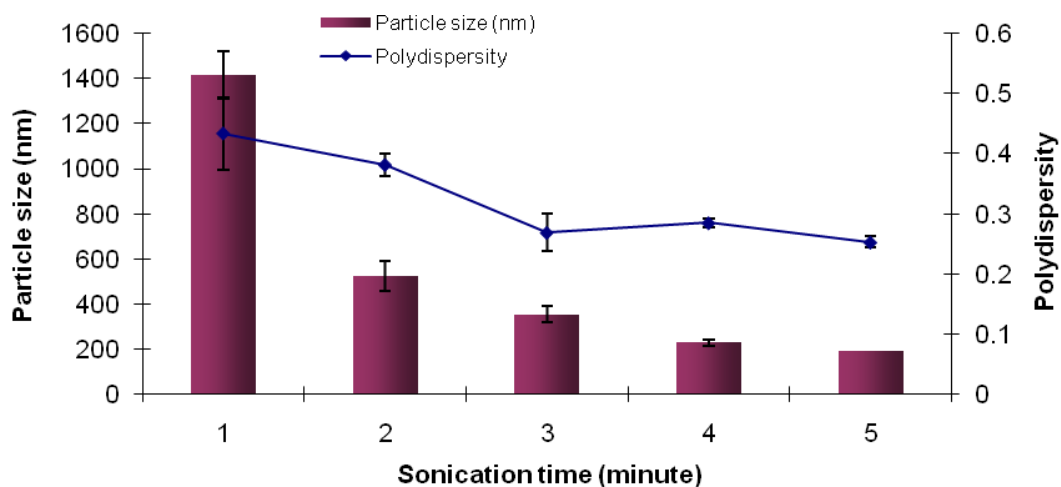


Figure 6. 14 The influence of sonication time on z-average diameter and polydispersity of the neutral liposomes. Liposomes were composed of DSPC: Chol at 16:1 molar ratio, with a requisite amount of enzyme inhibitor were formed in PBS and sonicated. Samples were then taken at various time points (1, 2, 3, 4 and 5 minutes). Upon increasing the sonication time, the size and polydispersity of the vesicles were considerably decreased. The polydispersity of the vesicles after 5 minutes sonication was in the proximity of 0.2, which is characteristic of such liposome based samples. Results denote mean \pm SD, n = 3.

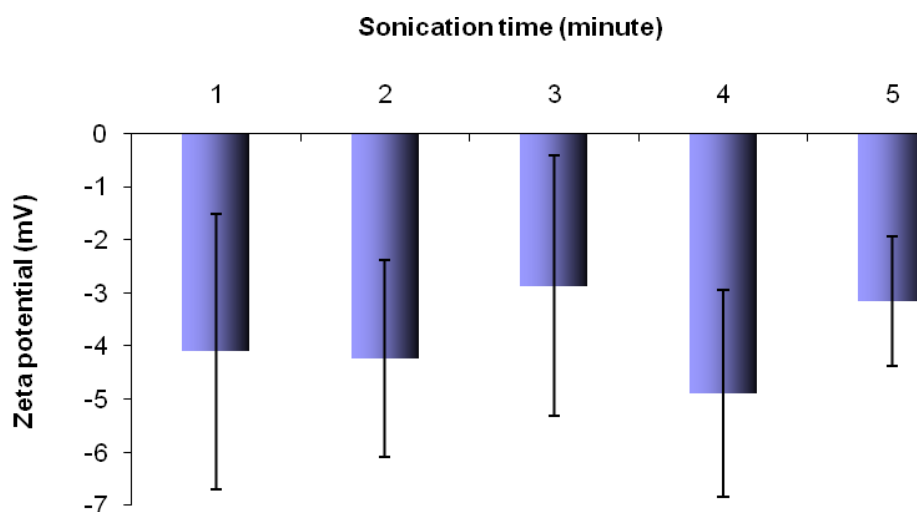


Figure 6. 15 The influence of sonication time on zeta potential of the neutral liposomes. Liposomes were composed of DSPC: Chol at 16:1 molar ratio, with a requisite amount of enzyme inhibitor were formed in PBS and sonicated. Samples were then taken at various time points (1, 2, 3, 4 and 5 minutes). In contrast to the particles size diameter, the zeta potential values remained constant for the duration of sonication. Results denote mean \pm SD, n = 3.

To optimize the formulation of SUV for the identified formulations, the effect of sonication time on z-average diameter, polydispersity and zeta potential of the TG2 incorporated liposomes composed of DSPC: Chol at 16:1 molar ratio formed in PBS was

investigated at a fixed frequency of 5 amplitude for 1, 2, 4 and 5 minutes and displayed in Figures 6.14 and 6.15. The particle size and polydispersity index of the vesicles demonstrated a progressive decline with an increase in the time of sonication as was expected. In terms of the particle size, vesicles were shown to reduce in size, from ~1400 nm to ~190 nm and in polydispersity index from ~ 0.5 to ~ 0.2. This decrease in particle size was extremely significant ($P < 0.01$, ANOVA). In term of surface charge, there was no substantial alteration ($P > 0.05$, ANOVA) during the sonication time and the zeta potential remained at around ~ -4 mV in all cases (Figure 6.15).

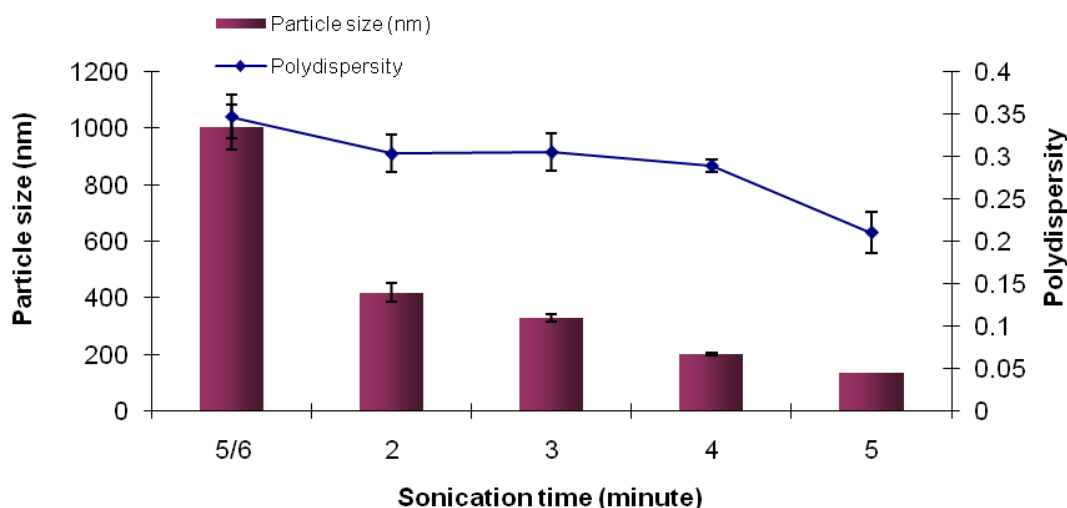


Figure 6.16 The influence of sonication time on z-average diameter and polydispersity of anionic liposomes. Liposomes composed of DSPC: Chol: PS at 12:1: 4 molar ratio, with a requisite amount of enzyme inhibitor were formed in PBS and sonicated. Samples were then taken at various time points (1, 2, 3, 4 and 5 minutes). Upon increasing the sonication time, the size and polydispersity of the vesicles were considerably decreased. Contrariwise, in the case of surface charge, there was no substantial change ($P > 0.05$, ANOVA) during the sonication time. Results denote mean \pm SD, $n = 3$.

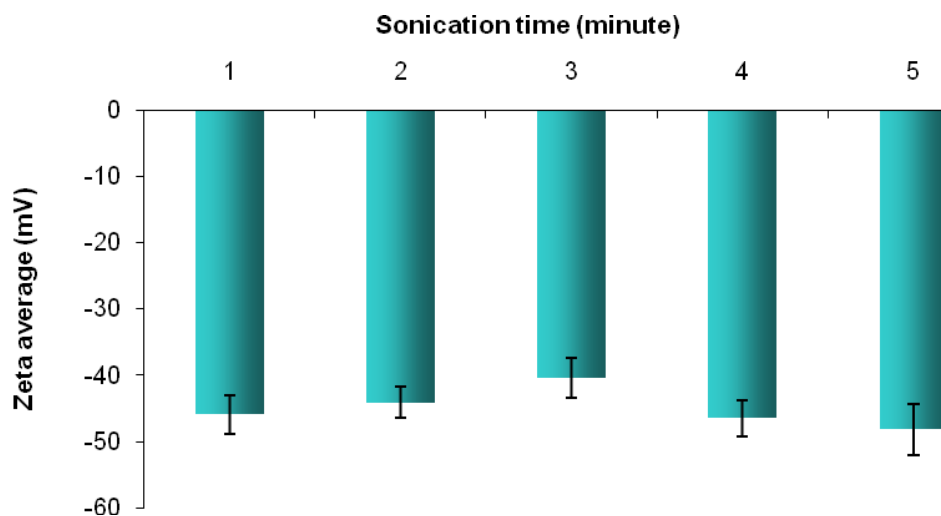


Figure 6. 17 The influence of sonication time on zeta potential of anionic liposomes. Liposomes composed of DSPC: Chol: PS at 12:1:4 molar ratio, with a requisite amount of enzyme inhibitor were formed in PBS and sonicated. Samples were then taken at various time points (1, 2, 3, 4 and 5 minutes). The same trend as with the neutral liposomes was observed. Once again, with the increased sonication time, both the polydispersity and particle size of the liposomes were significantly reduced. In contrast to the particles size diameter, the zeta potential values remained constant for the duration of sonication. Results denote mean \pm SD, $n = 3$.

The incorporation of PS lipid into the formulation and preparation of anionic liposomes, demonstrated the same trend as with the neutral liposomes. Once again with the increased sonication time, the polydispersity and particle size of the liposomes were significantly reduced ($P < 0.01$, ANOVA) from 0.34 ± 0.025 to 0.21 ± 0.024 and from 1004.4 ± 78.2 nm to 134.9 ± 0.6 nm respectively. The zeta potential values remained constant for the duration of sonication at around -45.03 ± 2.95 mV ($P > 0.05$, ANOVA), implying that irrespective of the liposome composition, the sonication time has no influence on the zeta potential of vesicles (Figures 6.16 and 6.17) (Labhasetwar et al., 1994).

6.6.5 Stability studies in serum

Stability in serum is one of the important parameters of liposome construction which can be affected by fatty acid chain length, saturation state of the phospholipids and the existence of cholesterol. Liposome stability depends on four categories of physical processes: loss of bi-layer components caused by desorption, loss of entrapped material caused by leakage, vesicle fusion, and vesicle aggregation. The fusion and aggregation of liposomes will result in alterations in liposome size distribution (Wu et al., 2003).

Accordingly, the stability of the liposome formulations was assessed by determining the quantity of drug retained within the liposomes, vesicle aggregation and any alterations in physicochemical characteristics (particle size and surface charge).

6.6.5.1 Liposome stability: drug retention

The ultimate efficacy of a liposomal dosage form will be judged on the ability of the formulator to reliably control the amount of free drug that reaches the site of action over a given period of time (Wiener et al., 1989, Gregoriadis, 1995). Previous work by other researchers has indicated that the drug retention for liposomes prepared from DSPC lipid is higher than that of liposomes produced from PC lipids. It is recognized that the ability of liposomes to retain drug during incubation in PBS at 37 °C could be affected by the lipid chain length and subsequently the lipid phase transition temperature (Senior and Gregoriadis, 1982). Alkyl hydrocarbon chain length is one of several factors which directly affect the phase transition temperature. As the hydrocarbon chain length is increased, van der Waals' interactions between the lipid chains get stronger, thus requiring more energy to disrupt the stable lipid bi-layer, and consequently the phase transition temperature increases. Therefore at 37 °C, PC liposomes ($T_c = 0\text{ °C}$) will be in the fluid state resulting in increased drug loss compared with a higher transition temperature lipid, such as DSPC ($T_c = 55\text{ °C}$), that will be in the ordered gel phase and retain a stable bi-layer (Mohammed et al., 2004). As a consequence these stable and strong bi-layers decrease the efflux of drugs from liposomes and thus impede the ability of these liposomes to retain drug during incubation (Massing and Fuxius 2000). Additionally, studies have shown that excess cholesterol in certain types of liposomes greatly improves bi-layer stability in the presence of blood and reduces their permeability (Gregoriadis, 1979). The inclusion of cholesterol impedes the diffusion of water deep into the lipid membrane, hence enhancing liposome stability by reducing hydrolytic degradation (Simon and McIntosh, 1986). Accordingly, the drug retention within the liposome bilayer was investigated for the two of the formulations tested *in vivo*; DSPC: Chol: PS in a molar ratio of 16:1:0 and 12:1:4 formed in PBS, for a period of 2 hours. According to the results, liposomes did not exhibit significant leakage of entrapped contents for the formulations tested. The percentage of drug leakage for the anionic

formulation was measured at $19.5 \% \pm 3.53$ and the neutral formulation was measured at $23 \% \pm 0.70$. The discrepancy in drug retention between anionic and neutral liposomes found in this study is not in accordance with the study by Mohammed et al. (2004), in which the addition of charged lipids to the liposome formulation resulted in increased drug release, signifying that the presence of charged lipids within the liposome bi-layer increased the permeability of the bi-layer or lipid drug binding.

6.6.5.2 Liposome stability: vesicle size and zeta potential studies

As previously discussed, using phospholipids such as DSPC with long hydrogenated fatty acid esters and a phase transition temperature higher than body temperature (55°C) makes the liposome bi-layer membrane more rigid and demonstrates a tighter film packing in physiological fluid (37°C) compared with membranes consisting of PC with shorter and less saturated hydrogenated fatty acid esters. As a consequence, these liposome membranes are more resistant to lipid exchange by serum proteins such as HDL. In view of this, particle size and surface charge of the two liposome formulations (DSPC: Chol and DSPC: Chol: PS in a molar ratio of 16:1 and 12:1:4 respectively) were measured over intervals of 2 hours incubation in PBS or PBS: FBS 50:50 (v/v) in a shaking water bath (37°C , 80 rpm) at various time points (0, 30, 60 and 120 minutes).

The liposome formulations developed for intravenous administrations should demonstrate no sign of aggregation in serum, for reasons of safety and to ensure their ability to cross the fenestrations of liver endothelium (Longmuir et al, 2006). According to Figures 6.18 and 6.19, the formulations tested remained relatively stable in PBS with regard to size and zeta potential during the observation period; however, these characteristics modified notably when placed in serum. A significant preliminary increase in liposome size (vesicle aggregation) from ~ 170 nm to ~ 340 nm for the neutral formulation and from ~ 140 nm to ~ 320 nm for the anionic formulation was observed in serum. Subsequent to the initial increase, the size of liposomes remained constant for the remainder of testing intervals for both formulations tested. Regarding the surface charge, an apparently common trend was that with an increase in incubation time in serum, the surface charge decreased gradually from the range of about -5 mV to about -20 mV for neutral liposomes and changed from

the range of about -40 mV to about -30 mV for anionic liposomes. The anionic lipid is not adding any protection against the effect of plasma with both types of formations interacting with plasma.

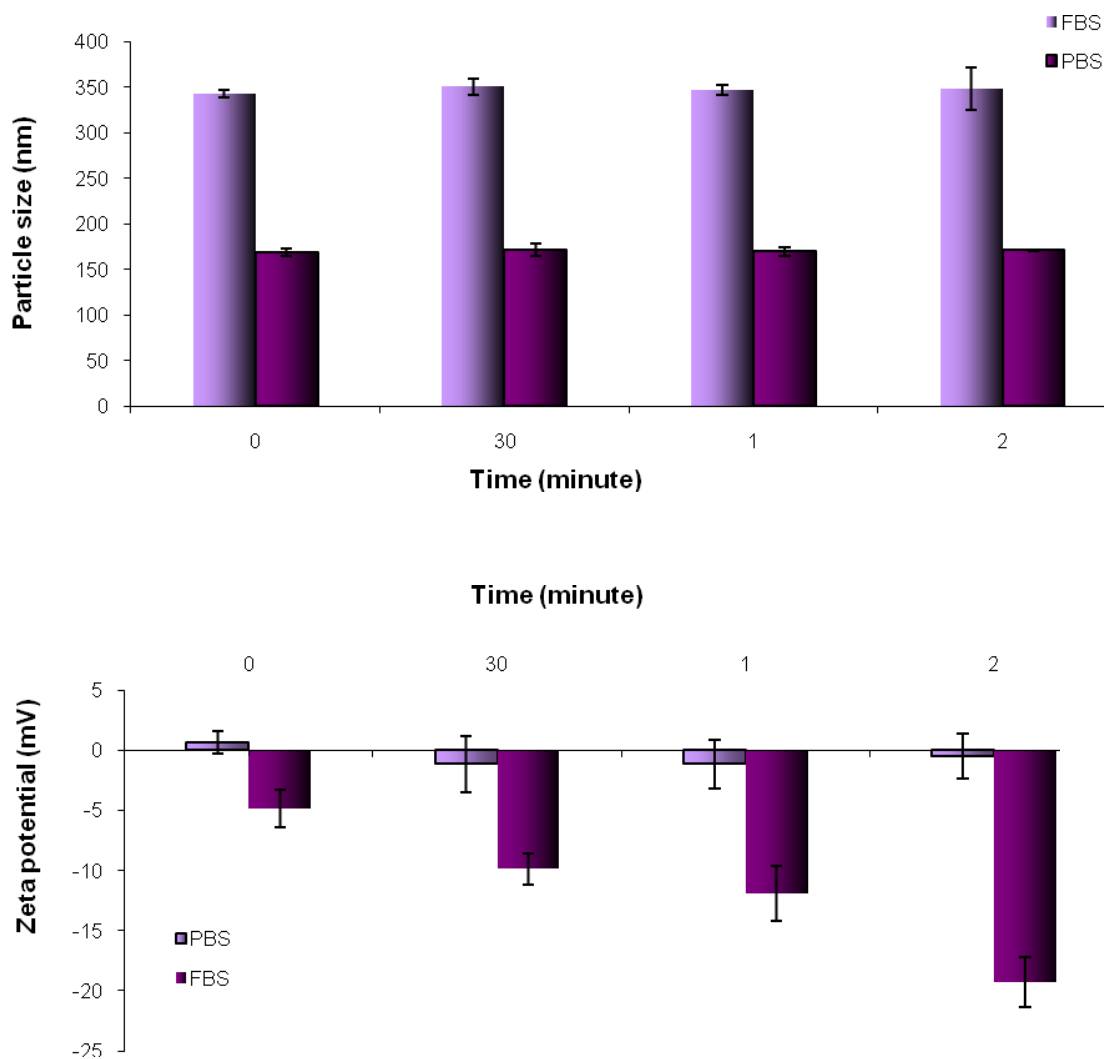


Figure 6. 18 Vesicle stability (size and zeta potential) of the neutral liposomes in serum. Liposomes were composed of DSPC: Chol (16:1) incubated in PBS or PBS: FBS 50:50 (v/v) in a gently shaking water bath (37 °C, 80 rpm) at various time points (0, 30, 60 and 120 minutes). The formulations tested remained relatively stable in PBS with regard to the size and zeta potential during the observation period. However, these characteristics changed notably when placed in serum. The data are expressed as means \pm standard deviation of three independent experiments.

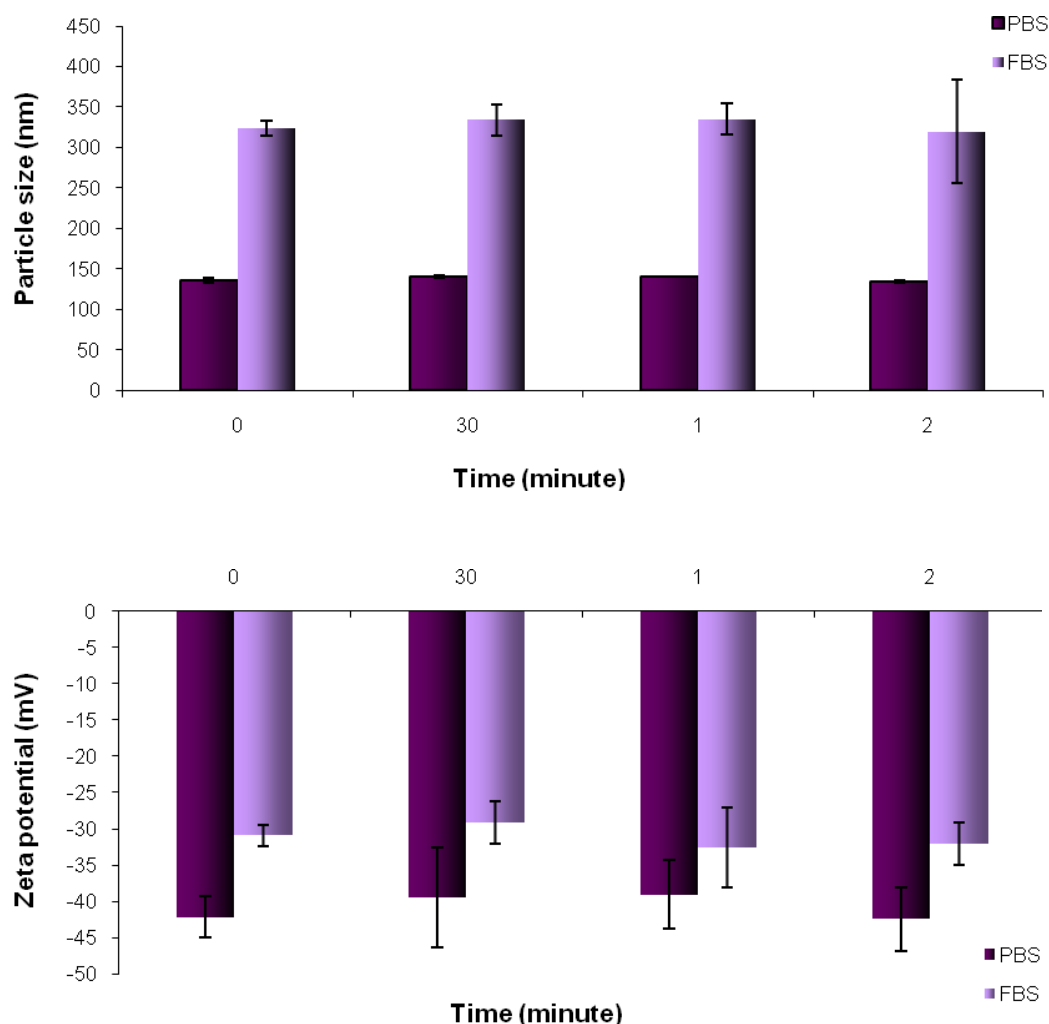


Figure 6. 19 Vesicle stability (size and zeta potential) of the anionic liposomes in serum. The liposomes were composed of DSPC: Chol: PS (12:1:4) incubated in PBS or PBS: FBS 50:50 (v/v) in a gently shaking water bath (37 °C, 80 rpm) at various time points (0, 30, 60 and 120 minutes). The formulations tested remained relatively stable in PBS with regard to the size and zeta potential during the observation period. However, these characteristics changed notably when placed in serum. The data are expressed as means \pm standard deviation of three independent experiments.

6.6.6 Bio-distribution studies of the liposome-TG2 inhibitor system in mice

Given liposomes could be formulated to incorporate the TG2 inhibitor, the next stage was to investigate their bio-distribution *in vivo* to assess their ability to deliver the drug target to the liver target site. Liposome composed of DSPC: chol: PS in a molar ratio of 16:1:0 with a mean particle size of 100 nm or 12:1:4 with a mean particle size of 100 nm or 500 nm used as drug carrier systems. To study the organ distribution of the liposome-TG2

inhibitor system subsequent to I.V. injection in mice, various types of organs were isolated and analyzed for radioactivity as described in the Material & Method section.

Figure 6.20 a-c illustrates the percentage of organ distribution of the liposomes-TG2 inhibitor system at various time points following I.V. injection. On a per organ basis, the uptake of the liposomal-drug delivery system by the liver was significantly higher ($P < 0.01$, ANOVA), than that taken up by other organs at all time points measured, independent of the formulation used. The percentage dose per organ for the liver was about 10 % to 18 % for the neutral formulation, about 4 % to 12 % for the anionic formulation with an average vesicle diameter of 500 nm and about 10 % to 18 % for the anionic formulation with an average vesicle diameter of 100 nm. Following the liver, the spleen demonstrated a higher liposome distribution amongst organs tested ($P < 0.05$, ANOVA). The dose percentage per spleen was at approximately of 1.30 %, 0.4 % and 0.96 % for the neutral preparation, anionic formulation with large and small vesicle size respectively. The inherent affinity of the liposomes for the liver is due to its being the largest internal organ in the body and Kupffer cells in the liver are part of the reticular endothelial system (Wu et al., 2003). Moreover, fenestrated capillaries in the liver and spleen could be another cause of liposome concentration in these organs following intravenous injection (Terwogt et al., 1999).

The liposomes with a mean particle size of 100 nm demonstrated a significantly higher concentration in the liver and spleen when compared with the liposomes of a larger particle size (500 nm), in terms of dose percent. These results are not in clear agreement with previous studies and suggest a higher uptake of small liposomes compared with larger liposomes, by the RES system. However, this could be attributed to the narrow range of vesicle size in the anionic formulations.

The uptake of negatively charged liposomes by the liver was not greater than that of neutral liposomes. As previously mentioned, the addition of negatively charged lipids (PS) increases the process of opsonization and thus the uptake by MPS-cells (Massing and Fuxius, 2000). The exposure of negatively charged lipid is thought to serve as a

signal for the removal of liposomes (Huong et al., 2001). Liposomes composed of DSPC have a relatively negative nature in PBS (~ -5 mV), the incubation of these liposomes in plasma affects the zeta potential and yields a higher negative charge (~ -20 mV). Therefore, these liposomes would not be considered to be neutral in the physiologic fluid and there would be less difference between the charges of the two formulations tested. This could account for the same level of organ uptake in neutral liposomes and in negatively charged ones.

The distribution of the liposomes in the kidney was insignificant for all the formulations tested (~ 0 %; Figure 6.18). The liposome accumulation in the lung was only detectable for the larger (500 nm) liposome (~ 1.85 %), suggesting that the larger sizes are filtered out rapidly in the lung capillaries. Due to the destabilization of liposomes in blood circulation and consequent rapid clearance of from the blood, only negligible amounts of radioactivity were found in the plasma at any time point subsequent to injection (results are not presented).

There was no apparent trend regarding the uptake of liposomes at different time points for any of the organs; this could be a result of employing short time points in the study.

Lack of significant differences in organ concentration of the three liposome formulations was most likely due to the same T_c of the lipids and a narrow range of vesicle size. These results suggest that the vesicle size could be one of the important factors affecting the fate of liposomes *in vivo*, but only with regards to a much wider size distribution than chosen for this study. However, there must clearly be a minimum size for the effective uptake of liposomes by RES. If they are below the minimum effective uptake size, the liposomes will most likely remain in higher concentration in circulation. In terms of future work, in order to investigate the effect of particle size on organ distribution of liposomes, a broader range of vesicle size and longer time points are recommended.

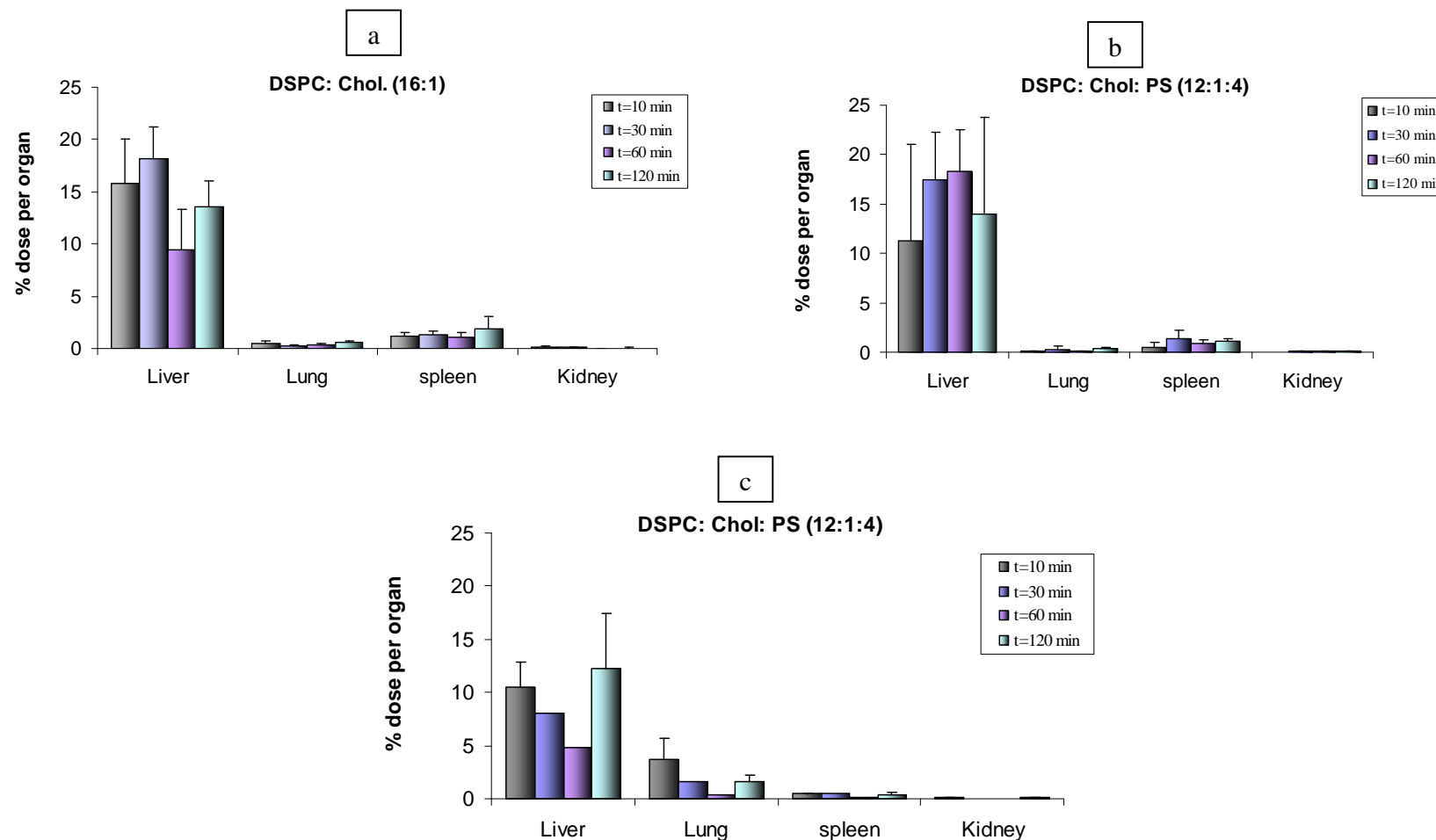


Figure 6. 20 Organ distribution of the liposomes-TG2 inhibitor system in mice at various time points following I.V. injection. Liposome were composed of DSPC: chol: PS in a molar ratio of 16:1:0 with a mean particle size of 100 nm (a) or 12:1:4 with a mean particle size of 100 nm (b) or 500 nm (c) used as drug carrier systems. Bio-distribution of liposome-encapsulated enzyme inhibitor was monitored using H^3 labeled cholesterol in the formulations as a marker. The uptake of liposomes by the liver was considerably higher than for other organs due to the inherent affinity of liposomes for the liver. Values denote mean \pm SD (n=3).

6.6.7 Conclusion

The presented results within this chapter indicate that the group of TG inhibitors used can be successfully incorporated into designed liposomes and delivered to the liver with very little distribution to the organs tested in this study. Upon I.V. administration of the TG inhibitor incorporated liposomes, the liver demonstrated relatively higher liposome distribution amongst all the organs tested. Therefore, liposomes can potentially be employed as a carrier system for site-specific delivery of this group of TG inhibitors into the liver, offering a potential new strategy for treating liver fibrosis and its end stage disease cirrhosis.

Chapter 7:

General discussion

7.1 Summary and Implications of Research Findings

The aim of this thesis was to investigate the therapeutic potential of a novel group of inhibitors of the enzyme TG for the treatment of catheter related complications such as bacterial infection and thrombosis, in addition to fibrotic diseases characterised by increased ECM deposition and cross linking such as liver fibrosis.

The low molecular weight, non-toxic FXIIIa inhibitors could prevent stabilisation of blood clots by inhibiting fibrin stabilisation by FXIIIa and consequently increase thrombolysis. Furthermore, they could reduce colonisation of catheters by *staphylococci* by inhibiting their FXIIIa dependant cross-linking to host proteins (fibrin and fibronectin) on the central venous catheter surface, preventing the release of bacteria into the blood where they would be susceptible to antibiotic action and host defences. The first part of this research was focused on incorporating of the FXIIIa inhibitor into catheters and other medical devices with the aim of prevention of thrombus formation and reduction in the associated incidence of bacterial infection. However, the release of FXIIIa inhibitor as a low soluble drug from the matrix systems is considered to be challenging. Therefore, various approaches were employed to improve its release profile from various systems. Silicone and polyurethane (PU) central venous catheters are amongst the most widely used central venous catheters in intensive care and in general medical wards. The FXIIIa inhibitor was incorporated into the polymer base coating of the PU strips. Optimum release of the FXIIIa inhibitor from the polyurethane catheters could be achieved by employing a blend solution of polymers for coating. It was deemed that utilization of the polymer blend (PVP and PLGA) for coating of the PU strips increased the amount of drug release significantly. With regard to silicone central venous catheters, initially the conventional silicone elastomer strips integrated the FXIIIa inhibitor were prepared for sustained release of the enzyme inhibitor. It was found that the release profile of the inhibitor could be enhanced by employing bicarbonate (SB) and citric acid (CA) as additives in the silicone formulations. From these findings it could be suggested that the FXIIIa inhibitor incorporated catheters could offer.

Further studies investigated the application of the TG2 inhibitors in treating of liver fibrosis and its end stage disease cirrhosis. Contrary to the conventional view that

cirrhosis is an irreversible process, recent evidence suggest that even advanced fibrosis is reversible (Friedman, 2000 ; Arthur, 2002 ; Bataller & Brenner, 2005). However, there is no efficient pharmaceutical intervention for liver fibrosis at present. Liver fibrosis is characterized by increased synthesis and decreased degradation of the extracellular matrix. Transglutaminase-mediated covalent cross-linking has been implicated in the stabilization and accumulation of ECM in number of fibrotic diseases. Thus, the use of tissue transglutaminase (TG2) inhibitors has potential in the treatment of liver fibrosis. It has been stated that pharmacological inhibition of TG2 may have adverse side effects, since TG2 demonstrates a protective role in liver injury by enhancing tissue stability and repair. However, it can be argued that intracellular and extracellular TG2 is catalytically inactive under normal physiological conditions, however physical or certain types of chemical injury can lead to rapid enzymatic activation. Therefore, the catalytic activity of TG2 must be activated rapidly when required, and inactivated almost immediately after its task is complete. Evidence shows that the tissue transglutaminase non-specific inhibitor (cystamine) ameliorates carbon tetrachloride (CCl₄) induced liver fibrosis via inhibition of TG2. A novel group of specific tissue transglutaminase inhibitors has been described recently, which has the advantage of targeting TG2 in the extracellular environment this limiting cell toxicity. These inhibitors have already indicated that they are successful candidates in the cure of kidney fibrosis in animal models. The ultimate aim of the work was to develop a drug delivery system which can be applied in the delivery of site-directed irreversible transglutaminase inhibitors to the liver which can then be further studied for the treatment of liver fibrosis in animal models. In an initial study carried out regarding *in-vivo* pharmacokinetics and biodistribution of these TG2 inhibitors in rats, the inhibitor demonstrated a rapid clearance and short half life. Hence, an appropriate carrier system was required to improve delivery and targeting of the inhibitor to the required side of action i.e. liver. Therefore, liposomes were used as drug delivery system for site specific delivery of these inhibitors of transglutaminase to the liver. Upon I.V. administration of the TG2 inhibitor-incorporated liposomes, on a per organ basis, the uptake of the liposomal-drug delivery system by the liver was significantly higher than that taken up by other organs at all time points measured, independent of the formulation used. The inherent biodistribution of the liposomes to the liver is due to the fenestrated capillaries in the liver, allowing the liposomes to escape from the

circulation and be taken up by cells of the MPS. Thus, liposomes incorporating TG inhibitor could potentially offer a novel strategy for treating of liver fibrosis and its end stage disease cirrhosis.

7.2 Future directions

- Determining the amount of FXIIIa sequestered by the inhibitor-and polymer-coated PU catheters and the inhibitor-incorporated silicone catheters.
- Production of fibrin clots on the inhibitor and polymer coated PU catheters and the inhibitor incorporated silicone catheters, assessing the inhibition of FXIIIa-mediated fibrin cross-linking and quantitative determination of fibrinolysis rate.
- Investigation of the effect of FXIIIa inhibitor integrated catheter on release of *Staphylococcus aureas* from human thrombi
- Inducing liver fibrosis by intraperitoneal (IP) injection of carbon tetrachloride (CCl₄) in mice and studying the efficacy of TG2 inhibitors (prior to and after incorporation into liposomes) in amelioration of liver fibrosis.

Thesis Publications

Journal Articles

Daneshpour, N., Griffin, M., Collighan, R., Rathbone, D. and Perrie, Y. (2010). Targeted delivery of a novel group of site directed transglutaminase inhibitors to the liver using liposomes: a new approach for the potential treatment of liver fibrosis. Accepted by *Journal of Drug Targeting*.

Daneshpour, N., Griffin, M., Collighan, R., Mongeot, A., Rathbone, D. and Perrie, Y. (2010). Indwelling catheters and medical implants with FXIIIa inhibitors: a novel approach to the treatment of catheter and medical device related infections. *In preparations*

Conference Proceedings

Daneshpour, N., Griffin, M., Collighan, R., Rathbone, D. and Perrie, Y. (2010). Using Transglutaminase inhibitors incorporated liposomes as a new approach for treatment of liver fibrosis. *American Association of Pharmaceutical Scientists (AAPS)*, New Orleans, U.S.A, November 2010

Daneshpour, N., Griffin, M., Collighan, R., Rathbone, D. and Perrie, Y. (2009). TG inhibitor incorporated liposomes: a potential drug delivery system for treatment of liver cirrhosis. *4th international liposome society conference*, London, U. K., December 2009.

Daneshpour, N., Collighan, R., Perrie, Y., Mongeot, A., Rathbone, D. and Griffin, M. (2009). Controlled release of FXIIIa inhibitors from self-lubricating silicone elastomers to produce a novel bioactive biomaterial for the treatment of catheters and medical device related infection. *Annual Meeting American Association of Pharmaceutical Scientists (AAPS)*, Los Angeles, U.S.A, November 2009.

Daneshpour, N., Collighan, R., Perrie, Y., Mongeot, A., Rathbone, D. and Griffin, M. (2009). A new approach to the treatment of liver cirrhosis: TG inhibitors and potential delivery systems. *Journal of Pharmacy and Pharmacology*, 61, A19, Suppl. 1, September 2009

Daneshpour, N., Perrie, Y., Collighan, R., Mongeot, A., Lambert, P., Rathbone, D. and Griffin, M. (2009). Inclusion of Factor XIIIa inhibitors as a new approach to the treatment of catheter and medical device related infections. *36th Annual Meeting and Exposition of the Controlled Release Society (CRS)*, Copenhagen, Denmark, July 2009.

Daneshpour, N., Perrie, Y., Collighan, R., Mongeot, A., Lambert, P., Rathbone, D. and Griffin, M. (2009) Investigation of a potential polymer coats with integrating FXIIIa inhibitors for catchers and other medical device related infection. *Young Pharmaceutical Scientists Meet in Nice*, Nice, France, June 2009.

Daneshpour, N., Perrie, Y., Collighan, R., Mongeot, A., Lambert, P., Rathbone, D. and Griffin, M. (2009). Indwelling catheters and medical implants with FXIIIa inhibitors using a biodegradable drug delivery technology. *UKICRS Symposium 2009*, London, U. K., April 2009

Daneshpour, N., Collighan, R., Perrie, Y., Mongeot, A., Rathbone, D. and Griffin, M. (2008). Investigation of fluorescent derivatives as potential probes for novel transglutaminase inhibitors. *Journal of Pharmacy and Pharmacology*, 60, A56-A57, Suppl. 1, September 2008.

Daneshpour, N., Collighan, R., Perrie, Y., Mongeot, A., Rathbone, D. Lambert, P. Griffin, M. (2008). Synthesis of a novel fluorescent transglutaminase inhibitor for controlled release from catheters and other implant devices. *35th Annual Meeting and Exposition of the Controlled Release Society (CRS)*, New York, U.S.A, July 2008.

Daneshpour, N., Collighan, R., Perrie, Y., Telci, D., Mongeot, A., Rathbone, D. and Griffin, M. (2008). Determination of efficacy and cytotoxicity of a novel group of transglutaminase inhibitors for targeted drug delivery. *Annual LHS Postgraduate Research Day*, Aston University, U.K., June 2008

2. Podium Presentations

The British Pharmaceutical Conference (BPC), Manchester, U.K., September 2009

Annual LHS Postgraduate Research Day, Aston University, U.K., 30th June 2008

35th Annual Meeting and Exposition of the Controlled Release Society, New York, U.S.A, July 2008

References

Adrian, J. A. et al. (2007). Addressing Liver Fibrosis with Liposomes Targeted to Hepatic Stellate Cells *Joannal. J. Liposome Res.*, 17 (3-4), 205-218.

Aeschlimann, D. T. (2000). *Connect. Tissue Res*, 41, 1.

Aeschlimann, D., Kaupp, O., & Paulsson, M. (1995). Transglutaminase-catalyzed matrix cross-linking in differentiating cartilage: identification of osteonectin as a major glutaminy substrate. *J. Cell. Biol.*, 129, 881-892.

Ahearn D.G. & Grace D.T. (2000). Effects of hydrogel/silver coatings on in vitro adhesion to catheters of bacteria associated with urinary tract infections. *Curr Microbiol*, 41, 120–125.

Ahl, P.L., Chen, L., Perkins, W.R., Minchey, S.R., Boni, L.T., Taraschi, T.F., Janoff, A.S. (1994). Interdigitation-fusion: a new method for producing lipid vesicles of high internal volume. *Biochimica et Biophysica Acta*, 1195, 237-244.

Allegiance Research & Technology (1999). Polymer coatings for powder-free medical gloves, *Choices*, 100;; <http://www.allegiance.net/hic/glvhand/Choic100.pdf>

Allen, T. M. & Cullis, P.R. (2004). Drug delivery systems: entering the mainstream. *Science*, 303, 1818–1822.

Allen, T. M. & Hansen, C. B. (1991). Pharmacokinetics of Stealth versus conventional liposomes: effect of dose. *Biochim. Biophys. Acta*, 1068, 133–141.

Anderson, ET., Fletcher, L., Severin, A., Murphy, E., Baker, SM., Matsuka, YV. (2004). Identification of factor XIIIa-reactive glutamine acceptor and lysine donor sites within fibronectin-binding protein (FnBA) from *Staphylococcus aureus*. *Biochemistry*. 43(37), 11842-52.

Ariens, R., Lai, T., Weisel, W., Greenberg, C., & Grant, P. (2002). Role of factor XIII in fibrin clot formation and effects of genetic polymorphisms. *Blood*, 100 (30), 743-754.

Armstrong, AW. et al. (2008). *Principles of pharmacology: the pathophysiologic basis of drug therapy*. Philadelphia: Wolters Kluwer Health/Lippincott Williams & Wilkins, 396.

Arthur, MJ. (2002). Reversibility of liver fibrosis and cirrhosis following treatment for hepatitis C. *Gastroenterology*.

Avgoustakis, K. (2005). Polylactic-Co-Glycolic Acid (PLGA), *Encyclopedia of Biomaterials and Biomedical Engineering*.

- Bangham, A. D. (1992). *Hospital Practice*, 27 (12), 51.
- Bangham, A. D. and Horne, R.W. (1964). Negative staining of phospholipids and their structural modification by surface-active agents as observed in the electron microscope. *J. Mol. Biol.* 8, 660–668.
- Bangham, A. D., Standish, M. M. & Miller, N. (1965). Cation Permeability of Phospholipid Model Membranes: Effect of Narcotics, *Nature*, 208, 1295 – 1297.
- Bataller, R. & Brenner, D. (2005). Liver fibrosis. *J. Clin. Invest.* 115(2), 209-218.
- Beau, P. & Matrat, S. (1999). A comparative study of polyurethane and silicone cuffed-catheters in long-term home total parenteral nutrition patients. *Clin Nutr*, 18(3), 175-77.
- Bereczky, Z. (2003/2004). Fibrin Stabilization (Factor XIII), Fibrin Structure and Thrombosis Pathophysiology of Haemostasis and Thrombosis. *Pathophysiol Haemost Thmmb*, 33, 30-437.
- Bologna R.A. & Tu L.M. (1999). Hydrogel/silver ion-coated urinary catheter reduces nosocomial urinary tract infection rates in intensive care unit patients: a multicenter study. *Urology*, 54, 982–987.
- Bondurant, Stuart, Virginia L. Ernster, & Roger Herdman, (eds.) (2000). *Safety of Silicone Breast Implants*. Retrieved May, 2010, available from http://books.google.co.uk/books?id=h1owCkaIg-oC&printsec=frontcover&dq=Safety+of+Silicone+Breast+Implants&source=bl&ots=6gzj9JJu0M&sig=wqUrKS1E8iShbOdWn8PAR0bUBJo&hl=en&ei=Q2vuS7bANY380wTNwPnhBw&sa=X&oi=book_result&ct=result&resnum=3&ved=0CCoQ6AEwAg#v=onepage&q&f=false
- Brismar, B., Hardstedt, C., and Jacobson, S. (1981). Diagnosis of thrombosis by catheter phlebography after prolonged central venous catheterization. *Ann Surg*, 194, 779–783.
- British Standard EN 1618 (1997). Catheters other than intravascular catheters—test methods for common properties.
- British Standard EN 30993 (1992). Biological evaluation of medical devices.
- Brook, M. A., Holloway, A. C., Ng, K. K., Hrynyk, M., Moore, C. & Lall, R. (2008). Using a drug to structure its release matrix and release profile. *International Journal of Pharmaceutics*, 358 (1, 2), 121-127.

- Cao, Y. & Li, H. (2002). Interfacial activity of a novel family of polymeric surfactants. *Eur. Polym. J.*, 38, 1457-1463.
- Catalano, P. et al. (2008). A System for Food Drying Using Humidity Control and Low Temperature. *Agricultural Engineering International: The CIGR EJournal*, X.
- Chaize, B., P. Colletier, J., Winterhalter, M., Fournier, D. (2004). Encapsulation of enzymes in liposomes: high encapsulation efficiency and control of substrate permeability, *Artif. Cells Blood Substit. Immobil. Biotechnol*, 32, 67–75.
- Chene, G., Boulard, G. & Gachie, J.P. (1990). A controlled trial of a new material for coating urinary catheters. *Agressologie*, 31 (8), 499–501.
- Chien, Y. W. & Dekker, M. (1992). *Novel drug delivery systems: Drugs and the Pharmaceutical Sciences* (Second ed., Vol. 50). New York: Marcel Dekker. 565–76.
- Choi, K. et al. (2005). Chemistry and biology of dihydroisoxazole derivatives: selective inhibitors of human transglutaminase 2. *Chem Biol*. 12(4), 469–475.
- Choi, K., Siegel, M., Piper, J.L., Yuan, L., Cho, E., Strnad, P., Omary, B., Rich, K.M., Khosla C. (2005). Chemistry and biology of dihydroisoxazole derivatives: selective inhibitors of human transglutaminase 2. *Chem Biol*, 12(4), 469-75
- Citron, B. A. et al. (2001). *J. Biol. Chem*, 276, 3295.
- Clarke, D.D., Mycek, M.J., Neidle, A. and Waelsch, H. (1957). The incorporation of amines into proteins. *Arch. Biochem. Biophys*, 79, 338–354.
- Clarke, D.D., Mycek, M.J., Neidle, A., Waelsch, H. (1959). The incorporation of amines into proteins, *Arch Biochem Biophys*, 79, 338–354.
- Collighan, R. & Griffin, M. (2009). Transglutaminase 2 cross-linking of matrix proteins - biological significance and medical applications. *Amino Acids*, 36 (4), 659-670.
- Commandeur, S., van Beusekom, H. M. & van der Giessen, W. J. (2006). Polymers, drug release, and drug-eluting stents. *J Interv Cardiol*, 19, 500-506.
- Cormio, L., Talja, M., Koivusalo, A., Makisalo, H., Wolff, H. and Ruutu M. (1995). Biocompatibility of various indwelling double-J stents. *J Urol*, 153, 494–496.
- Cox, A.J. (1987). Effect of a hydrogel coating on the surface topography of latex-based urinary catheters: an SEM study, *Biomaterials*, 8, 500–502.

Cox, A.J., Hukins, D.W.L. and Sutton, T.M. (1988). Comparison of in vitro encrustation on silicone and hydrogel-coated latex catheters. *Br J Urol*, 61, 156–161.

Cox, A.J., Millington, R.S., Hukins, D.W.L. and Sutton, T.M. (1989). Resistance of catheters coated with a modified hydrogel to encrustation during an in vitro test. *Urol Res*, 17, 353–356.

Crommelin, D.J.A. et al. (2002). Liposomes: Successful carrier systems for targeted delivery of drugs. In: *The Drug Delivery Companies Report Autumn/ Winter 2002*. PharmaVentures Ltd 2002.

Curelaru, I., Gustavsson, B., Hansson, A.H., Linder, L.E., Stenqvist, O., Wojciechowski, J. (1983). Material thrombogenicity in central venous catheterization II. A comparison between plain silicone elastomer, and plain polyethylene, long, antebrachial catheters. *Acta Anaesthesiol Scand*, 27(2), 158-64.

Damen, J., Regts, J., Scherphof, G. (1981). Transfer and exchange of phospholipid between small unilamellar liposomes and rat plasma high density lipoproteins. Dependence on cholesterol content and phospholipid composition., *Biochim. Biophys. Acta*, 665(3), 538-45.

Darouiche, R.O., Raad II, Heard, S.O., Thornby, J.I., Wenker, O.C., Gabrielli, A., Berg, J., Khardori, N., Hanna, H., Hachem, R., Harris, R.L., Mayhall, G. (1999). A comparison of two antimicrobial-impregnated central venous catheters. Catheter Study Group. *N Engl J Med*, 340(1), 1-8.

Day, C.P. (2002). Non-alcoholic steatohepatitis (NASH): where are we now and where are we going? *Gut*, 50, 585-8.

De Laurenzi, V. & Melino, G. (2001). Gene disruption of tissue transglutaminase. *Mol Cell Biol*. 21(1), 148–155.

Denstedt, J.D., Wollin, T.A. and Reid, G. (1998). Biomaterials used in urology: current issues of biocompatibility, infection, and encrustation, *J Endourol*, 12(6), 493–500.

Desgrandchamps, F. Moulinier, F. Daudon, M. Teillac P. and Le Duc, A. (1997). An in vitro comparison of urease-induced encrustation JJ stents in human urine. *Br J Urol*, 79, 24–27.

Devine, D.V., Wong, K., Serrano, K., Chonn, A., Cullis, P.R. (1994). Liposome-complement interactions in rat serum: implications for liposome survival studies. *Biochim Biophys Acta*, 1191, 43–51.

- Di Campli , C., Wu, J., Zern, M.A. (1999). Targeting of therapeutics to the liver: liposomes and viral vectors. *Alcohol Clin Exp Res*, 23 (5), 950-4.
- Dufour, M. C. Stinson, F. S. & Caces, M. F. (1993). Trends in cirrhosis morbidity and mortality: United States, 1979–1988. *Seminars in Liver Disease*, 13 (2), 109–125.
- Edwards, K. A. & Baeumner, J. A. (2006). Analysis of liposomes. *Talanta*, 68 (5), 1432-1441.
- Eggimann, P. & Pittet, D. (2001). Infection control in the ICU. *Chest*, 120, 2059 –2093.
- Eggimann, P., Sax, H., Pittet, D. (2004). Catheter-related infections. *Microbes and Infection*, 6 (11), 1033-1042.
- Elrick, L.J. et al. (2005). Generation of a monoclonal human single chain antibody fragment to hepatic stellate cells – a potential mechanism for targeting liver anti-fibrotic therapeutics. *J. Hepatol*, 42 (6), 888-896.
- Etienne, A. (1990). *S.T.P. Pharma. Sci*, 6, 33-40.
- Fan, L.T. & Singh, S.K. (1989). *Controlled Release: A Quantitative Treatment*. In: Cantow, H.-J. et al (eds.). New York: Springer-Verlag.
- Fang, Hsu-Wei et al. (2008). Dip coating assisted polylactic acid deposition on steel surface: Film thickness affected by drag force and gravity. *Materials Letters*, 62 (21-22), 3739-3741.
- Fesus, L. & Piacentini, M. (2002). Transglutaminase 2: an enigmatic enzyme with diverse functions. *Trends Biochem Sci*, 27(10), 534-9.
- Fletcher, SJ. (1999). Bodenham AR. Catheter-related sepsis: an overview—part 1. *Br J Intensive Care*, 9, 47–53
- Foster, TJ. and Hook, M. (1998). Surface protein adhesions of *staphylococcus aureus*. *Trends in Microbiology*, 6(12), 484-488.
- Fraley, R. et al. (1981). Liposome-mediated delivery of deoxyribonucleic acid to cells: enhanced efficiency of delivery by changes in lipid composition and incubation conditions. *Biochemistry*, 20(24), 6978–6987.
- Freshney, R. (1987). Freshney, R. (ed.), *Culture of Animal Cells: A Manual of Basic Technique*. New York: Wiley-Liss, Inc. 117.

- Freund, KF. et al. (1994) Transglutaminase inhibition by 2-(2-Oxopropyl)thioimidazolium derivative—mechanism of factor xiii inactivation. *Biochemistry*, 33(33), 10109–10119.
- Friedman, SL. (2000). Molecular regulation of hepatic fibrosis, an integrated cellular response to tissue injury. *J Biol Chem*, 275(4), 2247-50.
- Friedman, SL. (2003). Liver fibrosis - from bench to bedside. *J. Hepatol*, 38, Suppl. 1, S38-S53.
- Gabizon, A. & Papahadjopoulos, D. (1988). Liposome formulations with prolonged circulation time in blood and enhanced uptake by tumors. *Proc. Natl. Acad. Sci*, 85, 6949–6953.
- Gabizon, A. et al. (1990). Effect of liposome composition and other factors on the targeting of liposomes to experimental tumors: biodistribution and imaging studies. *Cancer Res*, 50, 6371–6378.
- Garg, S. Patel, S., Al-Shaikh, B. (2004). Coated central venous lines and catheter related blood stream infections. *CPD Anaesthesia*, 6(3), 136-139.
- Gombotz, W. R., & Pettit, D. K. (1995). *Bioconjug. Chem*, 6, 332.
- Gorman, S. P. & Tunney M, M. (1997). *J. Biomed. Mater. Res*, 12, 136–166.
- Goyal, P. et al. (2005). Liposomal drug delivery systems: Clinical applications. *Acta Pharm*, 55, 1–25.
- Grabielle-Madellmont, C. et al. (2003). Characterization of loaded liposomes by size exclusion chromatography. *J Biochem Bioph Meth*, 56(1-3), 189-217.
- Greenberg, CS., Birckbichler, PJ., Rice, RH. (1991), Transglutaminases: multifunctional cross-linking enzymes that stabilize tissues, *Faseb J*, 5(15), 3071-7.
- Gregoriadis, G. & Davis, C. (1979). *Biochem. Biophys. Res. Commun*, 89, 1287-1293.
- Gregoriadis, G. & Florence, A. T. (1993). Liposomes in drug delivery: Clinical, diagnosis and ophthalmic potential. *Drugs*, 45, 15-28.
- Gregoriadis, G. & Ryman, B. (1971). Liposomes as carriers of enzymes or drugs: a new approach to the treatment of storage diseases, *Biochem. J.*, 124, 58.
- Gregoriadis, G. (1973). Drug entrapment in liposomes. *FEBS Lett*, 36, 292–296.

- Gregoriadis, G. (1990). Immunological adjuvants: a role for liposomes. *Immunol Today*, 11 (3), 89- 97.
- Gregoriadis, G. (1995). Engineering liposomes for drug delivery: progress and problems. *Trends Biotechnol*, 13 (12), 527-537.
- Gregoriadis, G., da Silva, H., Florence, A.T. (1990). *Int. J. Pharmaceutics*, 65, 235.
- Grenard, P., Bates, M. K. and Aeschlimann, D. (2001). Evolution of transglutaminase genes: identification of a transglutaminase gene cluster on human chromosome 15q15. Structure of the gene encoding transglutaminase x and a novel gene family member, transglutaminase z. *J. Biol. Chem*, 276, 33066-33078.
- Grenard, P., Bresson-Hadni, S., El Alaoui, S., Chevallier, M., Vuitton, D. A., & Ricard-Blum, S. (2001). Transglutaminase-mediated cross- linking is involved in the stabilization of extracellular matrix in human liver fibrosis. *J Hepatol*, 35, 367-375.
- Griffin, M, Coutts, IG. & Saint, RE. (2004). *Novel compounds and methods of using the same*. World patent WO 2004/113363.
- Griffin, M. et al. (2004). *Novel compounds and methods of using the same*. World patent WO 2004/113363.
- Griffin, M., Casadio, R., & Bergamini, C. M. (2002). Transglutaminases: nature's biological glues. *Biochem J*, 368, 377–396.
- Griffin, M., Johnson, TS., Fisher, M., Haylor, JL., Hau, Z., Skill, NJ., Jones, R., Saint, R., Coutts, I., El Nahas, AM. (2008). Transglutaminase inhibition ameliorates tissue scarring and fibrosis: experience in a kidney model. (2008). *J American Society*, 14(8), 2052-2062.
- Griffin, M., Mongeot, A., Collighan, R., Saint, R. E., Jones, R. A., Coutts, I. C. (2008). Synthesis of Potent Water-soluble Tissue Transglutaminase Inhibitors. *Bioorg. Medicinal Chem. Lett.*, 18 (20), 5559-5562.
- Griffin, M., Smith, L. L., & Wynne, J. (1979). Changes in transglutaminase activity in an experimental model of pulmonary fibrosis induced by paraquat. *Br J Exp Pathol*, 60(6), 653–661.
- Haaf, F., Sanner, A. & Straub, F. (1985). Polymers of N-Vinylpyrrolidone: Synthesis, Characterization and Uses. *Polym. J.*, 17(1), 143–152.

- Haberland, M. E. & Reynolds, J. A. (1973). Self-association of Cholesterol in Aqueous Solution. *Proc Natl Acad Sci U S A*, 70 (8), 2313–2316.
- Hahn, U., Goldschmidt, H., Salwender, H., *et al.* (1995). Large-bore central venous catheters for the collection of peripheral blood stem cells. *J Clin Apheresis*, 10, 12-16.
- Haire, W. D., Edney, J. A., Landmark, J. D., *et al.* (1990). Thrombotic complications of subclavian apheresis catheters in cancer patients: prevention with heparin infusion. *J Clin Apheresis*, 5, 188-191.
- Harashima, *et al.* (1994). Enhanced hepatic uptake of liposomes through complement activation depending on the size of liposomes. *Pharm. Res*, 11, 402–406.
- Hiiragi, T., Sasaki H., Nagafuchi, A., Sabe, H., Shen, SC., Matsuki, M., Yamanishi, K., Tsukita, S. (1999). Transglutaminase type 1 and its cross-linking activity are concentrated at adherens junctions in simple epithelial cells. *J Biol Chem*, 274(48), 34148-54.
- Hillery, A. M. (2001). Advanced drug delivery and targeting: An Introduction. In: Hillery, A., Lloyd, A. W. & Swarbrick, J. (eds), *Drug delivery and targeting: for Pharmacist and Pharmaceutical scientists* (1st ed.). London: Taylor & Francis.
- Hoppe B. (1995). Central venous catheter-related infections: pathogenesis, predictors, and prevention. *Heart Lung*, 24(4), 333-9.
- Hoshal, VL., Ause, RG., and Hoskins, PA. (1971). Fibrin sleeve formation on indwelling subclavian central venous catheters, *Arch Surg*, 102, 353–358.
http://rais.ornl.gov/tox/profiles/acenaphthene_f_V1.html
- Huang, G., Gao, J., Hu Z., St John, JV., Ponder, BC., Moro, D. (2004). Controlled drug release from hydrogel nanoparticle networks. *J Control Release*. 94(2-3), 303-11.
- Huang, L. Haylor, JL., Hau, Z. Jones, RA., Vickers, ME., Wagner, B., Griffin, M. Saint, RE., Coutts, IGC., El Nahas, AM and Johnson, TS. (2009). Transglutaminase inhibition ameliorates experimental diabetic nephropathy, *Kidney Int*, 76, 383–394.
- Huie, S. A., Schmidt, P. F. & Warren, J. S. (1985). Testing adhesive and liner for transdermal drug delivery. *Adhes. Ageing*, 28, 30–35.
- Huong, T. M., Ishida T, T., Harashima, H., & Kiwada, H. (2001). The complement system enhances the clearance of phosphatidylserine (PS)-liposomes in rat and guinea pig. *Int J Pharm*, 215 (1-2), 197-205.

- Hwang, K. J. (1987). Liposome pharmacokinetics. In: M. J. Ostro (ed.), *Liposomes: from biophysics to therapeutics*. New York: Marcel Dekker, 109–156.
- Ichinose, A., et al. (1990). Structure of Transglutaminase. *JBC*, 265(23), 13411-13414.
- Ikada, Y. & Uyama, Y. (1993). *Lubricating Polymer Surfaces*. Lancaster, PA: Technomic Publishing Company.
- Iredale, JP. (2003). Cirrhosis: new research provides a basis for rational and targeted treatments. *BMJ*, 327, 143-7.
- Iredale, JP. (2007). Models of liver fibrosis: exploring the dynamic nature of inflammation and repair in a solid organ. *J. Clin. Invest*, 117(3), 539-548.
- Johansson, E., Hansson, M., Sollén Nilsson, A. & Engerwall, P. (1999). Vascular access devices used during harvest of peripheral blood stem cells: high complication rate in patients with long-term dialysis central venous catheter. *Bone Marrow Transplant*, 24, 793-797.
- John, SF., Derrick, MR., Jacob, AE., Handley, PS. (1996). The combined effects of plasma and hydrogel coating on adhesion of *Staphylococcus epidermidis* and *Staphylococcus aureus* to polyurethane catheters. *FEMS Microbiol Lett*, 144(2-3), 241-7.
- Johnson, T. S., Griffin, M., Thomas, G. L., Skill, J., Cox, A., Yang, B. (1997). The role of transglutaminase in the rat subtotal nephrectomy model of renal fibrosis. *J Clin Invest*, 99 (12), 2950–2960.
- Johnson, T. S., Skill, N. J., El Nahas, A. M., Oldroyd, S. D., Thomas, G. L., Douthwaite, J. A. (1999). *J. Am. Soc. Nephrol*, 10, 2146.
- Jones, M. (1995). The surface properties of phospholipid liposome systems and their characterisation. *Adv. Colloid Interface Sci.*, 54, 93-128.
- Jones, TC. (2000). Dip-Coating. *Metal Finishing*, 98 (6), 172-174(3)
- Juliano, R. L. & Stamp, D. (1975). Effects of particle size and charge on the clearance of liposomes and liposome-encapsulated drugs. *Biochim. Biophys. Acta*, 1113, 651–658.
- Kajihara, M., Sugie, T., Maeda, H., Sano, A., Fujioka, K., Urabe, Y., et al. (2003). Novel Drug Delivery Device Using Silicone: Controlled Release of Insoluble Drugs or Two Kinds of Water-Soluble Drugs. *Chem Pharm Bull*, 51 (1), 15-19.
- Kamps, JAAM. et al. (1999). Uptake of liposomes containing phosphatidylserine by liver cells in vivo and by sinusoidal liver cells in primary culture: in vivo-in vitro differences. *Biochem Biophys Res Commun*, 256 (1), 57-62.

- Kim, C.J. (2000). *Controlled Release Dosage Form Design* (1st ed.). Lancaster, PA: Technomic Publishing Company.
- Kipping, F. S. (1904). Organic derivative of silicone. Preparation of alkylsilicone chlorides. *Proc. Chem. Soc.*, 20, 15.
- Kirby, C. & Gregoriadis, G. (1984). Dehydration-rehydration vesicles (DRV): A new method for high yield drug entrapment in liposomes. *Biotechnology*, 2, 979-984.
- Kirby, C., Clarke, J., Gregoriadis, G. (1980). Transfer and exchange of phospholipid loss to high density lipoproteins in the presence of serum. *FEBS Lett*, 111, 324.
- Kirby, C.J. & Gregoriadis, G. (1999). Liposomes. In: Mathiowitz E (ed.), *Encyclopaedia of Controlled Drug Delivery*. New York: John Wiley & Sons, Inc. 461-492.
- Kutter, DJ. (2004). Thrombotic complications of central venous catheters in cancer patients, *Oncologist*, 9(2), 207-16.
- Labhasetwar, V. et al. (1994). A study on zeta potential and dielectric constant of liposomes. *J Microencapsul*, 11 (6), 663-668.
- Laennec, R.T.H. (1826). Traite de l'auscultation mediate. Hemorrhagic pleurisy of the left side with ascites and organic diseases of the liver.
- Lambert, PA. et al. (2007). *Medical devices and coatings therefor*. World patent. WO2007010201.
- Lawrence, EL. & Turner, IG. (2005). Materials for urinary catheters: a review of their history and development in the UK. *Med Eng Phys*, 27 (6), 443-53.
- Lee, C. H., Bagdon, R. E., Bhatt, P. P. & Chien, Y. W. (1997). Development of silicone-based barrier devices for controlled delivery of spermicidal agents. *J. Control. Release*, 44 (1), 43-53.
- Lee, H. B & Blaufox, M. D. (1985). Blood volume in the Rat, *J NuciMed*, 25, 72-76
- Leon, D. (2007). Rates for England and Wales (to 2004) and Scotland (to 2006) subsequently updated by Prof. David Leon and General Registrar for Scotland. *The Lancet*, 367 (9504), 52-56.
- Li, F. & Wang, J. Y. (2009). Targeted delivery of drugs for liver fibrosis. *Expert opinine drug delivery*, 6 (5), 531-541.

- Liedberg, H., Lundeberg, H. & Ekman, P. (1990). Refinements in the coating of urethral catheters reduces the incidence of catheter-associated bacteriuria. An experimental and clinical study. *Eur Urol*, 17, 236–240.
- Lin, CC. & Metters, AT. (2006). Hydrogels in controlled release formulations: network design and mathematical modeling. *Adv Drug Deliv Rev*, 58(12-13), 1379-408.
- Liu, D. L. et al. (1995). Recognition and clearance of liposomes containing phosphatidylserine are mediated by serum opsonin. *Biochim. Biophys. Acta*, 1235, 140–146.
- Liu, D., Mori, A., & Huang, L. (1992). Role of liposome size and RES blockade in controlling biodistribution and tumor uptake of GM1-containing liposomes. *Biochim. Biophys. Acta*, 1104, 95–101.
- Liu, X-Y., Yang, Q., Kamo, N., Miyake, J. (2001). Effect of liposome type and membrane fluidity on drug-membrane partitioning analyzed by immobilized liposome chromatography. *Journal of Chromatography A*, 913, 123-131.
- Longmuir, K. J., Robertson, R. T., Haynes, S. M., Baratta, J. L., Waring, A. J. (2006). Effective targeting of liposomes to liver and hepatocytes in vivo by incorporation of a plasmodium amino acid sequence. *Pharmaceutical Research*, 23(4), 759-769.
- Lorand, L. & Graham, RM. (2003). Transglutaminases: crosslinking enzymes with pleiotropic functions. *Nat Rev Mol Cell Biol*, 4(2), 140-56.
- Lorand, L. (1986). Activation of blood coagulation factor XIII. *Ann. N.Y. Acad. Sci*, 285, 144-158.
- Lowthian, P. (1998). The dangers of long-term catheter drainage, *Br J Nurs*, 7, 366–379.
- Madero, L., Diaz, MA., Benito, A. et al. (1997). Non-tunneled catheters for the collection and transplantation of peripheral blood stem cells in children. *Bone Marrow Transplant*, 20, 53-56.
- Maeda, H., Ohashi, E., Sano, A., Kawasaki, H. & Kurosaki, Y. (2003). Investigation of the release behavior of a covered rod-type formulation using silicone. *J. Control. Release*, 90 (1), 59-70.
- Maki, D., Weise, C., Sarafin, H. A. (1977). semiquantitative culture method for identifying intravenous-catheter-related infection. *N Engl J Med*, 296, 1305-9.

Malcolm, R. (2003). *Modified-Release Drug Delivery Technology*. In: M. J. Rathbone, J. hadgraft, & M. S. Roberts (ed.). New York: Marcel Dekker Inc.

Malcolm, R. K., McCullagh, S. D., Woolfson, A. D., Gorman, S. P., Jones, D. S. & Cuddy, J. (2004). Controlled release of a model antibacterial drug from a novel self-lubricating silicone biomaterial. *J. Control. Release*, 97 (2), 313-320.

Mangala, L. S. & Mehta, K. (2005). *Prog. Exp. Tumor Res*, 38, 125.

Mann, R. E., Smart, R. G., & Govoni, R. (2003). The epidemiology of alcoholic liver disease. *Alcohol Research & Health*, 27(3), 209–219.

Marion-Ferey, K., Pasmore, M., Stoodley, P., Wilso, S., Husson, G. P. & Costerton, J. W. (2003). *J. Hosp. Infect*, 53, 64–71.

Marzari, R., Sblattero, D., Florian, F., Tongiorgi, E., Not, T., Tommasini, A. (2001). *Immunology*, 166, 4170.

Mashak, A. (2008). In vitro drug release from silicone rubber–polyacrylamide composite. *Silicon Chemistry*, 3(6), 295-301.

Massing, U. & Fuxius, S. (2000). Liposomal formulations of anticancer drugs: selectivity and effectiveness. *Drug Resistance*, 3(3), 171-177.

Matsuka, YV., Anderson, ET., Milner-Fish, T., Ooi, P., Baker, S. (2003). Staphylococcus aureus fibronectin-binding protein serves as a substrate for coagulation factor XIIIa: evidence for factor XIIIa-catalyzed covalent cross-linking to fibronectin and fibrin. *Biochemistry*. 42(49), 14643-52.

Mayer, L.D., Hope, M.J., Cullis, P.R. (1986). *Biochim. Biophys. Acta*, 858, 161.

Mirza, A., Liu, S. L., Frizell, E., Zhu, J. L., Maddukuri, S., Martinez, J. (1997). A role for tissue transglutaminase in hepatic injury and fibrogenesis, and its regulation by NF-kappa B. *Am J Physiol-Gastroint Liver Physiol*, 35 (2), G281–G288.

Mohammed, A.R., Weston, N., Coombes, A.G.A., Fitzgerald, M., Perrie, Y. (2004). Liposome formulation of poorly water soluble drugs: optimisation of drug loading and ESEM analysis of stability. *International Journal of Pharmaceutics*, 285 (1-2), 23-34.

Monson, T. & Kunin, C.M. (1974). Evaluation of a polymer-coated indwelling catheter in prevention of infection. *J Urol*, 111, 220–222.

Morris, M. (2010). CENTRAL VENOUS CATHETER (CVC) CARE POLICY FOR ADULTS. Retrieved July 16, 2010, available from

http://www.ashfordstpeters.nhs.uk/attachments/1312_Central%20Venous%20Catheter%20Care%20Policy.pdf

Morris, NS., Stickler, DJ., Winters, C. (1997). Which indwelling urethral catheters resist encrustation by *Proteus mirabilis* biofilms? *Br J Urol*, 80, 58–63.

Motin, J., Fischer, G. and Evreux, J. (1964). Intérêt de la voie sous-clavière en réanimation prolongée. *Trav Originaux*, 40, 583–593.

Mughal, MM. (1989). Complications of intravenous feeding catheters. *Br J Surg*, 76, 15–21.

Nanda, N. et al. (2001). Targeted inactivation of Gh/tissue transglutaminase II. *J Biol Chem*. 276(23), 20673–20678.

Nardacci, R. et al. (2003). Transglutaminase Type II Plays a Protective Role in Hepatic Injury. *Am J Pathol*, 162 (4), 1293–1303.

O'Grady, NP. et al. (2002). Guidelines for the prevention of intravascular catheter-related infections. Centers for Disease Control and Prevention. *MMWR Recomm Rep*. 51(RR-10), 1-29.

Oussemaume, J. B., Noiret, N., Pereyre, M. & Saux, A. (1994). *Organometallics*, 13, 1034–1038.

Pan, CJ., Tang, JJ., Weng, YJ., Wang, J., Huang, N. (2007). Preparation and characterization of rapamycin-loaded PLGA coating stent. *J Mater Sci Mater Med*, 18 (11), 2193-8.

Papahadjopoulos, D. (1978). Liposomes and Their Uses in Biology and Medicine. *Ann. N.Y.Acad. Sci*, 308.

Pardin, C., Gillet, SM., Keillor, JW. (2006). Synthesis and evaluation of peptidic irreversible inhibitors of tissue transglutaminase. *Bioorg Med Chem*. 14(24), 8379–8385.

Park, JH., Cho, YW., Kwon, IC., Jeong, SY., Bae, YH. (2002). Assessment of PEO/PTMO multiblock copolymer/segmented polyurethane blends as coating materials for urinary catheters: in vitro bacterial adhesion and encrustation behavior. *Biomaterials*, 23(19), 3991-4000.

Patel, HM. (1992). Influence of lipid composition on opsonophagocytosis of liposomes. *Research in immunology*, 143, 242–244.

- Peppas, N., et al. (2000). Hydrogels in pharmaceutical formulations. *Eur J Pharm Biopharm*, 50 (1, 3), 27-46.
- Perrie, Y. & Rades, T. (2009). *FASTtrack Pharmaceuticals – Drug Delivery and Targeting*. London: Pharmaceutical Press.
- Perrie, Y., Barralet, J.E., McNeil, S., Vangala, A. (2004). Surfactant vesicle-mediated delivery of DNA vaccines via the subcutaneous route. *Int. J. Pharm.*, 284 (1-2), 31-41.
- Peterson, L., Zettergren, J. and Wuepper K. (1983). Biochemistry of Transglutaminases and Cross-Linking in the Skin. *Journal of Investigative Dermatology*, 81, 95-100
- Pinzani, M., Rombouts, K., Colagrande, S. (2005). Fibrosis in chronic liver diseases: diagnosis and management. *Journal of Hepatology*, 42, S22-36.
- Piozzia, A. et al. (2004). Antimicrobial activity of polyurethanes coated with antibiotics: a new approach to the realization of medical devices exempt from microbial colonization. *Int. J. Pharm.*, 280 (1-2), 173-183.
- Pisano, J. J., Finlayson, J. S. & Peyton, M. P. (1968). Cross-link in fibrin polymerized by factor 13: epsilon-(gamma-glutamyl)lysine, *Science*, 160, 892-893.
- Plowman, R. et al. (2001). The rate and cost of hospital acquired infections occurring in patients admitted to selected specialities of a district general hospital in England and the national burden imposed, *J Hosp Infect*, 47, 198–209.
- Pottecher, T., Forrler, M., Picardat, P., Krause, D., Bellocq, JP., Otteni, JC. (1984). Thrombogenicity of central venous catheters: prospective study of polyethylene, silicone and polyurethane catheters with phlebography or post-mortem examination, *Eur J Anaesthesiol*, 1 (4), 361-5.
- Press, OW., Ramsey, PG., Larson, EB. et al. (1984). Hickman catheter infections in patients with malignancies. *Medicine (Baltimore)*, 63, 189–200.
- Qiu, J. F., Zhang, Z. Q., Chen, W., & Wu, Z. Y. (2007). Cystamine ameliorates liver fibrosis induced by carbon tetrachloride via inhibition of tissue transglutaminase. *World J Gastroenterol*, 13 (32), 4328-32.
- Raad II, et al., (1994). The relationship between the thrombotic and infectious complications of central venous catheter. *JAMA*, 271, 1014–1016.
- Ranade, VV. (1989). Drug delivery systems.X 1. site-specific drug delivery using liposomes as carriers. *J Clin Pharmacol*, 29, 685–694.

Reitman, MTF. & McPeak, J. (2005). Protective Coatings for Implantable Medical Devices Proceedings, Society of Plastic Engineers. *ANTEC*, 3120–3124.

Rothkopf, C., Fahr, A., Fricker, G., Scherphof, G., Kamps, J. A. A. M. (2005). Uptake of phosphatidylserine-containing liposomes by liver sinusoidal endothelial cells in the serum-free perfused rat liver. *Biochimica et Biophysica Acta (BBA) – Biomembranes*, 1668 (1), 10-16.

Ruutu, M., Alfthan, O., et al. (1985). Cytotoxicity of latex urinary catheters, *Br J Urol*, 57, 82–87.

Salama, F.A. (1993). Application of polymers in urology, *38th International SAMPE Symposium*, 1, 573–581.

Santilli, J. (2002). Fibrin sheaths and central venous catheter occlusions: Diagnosis and management. *Techniques in Vascular and Interventional Radiology*, 5 (2), 89-94.

Sarem, M., Znaidak, R., Macias, M., & Rey, R. (2006). Hepatic stellate cells: its role in normal and its role in normal and pathological conditions. *Gastroenterol Hepatol*, 29, 93-101.

Saunders, L; Perrin, J; Gammack, D. (1962). Ultrasonic irradiation of some phospholipid sols. *J. Pharm. Pharmacol*, 14, 567–572.

Senior, J. & Gregoriadis, G. (1982). Is the half-life of circulating liposomes determined by changes in their permeability? *FEBS Lett*, 145, 109–114.

Sharma, A. & Sharma, U.S. (1997). Liposomes in drug delivery: Progress and limitations. *Int J Pharm*, 154 (2), 123-140.

Shintani, H. (2004). Modification of Medical Device Surface to attain Anti-Infection. *Trends Biomater. Artif. Organs*, 18 (1), 1-8.

Shweke, N. et al., (2008) Tissue transglutaminase contributes to interstitial renal fibrosis by favoring accumulation of fibrillar collagen through TGF-beta activation and cell infiltration. *Am J Pathol*, 173 (3), 631–642.

Siegel, M. & Khosla, C. (2007). Transglutaminase 2 inhibitors and their therapeutic role in disease states. *Pharmacol Ther*, 115 (2), 232–245.

Siegel, M., Strnad, P., Watts, R. E., Choi, K., Jabri, B., Omary, M. B., et al. (2008). Extracellular transglutaminase 2 is catalytically inactive, but is transiently activated upon tissue injury. *PLoS One*, 3 (3), 1861.

Sisirak, M., Zvizdic, A., Hukic, M. (2010). Methicillin-resistant *Staphylococcus aureus* (MRSA) as a cause of nosocomial wound infections. *Bosn J Basic Med Sci*, 10 (1), 32-7.

Skill, N. J., Griffin, M., El Nahas, A. M., Sanai, T., Haylor, J. L., Fisher, M., et al. (2001). Increases in renal epsilon-(gamma-glutamyl)-lysine crosslinks result from compartment-specific changes in tissue transglutaminase in early experimental diabetic nephropathy: pathologic implications. *Lab Invest*, 81 (5), 705–716.

Slaughter, T. F., Achyuthan, K. E., Lai, T. S., Greenberg, C. S. (1992). *Anal. Biochem*, 205, 166.

Stephens, LC., Haire, WD., Schmit, PK. et al. (1993). Granulocyte-macrophage colony-stimulating factor: high incidence of apheresis catheter thrombosis during peripheral stem cell collection. *Bone Marrow Transplant*, 11, 51-54.

Storm, G. & Crommelin, DJA. (1998). Liposomes: quo vadis? *Pharmaceutical Science & Technology Today*, 1 (1), 19-31.

Straubinger, R.M., Hong, K., Friend, D.S., Papahadjopoulos, D. (2003). Endocytosis of liposomes and intracellular fate of encapsulated molecules: encounter with a low pH compartment after internalization in coated vesicles. *Cell*, 32, 1069–1079.

Strnad, P. et al. (2006). Pharmacologic transglutaminase inhibition attenuates drug-primed liver hypertrophy but not Mallory body formation. *FEBS Lett.* 580(9), 2351–2357.

Strnad, P., Siegel, M., Toivola, DM., Choi, K., Kosek, JC., Khosl,a C., Omary, MB. (2006). Pharmacologic transglutaminase inhibition attenuates drug-primed liver hypertrophy but not Mallory body formation. *FEBS Letters*, 580 (9), 2351-2357.

Szoka, F. & Papahadjopoulos, D. (1978). Procedure for preperation of liposomes with lareg intrnal aqueous space an dhigh capture by reverse-phase evaporation. *Biochem*, 75, 4194-4198.

Tacconelli et al. (2009). Epidemiology, medical outcomes and costs of catheter-related bloodstream infections in intensive care units of four European countries: literature- and registry-based estimates, *Journal of Hospital Infection*, 72 (2), 97-103.

Talja, M., Korpela, A. and Järvi, K. (1990). Comparison of urethral reaction to full silicone, hydrogel-coated and siliconised latex catheters. *Br J Urol*, 66, 652–657.

Terwogt, JMM., et al. (1999). Clinical pharmacology of anticancer agents in relation to formulations and administration routes. *Cancer Treatment Reviews*, 25 (2), 83-101.

Terzano, C., Allegra, L., Alhaique, F., Marianecchi, C., Carafa, M., 2005. Nonphospholipid vesicles for pulmonary glucocorticoid delivery. *Eur J Pharm Biopharm*, 59, 57-62.

The National Nosocomial Infection Surveillance (2000). Monitoring hospital-acquired infections to promote patient safety—United States 1990–1999. *Morb. Mortal. Wkly Rep*, 49, 149–153.

Thibon, P., Le Coutour, X., Leroyer, R., Fabry, J. (2000). Randomized multi-centre trial of the effects of a catheter coated with hydrogel and silver salts on the incidence of hospital-acquired urinary infections. *J Hosp Infect*, 45, 117–124.

Tozer, T.N. & Rowland, M. (2006). *Introduction to Pharmacokinetics and Pharmacodynamics: The Quantitative Basis of Drug Therapy*. Baltimore: Lippincott Williams & Wilkins.

Tunney, M. M., Gorman, S. P. & Patrick, S. (1996). *Rev. Med. Microbiol*, 74, 195–205.

Tunney, M.M., Keane, P.F., Jones, D.S. and Gorman, S.P. (1996). Comparative assessment of ureteral stent biomaterial encrustation. *Biomaterials*, 17, 1541–1546.

U.S. EPA (U.S. Environmental Protection Agency) (1993a). Health Assessment Summary Tables. Annual FY-93. Prepared by the Office of Health and Environmental Assessment, Environmental Criteria and Assessment Office, Cincinnati, OH, for the Office of Emergency and Remedial Response, Washington, DC. Retrieved May 17, 2010, available from The Risk Assessment Information System http://rais.ornl.gov/tox/profiles/acenaphthene_f_V1.html.

U.S. EPA (U.S. Environmental Protection Agency) (1993b). Integrated Risk Information System (IRIS). Environmental Criteria and Assessment Office, Office of Health and Environmental Assessment, Cincinnati, OH. Retrieved May 17, 2010, available from The Risk Assessment Information System.

Ueki, T., Kaneda, Y., Tsutsui, H., Nakanishi, K., Sawa, Y., Morishita, R., et al. (1999). Hepatocyte growth factor gene therapy of liver cirrhosis in rats. *Nat Med*, 5 (2), 226-30.

Vemuri, S. & Rhodes, C.T. (1995). Preparation and characterization of liposomes as therapeutic delivery systems: a review. *Pharmaceutica Acta Helvetiae*, 70 (2), 95-111.

Vemuri, S., Yu, T., De Groot, J., Roosdrop, N. (1990). In-vitro interaction of sized and unsized liposome vesicles with high density lipoproteins. *Drug. Dev. Ind. Pharm*, 16, 1579–1584.

Wang, DA., Ji, J., Gao, CY., Yu, GH., Feng, LX. (2001). Surface coating of stearyl poly(ethylene oxide) coupling-polymer on polyurethane guiding catheters with poly(ether urethane) film-building additive for biomedical application. *Biomaterials*, 22 (12), 1549-62.

Wang, Z. & Shmeis, RA. (2005). Dissolution Controlled Drug Delivery Systems. In: Xiaoling, Li (ed.), *Design of controlled releases drug delivery systems*. Blacklick, OH, USA: McGraw-Hill Professional.

Watson, J. M. & Payne, P. A. (1990). *J. Membrane Sci*, 149, 171–205.

Weiner, N., Martin, F., Ria, M. (1989). Liposomes as a drug delivery system. *Drug Dev Ind Pharm*, 15 (10), 1523-1554.

Wheeler RA. and Griffiths, DM. (1992). Cuff Cath: an initial experience of cuffed polyurethane central venous catheters in children. *JPEN*, 16 (4), 384-5.

Wichterle, O. & Lim, D. (1960). Hydrophilic gels for biological use, *Nature*, 185, 117.

Wodzinska, JM. (2005). Transglutaminases as targets for pharmacological Inhibition *Mini Rev Med Chem*, 5 (3), 279-92.

Woolfson, A. D., Brown, A. f., Malcolm, R. K., Gorman, S. P., Jones, D. S. & McCullagh, S. D. (2003). Self-lubricating silicone elastomer biomaterials. *J. Mater. Chem*, 13, 2465–2470.

Woolfson, D., Elliott, G. E., Gilligan, C. A. & Passmore, C. M. (1999). Design of an intravaginal ring for the controlled delivery of 17 β -estradiol as its 3-acetate ester. *J. Controlled Release*, 61, 319-328.

Wu, J., Liu, P., Zhu, J., Maddukuri, S., Mark, A., Zern, M.D. (2003). Increased liver uptake of liposomes and improved targeting efficacy by labeling with asialofetuin in rodents. *Hepatology*, 27 (3), 772 – 778.

Xiang, DZ. et al. (1998). Composition and formation of the sleeve enveloping a central venous catheter. *J Vasc Surg*, 28 (2), 260-71.

Xiang, DZ., Verbeken, EK., Van Lommel, AT., Stas, M., De Wever, I. (2001). Sleeve-related thrombosis: a new form of catheter-related thrombosis. *Thromb Res*, 104 (1), 7-14.

- Yao, T., Degli Esposti, S., Huang, L., & Zernc, M. A. (1995). The use of liposomes in the therapy of liver disease. *Adv. Drug Delivery Rev.*, 17, 239-246.
- Yoon, Y.H & Yi, H. (2008). Liver Cirrhosis Mortality in the United States, 1970 -2005. *National Institute on Alcohol Abuse*, retrieved February 11, 2010, available from <http://pubs.niaaa.nih.gov/publications/surveillance83/Cirr05.pdf>
- Young, CD., Wu, JR. & Tsou, TL. (1998). High-strength, ultra-thin and fiber-reinforced pHEMA artificial skin. *Biomaterials*, 19, 1745–1752.
- Yu, H. Y. & Lin, C. Y. (1997). Uptake of charged liposomes by the rat liver. *J Formos Med Assoc*, 96 (6), 409-13.
- Yuan, L., Siegel, M., Choi, K., Khosla, C., Miller, CR., et al. (2006) Transglutaminase 2 inhibitor, KCC009, disrupts fibronectin assembly in the extracellular matrix and sensitizes orthotopic glioblastomas to chemotherapy. *Oncogene* 26(18), 2563–2573.
- Zheng, YF. et al. (2006). Surface characteristics and biological properties of paclitaxel-embedding PLGA coatings on TiNi alloy. *Materials Science and Engineering*, 438-440, 1119-1123.
- Zilberman. M. & Elsner. J. (2008). Antibiotic-eluting medical devices for various applications. *J. Control. Release*, 130 (3), 205-215.

Web image 1, tradeorea.com, retrieved July 29 2010, available from http://www.tradekorea.com/productdetail/P00023466/Multi_lumen_Venous_Catheter_Systems.html

Web image 2, retrieved July 29 2010, available from Chemo Prep, <http://mikehamel.wordpress.com/2009/03/22/chemo-prep/>

Web image 3 & 4, retrieved July 29 2010, available from The Internet Journal of Emergency Medicine, http://www.ispub.com/journal/the_internet_journal_of_emergency_medicine/volume_2_number_2_15/article/complication_of_venous_cut_down_migration_of_catheter_th_at_remaind_in_the_vein.html

Web image 5, retrieved July 29 2010, available from emedicine, <http://emedicine.medscape.com/article/1821257-treatment>

Web image 6, retrieved July 29 2010, available from Medscape, http://www.medscape.com/content/2004/00/47/23/472310/472310_fig.html

Web image 7, retrieved July 29 2010, available from TeleFlex Medical, http://www.arrowintl.com/products/pressurecvc/help_prevent_infection/default.asp

Web image 8, retrieved July 29 2010, available from Biochemistry, <http://www.ncbi.nlm.nih.gov/bookshelf/br.fcgi?book=stryer&part=A1378>.

Web image 9, retrieved July 29 2010, available from PDB, <http://www.rcsb.org/pdb/explore.do?structureId=3CDZ>

Web image 10, retrieved July 29 2010, available from Nutrition Soup, <http://nutritionsoup.wordpress.com/2008/09/30/let%E2%80%99s-stop-talking-about-fatty-liver-and-let%E2%80%99s-talk-about-the-real-issue/>

Web image 11, retrieved July 29 2010, available from PNAS, <http://www.pnas.org/content/99/5/2743/F2.expansion.html>

Web image 12, retrieved July 29 2010, available from Fascinating silicone, <http://www.dowcorning.com/content/discover/discovertoolbox/forms-rubber-structure.aspx>

Web image 13, retrieved July 29 2010, available from 2007 Encyclopaedia Britannica, Inc., <http://www.britannica.com/EBchecked/topic-art/342910/92244/Phospholipids-can-be-used-to-form-artificial-structures-called-liposomes>

Web image 14 & 15, retrieved July 29 2010, available from Nanolifenutra, http://www.nanolifenutra.com/liposome_technology.html

Web image 16 & 17, retrieved July 29 2010, available from Polynomial, <http://polynomial.me.uk/2009/07/>

| POLYMER | PERCENT SOLUTION (w/v) | The solubility and coating quality of the polymer within a range of solvents | | | | | | | | | | | | | | |
|---|---------------------------|--|---|-----------------------------------|---------|---|------------------------------------|---------|---|------------------------------------|------------|---|--|-----|---|-----------------------------------|
| | | Methanol | | comments | Ethanol | | comments | Acetone | | comments | Chloroform | | comments | DCM | | comments |
| Polythylene-glycol H(OCH ₂ CH ₂) _n OH MW:8000 | | S | C | Poor quality coating was observed | S | C | Polymer aggregates in ethanol | S | C | Polymer aggregates in acetone | S | C | Poor quality coating Insoluble solution | S | C | Polymer aggregates in DMC |
| | 2% | √ | X | | X | - | | X | - | | √ | X | | X | - | |
| | 5% | √ | X | | X | - | | X | - | | X | - | | X | - | |
| | 10% | √ | X | | X | - | | X | - | | X | - | | X | - | |
| Polythylene-glycol H(OCH ₂ CH ₂) _n OH MW:4600 | 2% | √ | X | Same as above | X | - | Same as above | X | - | Same as above | X | - | A thick white precipitate was observed | √ | X | Poor quality coating was observed |
| | 5% | √ | X | | X | - | | X | - | | X | - | | X | - | Insoluble solution |
| | 10% | √ | X | | X | - | | X | - | | X | - | | X | - | |
| Polythylene-glycol H(OCH ₂ CH ₂) _n OH MW:2000 | 2% | √ | X | Same as above | √ | X | Poor quality coating was observed. | √ | X | Poor quality coating was observed. | √ | X | yPoor quality coating was observed. | √ | X | Poor quality coating was observed |
| | 5% | √ | X | | √ | X | | √ | X | | √ | X | | √ | X | |
| | 10% | √ | X | | √ | X | | √ | X | | √ | X | | √ | X | |

Table 1 The solubility and coating quality of polyethylene-glycol of various molecular weights within a range of solvents. S = the solubility of the polymer in the solvent, C = the coating of the PU strips, √ = good, √√ = very good and X= analysis not applicable.

| POLYMER | PERCENT SOLUTION (w/v) | The solubility and coating quality of the polymer within a range of solvents | | | | | | | | | | | | | | |
|--|------------------------------|--|---|----------|---------|---|----------|---------|---|----------|------------|---|----------|-----|---|---------------------------------|
| | | Methanol | | comments | Ethanol | | comments | Acetone | | comments | Chloroform | | comments | DCM | | comments |
| Polyethylene oxide -(CH ₂ -CH ₂ -O) _n MW:1000,000 | | S | C | | S | C | | S | C | | S | C | | S | C | |
| | 2% | X | - | | X | - | | X | - | | X | - | | X | - | |
| | 5% | X | - | | X | - | | X | - | | X | - | | X | - | |
| | 10% | X | - | | X | - | | X | - | | X | - | | X | - | |
| Polyethylene oxide -(CH ₂ -CH ₂ -O) _n MW:300,000 | 2% | X | - | | X | - | | X | - | | X | - | | √ | √ | A fragile coating was observed. |
| | 5% | X | - | | X | - | | X | - | | X | - | | √ | √ | |
| | 10% | X | - | | X | - | | X | - | | X | - | | X | - | |
| Polyethylene oxide -(CH ₂ -CH ₂ -O) _n MW:5000,000 | 2% | X | - | | X | - | | X | - | | X | - | | X | X | |
| | 5% | X | - | | X | - | | X | - | | X | - | | X | - | |
| | 10% | X | - | | X | - | | X | - | | X | - | | X | - | |

Table 2 The solubility and coating quality of polyethylene oxide of various molecular weights within a range of solvents. S = the solubility of the polymer in the solvent, C = the coating of the PU strips, √ = good, √√ = very good and X= analysis not applicable.

| POLYMER | PERCENT SOLUTION (w/v) | The solubility and coating quality of the polymer within a range of solvents | | | | | | | | | | | | | | |
|--|------------------------|--|---|----------------------------|---------|---|-----------------------------------|---------|---|--------------------|------------|---|---|-----|---|--------------------------------------|
| | | Methanol | | comments | Ethanol | | comments | Acetone | | comments | Chloroform | | comments | DCM | | comments |
| Polyvinylpolypyrrolidone MW:360,000 | | S | C | A flimsy coat was observed | S | C | | S | C | | S | C | | S | C | |
| | 2% | √ | X | | √ | X | Not good coating | X | - | Insoluble solution | X | - | A milky white aggregate of the polymer was observed | √ | X | Poor quality coating was observed |
| | 5% | √ | X | | √ | √ | The coat splintered on drying. | X | - | | X | - | A milky white aggregate of the polymer was observed | X | - | Insoluble solution was observed |
| | 10% | √ | X | | √ | √ | coat dissolved in PBS | X | - | | X | - | | X | - | |
| Polyvinylpolypyrrolidone MW:10,000 | 2% | √ | X | Same as above | √ | X | Same as above | X | - | Same as above | √ | √ | The coat uncoupled when dried | √ | X | Poor quality coating was observed |
| | 5% | √ | X | | √ | √ | | X | - | | √ | √ | | √ | X | |
| | 10% | √ | X | | √ | √ | | X | - | | X | - | Insoluble | √ | √ | Coat dissol - ved in PBS |
| Polyvinylpolypyrrolidone MW:40,000 | 2% | √ | X | Same as above | √ | X | Poor quality coating was observed | X | - | Same as above | √ | √ | A good quality coating was obtained | √ | X | Poor quality coating was observed |
| | 5% | √ | X | | √ | | The coat splintered on drying. | X | - | | √ | √ | | √ | √ | A good quality coating was obtained. |
| | 10% | √ | X | | √ | √ | | X | - | | √ | √ | | √ | √ | |

Table 3 The solubility and coating quality of polyvinylpolypyrrolidone of various molecular weights within a range of solvents. S = the solubility of the polymer in the solvent, C = the coating of the PU strips, √ = good, √√ = very good and X= analysis not applicable

| POLYMER | PERCENT SOLUTION (w/v) | The solubility and coating quality of the polymer within a range of solvents | | | | | | | | | | | | | | |
|---------------------------------------|------------------------|--|---|--------------------|---------|---|--------------------|---------|---|--------------------|------------|----|-----------------------------------|-----|----|-----------------------------------|
| | | Methanol | | comments | Ethanol | | comments | Acetone | | comments | Chloroform | | comments | DCM | | comments |
| Poly(L-lactic acid) MW:300,000 | | S | C | | S | C | | S | C | | S | C | | S | C | |
| | 2% | X | - | Insoluble solution | X | - | Insoluble solution | X | - | Insoluble solution | √ | X | Poor quality coating was observed | √ | X | Poor quality coating was observed |
| | 5% | X | - | | X | - | | X | - | | √ | X | | √ | X | |
| | 10% | X | - | | X | - | | X | - | | X | - | Highly viscous solution | X | - | Highly viscous solution |
| Poly(L-lactic acid) MW:50,000 | 2% | X | - | Same as above | X | - | Same as above | X | - | Same as above | √ | X | Poor quality coating was observed | √ | X | Poor quality coating was observed |
| | 5% | X | - | | X | - | | X | - | | √ | √√ | | √ | √√ | |
| | 10% | X | - | | X | - | | X | - | | √ | √√ | | √ | √√ | |
| Poly(L-lactic acid) MW:2000 | 2% | X | - | Same as above | X | - | Same as above | X | - | Same as above | √ | √ | Coat dissol-ves in PBS | X | √ | Coat dissol-ves in PBS |
| | 5% | X | - | | X | - | | X | - | | √ | X | Poor quality coating was observed | X | X | Poor quality coat |
| | 10% | X | - | | X | | | X | - | | √ | X | | X | X | |

Table 4 The solubility and coating quality of poly(L-lactic acid) of various molecular weights within a range of solvents. S = the solubility of the polymer in the solvent, C = the coating of the PU strips, √ = good, √√ = very good and X= analysis not applicable.

| POLYMER | PERCENT SOLUTION (w/v) | The solubility and coating quality of the polymer within a range of solvents | | | | | | | | | | | | | | |
|---|------------------------|--|---|--------------------|---------|---|--------------------|---------|---|--|------------|----|--|-----|----|--|
| | | Methanol | | comments | Ethanol | | comments | Acetone | | comments | Chloroform | | comments | DCM | | comments |
| Poly(D,L-lactide-co-glycolide) 50:50 | | S | C | | S | C | | S | C | | S | C | | S | C | |
| | 2% | X | - | Insoluble solution | X | - | Insoluble solution | X | - | Insoluble solution | √ | √ | Good coating | √ | X | Coat dissolved in PBS |
| | 5% | X | - | | X | - | | X | - | | √ | √ | | X | X | |
| | 10% | X | - | | X | - | | X | - | | √ | √ | | X | - | Insoluble solution |
| Poly(D,L-lactide-co-glycolide) 85:15 | 2% | X | - | Same as above | X | - | Same as above | √ | √ | Good coating but the coat dissolved in PLA | √ | √ | A very good quality coating was observed | √ | √ | A very good quality coating was observed |
| | 5% | X | - | | X | - | | √ | √ | | √ | √√ | | √ | √√ | |
| | 10% | X | - | | X | - | | √ | √ | | √ | √√ | | √ | √√ | |

Table 5 The solubility and coating quality of poly(D, L-lactic-co-glycoside) of various molecular weights within a range of solvents. S = the solubility of the polymer in the solvent, C = the coating of the PU strips, √ = good, √√ = very good and X= analysis not applicable